The University Of Sheffield.

Novel aspects of the function and assembly of the electron transport chains in *Campylobacter jejuni*

Yang-Wei Liu

M.Sc. National Taiwan University

B.Sc. National Taiwan University

A thesis submitted in part fulfilment for the degree of Doctor of Philosophy

Department of Molecular Biology and Biotechnology

The University of Sheffield

September 2014

Summary

This thesis reports studies on novel aspects of the electron transport chains of the microaerophilic mucosal zoonotic pathogen *Campylobacter jejuni*. Surprisingly, growth under oxygen-limited conditions in strain 81116 was stimulated by tetrathionate, although *C. jejuni* does not possess any known type of tetrathionate reductase. A novel dihaem cytochrome *c* (C8j_0815; TsdA) was shown to be responsible for the enzyme activity. Kinetic studies with purified recombinant *C. jejuni* TsdA showed it to be a bifunctional tetrathionate reductase / thiosulphate dehydrogenase with a high affinity for tetrathionate. A *tsdA* null mutant still slowly reduced, but could not grow on, tetrathionate under oxygen limitation, lacked thiosulphate-dependent respiration and failed to convert thiosulphate to tetrathionate microaerobically. As TsdA represents a new class of tetrathionate reductase that is widely distributed among bacteria, energy conserving tetrathionate respiration will be far more common than currently appreciated. Many co-factored electron transport enzymes are localised by the twin-arginine translocase (TAT). Two paralogues of the TatA translocase component were identified in strain NCTC 11168, encoded by *cj1176c* (*tatA1*) and *cj0786* (*tatA2*). Deletion mutants constructed in either or both of the *tatA1* and *tatA2* genes displayed distinct growth and enzyme activity phenotypes. The specific rate of fumarate reduction catalysed by methyl menaquinone fumarate reductase (MfrA) was similar in the periplasmic fractions of both the *tatA1* and *tatA2* mutants and only the deletion of both genes abolished activity. Unprocessed MfrA accumulated in the periplasm of the *tatA1* mutant, indicating aberrant signal peptide cleavage. Despite being encoded in the *nap* operon, TatA2 is not essential for NapA maturation but may have a role in MfrA assembly. Several periplasmic *c*-type cytochromes encoded by *cj1153, cj1020c, cj0037c, cj0158c cj0854c* and *cj0874c* were mutated in *C. jejuni* NCTC 11168. Mutation of *cj1153* unexpectedly resulted in the loss of all other periplasmic *c*-type cytochromes and abolished electron transfer to the *cb*-oxidase. RT-PCR evidence suggested this phenotype was post-transcriptional and might be due to as yet undefined essential stabilising interactions of Cj1153 with other cytochromes. A large compensatory up-regulation of *cioAB* in the *cj1153* mutant suggested hitherto unappreciated regulatory flexibility. This study reveals additional complexity in the electron transport chains and offers a deeper insight into energy conservation in *C. jejuni*.

Acknowledgements

I would like to first thank my supervisor, Dave, for giving me the opportunity to do my PhD in England and his constant support, guidance and tolerance over the past four years. For me, you are more like a great friend who is always willing to share everything to us. It has been a privilege to work for you. I will always remember the joyful study and life time in the UK, especially with you. “You are ridiculously lucky to have a supervisor like Dave” if you still remember someone had told me so.

To everyone in F1 past and present, it has been my pleasure to work with you all. You are not only my colleagues but also good friends. I wish you all success and happiness always in the future. I will be so grateful if I can keep in touch with all of you. I would also like to thank our collaborator in the Bonn University, especially to Christiane. Without you, my first Mol Micro paper will not be published successfully in a squeezed time, thank you.

To my previous supervisors in Taiwan who always support me to study abroad and encourage me to carry out my dream, especially to Dr. Ya-Chun Chang and Dr. Ching-Tsan Huang in National Taiwan University, both of you are my mentors who were generous to give your sincere recommendations as my references when I applied my course.

To friends, both in and out of the department or those who are in Taiwan and around the world, I will never forget those memorable gatherings, conversations, drinks, and occasional dinners which are great energy to fulfil my life experience and also my English speaking of course. I am very thankful to know all of you.

To my family, especially to my mother, for their constant and unconditional love and financial support during my PhD, thank you so much. I am glad I have quite completed a big part of my life to be a student.

To Jo, who is the most important one in my life, thank you so much. Every single memory of us is speechless. I could not have done this without you, truly. I will return myself to you and the Fox Family unconditionally sooner or later.

This thesis is dedicated to my Grandma and Dad who are in the heaven. I wish you can see the glory of my success.

YWL Sep 2014

Publications and Presentations

Publications:

Liu, Y. W., A. Hitchcock, R. C. Salmon and D. J. Kelly (2014). It takes two to tango: Two TatA paralogues and two redox enzyme-specific chaperones are involved in the localization of twin-arginine translocase substrates in *Campylobacter jejuni*. *Microbiology* **160**(Pt 9): 2053-2066.

Liu, Y. W., K. Denkmann, K. Kosciow, C. Dahl and D. J. Kelly (2013). Tetrathionate stimulated growth of *Campylobacter jejuni* identifies a new type of bi-functional tetrathionate reductase (TsdA) that is widely distributed in bacteria. *Mol Microbiol* **88**(1): 173-188.

Presentations:

Duplicated *tatA* genes in *Campylobacter jejuni*: Distinct roles in assembly of the electron transport chains. **Yang-Wei Liu** and David Kelly., **CHRO, Aberdeen Scotland, 2013.**

Tetrathionate stimulated growth of *Campylobacter jejuni* identifies a new type of bi-functional tetrathionate reductase (TsdA) that is widely distributed in bacteria. **Yang-Wei Liu** and David Kelly., **SGM Spring Conference, Manchester UK, 2012**.

Thiosulfate dehydrogenase and tetrathionate reductase in *Campylobacter jejuni*: Novel enzymes implicated in mucosal growth? **Yang-Wei Liu** and David Kelly., **CampyUK, London, 2012**.

Dissection of the function of novel *c*-type cytochromes in *Campylobacter jejuni*. **Yang-Wei Liu**, Andy Hitchcock and David Kelly., **7th European Workshop on Bacterial Respiratory Chains, Höör Sweden, 2011.**

Abbreviations list

A_{xxx}	absorbance at xxx nm
aa	amino acid
Amp	ampicillin
APS	ammonium persulfate
ATP	adenosine triphosphate
BHI	brain heart fusion
bp	base pair
BSA	bovine serum albumin
BV	benzyl viologen
^{o}C	degrees Celsius
cat	chloramphenicol acetyl transferase
CCV	Campylobacter containing vesicle
cDNA	complementary DNA
CDC	Centers for Disease Control and Prevention, USA
CDT	cytoleathal distending toxin
CFE	cell free extract
Cio	cyanide-insensitive oxidase
Cj	*Campylobacter jejuni*
Cm	chloramphenicol
CO_2	carbon dioxide
Cyd	cytochrome *bd* oxidase
D	Dalton
DEPC	diethylpyrocarbonate
dH_2O	distilled water
ddH_2O	milli-Q water
DMS	dimethyl sulphide
DMSO	dimethyl sulphoxide
DNA	deoxyribonucleic acid
DNase	deoxyribonuclease
DTT	dithiothreitol
Δp	electrochemical proton potential
EDTA	ethylenediamine tetra-acetic acid
E_{M7}	midpoint redox potential at pH7
EMP	Embden-Meyerhof-Parnas
ETC	electron transport chains
FAD	flavin adenine dinucleotide
Fdh	formate dehydrogenase
Fe-S	iron sulphur

fla	flagellin
Frd	fumarate reductase
Fur	ferric uptake regulator
g	gram
GBS	Guillain-Barré syndrome
ggt	γ-glutamyltranspeptidase
GTP	guanosine triphosphate
h	hour
HCl	hydrochloric acid
HEPES	4-(2-hydroxyethyl)-1-piperazineethanesulfonic acid
H_2O	water
H_2O_2	hydrogen peroxide
Hyd	hydrogenase
HPLC	high performance liquid chromatography
IM	inner membrane
IPTG	isopropyl β-D-1-thiogalactopyranoside
ISA	isothermal assembly
Kan	kanamycin
kb	kilobase
kD	kiloDalton
l	litres
LB	Luria-Bertani
Ldh	lactate dehydrogenase
LOS	lipooligosaccharide
LPS	lipopolysaccharide
M	molar
mA	milliampere
Mfr	methylmenaquinol:fumarate reductase
mg	milligram
MH-S	Muller-Hinton plus 20 mM serine
min	minutes
MK/MKH_2	menaquinone/menaquinol
ml	millilitre
mM	millimolar
MOPS	3-(N-morpholino)propanesulfonic acid
mRNA	messenger ribonucleic acid
MV	methyl viologen
mV	millivolts
MW (or Mw)	molecular weight
MWCO	molecular weight cut off

µg	microgram
µl	microlitre
µM	micromolar
NAD(P)	nicotinamide adenine dinucleotide (phosphate)
NAD(P)H	nicotinamide adenine dinucleotide (phosphate) reduced
Nap	periplasmic nitrate reductase
nm	nanometer
nM	nanomolar
NMR	nuclear magnetic resonance
NO	nitric oxide
nt	nucleotide
OD_{xxx}	optical density at XXX nm
OM	outer membrane
ORF	open reading frame
Oor	2-oxoglutarate:acceptor oxidoreductase
PAGE	polyacrylamide gel electrophoresis
PBS(T)	phosphate buffered saline (with 0.05% Tween-20)
PCR	polymerase chain reaction
pH	hydrogen potential
pI	isoelectric point
PMF	proton motif force
Por	pyruvate:acceptor oxidoreductase
***p*-PD**	*p*-phenylenediamine
psi	pound force per square inch
QFR	quinol:fumarate reductase
ROS	reactive oxygen species
RNA	ribonucleic acid
RNase	ribonuclease
r.p.m.	revolutions per minute
RT	room temperature
RT-PCR	real time polymerase chain reaction
s	second
Sdh	succinate dehydrogenase
SDS	sodium dodecyl sulphate
Sec	general secretory pathway
SEM	scanning electron microscope
Sod	superoxide disumtase
Sor	sulphite:cytochrome *c* oxidoreductase
TAE	tris acetate EDTA solution
TAT (or Tat)	twin-arginine translocase

TBS(T)	tris-buffered saline (with 0.05% Tween-20)
TCA	tricarboxylic acid cycle
TEMED	N,N,N,N-tetramethylethylene-diamine
TMAO	trimethylamine-N-oxide
TMA	trimethylamine
TMPD	*N,N,N′,N′*-tetramethyl-*p*-phenylenediamine
Tor	trimethylamine N-oxide oxidoreductase
Tris	tris (hydroxymethyl) methylamine
UV	ultraviolet
V	volt
VitC	ascorbic acid
v/v	concentration, volume to volume
UQ/UQH$_2$	ubiquinone/ubiquinol
WT	wild type
w/v	concentration, weight to volume
x *g*	multiplied by gravitational force
X-gal	5-bromo-4-chloro-3-indolyl-β-D-galactopyranoside

Table of Contents

Chapter 3 – Identification of a novel type of bi-functional tetrathionate reductase (TsdA) in *C. jejuni* strain 81116

Chapter 4 – Two TatA paralogues are involved in the translocation of twin-arginine translocase substrates in *C. jejuni*

Chapter 1 Introduction

1.1 General microbiology of *Campylobacter jejuni*

Campylobacter jejuni is classified under the genus *Campylobacter* and belongs to the *Campylobacteraceae* family of the ε-proteobacteria. It is Gram-negative and its morphologic characteristics include slender, curved, S-shaped or spiral rods. The generic name *Campylobacter* is derived from the Greek word *Kampylos* meaning curved. The species name *jejuni* comes from the site where the organism does its damage, the jejunum and ileum. It is highly motile due to a polar unsheathed flagellum at one or both ends of the cell, which provides mobility for this bacterium (Vandamme, 2000). *C. jejuni* is non-spore forming and requires a microaerophilic environment for its propagation. The size of the cell ranges from 0.2 to 0.9 μm in width and 0.5 to 5.0 μm in length. The optimum temperature for its growth is between 37^{o}C to 42^{o}C (Kelly, 2001; Konkel *et al*., 2001). In the laboratory, the ideal atmosphere condition for culturing *C. jejuni* contains 3 to 15 % (v/v) oxygen and 2 to 10 % (v/v) carbon dioxide. Also, due to its physiological characteristics and metabolic complexity, *C. jejuni* can be only routinely cultured on plates containing blood or in very nutritious broth. It has a respiratory and chemoorganotrophic metabolism, deriving energy from amino acids and tricarboxylic acid (TCA) cycle intermediates, but not carbohydrates, which are neither fermented nor oxidized (Debruyne *et al*., 2008). However, it still can be propagated in less nutritious media with some additives like fumarate, formate and serine (Kelly, 2001; Sellars *et al*., 2002).

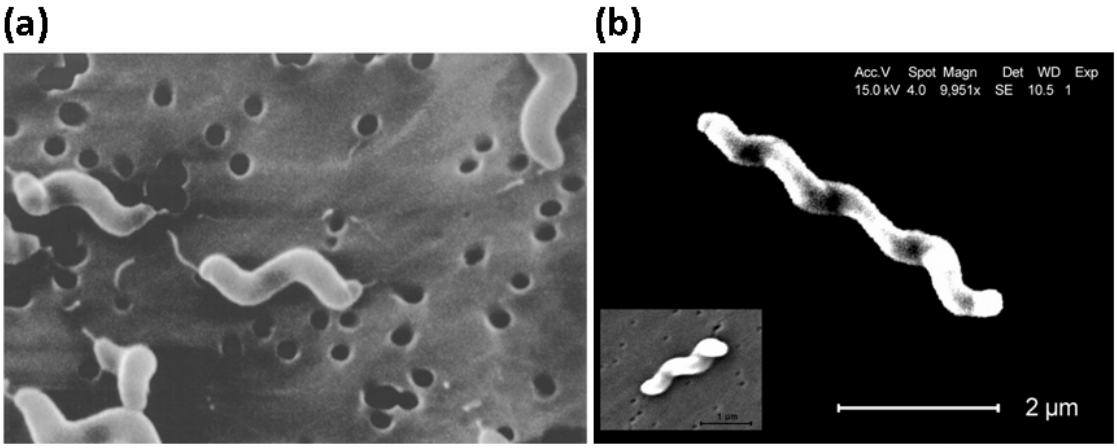

Figure 1.1 **The morphology of *Campylobacter jejuni* under SEM.** These images show its corkscrew appearance and bipolar flagella. Image Source: (a) Sean F. Altekruse / National Cancer Institute, Rockville. (b) Janice Carr / Centers for Disease Control and Prevention.

The history of *C. jejuni* could be traced back to 1886. A nonculturable spiral-shaped bacterium which caused enteritis in neonates was isolated by Theodor Escherich. Then, in 1927, Smith and Orcutt isolated a group of *Vibrio*-lke bacteria from cattle with diarrhea. In 1931, Jones and his colleagues proved a relationship between these microaerophilic vibrios and bovine dysentery. They named this organism *Vibrio jejuni*. Similar organisms were found in human's blood culture with gastroenteritis and aborted sheep fetuses. In 1972, *C.jejuni* was first isolated from human diarrheal specimens by a clinical microbiologist in Belgium using a filtration-culture system (Dekeyser *et al*., 1972; Butzler *et al*., 1979). With the development of improved media, the discovery of optimal temperature and reduced atmospheric requirements, *C. jejuni* finally was recognized as a significant cause of bacterial gastroenteritis. Due to its unusual growth requirements, this organism was neglected as a human pathogen for many years, all the while causing many undiagnosed cases of gastroenteritis.

C. jejuni is considered as a foodborne bacterial pathogen that is common in both industrialized and developing countries (Nauta *et al*., 2009). It can survive in natural environments and some specific hosts like human, cattle and chicken. Although it would cause acute bacterial gastroenteritis in humans, it could survive in the gastrointestinal tract of many avian species and has evolved a commensal relationship with them. Therefore, the main route of human infection is consumption of untreated, undercooked or contaminated food like unpasteurized milk, raw meat and poultry products which are contaminated by feces during processing (Ketley, 1997; Young *et al*., 2007; Fig. 1.2). Consequently, *C. jejuni* is one of the most common causes of acute food-borne gastroenteritis in man and is a major global public health and economic burden (Jacobs-Reitsma *et al*., 2008). The common symptoms of *C. jejuni* infection in humans include acute diarrhoea, fever, abdominal pain, headache, nausea and vomiting. In some cases, the infection leads to autoimmune disorders, including Guillain-Barré syndrome, a paralytic neuropathy that occurs following approximately 1 in every 1,000 cases of campylobacterosis, and Miller-Fisher syndrome, a variant of GBS (Jacobs *et al*., 2008).

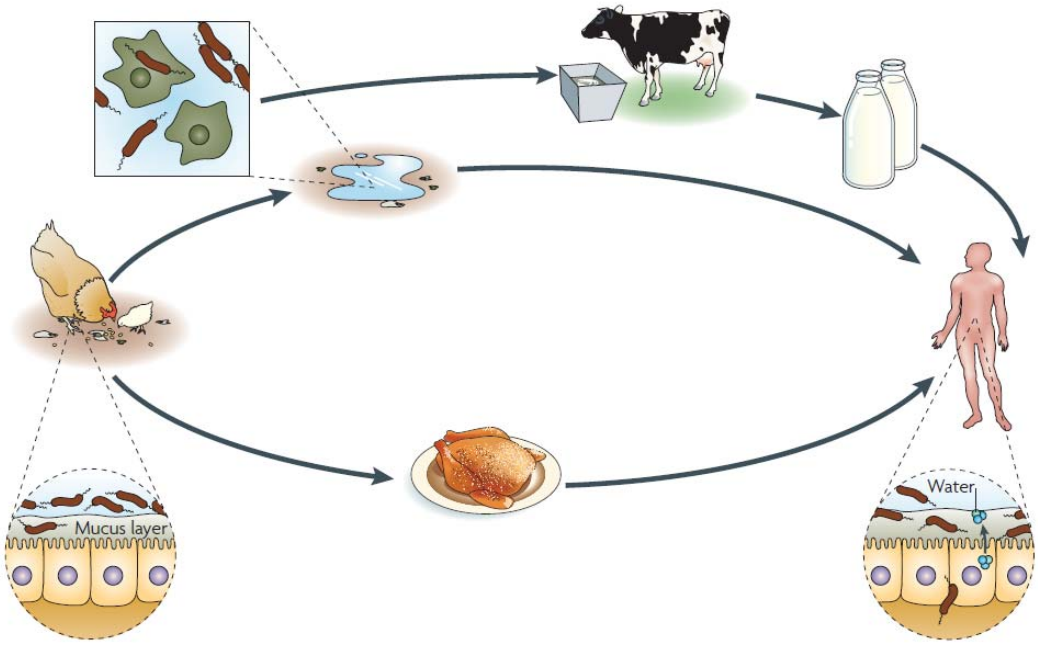

Figure 1.2 **Sources of *Campylobacter jejuni* infection,** several environmental reservoirs can lead to human infection by *C. jejuni*, including contaminated water, milk and undercooked poultry. After infection, *C. jejuni* can penetrate intestine cells and lead to some systemic syndromes in human. Figure adapted from Young *et al*., 2007.

1.2 Taxonomy

In addition to *Campylobacter* spp., *Wolinella* spp. and *Helicobacter* spp. also belong to the epsilon class of proteobacteria. They share some common physiological and biochemical features which are used as the traditional properties in taxonomy. In the past few years, genomic sequences of several ε-proteobacterial species from the *Campylobacterales* order have become available and this made the phylogenetic studies progress rapidly (Gupta, 2006). According to conventional methods, 16S rRNA genes of different strains were amplified with specific primers, and all amplified fragments could be sequenced, aligned and their phylogenetic relationships are determined by computative programs (Vandamme, 2000). However, based on comparative genomics concepts, phylogenetic data can be calculated via the alignment of amino acid sequences. The identified signature proteins and indels comprise rare genetic changes that have been introduced at various stages during the evolution of *Campylobacterales* and their species distribution patterns are supported by the branching order of these species in phylogenetic trees (Gupta, 2006; Fig. 1.3).

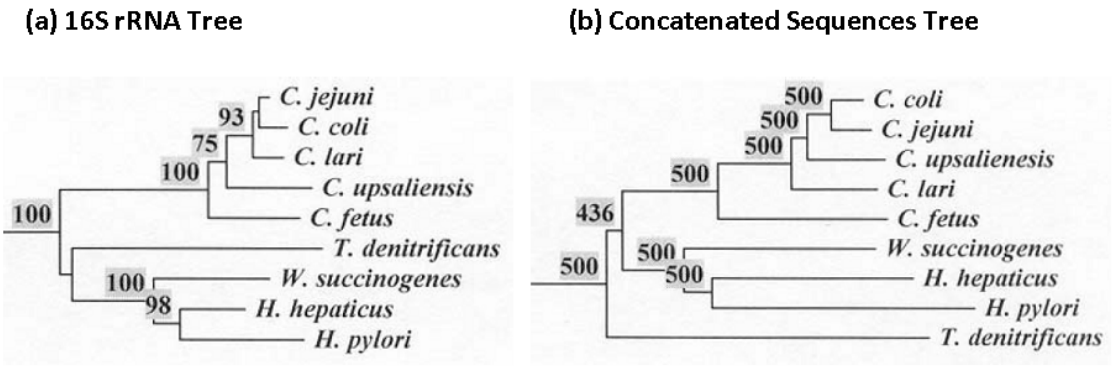

Figure 1.3 **Phylogenic relationships of *Campylobacteriales***, based on (a) 16S rRNA and (b) concatenated sequences for 9 proteins (AlaRS, Gyrase A, Gyrase B, EF-Tu, EF-G, Hsp70, RpoB and RpoC): four genera below *Campylobacteriales* are *Campylobacter*, *Helicobacter*, *Wolinella* and *Thiomicrospira*. Figure adapted from Gupta, 2006.

The phylogenic relationships of three main genera *Campylobacter*, *Helicobacter* and *Wolinella* are compared by the 16S rRNA and concatenated sequences which reflect different relationship within this class (Fig. 1.3). However, like *C. jejuni*, all members under these genera share some common features. They have relative smaller genomes (1.6 to 2.0 megabases) and can establish long-term association with their hosts, sometimes with pathogenic consequences (Young *et al*., 2007). The genus *Helicobacter* includes *Helicobacter pylori*, a well known pathogen that causes gastric ulcers, sometimes can survive in humans without any symptoms for decades. The genus *Wolinella* contains only one species, *Wolinella succinogenes*, which usually colonizes cattle as a commensal organism. Therefore, for these bacteria, it is usual to build long-term relationships with their hosts, which means they are highly host-adapted. For this reason, they can maintain their niches without generating any immunoresponse or syndromes in the host that has the ability for clearance (Young *et al*., 2007).

1.3 Genome Analysis of *Campylobacter jejuni* strains

The complete genome structure of *C. jejuni* strain NCTC 11168 was sequenced and published in 2000 (Parkhill *et al*., 2000). The whole genomic sequences made a renewed interest in some areas neglected previously and it also has been re-analysed and re-annotated (Gundogdu *et al*., 2007). The genome of *C. jejuni* NCTC 11168 is relatively small and compact and includes 1,641,481 base pairs (bp) in length with a low G+C content of 30.6%, comprising 1,654 predicted open reading frames (ORFs), of which, at least 20 probably represent pseudogenes and 54 stable RNA species.

Pseudogenes have similar sequences to those functional genes but are unable to produce functional products. It is one of the densest bacterial genomes to date because the average gene length is 948 bp and 94.3% of the genome is made up of coding sequences (Parkhill *et al*., 2000). It is also found that *C. jejuni* genome lacks repetitive sequences and there are only four repeated sequences within the entire sequence. According to the sequencing data, it is suggested that *C. jejuni* lacks DNA repair functions. For example, genes like *ada*, *phr*, *mutH*, *mutL* and *lexA* in *E.coli* can not be found in *C. jejuni* (Parkhill *et al*., 2000). Another interesting finding of the genome is the presence of hypervariable regions, which are short and homopolymeric, were mostly found in the genes for the biosynthesis or modification of surface structures (e.g. modification of the flagella and the biosynthesis of extracellular polysaccharide) which give the cell rapid variation of surface features. Taken together, both physiological traits may be relevant to colonization of the dynamic environment like the intestinal tract or evasion of the host immune system (Parkhill *et al*., 2000). Also, the genomic sequences suggested a highly branched respiratory chain in *C. jejuni,* which not only offers the potential for metabolic versatility but facilitates the research in molecular physiology and pathogenicity.

C. jejuni 81-176 is another strain which is considered as highly pathogenic and usually used in the research of colonisation (Hofreuter *et al*., 2006). The whole genome of *C. jejuni* 81-176 is composed of 1,594,651 bp in length. Therefore, comparing to that of strain NCTC 11168, there are 35 genes absent (Hofreuter *et al*., 2006; Gundogdu., 2007), including several metabolic and pathogenic genes like a dimethyl sulphoxide (DMSO) reductase; two DcuC homologues involved in succinate efflux and γ-glutamyltranspeptidase (*ggt*). Also, two plasmids were found in strain 81-176, pVir and pTet, which were considered as virulence factors in *C. jejuni* (Bacon *et al*., 2002).

C. jejuni strain RM1221 was discovered by Miller in 2000 (Miller *et al*., 2000). The total genomic sequencing was achieved in 2005 and its genome consists of 1,777,831 bp (Fouts *et al*., 2005). It also has a low G+C content as 30.31% and includes 1884 predicted ORFs. The average of length of its genes is 885 bp and 47 of them are pseudogenes (Fouts *et al*., 2005). Interestingly, it has shown that 12 of these pseudogenes are similar to those in the strain NCTC 11168.

1.4 Clinical aspects, diagnosis and treatment of campylobacteriosis

Many agents of foodborne infection cause similar clinical symptoms like diarrhoea, fever and pain. The diagnosis of *C. jejuni* relies on either isolating this bacterium in stools from patients, or performing immunological and molecular tests on a specimen to confirm the existence of this organism, antibodies or DNA fragments (Skirrow and Blaser, 2000). Most people who fall ill with *C. jejuni* have symptoms like diarrhoea (often bloody diarrhoea), cramping, abdominal pain and fever within 2 to 5 days after exposure to the organism and symptoms typically last for up to one week (Butzler and Skirrow, 1979). Although complications are rare, *C. jejuni* infection can lead to serious sequelae like acute cholecystitis, hemolytic uremic syndrome and Guillain-Barré syndrome which is the most common complication and causes neuromuscular paralysis in patients with campylobacteriosis (Rhodes and Tattersfield, 1982).

The incubation period of *C. jejuni* in human ranges one to seven days and the average is three days (Konkel *et al*., 2001). Some patients may have mild symptoms; others may have life-threatening illness with various complications. Comparing to other pathogens causing enteritis, *C. jejuni* has a low infectious dose of 500 cells, indicating the high risk of infection when consuming raw or undercooked poultry and contaminated water or milk (Black *et al*., 1988; Olson *et al*., 2008).

However, since the infection of *C. jejuni* is generally self-limiting, most of campylobacteriosis patients can recover without any clinical treatments of antibiotics. In cases of diarrhoea, the recommended therapy is to resupply fluid and electrolyte. For some severely dehydrated patients, rapid volume expansion with intravenous fluids is needed (Dryden *et al*., 1996). In order to shorten the duration of symptoms and eliminate this organism in gastrointestinal tracts, antibiotics such as erythromycin or fluoroquinolone can be used in some severe cases of infection. If antimicrobial therapy can be applied soon after the onset of symptoms, the duration of illness can be reduced from ten days to approximately five days (Dryden *et al*., 1996).

1.5 Pathogenic mechanisms of *Campylobacter jejuni*

Campylobacter jejuni was first recognized as a pathogen in 1977 (Byran and Doyle, 1995). However, without complete genomic information, for a long time researchers could only focus on some pathogenic traits like those in other bacterial pathogens. The

lack of knowledge concerning the pathogenic mechanisms has limited our means of preventing humans from obtaining this organism. Until recently, the whole genome information was sequenced and lots of gene-based pathogenic factors of *C. jejuni* were revealed (Parkhill *et al*., 2000). According to previous studies, complex interactions between the pathogen and host tissues lead to the gastrointestinal tract infection, where *C. jejuni* is able to develop some pathogenic mechanisms like invasion, adhesion, glycosylation and motility. All of them would challenge the immune system of specific hosts and cause some syndromes of campylobacteriosis.

1.5.1 Virulence and colonisation factors

1.5.1.1 Motility and taxis

The mobility/chemotaxis of *C. jejuni* is vital to many aspects for the survival, including host colonization, virulence in some animal models, secretion and host-cell adhesion and invasion. A mutant deficient in motility was unable to maintain persistent infection with the host and also showed reduced adhesion and invasion of human cells (Wassenaar *et al*., 1991; 1993; Golden and Acheson 2002; Hendrixson and DiRita, 2004). Previous studies indicated that *C. jejuni* could penetrate the mucus of the small bowel of human due to its spiral shape and flagellar motility (Golden and Acheson, 2002; Yao *et al*., 1994). Both of these characteristics facilitated the corkscrew motion of this pathogen which first colonised and then grew in the intestinal mucus layer. The bipolar unsheathed flagella are composed of a basal body, a hook and filaments. The filament is built up by the flagellins FlaA (Cj1339) and FlaB (Cj1338; Guerry *et al*., 1991), which *flaA* shows a higher expression level (Konkel *et al*., 2001). A transcriptional hierarchy exists in the regulatory mechanism of the flagella of *C. jejuni*. The regulatory cascade includes σ^{54} (encoded by *rpoN*) and σ^{28} (encoded by *fliA*) as the flagellar σ-factors (Hendrixson *et al*., 2001) and the two-component system Flg/S/R (Cj0793/Cj1024; Wösten *et al*., 2004). However, the flagellar master regulators FlhC and FlhD, which are crucial for the flagellar gene expression in other species, have not been identified in the *C. jejuni* genome (Parkhill *et al*., 2000). Flagella offer an advantage for *C. jejuni* to invade through the epithelial surface to the underlying tissues with resisting expulsion caused by gut peristalsis (Hendrixson and DiRita, 2004), and it could also act as a secretion apparatus for invasion antigens, which are able to elaborate other virulence factors to cause inflammation and epithelial damage with leakage of fluid.

The mobility caused by chemical stimulation is called chemotaxis. Environmental factors like the concentration of carbon sources will trigger the signal transduction system in *C. jejuni,* which makes cells sense surrounding changes and start to response by flagellar movements toward or away from the source of stimuli. The genome sequence analysis has shown that *C. jejuni* encodes most features of the *E. coli* chemotaxis system. Several homologues like the histidine kinase CheA (Cj0284), scaffold protein CheW (Cj0283) and response regulator of controlling flagellar rotation CheY (Cj1118) are present (Parkhill *et al*., 2000; Marchant *et al*., 2002), along with the receptor adaption proteins CheR (Cj0923) and CheB (Cj0924; Kanungpean *et al*., 2011). *C. jejuni* lacks a homologue of the phosphatase CheZ but Cj0700 might be a functional substitute (Korolik and Ketley, 2008). The poorly understood CheV protein was also found in *C. jejuni* which has a N-terminal CheW like domain and a C-terminal CheY-like domain. It is supposed to be a phosphate sink for the signal-transduction machinery of chemotaxis (Marchant *et al*., 2002; Pittman *et al*., 2001).

C. jejuni displays chemotactic mobility towards amino acids which are found in high levels in the chick gastrointestinal tract (Hugdahl *et al*., 1988). There are ten methyl-accepting chemotaxis receptors (MCPs) anchoring on the membrane of *C. jejuni*, which are also termed Tlps (transducer-like proteins; Marchant *et al*., 2002). Mutants that lack either Cj0019c (DocB) or Cj0262c, which are both MCPs, show decreased chick colonisation. According to the genomic and genetic analysis, *C. jejuni* is also able to transduce an energy taxis (or aerotaxis) signal using CetA and CetB (Cj1190/Cj1189) proteins, and migrate in response to either the redox state of electron transport chain components or the proton motive force (Hendrixson *et al*., 2001).

1.5.1.2 Adhesion and invasion

To colonise hosts, bacteria typically require specific components on the cell surface to attach host cells. Fimbriae and pili are the most common structures which facilitate the adhesive progress during colonization. The genomic sequence analysis revealed that *C. jejuni* does not encode either of them (Parkhill *et al*., 2000), but relies on surface-exposed adhesins which make pathogens attach on human cells, especially bind to host target cells associated with the intestinal mucus-filled crypts (Pei *et al*., 1998). The adhesins discovered in previous studies includes the flagellin (Grant *et al*., 1993) and the FlaC (Cj0720) secreted by flagella (Song *et al*., 2004); the lipooligosaccharide

(LOS; McSweegan and Walker, 1986); the surface attached lipoprotein JlpA which is crucial for the HEp-2 cell binding (Cj0983; Jin *et al*., 2001); the periplasmic binding protein PEB1a (or called CBF1, Cj0921**;** Pei *et al*., 1998); the outer membrane proteins CadF which binds specifically to fibronectin (Cj1478; Konkel *et al*., 1997) and FlpA (Cj1279; Flanagan *et al*., 2009); the autotransporter protein CapA (Cj0628/Cj0629; Ashgar *et al*., 2007); the surface exposed P95 (Kelle *et al*., 1998); the major outer membrane protein (MOMP) encoded by *porA* (*cj1259*; Schroder and Moser, 1997); the surface capsular polysaccharide (Bacon *et al*., 2001); and the magnesium transporter glycoprotein Cj1496c which is present in the periplasm (Kakuda and DiRita, 2006).

Intracellular *C. jejuni* have been observed in patients, which indicates the bacteria apparently invade intestinal epithelial cells and this could be reproduced in cell lines *in vitro*. All *C. jejuni* strains require microtubule polymerization for a maximal invasion and the disruption of actin-based process has also been well described (Monteville *et al*., 2003; Oelschlaeger *et al*., 1993). *C. jejuni* undergoes physiological changes in oxygen sensitivity and metabolism inside the host cells and a modified membrane bound compartment called *C. jejuni* containing vacuoles (CCVs) allows the survival and replication of this pathogen (Watson and Galán, 2008). The synthesis of *Campylobacter invasion antigens* (Cia) is stimulated by the bile component deoxycholate and the secretion of Cia is probably mediated by the flagellar type-III secretion system (Konkel *et al*., 2004). The Cia has been demonstrated to cause invasion (Rivera-Amill *et al*., 2001; Konkel *et al*., 1999; Christensen *et al*., 2009; Buelow *et al*., 2011), as do the polysaccharide capsule (Bacon *et al*., 2001) and sialylated LOS (Louwen *et al*., 2008).

1.5.1.3 Toxin production

The well-studied CdtABC (Cj0079c – Cj0077c) tripartite complex has revealed the first cytolethal distending toxin (CDT) in *C. jejuni* (Lara-Tejero and Galán, 2001). The toxin causes an arrest at the G_1/S or G_2/M transition of the cell cycle, blocks cell division and leads to cell death of lymphocytes and has been recognized as a major pathogenicity-associated factor (van Vliet and Ketley, 2001). CdtB is thought to act as a DNase, as it shares similarity with a family of DNase I-like proteins. The functions of CdtA and CdtC are still unclear, but one or both might mediate binding to host cells (Lara-Tejero and Galán, 2001). In addition, several proteins were found to act as CDTs while the infection process of *C. jejuni*, including a phospholipase, *pldA* (*cj1351*; Ziprin

et al., 2001); a putative contact dependent haemolysin, *tlyA* (*cj0588*) and a putative integral membrane protein with a haemolysin domain (*cj0183*; Sałamaszyńska-Guz and Klimuszko, 2008). The CDT is present in the outer membrane vesicles of *C. jejuni* (Lindmark *et al*., 2009). However, its role in the virulence process is still unclear and the *cdt* mutant shows similar enteric colonization and host cell adhesion as wild type but the reduction of invasion was observed in it (Purdy *et al*., 2000; Biswas *et al*., 2006).

1.5.1.4 The homeostasis of iron

The iron homeostasis is crucial to bacterial survival and it is also essential for living organisms in the cellular processes including metabolism, electron transport and gene regulation. Also, the availability of iron plays a central role in the pathogenesis of bacterial pathogens (Braun, 2001). The ferric iron (Fe^{3+}) occurs in the host mostly and the specific iron-binding proteins like lactoferrin and transferring allow the ferric iron to be isolated from pathogens in the host. In order to overcome this situation, the commensal and pathogenic bacteria secret a specific iron-chelator called siderophore, which shows higher affinity to Fe^{3+}. However, the genomic sequence analysis shows that no siderophores are encoded in *C. jejuni* (Gundogdu *et al*., 2007). Instead, this pathogen is able to utilise several iron uptake systems to obtain iron from siderophores secreted by other bacteria like ferric-enterobactin and salmochelin or host-derived iron-binding proteins like lactoferrin and hemoglobin (Miller *et al*., 2009; Naikare *et al*., 2013). CfrA (Cj0755) located in the outer membrane of *C. jejuni* NCTC 11168 is a ferric-enterobacterin receptor, which coordinates with the CeuBCDE (Cj1352 - Cj1355) ABC transporter system to mediate enterbactin/enterochelin uptake into *C. jejuni* (Palyada *et al*., 2004). Another iron uptake system that facilitates iron acquisition from host compounds like hemoglobin and hemin is the *chuABCDZ* (*cj1613 – cj1617*) gene cluster (Ridley *et al*., 2006). Furthermore, *C. jejuni* is also able to utilize ferrous (Fe^{2+}) iron by the FeoB (Cj1398) transport protein (Naikare *et al*., 2006) and the major iron-storage protein in *C. jejuni* is the ferritin-like Cft (Cj0612; Wai *et al*., 1995).

1.5.1.5 Protein glycosylation

Glycosylation is a kind of post-translational modification of proteins with oligosaccharide conjugation. Two protein glycosylation systems were found in *C. jejuni*: *O*-linked glycosylation modifies serine or threonine residues on flagellin, while the other modifies asparagine residues on many proteins (*N*-linked glycosylation).

Interestingly, the *N*-linked glycosylation had been observed only in eukaryotes and archaea before the discovery of the *N*-linked modification system in *C. jejuni* (Szymanski *et al*., 1999). The biochemical functions and biosynthesis pathway of *O*-linked glycosylated proteins were well studied and this system plays an important role in the synthesis of flagella in *C. jejuni*. Previous studies indicate that the flagellin in strain 81-176 is glycosylated with pseudaminic acid, synthesized by the *pse* genes (McNally *et al*., 2006) and homologues of genes involved in flagellin glycosylation of *Campylobacter coli* are wildly distributed among different *C. jejuni* strains (McNally *et al*., 2007). *O*-linked glycosylation of flagellin is necessary for the proper assembly of the flagellar filaments, and suggests a deficiency of this mechanism will result in severe consequences, such as the loss of motility, a decrease in the adherence to and invasion of human epithelial cells (Szymanski *et al*., 2002) and decreased virulence in ferrets (Guerry *et al*., 2006). However, to date, there is still no evidence for the role of *O*-linked glycosylation in immune avoidance or the host cell interaction. On the contrary, *N*-linked glycosylation plays a more fundamental role in the biology of *C. jejuni* and the *N*-linked glycans are conserved in all strains that have been examined (Dorrell *et al*., 2001; Szymanski *et al*., 1999). The *pgl* gene cluster (*cj1119c – cj1130c*) is responsible for the synthesis of *N*-linked glycans which consist of *N*-acetylgalactosamine-containing heptasaccharides (Young *et al*., 2002) at the conserved sequence – D/E-X_1-N-X_2-S/T (where X_1 and X_2 can be any amino acids except proline; Wacker *et al*., 2002; Young *et al*., 2002). Over more than 30 periplasmic and membrane proteins are *N*-linked glycosylated and participating in the process of colonisation, adherence and invasion (Wacker *et al*., 2002; Linton *et al*., 2005) while the strain with *pgl* mutations exhibit reduced adherence and invasion in the INT 407 intestinal cell lines (Kakuda and DiRita, 2006). Furthermore, *N*-linked glycosylation changes the immunoreactivity of some glycosylated proteins, which suggests *N*-linked glycosylation might be involved in the evasion of the immune system (Szymanski *et al*., 1999). However, the biological function of *N*-linked glycosylation in *C. jejuni* is still not fully clear to date.

1.6 Physiology of *C. jejuni*

In the lack of genetic information, most previous studies focused on the virulence and colonisation of *C. jejuni* before the revealing of its genomic sequences. However, the particular metabolic properties of this organism are important because they directly or indirectly relate to the ability of pathogenicity. Also, *C. jejuni* needs complex

environmental conditions for culturing and a complex medium like undefined blood products are always used, which leads to the difficulty of understanding its metabolic pathway and the utilization of various substrates (Kelly, 2001). Now the complete genome information provides many new insights of the physiology of *C. jejuni* (Parkhill *et al*., 2000).

1.6.1 Carbon catabolism

1.6.1.1 The non-glycolytic nature of *C. jejuni*

The glycolysis pathway is the first and critical step of carbon metabolism in prokaryotic and eukaryotic cells and yields ATP and NADH. ATP can be utilized by cells directly whereas NADH drives the production of ATP via electron transport chain and ATPase. Due to the lack of the nonreversible glycolytic enzyme 6-phosphofructokinase, *C. jejuni* has an interrupted Embden-Meyerhof-Parnas (EMP) pathway, so it can not utilize the most common carbon source in the environment: glucose (Parkhill *et al*., 2000; Kelly, 2008). Also, the result of BIOLOG phenotype microarray analyses showed that the respiratory activity of *C. jejuni* was not enhanced either by adding hexoses and pentoses like fructose, galactose, trehalose, ribose, rhamnose or the presence of disaccharides lactose, maltose and sucrose (Gripp *et al*., 2011; Line *et al*., 2010; Muraoka and Zhang, 2011). However, recent studies revealed that L-fucose can be utilized as a growth supporting carbon/energy source in certain strains (Muraoka and Zhang, 2011; Stahl *et al*., 2011). A genomic island (9 kb) which is comprised of 11 open reading frames from *cj0480* to *cj0490*, is found in strain NCTC 11168 but not in 81-176. The gene region encodes fucose-inducible enzymes which constitute a unique pathway for the uptake and metabolism of the sugar and facilitate the colonisation of the host guts since L-fucose is the predominant saccharide in mucins (particularly in the small intestine and cecum). The *fucP* (*cj0486*) gene encodes a putative fucose permease which enhances the growth of *C. jejuni* NCTC 11168 supplemented with fucose *in vitro* and provides a competitive advantage during the colonisation in the porcine pathogenic model (Stahl *et al*., 2011). In addition to mucins, the source of fucose in the intestine might be from the degradation of host glycans by commensal bacteria or the up-regulation of host's fucosidase stimulated by the infection of other pathogens like *H. pylori* (Liu *et al*., 2009). The fucose transported by FucP might be further metabolised to dihydroxyacetone phosphate (DHAP) and then to pyruvate which provides a rationale for the lower part of the EMP pathway in *C. jejuni* (Muraoka and Zhang, 2011).

1.6.1.2 Gluconeogenesis and anaplerotic reactions

C. jejuni does not encode for enzymes like 6-phosphogluconate dehydratase and 2-keto-3-deoxyphosphogluconate aldolase in the Entner–Doudoroff pathway (Fouts *et al*., 2005; Parkhill *et al*., 2000), also a glucose uptake system like the phosphoenolpyruvate (PEP)-dependent phosphotransferase in *E. coli* (Gosset, 2005) was not found in *C. jejuni*. Consequently, gluconeogenesis is necessary for the biosynthesis of glucose, which is used for the LPS and capsule biosynthesis and the *O*- or *N*-linked glycosylation of various proteins (Karlyshev *et al*., 2005). Though the gluconeogenesis has not been experimentally proven yet, several anaplerotic enzymes which bridge the TCA cycle to the EMP pathway were discovered and they are homologues of pyruvate carboxylase PycA and PycB (Cj1037 and Cj0932), the phosphoenolpyruvate carboxykinase PckA (Cj0932) and the pyruvate kinase Pyk (Cj0392c; Velayudhan and Kelly, 2002). These enzymes are required for the oxaloacetate – PEP – pyruvate conversion that composes a metabolic triangle in the controlling of the carbon flow. Interestingly, the irreversible pyruvate kinase Pyk which catalyses the final step of glycolysis is in the absence of function forwards EMP-pathway, thus the catabolic role of Pyk might involve in the lower part of the pathway with unknown substrates. Besides, PckA which catalyses the synthesis of PEP by the decarboxylation of oxaloacetate, was considered essential for *C. jejuni* because the *pckA* gene could not be inactivated by site-directed mutagenesis in strain NCTC 11168 (Velayudhan and Kelly, 2002).

1.6.1.3 The tricarboxylic acid cycle

The genome sequence indicates that *C. jejuni* possesses all critical enzymes which are necessary for operating a complete oxidative tricarboxylic acid (TCA) cycle (Parkhill *et al*., 2000). Homologues of succinate dehydrogenase (*cj0437-0439*, or type B fumarate reductase), the α and β subunit of succinyl-coA synthetase, fumarate reductase complex (*frdABC*), NAD-linked malate dehydrogenase and a malate:quinine oxidoreductase are present (Kelly, 2001). However, the pyruvate dehydrogenase and 2-oxoglutarate dehydrogenase complexes are absent and replaced by another two oxidoreductases as alternatives: Por and Oor. The flavodoxin/ferredoxin-dependent pyruvate: acceptor oxidoreductase (Por; encoded by *cj1476c*) is responsible for the oxidative decarboxylation of pyruvate to acetyl-CoA and the related 2-oxoglutarate: acceptor oxidoreductase (Oor; encoded by *oorDABC*, *cj0535* to *cj0538*) catalyses the conversion

of oxoglutarate to succinyl-CoA. Both Por and Oor contain iron-sulphur (Fe-S) clusters which are very sensitive to inactivation by oxygen and commonly found in obligate anaerobes. The presence of these two proteins might partially contribute to the microaerophilic phenotype of *C. jejuni* (Kelly, 2008; Kendall *et al*., 2014). It has been demonstrated that an additional redox protein might mediate the transfer of electrons from Por-reduced flavodoxin to NADP in *H.pylori* (Hughes *et al*., 1998) and this is crucial for the reoxidising of reduced flavodoxin to ferrodoxin produced in the Por/Oor reactions. The flavodoxin:quinone reductase homologue in strain NCTC 11168 is Cj0559 (St Maurice *et al*., 2007) but it has not been proved yet whether this might contribute the similar electron transfer as that in *H .pylori*.

1.6.1.4 Organic acids and amino acids are the main sources of carbon for *C. jejuni*

Due to the significance of gluconeogenesis in *C. jejuni* for maintaining its physiological activity, the substrates which are utilised efficiently in the intermediary metabolism will be able to satisfy the necessities for carbohydrate, lipid and protein biosynthesis of this pathogen. Previous studies revealed that *C. jejuni* is able to catabolise organic acids like lactate, pyruvate, acetate and intermediates of the TCA cycle as well as a restricted number of amino acids (Elharrif and Megraud, 1986; Westfall *et al*., 1986; Mohammed *et al*., 2004; Guccione *et al*., 2008; Hinton, 2006; Velayudhan and Kelly, 2002; Wright *et al*., 2009) and several systems for active transport of organic acids across the inner membrane are deduced from the genomic information (Parkhill *et al*., 2000). Also, organic acids like pyruvate, 2-oxoglutarate, fumarate, succinate, malate and lactate are chemoattractants of *C. jejuni*, suggesting their importance for the proliferation of *C. jejuni* (Hugdhal *et al*., 1988; Vegge *et al*., 2009). The C4-dicarboxylate antiporters DcuA (Cj0088) and DcuB (Cj0671) on the inner membrane are able to transport aspartate into *C. jejuni* under oxygen-limited conditions (and excrete succinate electroneutrally with fumarate uptake), then aspartate is converted into fumarate by deamination catalysed by the aspartase AspA (Cj0087) within the cell and fed directly into the TCA cycle. The AspA has also been shown to be important in fumarate respiration in *C. jejuni* (Guccione *et al*., 2008). Furthermore, only the *dcuAdcuB* double mutant was unable to grow supplemented with aspartate/fumarate, indicating their activities were redundant. Nevertheless aspartate uptake still occurs, suggesting the transportation might be achieved by the PEB1 aspartate/glutamate ABC-transporter

(Leon-Kempis *et al*., 2006) and possibly by the homologue of DctA: Cj1192, which is a predicted dicarboxylate/amino acid:cation symporter (Parkhill *et al*., 2000). Although there is another system accounting for the specific efflux of succinate (DcuC; Zientz *et al*., 1999), the homologous genes found in *C. jejuni* NCTC 11168 are inactive pseudogenes (*cj1389* and *cj1528*), and this probably explains the growth defect of the *dcuAdcuB* mutant.

It is well established that the utilization of amino acids plays an important role in fuelling the central metabolism of *C. jejuni.* However, only few glucogenic amino acids support the growth of this pathogen and some of them like arginine and lysine have been proved as chemorepellents (Rahman *et al*., 2014). The amino acids which are utilised by most *C. jejuni* strains for proliferation include aspartate, glutamate, proline and serine (Guccione *et al*., 2008; Hofreuter *et al*., 2008; Velayudhan *et al*., 2004; Leach *et al*., 1997). This correlates well with the metabolic profiling of supernatants from *C. jejuni* liquid culture, which demonstrates the utilization of these four amino acids (Guccione *et al*., 2008; Wright *et al*., 2009) and the amino acid composition of chicken excreta (Parsons *et al*., 1982). The order of importance for these four amino acids *in vivo* was validated by the catabolic test and the colonisation of animal models of infection with mutants. Serine is first catabolized and facilitated the rapid growth for *C. jejuni* (Velayudhan *et al*., 2004), followed by the usage of aspartate (Guccione *et al*., 2008; Novik *et al*., 2010), glutamine/glutamate (Hofreuter *et al*., 2006; Barnes *et al*., 2007) and proline (Leach *et al*, 1997). Due to the presence of an active serine transporter SdaC (Cj1265c) and dehydratase SdaA (Cj1264c), serine becomes the most favoured amino acid for *C. jejuni* growth. Within the cell, serine is efficiently converted to pyruvate which can be fed directly into the TCA cycle by the conversion to acetyl-CoA mediated by Por (Velayudhan *et al*., 2004).

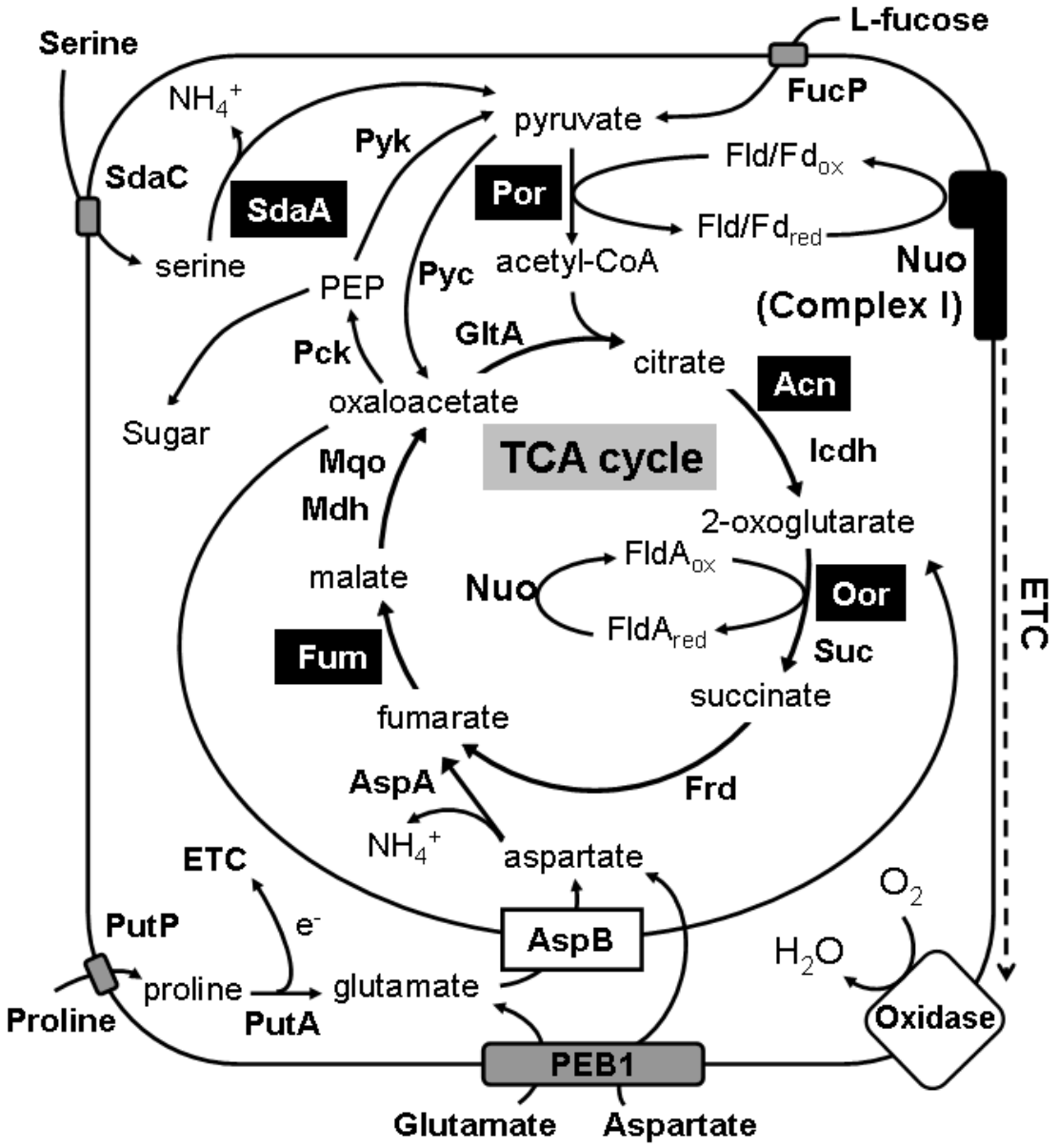

Figure 1.4 Central carbon metabolism and amino acid utilisation in *C. jejuni*. Major enzymes are shown next to the reaction they catalyse and pathways are partially elucidated. Transporters are shown as grey rectangles and O_2-sensitive enzymes are shown in black boxes. The outer and inner membranes and the periplasm are demonstrated as a single border. Enzymes and proteins, from top: FucP, L-fucose transporter; SdaC, serine transporter; SdaA, serine dehydratase; Pyk, pyruvate kinase; Por, pyruvate: acceptor oxidoreductase; Nuo, NADH: quinone oxidoreductase; Pyc, pyruvate carboxylase; Pck, PEP carboxykinase; GltA, citrate synthase; Acn, aconitase; Icdh, isocitrate dehydrogenase; Mqo, malate:quinone oxidoreductase; Mdh, malate dehydrogenase (NAD linked); Oor, 2-oxoglutarate: acceptor oxidoreductase; Suc, succinyl-CoA synthetase; Fum, fumarase; Frd, fumarate reductase; AspA, aspartate deaminase; AspB, glutamate transaminase; PutP, proline transporter; PutA, proline dehydrogenase; PEB1, aspartate/glutamate ABC-transporter. ETC is electron transport chain and PEP is phosphoenol pyruvate. Figure revised from Kelly, 2008.

Still some *C. jejuni* strains are able to utilize asparagine and glutamine/glutathione for growth. For the deamination of asparagine, an additional sec-dependent secretion signal is necessary for the transportation of L-asparaginase AnsB ($AnsB^S$; secreted AnsB) into periplasm that was only found in certain strains such as 81-176. Also, *C. jejuni* strains which encode for a secreted γ- glutamyltranspeptidase (GGT) are able to utilize glutamine for growth (Hofreuter *et al*., 2008). Taken together, the $ansB^s$ and *ggt*-positive *C. jejuni* isolate relies on the conversion of both amino acids to aspartate and glutamate respectively in the periplasm, then these deaminated amino acids are transported through the membrane bound DcuAB, DctA and PEB1 into the cell (Guccione *et al*., 2008; Leon-Kempis *et al*., 2006). Furthermore, proline is the least well-used amino acid and the presence of PutP (CJJ81176_1494; Cj1502), a sodium/proline symporter, allows proline entering the TCA cycle where the PutA (CJJ81176_1495; Cj1503), a bifunctional enzyme, converts proline to glutamate in a two-step reaction (Stahl *et al.*, 2012). In addition to the systems described above, the CjaA (Cj0982c) protein constitutes the cysteine-binding component of an ABC transporter (Müller *et al*., 2005) and the homologues of LIV transport system might contribute the transportation of branched-chain amino acids such as leucine, isoleeucine and valine (Ribardo and Hendrixson, 2011).

1.6.2 Microaerophilly

The dependence on oxygen for *C. jejuni* is a dilemma since it is well known as microaerophile, which means that *C. jejuni* although requiring oxygen for growth, is unable to grow at normal atmospheric oxygen tensions. This unusual physiological characteristic may offer this pathogen a niche for surviving at low oxygen concentrations (Kreig and Hoffman, 1986; Kelly *et al*., 2001). Most strains of *C. jejuni* grow best at 3 – 10 % (v/v) oxygen, and their growth will be inhibited under both extreme conditions: atmospheric oxygen tensions and strict anaerobic environments like human guts. The life cycle of *C. jejuni* reflects its exposure to various oxygen concentrations but the knowledge about its microaerobic requirement of oxygen and the oxygen-sensing system is still unclear although the possible explanation of the former is the presence of oxygen dependent/sensitive enzymes. *C. jejuni* is equipped with various enzymes facilitating oxygen-independent respiration with alternative electron acceptors to oxygen but no growth can be observed under strictly anaerobic conditions (Veron *et al*., 1981). The possible explanation of this phenomenon is the requirement of low amounts of oxygen for the deoxynucleotides synthesis which is catalyzed by the

oxygen-sensitive class I ribonucleotide reductase (NrdAB-type RNR; Sellars *et al*., 2002).

C. jejuni encodes for several oxygen sensitive enzymes, which might be part of the reason for the microaerobic requirement. The oxygen-labile, iron-sulphur (Fe-S)-containing metabolic enzymes Por and Oor in the TCA cycle are sensitive to molecular oxygen. Although they are partially protected by the hemerythrin proteins HerA (Cj0241c) and HerB (Cj1224), no sufficient mechanisms are found to repair Por and Oor once damaged through exposure to atmospheric oxygen concentrations (Hughes *et al*., 1998; Kendall *et al*., 2014). The L-serine dehydratases SdaA in most aerobes are pyridoxal 5' phosphate (PLP)-dependent, but instead of binding to PLP, the SdaA homologue in *C. jejuni* contains an oxygen labile Fe-S cluster, similar to enzymes mostly found in anaerobes (Velayudhan *et al*., 2004). Another example of oxygen sensitive enzymes is rubredoxin oxidoreductase/rubrerythrin (Rbo/Rbr)-like Rrc protein (Cj0012c). It has been shown that reactive oxygen species (ROS) and aerobic stress severely affect the enzyme activity (Yamasaki *et al*., 2004).

However, *C. jejuni* is adapted to this unfavourable circumstance during the process of colonisation in the host. This pathogen is in preference colonising the mucus layer and the intestinal crypt close to the epithelium (Beery *et al*., 1988; Lee *et al*., 1986) where the oxygen tension is higher than in the intestinal lumen. Also, the preferred colonisation site of *C. jejuni* is between the mid small intestine and the mid colon, which holds higher oxygen tensions than the distal colon and rectum (He *et al*., 1999).

The facile explanation for the molecular basis of the microaerophily is a deficiency of oxidative stress defences. Non-specific electron transfer from the respiratory chain to oxygen occurs in most of oxygen-dependent bacteria (Cabiscol *et al*., 2000). The stepwise one-electron reduction of O_2 results in the formation of the reactive oxygen species (ROS) such as superoxide radical (O_2^-), hydrogen peroxide (H_2O_2) and hydroxyl radical ($HO^\cdot$), which are also arising from the host immune system in response to bacterial infection; their cellular targets including DNA, proteins and membranes. Basically, this hypothesis is unlikely in *C. jejuni* due to the harboring of a variety of ROS-detoxifying enzymes including the superoxide dismutase SodB (Cj0169; Pesci *et al*., 1994), the alkyl hydroxide reductase AhpC (Cj0334; Baillon *et al*., 1999), the catalase KatA (Cj1385; Day *et al*., 2000), the thiol peroxidases Tpx (Cj0779; Atack *et*

al., 2008), the bacterioferritin comigratory protein Bcp (Cj0271; Atack *et al*., 2008), the cytochrome *c* peroxidases (Cj0020c and Cj0358; Parkhill *et al*., 2000), and the methionine sulfoxide reductases MsrA and MsrB (Cj0637 and Cj1112; Atack and Kelly, 2009). However, the regulation of oxidative stress response in *C. jejuni* is still poorly understood but PerR (Cj0322) is thought to be involved in it (Palyada *et al*., 2009).

1.6.3 Capnophily

Like oxygen, carbon dioxide is also essential for the proliferation of *C. jejuni*. The ideal atmospheric level of carbon dioxide (CO_2) for the growth of *C. jejuni* is 5 – 10 % (v/v). Although the reasons for this are unclear, CO_2 requiring enzymes including those involved in anaplerotic CO_2 fixation like phosphoenolpyruvate (PEP) carboxykinase and pyruvate carboxylase (Kelly, 2001; Velayudhan and Kelly, 2002) may be important. The multi-subunit acetyl-CoA carboxylase in *H. pylori* shows a low affinity for CO_2 but it is essential for fatty acid biosynthesis. This might be a major reason to explain the necessity of carbon dioxide for this organism (Burns *et al*., 1995; Hughes *et al*., 1995). Still the presence of carbonic anhydrases which regulate the balance of CO_2/bicarbonate is also considered as a contributor to the capnophilic phenotype (Kelly, 2001). This emzyme is the IcfA homologue, which is encoded by *cj0237*/*cynT* according to the genomic information of *C. jejuni* (Parkhill *et al*., 2000)

1.7 Electron transport chains

1.7.1 Overview

C. jejuni is considered as a non-fermentative bacterium and its energetic requirement must be fulfilled by oxidative phosphorylation, which is achieved by the electron transport system in the cell. A complicated electron transport system allows energy conservation and supports bacteria to grow under a wide range of environmental niches. The metabolic flexibility of bacteria is determined by the composition and the degree of branching of the electron transport chain (ETC), which consists of diverse electron donors and acceptors that allow the cell to survive under different conditions including the human intestine, which is considered as the most competitive environment for *C. jejuni* growth.

A typical electron transport chain is comprised of four parts: dehydrogenases for electron donors like the intermediate products of central metabolism or natural compounds in the environment; the membrane soluble quinone pool which is able to carry electrons in the form of hydrogen atoms; the electron transfer enzymes which mediate the main flow of electrons and a terminal oxidase under the aerobic condition or terminal reductases in the oxygen-limited environment. The crucial properties of electron transport chains are (i) the degree of branching at both dehydrogenase and reductase ends of the chain which determines the diversity of substrate utilisation and provides the growth advantage of bacteria; (ii) given due consideration of applicable positive midpoint redox potentials (E_{M7}), the competence of cells to utilize alternative electron acceptors to molecular oxygen; (iii) the presence of a variety of types of cytochromes as additional electron carriers and often more than one type of quinone; (iv) the proper interaction between electron pathways, the efficiency of electron transfer will be maximized if every reductant is able to be paired with a range of oxidants; and (v) the optimum degree of proton translocation and energy transduction which is contributed by each electron transport chain.

The complicated respiratory chain of *C. jejuni* was identified in early detailed studies on the physiology of *Campylobacters* (Carlone and Lascelles, 1982; Hoffman and Goodman, 1982) with the presence of abundant cytochromes. The details of ETC could be depicted more precisely after the revelation of the genome sequences of *C. jejuni* (Parkhill *et al*., 2000) and its highly branched and complex ETC is uncommon since the genome size (1.6 to 1.9 Mb) is smaller than that of other enteropathogenic bacteria like *E. coli* (4.6 Mb; Blattner *et al*., 1997) and *Salmonella typhimurium* (4.8 Mb; McClelland *et al*., 2001). In the strain NCTC 11168, the major predicted electron transport pathways which were deduced by genomic information and biochemical evidence is shown in figure 1.5. Electrons are fed into the menaquinone pool from a variety of organic/inorganic electron donors catalyzed by corresponding dehydrogenases. The most efficient energy conservation occurs under aerobic conditions, the electrons in the menaquinone pool will be further transferred to either the electrogenic quinol oxidase CioAB (Jackson *et al*., 2007) directly or the terminal *cb*-oxidase via the route of the proton-translocating cytochrome bc_1 complex and periplasmic *c*-type cytochromes. However, the oxygen-limited or even strict anaerobic conditions like the host gut might occur in the life cycle of *C. jejuni* and a variety of alternative electron acceptors have been identified, which still allow the growth and

energy conservation. In short, the complexity of *C. jejuni* ETC is currently underestimated because some cytochromes and redox proteins are still uncharacterised.

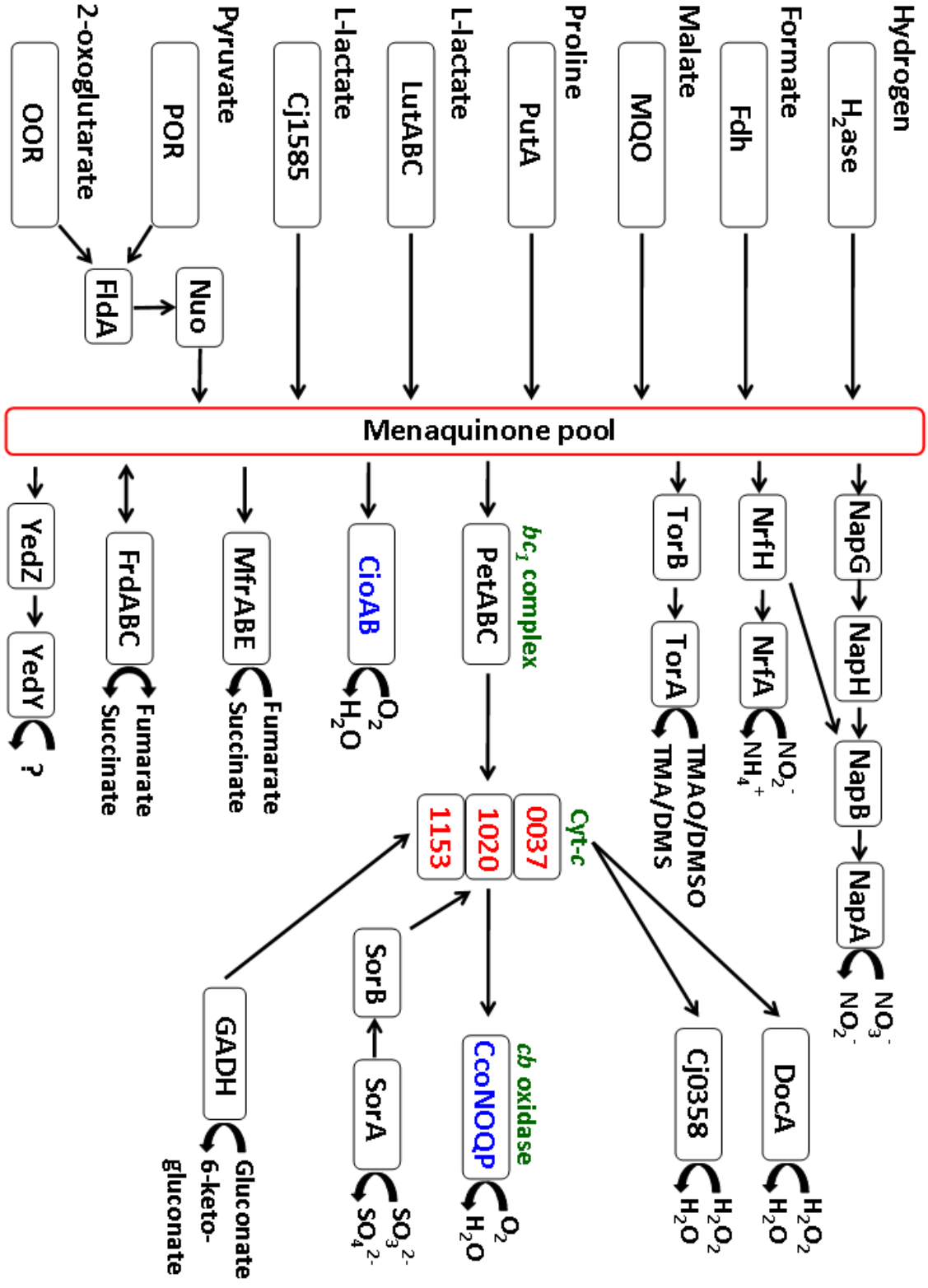

Figure 1.5 Major electron transport pathways in *Campylobacter jejuni*. A variety of electron donors, including molecular hydrogen, organic acids and amino acids, are catalysed by a series of dehydrogenases, which transfer electrons to menaquinone pool in the lipid bilayer of the inner membrane. Under microaerobic conditions, menaquinone will further reduce the cytochrome *bc1* complex which in turns reduces periplasmic *c*-type cytochrome(s). Cytochrome *c* is reoxidised by one of the terminal oxidases, the high affinity *cb* type cytochrome *c* oxidase (blue). The cyanide-resistant, low affinity CioAB-type menaquinol oxidase is also present. Cytochrome *c* may also be reoxidised by hydrogen peroxide in the periplasm through the activity of two separate CCPs. Besides, electrons can also be fed directly into *c*-type cytochromes, bypassing the menaquinone pool. Under oxygen-limited or extremely anaerobic conditions, several alternative electron acceptors to oxygen can terminate respiration. The individual components of the *C. jejuni* electron transport chains will be further discussed in the text. Terminal oxidases are shown in blue and possible *c*-type cytochromes are shown in red.

1.7.2 Electron donors

1.7.2.1 Hydrogen and formate

Hydrogen and formate may be key energy sources *in vivo*. *C. jejuni* shows high respiratory activity with gaseous hydrogen which is an excellent electron donor. The hydrogenase activity has been proved with the membrane fraction of *C. jejuni*. (Carlone and Lascelles, 1982; Hoffman and Goodman, 1982). Due to the catabolic activity of the host gut microbiota, some by-products produced by obligate anaerobes are important energy sources for metabolic cross-feeding of *C. jejuni* and the molecular hydrogen in the intestine might be caused by the redox reactions during the fermentative process. The gaseous hydrogen has been shown in the mouse stomach at concentrations much higher than the K_m of the hydrogenase (Olson and Maier, 2002). The *C. jejuni* genome encodes the membrane-bound NiFe-type hydrogenase HydABCD (Cj1267c – Cj1264c) (Parkhill *et al*., 2000; Weerakoon *et al*., 2009), which faces the periplasm (Hoffman and Goodman, 1982). It is proposed to be translocated across the cytoplasmic membrane via the TAT (twin-arginine translocation) system because the HydA (Cj1267c) protein, a small subunit containing the Fe-S cluster, carries the TAT signal peptide at the amino-terminus. The NiFe active site containing large subunit is encoded by *hydB* (*cj1266c*). HydC (Cj1265c) is a *b*-type cytochrome which is anchored on the cytoplasmic membrane and HydD (Cj1264c) is a protease involved in enzyme

maturation (Vignais *et al*., 2001). The pleiotropic accessory factors encoded by the *hypFBCDEA* operon (*cj0622 – cj0627*) are necessary for the assembling of the enzyme complex and the insertion of the nickel cofactor, which are essential for the hydrogenase activity. Also, the acquisition of nickel ion as a cofactor via an ABC transporter system (Cj1584c – Cj1580c) of *C. jejuni* NCTC 11168 has been identified recently. This uptake system showed high-affinity to nickel ion and is named NikZYXWV (Howlett *et al*., 2012). The inactivation of periplasmic binding protein *nikZ* (*cj1584c*) under low nickel concentrations would result in a decreasing hydrogenase activity in the mutant strain, indicates an important role of the Nik-transport system in the nickel ion acquisition. However, the hydrogenase activity of the *nikZ* mutant was restored at high nickel concentrations, suggests the presence of additional nickel transporters (Howlett *et al*., 2012). The nickel chaperone SlyD is crucial for the hydrogenase activity in *E. coli*; however the nickel uptake capacity and the hydrogenase activity are not altered in the mutant of *cj0115* which is the s*lyD* orthologue gene in *C. jejuni* NCTC 11168 (Howlett *et al*., 2012).

In addition to hydrogen, formate is another important energy source in *C. jejuni*, which is generated mainly by the mixed-acid fermentation of the intestinal microbiota and sensed as a chemoattractant through the Tlp7 chemoreceptor (Tareen *et al*., 2010; Vegge *et al*., 2009). The formate/bicarbonate couple has a highly negative redox potential (E_{M7} = -420 mV), which makes formate an excellent electron donor and oxidized by the formate dehydrogenase in *C. jejuni.* Previous respiration study of *C. jejuni* membrane vesicles revealed the respiratory activities with formate or hydrogen as substrates were 50 - 100 times greater than the rates achieved with lactate, malate, succinate and NADH (Hoffman and Goodman, 1982; Myers and Kelly, 2005). The formate dehydrogenase (Fdh) in *C. jejuni* is membrane bound, periplasmic facing, and comprised of the selenocysteine and pterin cofactor containing large subunit FdhA (Cj1511c), the Fe-S subunit FdhB (Cj1510c), the formate dehydrogenase cytochrome-*b* subunit FdhC (Cj1509c) and FdhD (Cj1508c), a protein of unknown function required for Fdh activity (Berg *et al*., 1991). The structure of *C. jejuni* FdhABCD is similar to the Fdh-N and Fdh-O enzymes in *E. coli* and the transportation of Fdh relies on the TAT system due to the signal peptide found at the N-terminus of FdhA. Recent studies indicate that the Fdh activity of *C. jejuni* is controlled by FdhT (Cj1500), FdhU (Cj1501) and a high-affinity TupABC-like tungstate transporter (Cj1538 – Cj1540), suggests that

tungsten might be incorporated into the Fdh complex (Pryjma *et al*., 2012; Shaw *et al*., 2012; Smart *et al*., 2009).

Hydrogen and formate produced by the fermentation in the host gut are the abundant source of electrons for *C. jejuni in vivo*. The result of colonisation test in chicks showed that either Hyd or Fdh mutant only caused a modest decreasing but the colonisation was severely abolished by feeding a double mutant. (Weerakoon *et al*., 2009). Furthermore, due to a less redundant ETC and the absence of Fdh, the mutant of Hyd in the closely related *H. pylori* was unable to colonise in the mouse model of infection (Olson and Maier, 2002). Taken together, this information suggests the absence of Hyd or Fdh is able to be complemented by the other in the single mutant of *C. jejuni*, indicating the importance of both hydrogen and formate as energy source like electron donors in the chick caecum (Weerakoon *et al*., 2009).

1.7.2.2 NAD(P)H

Reduced nicotinamide adenine dinucleotide (NADH) and flavin adenine dinucleotide (FADH) are the major electron sources for the ETC of many bacteria. The negative redox potential (E_{M7} = -340mV) of NADH/NAD couple makes NADH the major electron donor for oxidative phosphorylation which is driven by a proton gradient generated through the proton-translocating NADH:quinone oxidoreductase (Nuo or NDH-1) complex (Haddock and Jones, 1977). However, unlike FADH in *C. jejuni*, NADH is a poor respiratory electron donor which showed 50 fold lower respiration rate compared to hydrogen/formate respiration (Hoffman and Goodman, 1982) and Mdh is the only NADH generating enzyme in the TCA cycle since both pyruvate dehydrogenase and oxoglutarate dehydrogenases are absent. The Nuo complex is an intrinsic membrane protein which is composed of 14 subunits, (Friedrich, 1998; Friedrich *et al*., 1998) but *nuoE* and *nuoF* subunits which are essential for the function of NADH dehydrogenase are absent in the *nuo* gene cluster (*cj1566c – cj1579c*; Parkhill *et al*., 2000) and replaced by the genes *cj1575c* and *cj1574c*, which lack an obvious NAD(P)H-binding motif in *C. jejuni* NCTC 11168 (Smith *et al*., 2000; Parkhill *et al*., 2000). It has been shown that Cj1574c might associate with Cj1575c and mediates the electron transfer from the reduced, flavin mononucleotide containing flavodoxin FldA to the Nuo complex (Weerakoon and Olson, 2008). Consequently, the Nuo complex of *C. jejuni* and *H. pylori* (which has a similar unusual *nuo* operon) seems to participate

rather in the oxidation of flavodoxin than of NADH. It was hypothesised that flavodoxin/ferredoxin reduced by Por/Oor complexes in the TCA cycle might act as the donor substrate; and the reduced FldA is generated by the oxidation of 2-oxoglutarate to succinyl-CoA catalyzed by the Oor but the putative ferredoxin FdxA (Cj0333c) and Cj0369c are not electron acceptors for Oor. Mutagenesis of the *nuo* operon also demonstrates its importance: mutation of any of the 12 *nuo* genes results in a growth defect in the absence of any alternative respiratory substrate, which suggests the Nuo complex is the major point of entry for electrons into the respiratory chain. Moreover, Cj1574c is essential for the re-oxidation of flavodoxin, which can continuously accept electrons from Por/Oor (Weerakoon and Olson, 2008) and it is also crucial in the colonisation of chicks. The polar effect on *cj1574c* generated by the mutation of *nuo* complex leads to a reduce ability for colonisation of *C. jejuni* NCTC 11168 (Weerakoon *et al*., 2009).

1.7.2.3 Lactate

Lactate dehydrogenase activity in oxygen-linked respiration of *C. jejuni* was demonstrated some years ago (Hoffman and Goodman, 1982). Recent studies have elucidated the role of the L-iLDHs which is the membrane-associated NAD-independent respiratory enzyme, mediating the oxidation of lactate to pyruvate in *C. jejuni*. The L-iLDH is a three-subunit non-flavin Fe-S cluster containing enzyme and is comprised of *cj0075c*, *cj0074c* and *cj0073c* in *C. jejuni* NCTC 11168, although inactivation of any of these genes did not abolish the growth of respective mutants (Thomas *et al*., 2011). However, a second L-iLDH is a FAD and Fe-S containing oxidoreductase Cj1585c which is responsible for the observed redundancy in the respiration of L-lactate. In *C. jejuni* NCTC 11168, the *cj0075c* and *cj1585c* double mutant strain shows a poor growth with 20 mM L-lactate as a carbon source but the utilization of D-lactate is not affected (Thomas *et al*., 2011). The gene locus of *cj1585c* is not conserved in *C. jejuni* and is replaced by a gene cluster *dmsABC*, which encodes a DMSO reductase in strains such as 81-176, 81116, M1 or 327 (Hofreuter *et al*., 2006; Pearson *et al*., 2007; Friis *et al*., 2010; Takamiya *et al*., 2011). Moreover, in the wild-type strain 81116 lacking the L-iLDH Cj1585c naturally, a mutant in the *cj0075c* homologue was unable to grow with L-lactate. The mechanism of utilizing D-lactate is still unclear but important in *C. jejuni* since both L- and D-lactate have highly negative redox potential coupled with pyruvate (E_{M7} = -190 mV), which indicates they are good

electron donors. *C. jejuni* might be benefit from the cross-feeding of lactate, which is produced by the microbiota in the mammalian or avian gut and therefore likely to be important carbon sources for *in vivo* growth (Thomas *et al*., 2011).

1.7.2.4 Malate

Previous studies revealed that malate could stimulate respiration in *C. jejuni* and produced a H^+/O ratio of 2.0 (Hoffman and Goodman, 1982). Malate is also considered as a good electron donor to the quinone pool as its negative redox potential coupled with oxaloacetate (E_{M7} = -166 mV). Two possible enzymes responsible for malate catabolism are the NAD-independent, flavoprotein-type malate:quinone oxidoreductase (Mqo; Cj0393) and the NAD-linked malate dehydrogenase (Mdh; Cj0532). The former shows 49.3% similarity to the related malate:quinone oxidoreductase in *H. pylori* and Mqo is also a FAD-dependent, membrane-bound and cytoplasmic-facing enzyme, which permits malate to act as a direct electron donor to the quinone pool (Kather *et al*., 2000).

1.7.2.5 Succinate

The TCA cycle intermediate succinate is not only a carbon source for *C. jejuni* but serves also as an electron donor. Therefore succinate is oxidised to fumarate by succinate dehydrogenase (Sdh) accompanied with the formation of $FADH_2$ and the following electron transfer to the menaquinone pool. The respiration of succinate has been elucidated in *C. jejuni* with a H^+/O ratio of 2.01 (Hoffman and Goodman, 1982) and a membrane-bound succinate dehydrogenase (succinate:quinone oxidoreductases) SdhABC (Cj0437 – Cj0439) comprised of three subunits including flavoprotein (Cj0437), Fe-S subunit (Cj0438) and cysteine rich SdhE homologue (Cj0439) was originally identified from the genome sequence. However, the SdhABC complex was incorrectly annotated and is not involved in the conversion of succinate to fumarate (Parkhill *et al*., 2000; Weingarten *et al*., 2009). It is actually a novel type of methylmenaquinol:fumarate reductase (Mfr) which is a periplasmic enzyme and able to convert fumarate to succinate in a unidirectional manner(Guccione *et al*., 2010; Hitchcock *et al*., 2010). Also, another putative fumarate reductase FrdABC complex was also found and comprised of a membrane-associated diheme cytochrome *b* containing subunit FrdC (Cj0408), the flavoprotein FrdA (Cj0409) and the Fe-S protein FrdB (Cj0410). FrdABC has been shown to be bi-directional and has properties of a

succinate:quinone reductase (Fig. 1.5) and it is the only enzyme accounting for the oxidation of succinate to fumarate in *C. jejuni* to date (Guccione *et al*., 2010).

1.7.2.6 Sulphite

The inorganic anion sulphite is usually utilized by free-living chemolithotrophic sulphur-oxidizing bacteria but it is found as an excellent electron donor in *C. jejuni* due to the highly negative redox potential (E_{M7} of the sulphite/sulphate = -454 mV) and the better stability in the low-oxygen atmosphere. *C. jejuni* has respiratory capacity using sulphite and metabisulphite with oxygen as the terminal electron acceptor (Myers and Kelly, 2005). The sulphite:cytochrome *c* oxidoreductase (Sor) is a periplasmic enzyme which is composed of two-subunits: SorA (Cj0005c), a molybdopterin oxidoreductase with a TAT signal peptide at the N-terminus and SorB (Cj0004c), a monohaem cytochrome c_{552}. The Sor system in *C. jejuni* which is similar to that in *Starkeya novella* is conserved and can be also found in *C. lari* but not in any other examined *Campylobacter* and *Helicobacter* species. Inhibitor studies show electrons derived from sulphite enter the respiratory chain after the bc_1 complex and will be transferred directly to cytochrome *c*, which is then oxidised by the high affinity *cb*-type terminal oxidase (Myers and Kelly, 2005), indicating the capability of respiring sulphite in the low oxygen environments such as the human gut and soil. Sulphite (or metabisulphite) has an inhibitory effect on the growth of several microorganisms like *H. pylori* (Jiang and Doyle, 2000). Therefore, the sulphite respiration system in *C. jejuni* may confer a detoxification mechanism and offer a surviving niche to this enteropathogenic bacterium. Also, a recent study showed the mutation of *cj0005c* in *C. jejuni* leads to a diminished adherence and invasion of host cells cultured *in vitro* (Tareen *et al*., 2011).

1.7.2.7 Gluconate

Due to the absence of the oxidative pentose phosphate pathway and Entner-Doudoroff pathway, *C. jejuni* is unable to catabolise glucose or the oxidised form gluconate. However, gluconate can be utilised by *C. jejuni* as electron donor for respiration through a temperature-regulated flavin-containing gluconate dehydrogenase (GADH) which is encoded by the two-gene operon *cj0414* and *cj0415* (Pajaniappan *et al*., 2008). GADH is linked to the electron transport chain by a co-transcribed cytochrome in most bacteria but this is not observed in *C. jejuni*, moreover, inhibitor studies showed that electrons derived from gluconate are predicted to enter the electron transport chain in *C.*

jejuni via periplasmic cytochromes *c*, suggesting GADH might locate in the periplasm peripherally associated with the cytoplasmic membrane (Pajaniappan *et al*., 2008; Kelly, 2008). Transcriptional and proteomic analysis showed that the upregulation of *cj0414* and *cj0415* and the elevated expression of GADH in *C. jejuni* upon a temperature shift from 37^{o}C to 42^{o}C correlated with the higher GADH activity and gluconate-dependent oxygen consumption rate (Pajaniappan *et al*., 2008). This observation might explain that GADH is necessary for high-level colonisation of chicks but not for mice, reflecting the different temperatures of the caecal environments of the two hosts (Pajaniappan *et al*., 2008). Since the TAT signal motif was found at the N-terminus of Cj0414, GADH in *C. jejuni* is predicted to be translocated across the cytoplasmic membrane by the TAT system.

1.7.2.8 Proline

Proline is generally considered as a carbon source supporting the growth of *C. jejuni* (Guccione *et al*., 2008; Hofreuter *et al*., 2008) and is also predicted to act as electron donor during its catabolism. The uptake of proline in *C. jejuni* is facilitated by the putative proline transporter PutP (Cj1502) and proline will be further oxidised by the predicted bifunctional proline dehydrogenase PutA (Cj1503) which converts proline to glutamate in a two-step reaction (via the intermediate delta-1-pyrroline-5-carboxylate) (Stahl *et al.*, 2012); and the electrons produced in this reaction could feed into the quinone pool directly (Kelly, 2008).

1.7.3 The quinone pool

Unlike the utilisation of higher potential ubiquinone (E_{M7} = +110 mV) in aerobic respiration of *E. coli*, *Campylobacter* species contain menaquinone (E_{M7} = -75 mV) as the sole respiratory quinone, which are able to transfer electrons from electron donors to (i) the cytochrome bc_1 complex, (ii) alternative electron acceptors, and (iii) the cyanide-resistant quinone oxidase CioAB (Fig. 1.5) (Ingledew and Poole, 1984; Carlone and Anet, 1983; Collins *et al*., 1984; Jackson *et al*., 2007). Two types of menaquinones with six isoprene units were found in *C. jejuni*: MK-6 and a methyl-substituted MK-6 of which the latter has not been reported in *H. pylori*. The highest level of menaquinone was found at the optimum growth concentrations of oxygen of 5 to 10 % (v/v) and the oxygen levels between 2 – 15 % (v/v) did not alter the quinone type in *C. jejuini*. (Carlone and Anet, 1983; Collins *et al*., 1984).

1.7.4 The cytochrome bc_1 complex

The membrane-bound cytochrome bc_1 complex is comprised of three subunits and four redox centres, and is responsible for receiving electrons from the low potential menaquinone and transferring them to cytochrome *c*, accompanied with a proton gradient across the cytoplasmic membrane (Trumpower, 1990; Thöny-Meyer, 1997; Myers and Kelly, 2005). The bc_1 complex is widely distributed among prokaryotic and eukaryotic organisms containing ubiquinone, including aerobic, anaerobic and photosynthetic bacteria and in mitochondria of lower and higher eukaryotes although it is not found in *E. coli* (Ingeldew and Poole, 1984). The cytochrome *b* and cytochrome *c* redox centres of the bc_1 complex in *C. jejuni* have been detected in early work (Carlone and Lascelles, 1982) and the genomic sequences in *C. jejuni* (*cj1184c – cj1186c*) referred that the *petB* (*Cj1185c*) gene encodes the cytochrome *b* subunit containing a pair of non-covalently bound *b*-type heams; PetC (Cj1184c) is the cytochrome c_1 subunit with its covalently attached *c*-type haem; and PetA (Cj1186c) is a Rieske protein which has the 2Fe-2S cluster and the N-terminal TAT-dependent signal peptide (Parkhill *et al*., 2000; Smith *et al*., 2000). The operation of this complex has been shown by the genome sequence information and respiratory inhibitor studies in *H. pylori* (Alderson *et al*, 1997; Chen *et al*., 1999)

1.7.5 *c*-type cytochromes

1.7.5.1 General biochemistry

Cytochrome *c* is abundant in the *C. jejuni* cell and covalently binds the haem group, which allows the pink appearance of cells. The *c*-type cytochrome catalyses various redox reactions (Bertini and Rosato; 2006) and also plays a major role in electron transfer from the bc_1 complex to the terminal *cb*-type oxidase in *C. jejuni* (Kelly, 2008). Also, *c*-type cytochromes are predicted to directly mediate the electron flux from the periplasmic dehydrogenases for electron donors like sulphite and gluconate to the terminal oxidase (Myers and Kelly, 2005; Kelly, 2008). Two types of cytochrome *c* are found among most of prokaryotic and eukaryotic organisms: the water soluble protein which is present in the periplasm of Gram-negative bacteria or in the thylakoid lumen of some chloroplasts and membrane-anchored proteins which link with the membrane via an N-terminal hydrophobic extension (Thony-Meyer, 1997) and the latter are often tightly associated with a redox centre of the oxidase/reductase, such as in the case of the

cytochrome bc_1 complex. The formation of *c*-type cytochromes requires the formation of two thioester bonds between the two cysteine sulphurs in a -CXXCH- motif (called haem attachment motif; where 'X' in the motif is any residue) in the protein and the vinyl group of haem. The histidyl usually serves as the fifth (proximal) axial ligand to the haem iron in the assembled cytochrome *c* (Thony-Meyer, 1997). The transportation of soluble periplasmic cytochrome *c* in Gram-negative bacteria depends on the Sec translocation system which is able to recognize the signal motif at the N-terminus of the apocytochrome polypeptide (Thony-Meyer and Kunzler, 1997).

A previous study revealed the presence of a soluble *c*-type cytochrome in *H. pylori*, which in the cell free extracts were able to be reduced by ascorbic acid and a low molecular mass cytochrome *c* was assumed to be responsible for this phenomenon (Ødum and Anderson, 1995). It was then confirmed by spectroscopic studies and characterized spectroscopically as cytochrome c_{553} (Marcelli *et al*., 1996; Nagata *et al*., 1996; Evans and Evans, 1997; Koyanagi *et al*., 2000), which has been identified as a potential electron donor to the *cb*-type cytochrome *c* oxidase and the redox potential is +170 mV (E_{M7}) (Koyanagi *et al*., 2000). In *C. jejuni*, the putative mono-haem cytochrome *c* Cj1153 has been identified as the most likely candidate for bridging the electron flux from the bc_1 complex to the terminal oxidase with the 34.6% identity to the cytochrome C_{553} of *Desulfovibrio vulgaris* (Parkhill *et al*., 2000).

1.7.5.2 The biogenesis of *c*-type cytochromes

The biosynthesis of *c*-type cytochromes is complicated and three essential steps are required in all types of cells: (i) the translocation of apocytochrome polypeptide and haem *b* across at least one membrane lipid bilayer, (ii) the periplasmic reduction of cysteine residues in the haem *c* attachment motif of the apocytochrome, and (iii) the stereospecific covalent bonds forming between haem *b* to the sulphur atoms of the two cysteine residues in the -CXXCH- motif in the polypeptide by a membrane-associated machinery. A previous study showed that it was possible to synthesise cytochrome *c in vitro* by incubating apocytochrome with ferrous ions and the formation of *b*-type cytochrome was observed first followed by the formation of the thioester bonds to give the *c*-type products (Daltrop *et al*., 2002). This indicates that the formation of the cytochrome *c* thioester bonds requires reducing conditions; otherwise, a disulfide bond is readily formed between neighboring cysteine residues in polypeptides and the ferrous

ions are also further oxidised, especially under an oxidizing environment such as on the outer side of the cytoplasmic membrane. Furthermore, an intriguing phenomenon was observed in all known biogenesis systems, that is the same stereochemistry and orientation of haem attachment to the protein. The N-terminal and C-terminal cysteines are always associated to the 2-vinyl and 4- vinyl groups of haem, respectively (see Fig. 1.6) (Barker and Ferguson, 1999; Stevens *et al*., 2004). In order to overcome these issues, a post-translational modification system for forming these bonds is a necessity for most organisms. At present, there are at least five cytochrome *c* biogenesis systems (System I to V) discovered and the System I and II are prevalent among most of Gram-positive and -negative bacteria. The System I is also called Ccm system (cytochrome *c* maturation), which was discovered in *E. coli* and also found in plant mitochondria (Thöny-Meyer *et al*., 1994); and the System II (Ccs; cytochrome *c* synthase module) was first revealed in *Chlamydomonas reinhardtii* (Howe and Merchant, 1992) and is also employed by ε-proteobacteria, including *C. jejuni* (Parkhill *et al*., 2000; Kranz *et al*., 2009). The details of both systems will be further discussed in the following section.

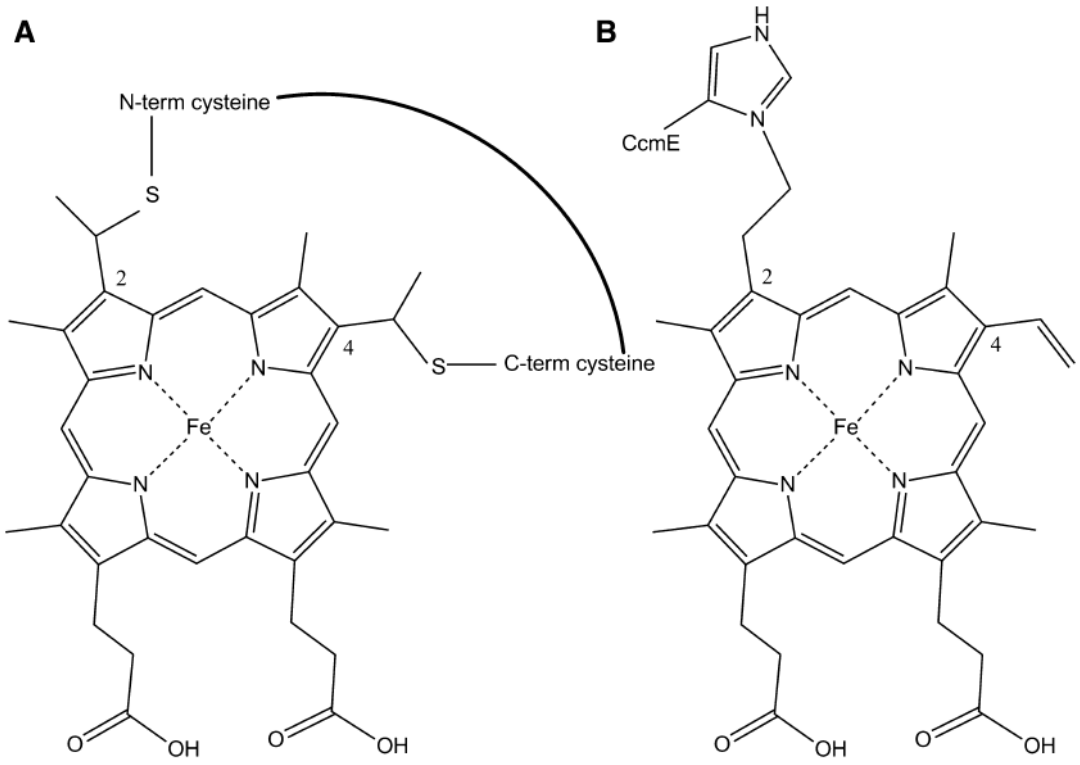

Figure 1.6 The thioester bond forming between a haem molecule and cysteine residues or CcmE protein. (A) Haem attachment to cytochrome *c* indicating the thioester bonds formed at the 2-vinyl and 4-vinyl haem positions to the two cysteine residues on the apocytochrome polypeptide. The N' and C' orientations of two cysteines are shown. (B) Haem attachment to the histidine side chain of CcmE (Lee *et al*., 2005). Figure adapted from Stevens *et al*., 2011.

1.7.5.2.1 Cytochrome *c* biogenesis System I (Ccm system)

The Ccm system was found in plant mitochondria, archea and many Gram-negative bacteria. According to the findings in *E. coli* and *Rhodobacter capsulatus*, the Ccm system is composed of eight cytochrome *c* maturation proteins (CcmABCDEFGH) which are expressed from a single operon and it is the most complex of the known cytochrome *c* biogenesis system to date. In addition, two proteins DsbD and DsbA are also involved in the maturation of cytochrome *c*, in which the former plays a reducing role which transfers reductant from cytoplasmic thioredoxin across the membrane via a thiol:disulphide cascade and assists disulphide bond formation between two cysteines within a -CXXCH- motif in the oxidizing environment of the periplasm (Daltrop *et al*., 2002; de Vitry, 2011). DsbA is a powerful periplasmic oxidase, which causes oxidation of the apocytochrome cysteine and incorporates disulphides into extracytoplasmic proteins (Shouldice *et al*., 2011). CcmG is a periplasmic thioredoxin that is reduced by DsbD and two possible candidates will further receive reductant from CcmG as shown in Fig. 1.8. The redox-active pair of cysteine in CcmG might directly interact with the -CXXCH- motif of the apocytochrome and the synthesis will be abolished in the *ccmG* mutant, which is unable to be reversed by an exogenous reductant or by the removal of the strongly oxidizing protein DsbA. Alternatively, the cysteines in the -CXXC- motif of CcmH are possible redox partners of the apocytochrome *c* and the reduction of CcmG requires a functional CcmH (N-CcmH), suggests that CcmH is the reductant for CcmG (Di Matteo *et al*., 2007; Meyer *et al*., 2005; Reid and Eaves, 2001). CcmH is a fusion protein found in *E. coil* but is expressed separately in other organisms (CcmH and CcmI). The N-terminal of CcmH (N-CcmH) is a membrane-anchored three helix bundle with a conserved pair of cysteines that is considered as a thiol-disulphide oxidoreductase (Di Matteo *et al*., 2007). CcmI is a tetratricopeptide repeat (TPR)-containing protein which has been proposed to interact with the apocytochrome polypeptide and the TPR domain is considered to help the formation of cytochromes. Although CcmI is dispensable for *c*-type cytochromes production in *E. coli* (Fabianek *et al*., 1999; Robertson *et al*., 2008), the same is not true in *R. capsulatus* (Sanders *et al*., 2010).

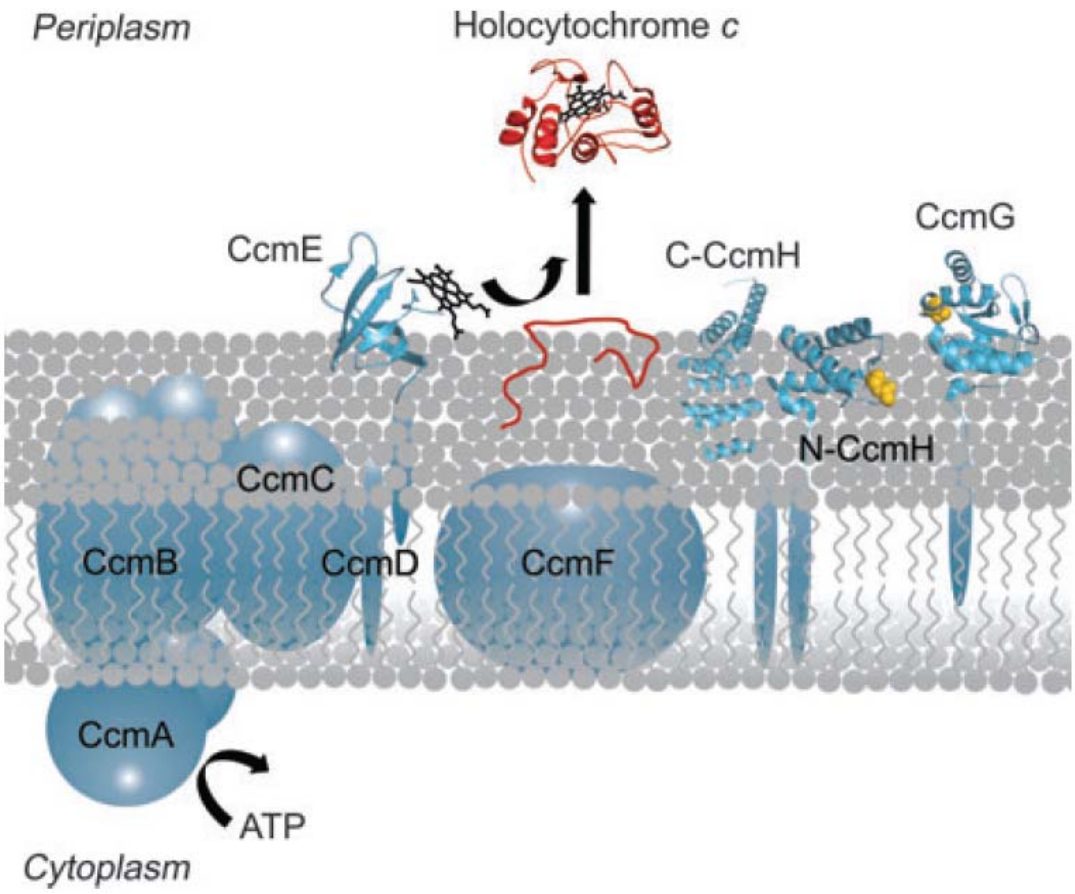

Figure 1.7 The cytochrome *c* maturation System I. The Ccm proteins (in blue) are all integral proteins or are membrane-anchored with soluble domain in the periplasm (with the exception CcmA, which hydrolyses ATP in the cytoplasm). The structures of the soluble domains of CcmE, ccmG and N-terminal domain of CcmH have been solved and are shown on the periplasmic side. The structure of a paralog of the C-terminal domain of CcmH, NrfG, is also shown. The holocytochrome *c* shown is from *Paracoccus denitrificans*. CcmH in *E. coli* is a fusion of two proteins that occur separately in other organisms (CcmH and CcmI, labeled N-CcmH and C-CcmH). The apocytochrome c protein is shown in red, as is the holocytochrome c produced when haem (shown in black) becomes covalently attached. The cysteine residues, assumed to be involved in reducing the -CXXCH- motif in the apocytochrome, are shown in yellow. Figure adapted from Stevens *et al*., 2011.

Haem is synthesized in the bacterial cytoplasm and has to be delivered to CcmE on the other side of the membrane. The complex formed by CcmAB and CcmC is involved in delivering haem across the membrane to CcmE, which is a haem chaperone (Christensen *et al*., 2007; Feissner *et al*., 2006). The CcmA and CcmB proteins are members of the ATP-binding cassette family and were initially postulated to be haem transporters to the periplasm in bacteria. CcmC is able to interact with the haem molecule and mediate the haem attachment to CcmE (Richard-Fogal and Kranz, 2010).

However, the function of haem transferring across the membrane of CcmC is still unclear; especially there is no conserved histidine residue in transmembrane helices (Richard-Fogal and Kranz, 2010). The haem chaperone CcmE shows a unique mode of covalent binding of the haem cofactor. It has a membrane-anchoring N-terminal helix and a globular domain exposed to the periplasm and histidine residues of the latter are able to form covalent bonds with haems (Schulz *et al*., 1998). The histidine residues of CcmE are crucial because the point mutation not only prevents the covalent attachment but blocks the whole *c*-type cytochrome biogenesis pathway. It has been shown that covalently bound haem on CcmE transfers *in vivo* to an apocytochrome *c* (Schulz *et al*., 1998), furthermore, it is noteworthy this transfer will only occur in the presence of the ATPase activity of CcmA (Christensen *et al*., 2007; Feissner *et al*., 2006). CcmD is a small transmembrane protein and it has been shown to interact with CcmC and CcmE (Ahuja and Thöny-Meyer, 2005) and also be required for the release of CcmE with haem bound from a complex including CcmC (Richard-Fogal *et al*., 2008).

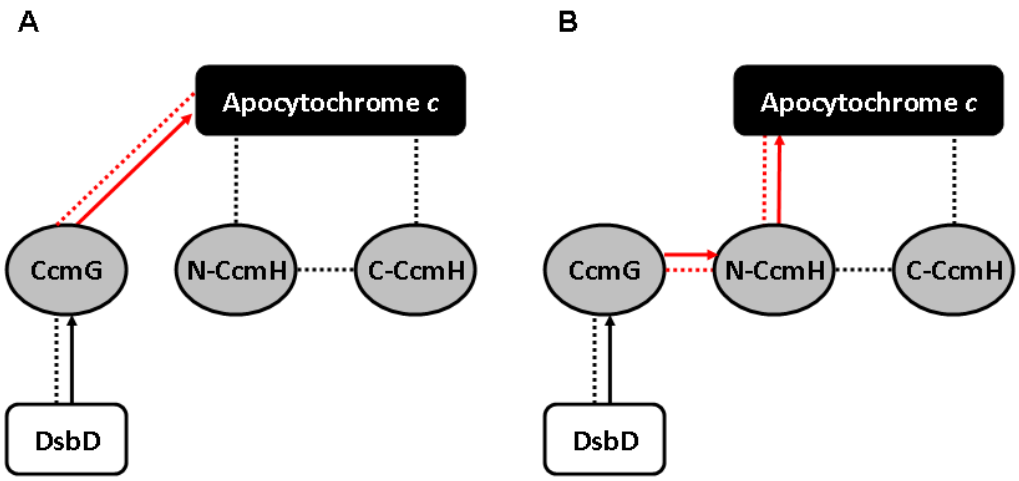

Figure 1.8 Possible interaction networks between CcmG, N-CcmH and the apocytochrome *c*. The arrows indicate possible pathways of reductant transfer and dotted lines specify protein-protein interactions. (A) Direct provision of the reducing power from CcmG to the apocytochrome. N-CcmH and C-ccmH would be involved in interactions with each other and with the apocytochrome *c* to assist haem attachment. (B) In the case of indirect provision of reductant, CcmG would reduce N-CcmH which, in turn, would reduce apocytochrome *c*. Figure revised from Stevens *et al*., 2011.

Basically, the System I recognizes only, or very little more than, the -CXXCH- motif of the apocytochrome. Surprisingly, the polypeptides with a -CXXCH- motif, but of only 12 amino acids can undergo haem attachment by the Ccm system (Braun and Thöny-Meyer, 2004), as well as the occurrence of close spacing of some -CXXCH- motifs in multihaem cytochromes. CcmG and CcmH can interact with CcmF which is the core of attaching haem to cytochromes (Ahuja and Thöny-Meyer, 2003; Ren *et al*., 2002). CcmH has been shown to interact with apocytochrome in a plant system (Meyer *et al*., 2005), suggests CcmH binds the apocytochrome and then bestows it to CcmF for haem attachment, with haem provided by CcmE. As a membrane-anchoring protein, CcmF has many (> 11) transmembrane helices and water-soluble loops facing to the periplasm. Tryptophan are the most conserved residues in the periplasmic loop which are envisaged to be involved in handling haem as it is incorporated into the apocytochrome (Ren *et al*., 2002), also the transmembrane structure suggests a role as a transport protein. The evidence from a recent study shows that a covalent bond is formed between haems and the CcmF protein and the role of CcmF is to supply reductant to maintain the haem attached to CcmE, which is destined to be transferred to an apocytochrome, in the ferrous state (Richard-Fogal *et al*., 2009). However, the interaction between CcmF, CcmE and CcmH is still not clear, also there are clearly many key issues that need to be studied to allow an understanding of this post-translational system.

1.7.5.2.2 Cytochrome *c* biogenesis System II (Ccs system)

In contrast to the System I, fewer proteins are involved in the cytochrome *c* biogenesis System II (Ccs system) which is employed by β-, δ-, and ε-proteobacteria, Gram-positive bacteria, Aquificales and cyanobacteria, as well as by algal and plant chloroplasts. Ccs system is composed of four membrane-bound proteins with at least one transmembrane (TM) segment: CcsA (or ResC) and CcsB (ResB) are the components of the cytochrome *c* synthase, whereas CcdA and CcsX (ResA) are able to generate a reduced haem *c* attachment motif. Some ε-proteobacteria make use of a CcsBA fusion protein (Feissner *et al*., 2006; Goddard *et al*., 2010; Kern *et al*., 2010), which is constituted by a single polypeptide cytochrome *c* synthase. In *B. subtilis*, CcsA and CcsB are called ResC and ResB because they are found in the *resABCDE* cluster (Sun *et al*., 1996). ResDE constitutes a two-component regulatory system with a role in the control of gene expression which is important for synthesis of respiratory enzymes.

Three components, ResA which is the ortholog of CcsX in *Bordetella pertussis*, CcdA and *B. pertussis* DsbD constitute a thiol-disulphide redox module that functions to keep apocytochrome *c* cysteine reduced (Schiött *et al*, 1997; Beckett *et al*., 2000).

In the system II, the apocytochrome polypeptide transported by the Sec pathway, is in the reduced (thiol) state during export across the cytoplasmic membrane. The *B. subtilis* BdbD protein which locates on the outer surface of the cytoplasmic membrane, will efficiently recognise and oxidise thiols in polypeptides, leading to the formation of intra- and intermolecular disulphide bonds (Kouwen and van Dijl, 2009). BdbD is a highly oxidizing thiol-disulphide oxidoreductase and is anchored to the membrane by a single N-terminal TM segment (Crow *et al*., 2009). The catalytic domain of BdbD is functionally analogous to the DsbA protein in the System I and the BdbC, a four TM segment protein homologue to *E. coli* DsbB, keeps BdbD oxidized and reduces menaquinone in the membrane (Kouwen and van Dijl, 2009). The disulphide bond formed by BdbD activity is believed to protect secreted apocytochrome *c* from proteolytic degradation or from being cross-linked to other thiol-containing proteins.

The role of ResA is probably to break disulphide bridges in apocytochrome *c* to allow the ligation of haem *b* (Fig. 1.9), and then ResA in turn is reduced by CcdA that receives its reducing equivalents from thioredoxin in the cytoplasm (Moller and Hederstedt, 2008). In addition to ResA, CcdA is able to reduce other proteins on the outer side of the membrane and serves as a redox hub in the membrane. CcdA is a homologue to the central of *E. coli* DsbD and is composed of six TM segments with one conserved cysteine residue in each of TM1 and TM4 (Porat *et al*., 2004; Schiött *et al*, 1997; Page *et al*., 2004; Deshmukh *et al*., 2000). ResA in *B. subtilis* is presumably reduced by direct interaction with CcdA (Erlendsson *et al*., 2003). The structure of ResA shows redox-dependent conformational changes including the active site helix and affecting a surface cavity proposed to be the binding surface for oxidized apocytochrome *c* (Crow *et al*., 2004; Colbert *et al*., 2006). Also, the substrate-specific recognition enhances the activity of ResA, indicates the binding of oxidized apocytochrome *c* to reduced ResA facilitates the subsequent docking of the histidine residue of the haem *c* attachment motif of ResA in the cavity of reaction (Lewin *et al*., 2008; Hodson *et al*., 2008).

The prototypical System II CCS (cytochrome *c* synthase) is a multifunctional heterodimeric membrane protein complex formed by CcsA and CcsB in an assumed 1: 1 stoichiometry. The CcsBA-type CCSs are found in ε-proteobacteria such as *H. pylori*, *W. succinogenes* and *C. jejuni* (Feissner *et al*., 2006; Kern *et al*., 2010). Bacterial CcsA proteins are composed by from six up to possibly fifteen TM seqments and are evolutionary related to the CcmC and CcmF proteins of System I (Lee *et al*., 2007). The CcsB protein has from four to six TM segments and contains a large extracytoplasmic domain (between TM3 and TM4 in the case of four TM segment proteins, Fig. 1.9). The proposed function of CcsBA is to catalyse: (i) the transportation of reduced haem from the cytoplasm (*n*-side) to the periplasm (*p*-side) of the energized membrane in bacteria; (ii) the recognition one or several different apocytochromes with a reduced haem *c* attachment motif; and (iii) the formation of the thioester bonds between haem and the thiol groups of two cysteine residues in the apocytochrome polypeptide. There are four conserved histidine residues (one in the CcsB and three in the CcsA part of the fusion protein) found to be essential for cytochrome *c* biogenesis and the transient linkage between the haem and these histidine residues will protect the haem molecule from oxidation (Frawley and Kranz, 2009). CcsA contains a conserved and characteristic tryptophan-rich domain, the so-called WWD motif, which is also present in two Ccm system proteins CcmC and CcmF and interacts with haem *b* during cytochrome *c* maturation (Kranz *et al*., 2009; Richard-Fogal *et al*., 2009). The CcsB (ResB) and CcsA (ResC) proteins from *B. subtilis* have both been described as haem-binding proteins and the haem is bound to CcsB via one thioether bond (Ahuja *et al*., 2009). However, the functional significance of this bond remains unclear and the role of CcsB has still to be elucidated.

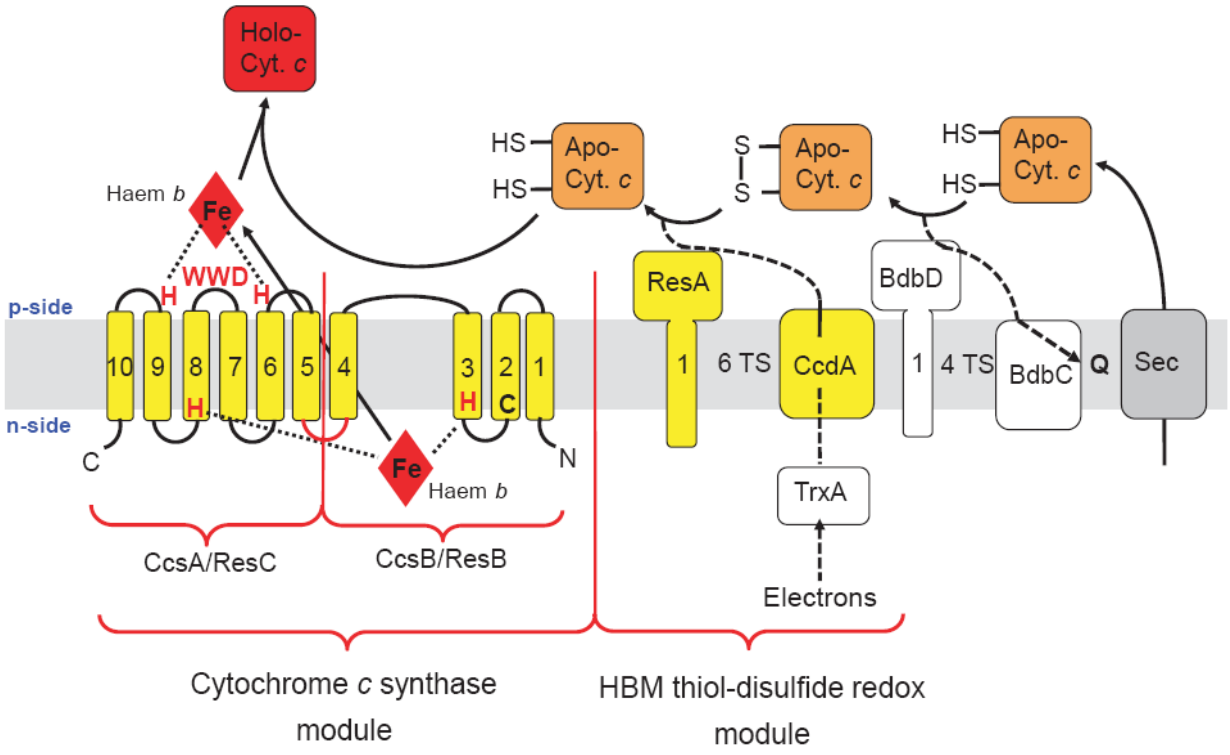

Figure 1.9 The cytochrome *c* biogenesis System II. Left: the CCS module illustrated by the CcsBA fusion protein found in *Helicobacter* spp. and *Wolinella succinogenes*. The fusion part between the CcsA and ccsB proteins is the loop between TM segments 4 and 5 and shown in red. Right: the thiol-disulphide redox module for breaking a disulphide bond between the two cysteine residues of the -CXXCH- motif and protein dithiol oxidation (BdbD and BdbC) enzymes illustrated by the situation in *B. subtilis* membranes. Additional details will be further discussed in the text. C, cysteine residue (in the TM segments 2 of CcsB) found to bind haem covalently in *B. subtilis* CcsB (ResB); H, essential histidine residues in CCS module; HBM, haem attachment motif; Q, quinone; Sec, polypeptide secretion translocation; TrxA, thioredoxin; TS, transmembrane segment; WWD, tryptophan-rich motif. Figure adapted from Kern and Simon, 2011.

Different CCS isozymes might be present in various bacteria. For example, the *W. succinogenes* genome encodes three CcsBA-type proteins designated as CcsA2, CcsA1 and NrfI (Kern *et al*., 2010; Kern and Simon, 2011; Hartshorne *et al*., 2007). NrfI is able to mediate the covalent linkage between the haem molecule and the unique haem *c* binding site, the -CXXCK- motif, of the cytochrome *c* nitrate reductase NrfA. The lysine residue of this motif serves as an unusual proximal haem *c* iron ligand (Einsle *et al*, 1999; Einsle *et al*., 2000). CcsA1 is related in the maturation of the octahaem cytochrome *c* MccA which contains one conserved -$CX_{15}CH$- (15 any residues between

two separated cysteine) and seven copies of -CXXCH- motifs. Both cysteine residues in -CX_{15}CH- motif have been shown the covalent attachment to haem. CcsA2 is essential for *W. succinogenes* growth, and most likely recognises the conventional -CXXCH- motif. The expression of different CcsAs in a System I-deficient *E.coli* strain showed that CcsA2 is able to mediate the covalent binding between haem *b* molecules and the -CXXCH- motif (Kern *et al*., 2010) but neither NrfI nor CcsA1 is capable to achieve the attachment to the -CXXCK- or -CX_{15}CH- motifs respectively under the same condition (Kern *et al*., 2010), which implies that the specialized CCSs recognize specific structural features in their cognate apocytochromes (Kern *et al*., 2010). Furthermore, in *C. jejuni* 81116 a gene cluster (*c8j_0029* to *c8j_0032*) has been identified which may be involved in sulphite metabolism, containing two unusual genes *c8j_0029* and *c8j_0030* encoding putative *c*-type cytochromes harboring multiple-haems (6 to 8 -CXXCH- motifs of both and a -CX_{17}CH- motif in the C8j_0029 protein) and a rhodanese (sulphur transferase) domain. Thus the CCSs system(s) which is not identified yet will be significant in the energy utilizing and colonisation of *C. jejuni* in the hosts.

1.7.6 Oxygen as a terminal electron acceptor

Two different terminal oxidases were identified in *C. jejuni* by the spectroscopy and cyanide-resistant assays in early studies (E_{M7} of O_2/H_2O couple = +815 mV) (Carlone and Lascelles, 1982; Hoffman and Goodman, 1982). The genomic sequences analysis further confirmed that a *cb*-type cytochrome *c* (or cytochrome cbb_3-type) oxidase and a cytochrome *bd*-type quinone oxidase are present in *C. jejuni* (Parkhill *et al*., 2000). According to the parallel sequence analysis, the *cb*-type cytochrome *c* oxidase in *C. jejuni* is similar to that of *H. pylori* (Nagata *et al*., 1996) and is encoded by *ccoNOQP* (*cj1490c - cj1487c*; Parkhill *et al*., 2000). This enzyme is sensitive to cyanide in either 5% or 10 % (v/v) oxygen content and shows a very high affinity for oxygen (Jackson *et al*., 2007). Due to the physiological importance of cytochrome *cb* oxidases for microaerobic respiration (Pitcher *et al*., 2002), it was thought that a knockout mutant of this enzyme in *C. jejuni* might not be viable (Jackson *et al*., 2007). However, in order to avoid the whole *cco* module abolishment, a *ccoN* mutant was constructed and it is highly sensitive to oxygen. The mutant also showed a growth defect in microaerobic condition (less than 7 % (v/v) O_2) and was unable to colonise chicken (Weingarten *et al*., 2008) although it was not confirmed that the mutant ever reached the cecum (about 1% oxygen). A previous transcriptional study also indicated the importance of this oxidase

in colonisation: the *cco* gene cluster was up-regulated about fourfold in chicks, suggesting a microaerobic environment niche (Woodall *et al*., 2005). The observed oxygen toxicity of this mutant may be due to one of the following reasons: (i) the reactive oxygen species like H_2O_2 produced by cyanide-insensitive oxidase CioAB in *C. jejuni* might overwhelm the oxidative-production enzymes such as catalase and alkyl hydroperoxide reductase; and (ii) in order to keep the function of oxygen-sensitive metabolic enzymes in the cytoplasm, the cbb_3-type oxidase might keep cytoplasmic oxygen tensions at low level. To conclude, the latter hypothesis seems more related to the microaerobic feature of the *C. jejuni* growth (Weingarten *et al*., 2008).

Two genes (*cj0081 - cj0082*) which are similar to the *cydAB* operon in *E.coli,* encode a cytochrome *bd*-type quinol oxidase have been found in *C. jejuni* (Thöny-Meyer, 1997; Parkhill *et al*., 2000) and it has been a long time that *C. jejuni* is considered as possessing a cytochrome *bd*-type terminal oxidase. However, the high-spin haems of b_{558}, b_{595} and *d*-type, which are typical characteristics of *bd*-type cytochromes, are absent in *C. jejuni*, indicating the possibility of the presence of a different type of cytochrome *bd*-type oxidase. The peptides encoded by the *cioAB* genes in *Pseudomonas aeruginosa* is a homologue to the two subunits of bacterial *bd* oxidase but lacks the feature of association with the haems (Jackson *et al*., 2007; Cunningham and Williams, 1995). It seems likely that the *cioAB*-encoded oxidase of *P. aeruginosa* and *C. jejuni* belong to the same family of poorly characterized enzymes in which the haems are replaced by other redox centres, thus the oxidase in *C. jejuni* is renamed as CioAB (Jackson *et al*., 2007). The CioAB oxidase is cyanide-insensitive and has a much lower affinity for oxygen than the *cb*-type cytochrome *c* oxidase (Jackson *et al*., 2007) or the cytochrome *bd* type oxidase in *E. coli* (D'Mello *et al*., 1996). The growth defect was only reflected by the viable count of the *cioAB* mutant under 5 % oxygen (v/v) whereas the optical density of the wild-type and mutant were similar. The CioAB showed a low affinity to oxygen (see the discussion below) and the mutation of *cioAB* in *C. jejuni* may result in up-regulation of synthesis of the high-affinity *cb*-type oxidase or diverting the electron flow to the high-affinity oxidases, particularly at the low oxygen tensions. Thus, the role of CioAB might be involved in maintaining a microaerobic environment and oxygen detoxification, as proposed for *Azotobacter vinelandii* CydAB, where cytochrome *bd* protects the oxygen-labile nitrogenase (Jackson *et al*., 2007; Kelly *et al*., 1990). Furthermore, the quinol oxidase bypasses the cytochrome bc_1 complex and accepts electrons directly from quinol, suggesting that the presence of this oxidase

offers a protective mechanism against competing microorganisms that produce toxins which inhibit the cytochrome bc_1 complex (Trumpower, 1990).

1.7.7 Respiration with alternative electron acceptors under oxygen-limited conditions

Under oxygen-limited conditions, *C. jejuni* is capable of utilising several inorganic and organic compounds as alternative electron acceptors for respiration in addition/instead of molecular oxygen, including nitrate (E_{M7} of nitrate/nitrite couple = +421 mV), nitrite (E_{M7} of nitrite/ammonium couple = +440 mV), trimethylamine-*N*-oxide (TMAO; E_{M7} of TMAO/trimethylamine couple = +130 mV), dimethyl sulphoxide (DMSO; E_{M7} of DMSO/dimethyl sulphide couple = +160 mV) and fumarate (E_{M7} of fumarate/succinate couple = +30 mV). Several corresponding enzymes, such as nitrate reductase, nitrite reductase, TMSO/DMSO reductase (termed an SN oxide reductase) and fumarate reductase, were identified in the reduction of alternative electron acceptors (Parkhill *et al*., 2000; Kelly, 2001; Sellars *et al*., 2002; Myers and Kelly, 2005; Pittman *et al*., 2007). The utilization of these compounds offers *C. jejuni* a survival niche in the extremely low oxygen environments like the avian and mammalian guts, augmented by the presence of metabolic intermediates produced by the microbiota. Thus anaerobic respiration is considered crucial for energy conservation and growth of this pathogen.

1.7.7.1 Fumarate reduction to succinate

Under oxygen-limited conditions, fumarate respiration is important in energy conservation in *C. jejuni*. Fumarate reduction is carried out by succinate:quinone oxidoreductases (SQOR) which are membrane bound multisubunit complexes that catalyse the two-electron transfer between the succinate/fumarate and quinone/quinol couples (Lancaster, 2002). Two fumarate reductases found in *C. jejuni*, Frd (see section 1.7.2.5) and Mfr (encoded by *mfrABE*, *cj0437* - *cj0439*), belong to SQORs, which are comprised of a soluble domain attached to the cytoplasmic membrane. The soluble domain is made up of two subunits; subunit A contains an FAD cofactor and is the site of fumarate reduction and subunit B contains three Fe-S centres (Lancaster, 2002; Lemos *et al*., 2002). The membrane-associated domain may contain one or two haems which conduct electrons from/to the quinone pool. The FrdABC complex is a cytoplasmic-facing bifunctional enzyme which is capable of oxidising succinate to fumarate aerobically and reduces fumarate in oxygen-limited conditions whereas the

Mfr enzyme can only reduce fumarate. An oxygen-limited growth defect on fumarate only occurs in the *frdA* but not in *mfrA* mutant, suggesting the significant role of Frd under oxygen-limited conditions (Guccione *et al*., 2010). However, the *mfr* genes are highly upregulated under oxygen limitation *in vitro* or *in vivo* (Guccione *et al*., 2010; Woodall *et al*., 2005), suggesting the possible role of Mfr is to allow more rapid adaption to fumarate-dependent growth, as coupled fumarate transport and succinate efflux through the DcuAB system is required, before fumarate reduction catalysed by Frd can occur (Guccione *et al*., 2010, Fig. 1.10). Like the transportation of periplasmic Mfr complex in *W. succinogenes*, a TAT signal peptide is also found at the N-terminus of the flavoprotein subunit, MfrA (Juhnke *et al*., 2009). In contrast to the situation in *W. succinogenes*, the periplasmic MfrA protein and corresponding activity is detectable in *C. jejuni* (Guccione *et al*., 2010; Juhnke *et al*., 2009). Since MfrA is the only subunit with the TAT signal peptide, the transportation of the whole complex is predicted as a "hitch-hiker" mechanism (Berks *et al*., 2005) with the association between the MfrE subunit and the cytoplasmic membrane (Guccione *et al*., 2010).

Furthermore, Mfr in *C. jejuni* also has been shown to reduce mesaconate and crotonate as alternative substrates which are metabolic intermediates of various common gut anaerobes (Buckel, 2001; Bader *et al*., 1980). Although Frd is also able to utilize both substrates in some extent, these electron acceptors do not appear to be transported across the cytoplasmic membrane, providing a further rationale for the periplasmic location of a reductase able to reduce such compounds (Fig. 1.10; Guccione *et al*., 2010). In ε-proteobacteria, the operation of Frd enzyme has been shown to be non-electrogenic due to the un-coupling 'E-pathway' (Lancaster *et al*., 2005). However, in *C. jejuni* the reduction of fumarate by the Frd activity and the MfrABE complex in the periplasm will result in no difference in the overall energetics of the two complexes, although the operation of the periplasmic Mfr is solely non-electrogenic. The possible model of Frd and Mfr complexes is depicted in figure 1.10 (Guccione *et al*., 2010).

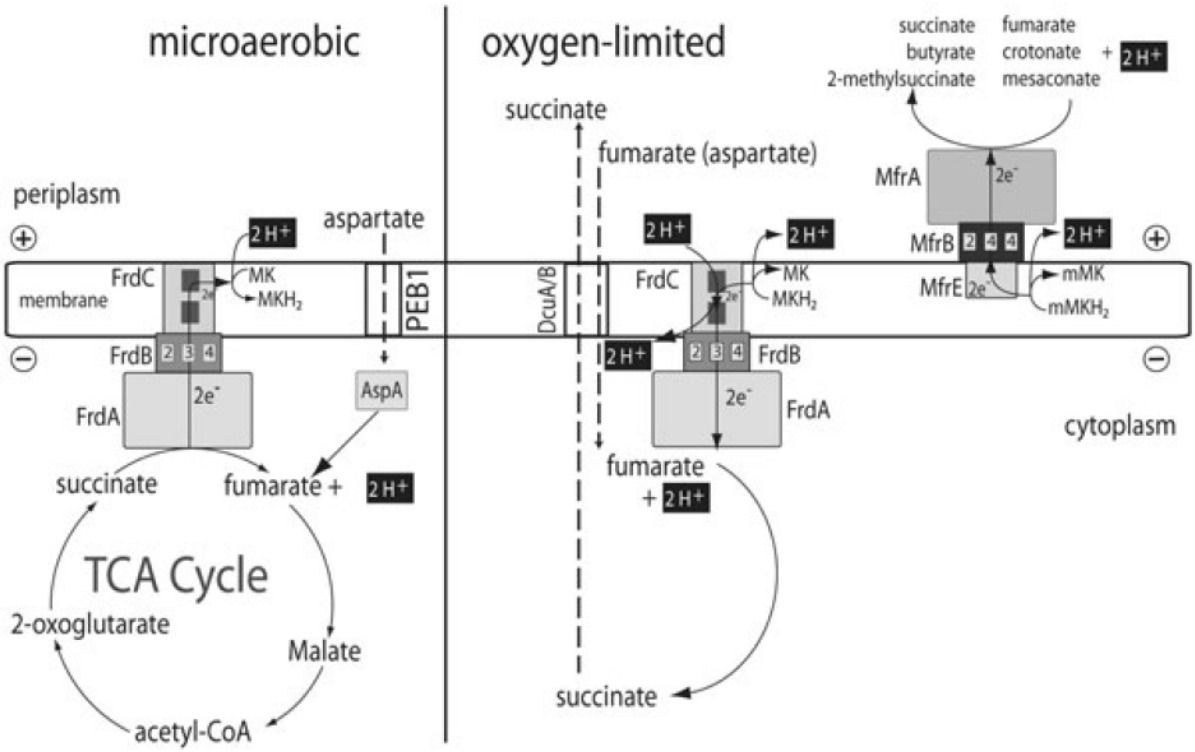

Figure 1.10 The operation of FrdABC and MfrABE in *C. jejuni*. The left : the role of the bifunctional FrdABC complex under microaerobic conditions. FrdABC acts as a TCA cycle enzyme converting succinate to fumarate and donating electrons to the menaquinone (MK) pool. The right: under oxygen-limited conditions, the FrdABC complex acts as a fumarate reductase, accepting electrons from the MKH_2 pool. The MfrABE complex is periplasmic facing and likely to be translocated as a preformed complex to the periplasm via the TAT system. It acts as a methylmenaquinol ($mMKH_2$) dependent C4-mono/di-carboxylic acid reductase with a preference for fumarate. It is also able to reduce mesaconate and crotonate, substrates that cannot easily cross the cytoplasmic membrane. Numbers within boxes in the FrdB and MfrB subunits refer to differences in the iron–sulfur centres in these proteins, either 2Fe-2S [2], 3Fe-4S [3] or 4Fe-4S [4] (see Lemos *et al*., 2002). Figure adapted from Guccione *et al*., 2010.

1.7.7.2 Nitrate reduction to nitrite

Several human pathogens harbor nitrate and nitrite respiration systems (Sparacino-Watkins *et al*., 2014). During intestinal inflammation, higher nitrate concentrations in the host can be observed and provides a benefit for the growth of bacteria which are able to utilise nitrate as electron acceptor under oxygen-limited conditions (Winter *et al*., 2013). There are two major systems responsible for nitrate reduction in bacteria: the periplasmic-type Nap and the membrane bound complex Nar. The Nap system is prevalent among all members of the ε-proteobacteria including *C. jejuni* (Pittman *et al*., 2007; Kern and Simon 2009a). Both Nap and Nar systems are present in *E.coli*; Nap shows a significantly higher affinity for nitrate and is considered as the major system operated under conditions of nitrate limitation, while Nar is functional in nitrate-rich environments (Potter *et al*., 1999). Since the nitrate concentration may be as low as 10 to 50 μM *in vivo*, the Nap system might be important for the bacterial pathogenicity in the host (Potter *et al*., 2001) and a *nap* mutant of *C. jejuni* has been demonstrated to show mildly reduced colonisation of the chick host (Weingarten *et al*., 2008). The *nap* operon found in *C. jejuni* (*napAGHBLD*) is similar in composition and arrangement to that of the other ε-proteobacteria such as *W. succinogenes*, where the function and assembly of most of gene products of dissimilatory Nap enzymes have been fully indentified and characterized (Pittman *et al*., 2007; Kern *et al*., 2007). The *C. jejuni* NapA was identified as a molybdoenzyme (Smart *et al*., 2009; Taveirne *et al*., 2009) that binds a *bis*-molybdenum guanine dinucleoside cofactor and a [4Fe-4S] cluster in the cytoplasm prior to the transport by the TAT system across the cytoplasmic membrane (van Mourik *et al*., 2008). NapB is a di-haem *c*-type cytochrome which forms the catalytic nitrate reducing complex with NapA (Potter and Cole, 1999). In. *C. jejuni*, the mechanism of electron flux to nitrate is not obvious because the Nap system in other bacteria is usually coupled to quinol oxidation by a membrane-anchored tetrahaem cytochrome *c*, NapC (Potter and Cole, 1999). The functional homologue of *napC* is generally absent in the *nap* gene cluster of ε-proteobacteria and in *W. succinogenes* the function of the Nap system is totally independent of a NapC-type cytochrome (Simon *et al*., 2003). However, in *C. jejuni* the *napC* homologue *nrfH* (*cj1358c*), which seems irrelevant to the nitrate reduction, has been discovered and is directly upstream of the *nrfA* nitrite reductase gene (*cj1357c*), implying that is part of the nitrite reductase system. NapG and NapH are putative Fe-S proteins and it has been demonstrated that in *E. coli* they may able to form an ubiquinol

dehydrogenase which donates electrons to NapA, via NapC and NapB (Brondijk *et al*., 2002; 2004). Instead of the function of NapC, in ε-proteobacteria the NapGH complex is considered to form a cytochrome *c* independent membrane bound menaquinol dehydrogenase complex (Kern and Simon, 2008). In *C. jejuni*, NapGH is the major route of electron transfer to NapA; however the NapG mutant shows a slow nitrate-dependent growth, suggesting less efficient electron transfer is mediated by NrfH, the electron donor to the nitrite reductase NrfA (Pittman *et al*., 2007).

NapD is a chaperone necessary for the export of NapA by the TAT translocation system in *E. coli* (Maillard *et al*., 2007) and is essential for NapA maturation and growth by nitrate respiration (Potter and Cole, 1999; Kern *et al*., 2007). NapL is predicted to be a soluble periplasmic protein localised by the Sec system and also widely distributed among the ε-proteobacteria. The *napL* mutation in *W. succinogenes* and *C. jejuni* leads to a decrease in NapA-dependent nitrate reduction but the function of NapL is still unknown to date. NapF is a Fe-S protein and associates with a membrane bound complex with NapGH on the cytoplasmic side. It is required for full maturation of NapA in *W. succinogenes* but the homologue is absent in *C. jejuni* (Kern and Simon, 2009b; Kern *et al*., 2007).

1.7.7.3 Nitrite reduction to ammonium

In *C. jejuni*, the nitrite reductase (Nrf) system is comprised of two components: NrfA and NrfH. NrfA is a periplasmic pentahaem cytochrome *c* and functions as a terminal reductase which is connected to the quinone pool by NrfH, a tetrahaem-containing NapC-like cytochrome *c* (Pittman *et al*., 2007). The NrfA enzymes in most bacteria contain an unusual -CXXCK- instead of the *C. jejuni* conventional -CXXCH- motif at the haem 1 binding site and require a dedicated lyase for covalent attachment of the active site haem (e. g., *W. succinogenes*, see section 1.7.5.2.2) (Pisa *et al*., 2002). This probably explains the absence of the gene encoding for Nrf-specific lyases in *C. jejuni*. NrfH is predicted to be a periplasmic-facing enzyme which is anchored on the cytoplasmic membrane by an uncleaved TAT-like signal peptide. The parallel genome sequence analysis of all ε-proteobacteria to date indicates the *nrfH* gene is encoded upstream of *nrfA* (Kern and Simon, 2009a). The catalytic complex, which is formed by NrfH and NrfA, couples menaquinol oxidation to nitrite reduction in an electroneutral process (Simon *et al*., 2000; Pittman *et al*., 2007) and nitrite reduction is highly

dependent on the specific activities of NrfA in *C. jejuni* (Sellars *et al*., Pittman *et al*., 2007).

Nitrite reductase can also perform the five electron reduction of nitric oxide (NO) to ammonium (NH_4^+) (Costa *et al*., 1990). In addition to flavohemoglobin (Hmp) and flavorubredoxin (NorV), in *E.coli* the NrfA enzyme might play a significant role in nitric oxide detoxification (Poock *et al*., 2002). Hmp and NorV are absent in *C. jejuni* and nitrosative stress and NO, an anti-microbial mechanism employed by the mammalian immune system in response to bacterial infection, will be raised during the growth with nitrite (Pittman *et al*., 2007; Kern *et al*., 2011a). However, in addition to NrfA, a cytoplasmic single domain globin (Cgb) which has been shown to protect against nitrosative stress, is inducible by the regulatory protein NssR (Elvers *et al*., 2004; Pittman *et al*., 2007). In contrast to the constitutive expression of NrfA, the NssR-mediated induction of *cgb* against nitrosative stress is slow, which explains the phenotype of hypersensitivity to nitrosative stress in the *nrfA* mutant (Elvers *et al*., 2005; Pittman *et al*., 2007). Taken together, the periplasmic NrfA and cytoplasmic Cgb are present on the opposite side of the cytoplasmic membrane and constitute a robust defense against nitrosative stress. Also, NrfA can mediate the stress response to NO in *W. succinogenes* (Kern *et al*., 2011b). However, a *nrfA* mutant still colonises the avian intestine (Weingarten *et al*., 2008), suggesting Nrf may be more important in the mammalian host.

1.7.7.4 *S*- and *N*- oxides as electron acceptors

TMAO and DMSO are structurally similar compounds and widely distributed in aquatic environments and soil; TMAO is an excretory product of many marine organisms and DMSO is produced by some algae as a cryoprotectant (McCrindle *et al*., 2005). TMAO is also known to be made in the mammalian gut from the dietary lipid phosphatidylcholine (Wang *et al*., 2011). It is therefore likely that *Campylobacters* will encounter the structurally similar compounds in the host or natural habitats with adequate concentrations to support their respiration. A variety of microorganisms are capable to catalyze the two electrons reduction of TMAO and DMSO by the corresponding reductases (often by the same enzyme) which are induced by low oxygen levels, yielding trimethylamine (TMA) / dimethyl sulphide (DMS), respectively. Several distinct enzymes were found in *E. coli* where the DMSO reductase encoded by

dmsABC is able to reduce various S- and N- oxide; the TMAO reductase TorACD is highly specific for TMAO; and the TorYZ enzyme which prefers TMAO but is also able to reduce other S- and N- oxides (Bilous and Weiner, 1988; Mejean *et al*., 1994; Gon *et al*., 2000). In the periplasmic Tor system, the histidine kinase-response regulator TorSR is capable to sense the concentration of TMAO, which induces the expression of the *torCAD* operon (Jourlin *et al*., 1996). The terminal reductase TorA is a molybdoenzyme which is fed electrons from menaquinone via the membrane-anchored pentahaem cytochrome *c*, TorC (Gon *et al*., 2001). The maturation of TorA needs a cytoplasmic chaperone TorD which ensures the correct conformation of TorA prior to the transportation across the membrane via the TAT system. The DmsABC DMSO reductase in *E.coli* is comprised of a large extrinsic membrane associated molybdoprotein DmsA, a smaller electron transferring Fe-S subunit DmsB and an intrinsic membrane anchor and menaquinol binding subunit DmsC (Weiner *et al*., 1993). Electrons would be transferred from the menaquinone via DmsC then DmsB to DmsA in the periplasm, where the reduction of DMSO would take place. The expression of *dmsABC* is inducible under oxygen-limited conditions, which is controlled by the FNR (fumarate and nitrate reductase regulation protein; McCrindle *et al*., 2005) and is influenced by ModE, a molybdate binding transcription factor (McNicholas *et al*., 1998).

In *C. jejuni* NCTC 11168, the TorA homologue Cj0264c is solely responsible for both TMAO and DMSO reduction (Sellars *et al*., 2002). It is a periplasmic molybdoprotein which is translocated to the periplasm by the TAT system, via the recognition of the signal peptide -DRRKFLK- at its N-terminal sequence. The upstream gene *cj0265c* encodes a monohaem *c*-type cytochrome with similarity to the C-terminus of the membrane-anchored TorC of *E. coli* (Sellars *et al*., 2002). However, due to the lack of extra haem binding, the Cj0265c protein seems unable to transfer electrons from menaquinone to the Cj0264c protein. A NapC-like multihaem cytochrome *c* is often involved in connecting terminal reductases in the periplasm with the quinol pool and TorC in *E. coli* has this function. In *C. jejuni*, the anaerobic growth of the *nrfH* mutant with TMAO/DMSO suggests the NapC homologue NrfH does not carry out this role (Pittman *et al*., 2007). Like the *torYZ* system in *E. coli*, the TorD homologue is also absent in the *C. jejuni* operon. The level of avian colonisation of both wild type and the *cj0264c* mutant are similar, suggesting TMAO or DMSO are not important electron acceptors in the avian hosts (Weingarten *et al*., 2008). In *C. jejuni* 81-176, a system

similar to the DmsABC DMSO reductase in *E. coli* has been found and the mutagenesis of *dmsA* leads to a colonisation defect in the mouse, indicating this enzyme is significantly involved in the colonisation process of the mammalian host (Hofreuter *et al*., 2006).

1.7.7.5 Hydrogen peroxide

Several toxic intermediates are formed during the incomplete reduction of molecular oxygen to water, including hydrogen peroxide (H_2O_2; see section 1.6.2) which can be degraded to H_2O and O_2 by the cytoplasmic catalase and the periplasmic cytochrome *c* peroxidase (CCP). Bacterial CCPs are usually dihaem proteins that utilize reduced cytochrome *c* as an electron donor to detoxify H_2O_2 to H_2O (Atack and Kelly, 2007). Although the exposure of bacterial cells to excess oxygen increases H_2O_2 levels (Seaver and Imlay, 2004), the *ccp* genes seem to be upregulated preferentially under microaerobic or anaerobic environments and this may be relevant in pathogenic bacteria like *C. jejuni*. For example, the low oxygen environment such as the human gut will trigger the expression of periplasmic CCPs which is the first line of defense against the attack of H_2O_2-producing phagocytes. Two putative CCPs encoded by *cj0020c* and *cj0358* are found in *C. jejuni* NCTC 11168 (Parkhill *et al*., 2000) and the corresponding gene (*cjj0047c* and *cjj0382*) products have been characterized in strain 81-176 (Bingham-Ramos and Hendrixson, 2008). Cjj0047 is solely needed for the colonization of chicks but neither mutant shows significant sensitivity to H_2O_2, suggesting they are not redundant and might have distinct physiological roles (Hendrixson and DiRita, 2004; Bingham-Ramos and Hendrixson, 2008). However, in *C. jejuni* NCTC 11168, both *cj0020c* and *cj0358c* mutants show higher sensitivity to killing by H_2O_2 (Kelly, 2008) and the expression of the latter is increased significantly in the chick cecum (Woodall *et al*., 2005), which is thought to be a low-oxygen niche. The studies to date indicate that CCPs in *C. jejuni* are unlikely to play a major role in the detoxification of H_2O_2 in the periplasm (Bingham-Ramos and Hendrixson, 2008). Although the periplasmic CCPs are not energy conserving, the coupling of H_2O_2 reduction and a proton translocating dehydrogenase or cytochrome bc_1 complex still allows the generation of proton motive force (PMF) (Kelly, 2008). The periplasmic H_2O_2 is also generated by a side reaction of the formate dehydrogenase (Fdh), thus CCPs may be important during growth on formate (Goodhew *et al*., 1988).

1.8 Protein translocation across the bacterial cytoplasmic membrane

1.8.1 Overview

Proteins that reside partially or completely outside the bacterial cytoplasm require specialized pathways to facilitate their localization. Functional proteins in the periplasm must be translocated across the hydrophobic barrier of the inner membrane. Although the Sec pathway transports proteins in a predominantly unfolded conformation, the TAT pathway exports fully-folded protein substrates. The Sec pathway is universally conserved, essential and normally the main route of protein export. The TAT pathway, by contrast, is found in some bacteria and archea and has been identified as essential in only a few organisms. The TAT pathway is an active transport system that is energized solely by the transmembrane protein motive force (PMF) and the Sec system needs the energy derived from both ATP hydrolysis and the PMF.

1.8.2 The signal peptides of the Sec and TAT systems

The recognition of the signal sequences harbored within corresponding substrates (mostly apoproteins) is a prerequisite of the protein translocation system. Proteins targeted to the Sec and TAT machineries have N-terminal signal peptides that have similar overall architecture and are normally cleaved by an externally facing signal peptidase (Thompson *et al*., 2010; Yahr and Wickner, 2001; Luke *et al*., 2009). Signal peptides have a tripartite structure with a basic n region at the N-terminus, a hydrophobic h region in the middle and a polar c region at the carboxyl terminus. The signal peptidase recognition site generally locates in the c region, which is suitable for the cleavage by either a type I or a type II signal peptidase. Type II signal peptidase, also known as lipoprotein signal peptidase, has a consensus recognition sequence that is typically -L_{-3}(A/S/T)$_{-2}$(G/A)$_{-1}$- along with an absolutely conserved cysteine at the +1 position of the mature protein and this cysteine residue is lipidated prior to cleavage. The lipid modified mature domain then remains membrane surface associated through the lipid anchor or is further sorted to the outer membrane. Although Sec- and TAT-dependent signal peptides share some common features, there are several key differences that are crucial for targeting to the correct export pathway and avoiding mistargeting to the incorrect machinery. The n region of the Sec signal peptide is positively charged without any conserved residues, which has been implicated in electrostatic interactions with membrane phospholipids. Both the h and n regions are

critical structural elements recognised by signal recognition particles (SRP) and the motor protein SecA (Peterson *et al*., 2003; Lee and Bernstein, 2001; Cunningham and Wickner, 1989). The TAT signal peptides contain a highly conserved twin-arginine motif, defined as -SRRXFLK-, in which the consecutive arginines are almost always invariant; the other motif residues occur with a frequency of > 50%, and the amino acid at the X position is usually polar (Berks, 1996; Joshi *et al*., 2010; Stanley *et al*., 2000). Previous studies have shown that the twin arginines are crucial for the TAT-dependnet transportation, whereas the mutation of other residues in the TAT motif results in less notable transport defect (Palmer *et al*., 2010). In addition, naturally occurring TAT-dependent substrates with a -KR- rather than -RR- pair have been also identified (Hinsley *et al*., 2001). Although the presence of the twin arginine motif is able to prevent the interaction with the Sec pathway, some Sec-dependent substrates harbor twin arginines in their signal sequence, such as DacD (see Fig. 1.11). Still, other features of the TAT signal peptide and the passenger domain of TAT-dependent substrates allow the Sec incompatibility. The hydrophobicity of h region in the TAT signal peptide is usually less than that of the Sec-targeting sequence, and this is a major discriminating feature for these two peptides. With the increasing of the hydrophobicity in the TAT signal peptide via the substitution of residues, the TAT-dependent substrate will reroute to the Sec pathway (Cristobal *et al*., 1999). Moreover, the basic residues are present in the c region of some TAT signal peptides, which are occasionally found in the c region of Sec signal sequences. Although the presence of a basic amino acid in the c region is not a requirement by the TAT machinery, it has been shown to prevent involvement of the signal peptide with the Sec machinery (Cristobal *et al*., 1999; Blaudeck *et al*., 2003; Bogsch *et al*., 1997). Several web-based bioinformatics programs, such as TATFIND and TatP, are available for the prediction of TAT signal peptides. (Dilks *et al*., 2003; Rose *et al*., 2002; Bendtsen *et al*., 2005; Bagos *et al*., 2010).

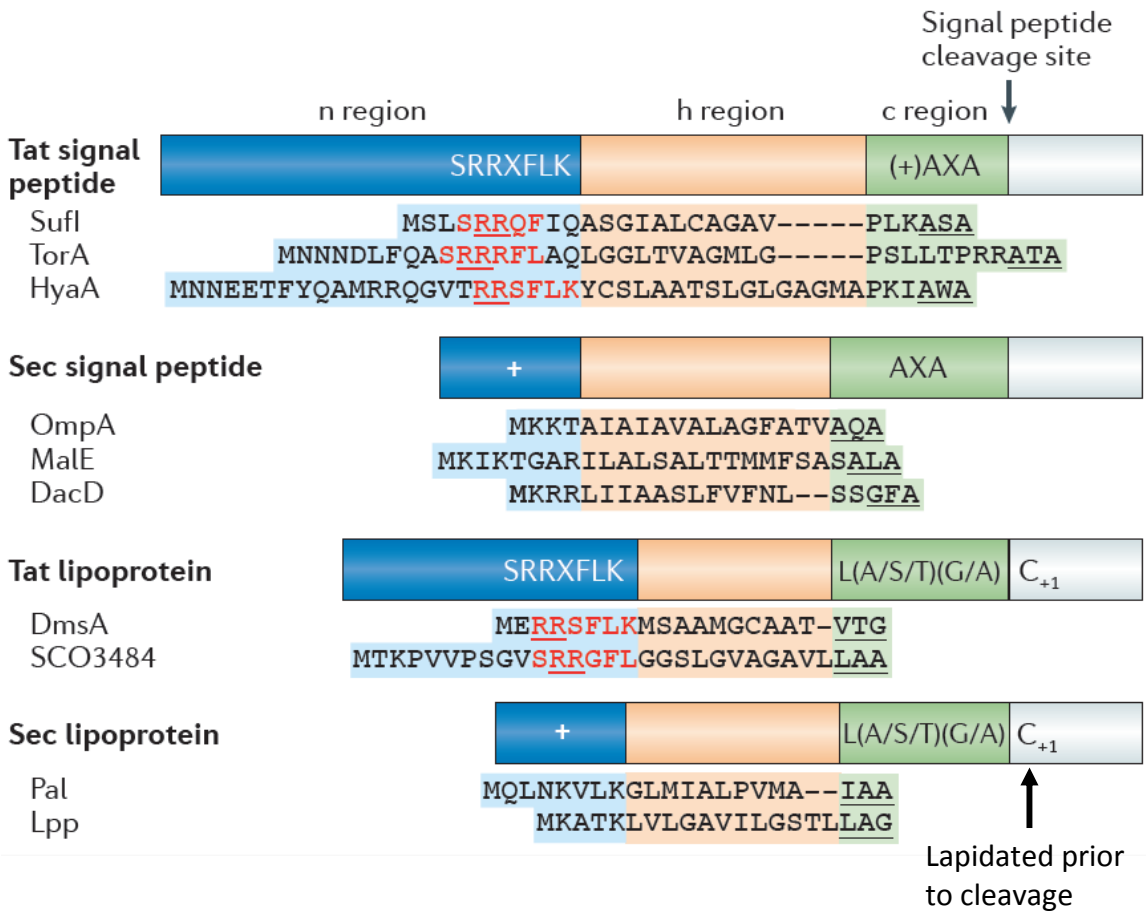

Figure 1.11 The Sec- and TAT-dependent signal peptides of various substrate. In the figure, residues that match the TAT consensus are shown in red, with the twin arginines underlined. A'+' indicates a basic region. Signal peptidase recognition sequences in the c regions are underlined. Proteins listed in this figure are found in *E. coli* but DmsA and SCO3484 are not included. SufI, a divisomal protein; TorA, TMAO reductase; HyaA, hydrogenase 1 small subunit; OmpA, outer-membrane protein A; MalE, maltose-binding periplasmic protein; DacD, $_D$-alanyl-$_D$-alanine carboxypeptidase; DmsA, DMSO reductase in *Shewanella oneidensis*; SCO3484, DMSO reductase in *Streptomyces coelicolor*; Pal, peptidoglycan-associated lipoprotein; Lpp, major outer-membrane lipoprotein. Figure revised from Palmer and Berks, 2012.

1.8.3 The Sec-dependent pathway

The general secretion (Sec) system is the major route involved in both the secretion of unfolded proteins across the cytoplasmic membrane and the insertion of membrane proteins into the membrane, which is well studied and characterized. Extensive genetic analysis, using *E. coli* as a model organism, has resulted in the identification of all major genes and proteins (for a recent review, see Kudva *et al*., 2013). Here, the general concept of the Sec pathway is included to allow comparison to the TAT system. In *E. coli*, major components of the Sec transport machinery were initially identified via genetic screens, including SecA, SecB, SecE, SecY and SecG. SecB is a secretion specific chaperone which can partially compensate for the loss of functions in *E. coli* strains deficient in general chaperones (Fekkes and Driessen, 1999; Ullers *et al*., 2004). In the Sec machinery, SecB binds to the polypeptide domains of long nascent secretory proteins while they emerge from the ribosome exit tunnel and stabilizes them in an unfolded conformation (Kumamoto, 1989). A property that discriminates SecB from other chaperones is that it binds specifically to the protein conducting channel (PCC)-associated SecA, where this reaction initiates the transfer of unfold secretory proteins from SecB to SecA (Zhou and Xu, 2005; Mitra *et al*., 2006). The ATPase secA functions as receptor for secretory proteins and as an ATP-dependent motor that drives the protein translocation reaction when associated to the PCC (Hartl *et al*., 1990). SecA is the central component of the bacterial Sec system as it interacts with almost all other components of the translocase. The characteristic of a conserved Walker A and B ATP binding motif and the homology to DEAD-box RNA and RecA-like DNA helicase indicates that SecA is molecular motor that drives the protein translocation reaction (Walker *et al*., 1982; Koonin and Gorbalenya, 1992). The homodimeric form of SecA has been implicated as the active conformation in protein translocation. The PCC forms a hydrophilic pore for secretory proteins to pass the membrane (Joly and Wickner, 1993; Cannon *et al*., 2005) and it is composed of the dimer of SecYEG complex, including SecY, SecE and SecG in bacteria. The central pore in the SecYEG complex can be widened to a sufficient extent that it can accommodate unfold polypeptide chains, without the need for a lateral opening of the translocation channel (Tian and Andricioaei, 2006; Haider *et al*., 2006). The dynamic model of the protein translocation was proposed by the interaction between SecA and SecY. Due to the conformational change of SecA by binding to SecY, the translocation is proposed to be the result of nucleotide dependent cycles of insertion and dislodgment of SecA domains with bound secretory

protein into the PCC (Economou and Wickner, 1994; Price *et al*., 1996; van der Wolk *et al*., 1997). The *C. jejuni* genome encodes the key components of a functional Sec-translocase but lacks the non-essential SecB (Parkhill *et al*., 2000), which is found mainly in the α-, β-, and γ-proteobacteria (van der Sluis and Driessen, 2006).

Taking all components together, in *E.coli* proteins can be targeted to the Sec translocase by two different mechanisms, as shown in Fig. 1.12. Secretory proteins are guided to the SecYEG-associated SecA by the secretion specific chaperone SecB that maintains these proteins in a translocation-competent, unfolded state (Driessen, 2001), where ATP is a main source of energy to drive protein segments through the pore of PCC (Wickner, 1994). During co-translational targeting, the signal recognition particle (SRP) binds to the signal sequence of the secretory protein while it emerges from the ribosome (Luirink *et al*., 2005) and the entire ternary complex of SRP/ribosome/nascent secretory protein chain is targeted to the Sec-translocase by the expanse of GTP. In bacteria, the PMF also contributes as a driving force to the Sec translocation reaction.

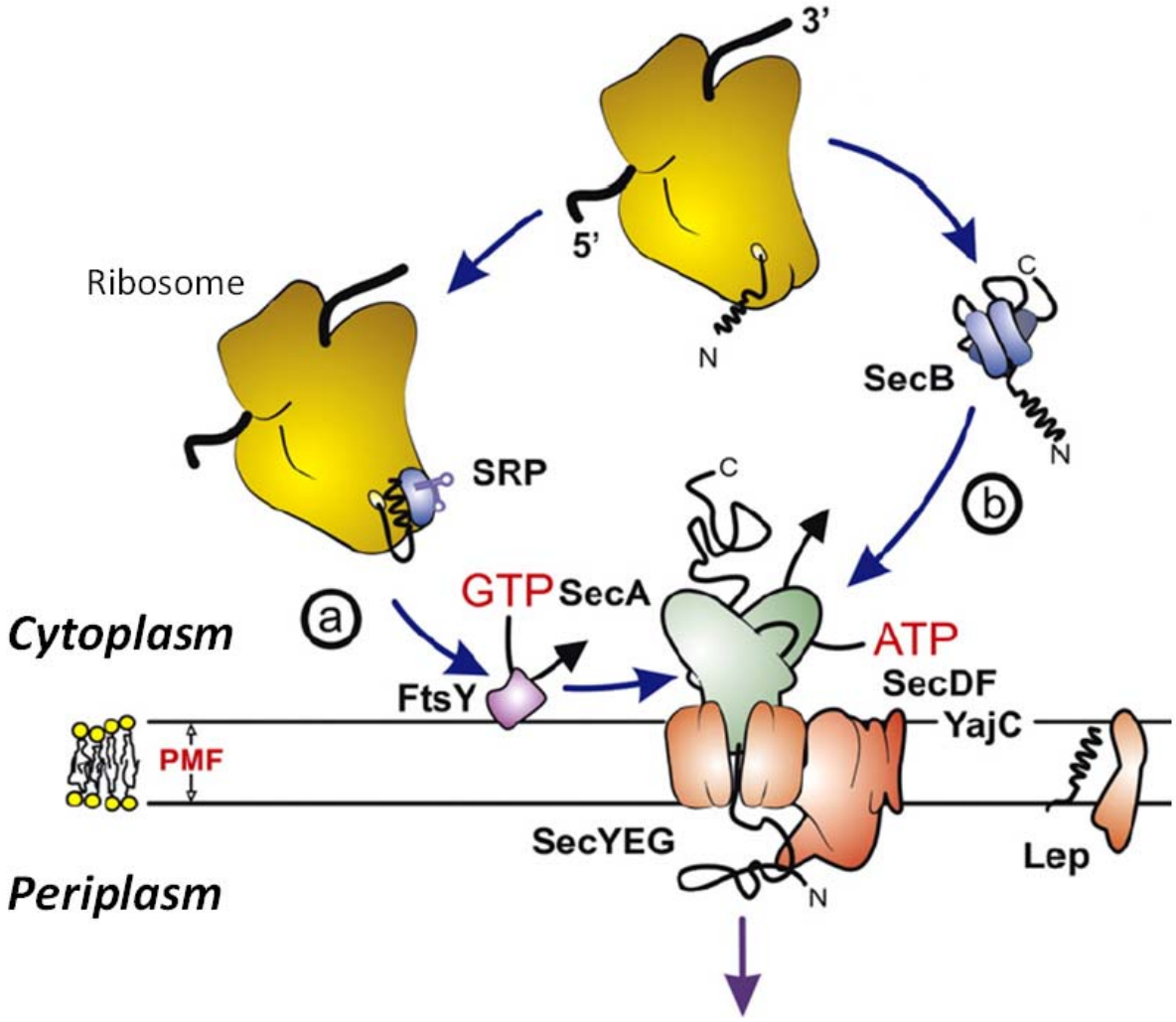

Figure 1.12 Schematic view of the *Escherichia coli* Sec translocase.

The bacterial Sec translocase is a protein complex in the cytoplasmic membrane, which comprises a peripheral motor domain SecA (green), the protein-conducting channel, SecYEG (orange), and the accessory protein SecDF(or called YajC; pink). Signal peptidase (Lep) is a membrane-bound peptidase that cleaves the signal sequence from preproteins at the periplasmic face of the membrane. (a) Membrane proteins and some preproteins utilize the co-translocation targeting route with the binding between ribosome-bound nascent chains and signal recognition particle (SRP) and the SRP-receptor FtsY, the process is energized by GTP. (b) Post-translational targeting route with the assistance of secretion specific chaperone SecB. ATP is the energy source during protein translocation. PMF is also the energy source for both mechanisms of translocation. Figure revised from Natale *et al*, 2007.

1.8.4 The TAT-dependent pathway

Unlike the Sec machinery, the TAT pathway usually transports pre-folded proteins across the cytoplasmic membrane (Robinson and Bolhuis, 2004). Functional TAT systems occur in many bacteria and archea, as well as in thylakoid membranes of plant plastids (Müller and Klösgen, 2005). TAT translocases consist of two or three membrane integrated subunits, i.e. TatA and TatC or TatA, TatB and TatC, that together form a receptor and a protein conducting machinery for TAT-dependent substrates which are often cofactor containing proteins and the insertion of cofactors is mainly restricted in the cytoplasm. The energy source for translocation is only provided by the PMF (Yahr and Wickner, 2001). Although the TAT system normally transports fewer substrates than the Sec system (Dilks *et al*., 2003), it has key roles in many cellular process, including respiratory and photosynthetic energy metabolism, iron and phosphate acquisition (Ize *et al*., 2004; Letoffe *et al*., 2009; Mickael *et al*., 2010; Monds *et al*., 2006), cell division (Stanley *et al*., 2001), cell motility (Ochsner *et al*., 2002), quorum sensing (Stevenson *et al*., 2007), resistance to heavy metals (Ize *et al*., 2004) and antimicrobial peptides (Weatherspoon-Griffin *et al*., 2011). Importantly, the TAT pathway is required for the bacterial pathogenicity in the tested animal and plants (De Buck *et al*., 2008).

In the light of experimental evidence, the rationales for the use of the TAT pathway in bacteria include: the need for the insertion of complex cofactors; the avoidance of metal ions that compete for insertion into the active site of the proteins (Tottey *et al*., 2008); the transport as a hetero-oligomeric complex (termed hitch-hiking; Sauve *et al*., 2007); and difficulties in keeping the protein unfolded before post-translational transport (Pohlschroder *et al*., 2004). In *C. jejuni* most enzymes in electron transport chains show these necessities but the 'hitch-hiking' phenomenon is crucial for several reductase, such as the bc_1 complex, nitrate reductase (Nap) and fumarate reductase (Mfr) (Bachmann *et al*., 2006; De Buck *et al*., 2007; Hitchcock *et al*., 2010). The knowledge of the TAT system in Gram-negative bacteria has been established in the model organism *E. coli* where the *tat* operon, *tatABCD*, with the monocistronic *tatE* gene located elsewhere are found; both transcription units are constitutively expressed suggesting the TAT pathway is important under all growth conditions (Jack *et al*., 2001). TatA is a small protein consisting of an N-terminal transmembrane anchor (TMH), a short hinge region, an amphipathic helix (APH) and a charged C-terminal tail and TatB

shares the same modular structure with TatA but usually has a longer C-tail (Hicks *et al*., 2003). The transport of endogenous TAT substrates are abolished in the *tatB* mutant of *E. coli*, while it still allows the low level of export of TAT signal-fused reporter proteins, reflecting some residual TatB-like activity of TatA (Blaudeck *et al*., 2005; Chanal *et al*., 1998). TatC is a polytopic membrane protein with six transmembrane domains (Behrendt *et al*., 2004), which harbors a recognition site for the twin-arginine motif of the TAT signal peptide (Fig. 1.15; Alami *et al*., 2003; Gerard and Cline, 2006; Rollauer *et al*., 2012). Both TatC and TatA/B family members tend to form homo-oligomeric and hetero- oligomeric complexes in the core of the TAT system. TatA and TatC form together the minimal Tat translocase in Gram-positive bacteria *B. subtilis* (Pop *et al*., 2002; Jongbloed *et al*., 2004) whereas in proteobacteria like *E. coli* the system is more complex, as the TatB and TatC will form a stable integral membrane TatBC complex containing an estimated 6-8 copies of each protein, which is stable to bind TAT substrates (Bolhuis *et al*., 2001; Tarry *et al*., 2009; McDevitt *et al*., 2006). The transport cycle is initiated by substrate binding to the TatBC complex via their signal peptides (Gerard and Cline, 2007). Some substrates proteins are able to interact with the phospholipid surface of the membrane and possibly find the TatBC complex by two-dimensional diffusion on the membrane surface (Shanmugham *et al*., 2006; Bageshwar *et al*., 2009). When the TAT-dependent substrate binds to the TatBC, the twin-arginine motif is positioned close to TatC, whereas the hydrophobic h region of the signal peptide and the folded passenger domain are in the vicinity of TatB (step 1 and 2 in Fig. 1.13). The specific binding site of TatC mediates the selectivity of binding to the TatBC complex (Cline and Mori, 2001). Recent evidence from studies of the chloroplast TAT system (Aldridge *et al*., 2014) suggests that TatC subunits are arranged in a concave face-to-face arrangement, creating a closed chamber. The substrate signal peptide seems to insert into spaces between the TatC subunits, forcing them apart and allowing access of TatA to the chamber, which is proposed to seed TatA polymerisation and translocase assembly (Aldridge *et al.,* 2014). The association of TatA with TatBC requires the PMF and lasts until the substrate has crossed the membrane. During the translocation process, the substrate is probably contact with all three TAT components, suggesting that a TatABC complex mediates transport (Mori and Cline, 2002). Nevertheless, it has been proposed that the substrate is transferred from TatBC to TatA (Alami *et al*., 2003).

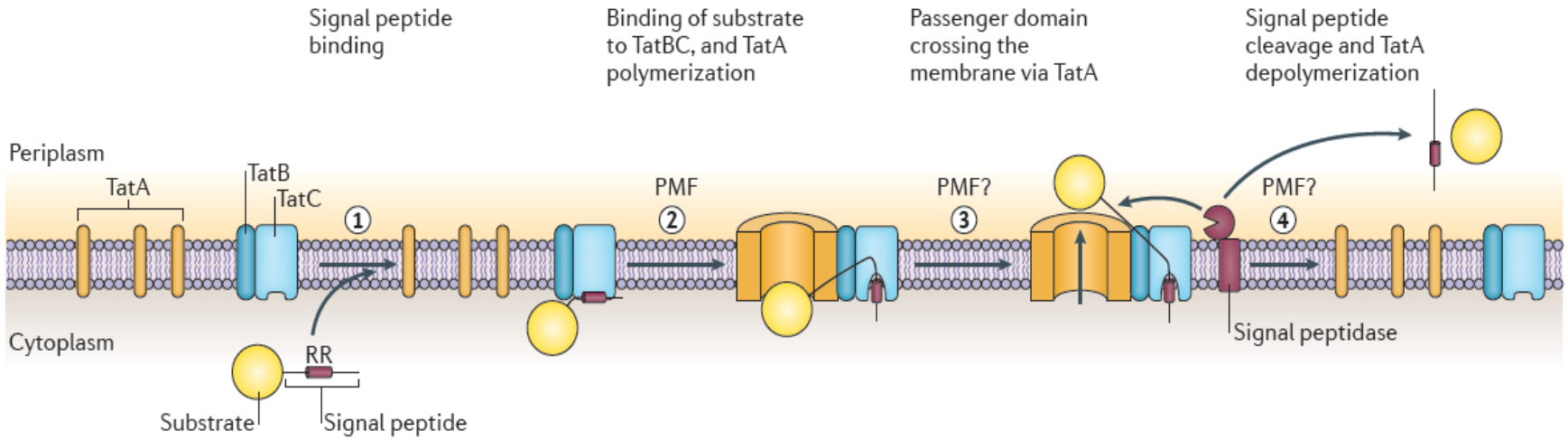

Figure 1.13 Model of the TAT translocation cycle in *E. coli*. At the start of the cycle, TatB and TatC associate as a complex, whereas TatA is present as dispersed promoters. The TatBC complex contains multiple copies of each protein, but only single copy depicted. The number of subunits in a TatA promoter is still unclear. Step1: the initiation of substrate translocation, the TatBC complex binds the signal peptide of a substrate protein in an energy-independent step; the twin-arginine (RR) motif in the signal peptide is specifically recognized by a site in TatC. The reminder of the signal peptide and the substrate passenger domain are close to TatB. Step2: the recruitment of TatA promoters by the TatBC complex, although some evidence suggests that the interaction between the TatBC and substrates is strengthened in a PMF-independent manner, TatA promoters are recruited to the TatBC complex and polymerized in a step that depends on the PMF. The resulting TatABC complex is the active translocation site. Also, the signal peptide is in contact with all three Tat components at this stage (Alami *et al*., 2003). Step3: the passenger domain of the substrate protein cresses the membrane via the polymerized TatA components, and the signal peptide remains bound to the TatBC complex. It is not known whether this step requires PMF as the energy source. Step4: the signal peptide will be normally proteolytically removed by a signal peptidase until the passenger domain has reached the far side of the membrane. The TatA component will dissociates from TatBC and depolymerise back to free promoters. The fate of the signal peptide following transport is uncertain, so this peptide is arbitrarily shown as being released into the periplasm. Figure revised from Palmer and Berks, 2012.

Following assembly of a TatABC-substrate complex, the substrate is translocated across the membrane to the periplasm, where the signal peptide is normally removed by a signal peptidase (Yahr and Wickner, 2001; Luke *et al*., 2009). The TatABC complex then disassembles until the next transport starts. TatD and E proteins are present in some organisms. TatD is a soluble cytoplasmic protein with DNase activity but is not a component of the TAT pathway (Wexler *et al*., 2000; Lindenstrauss *et al*., 2010). The *tatE* gene is a shorter paralogue of *tatA* thought to have arisen from a cryptic gene duplication; TatE is at least partially functionally interchangeable with TatA but appears to be largely redundant (Sargent *et al*., 1998). It should be noted that some Gram-positive bacteria may differ in their *tat* gene complement and can contain several independent TatA-TatC systems (Goosens *et al*., 2014).

A major role of TatA in the translocation process was originally derived from the findings and three major ideas were developed of how TatA might achieve the ensuing membrane passage of TAT substrates. In the first model TatA is assumed to form size-fitting pores for folded TAT substrates (Gohlke *et al*., 2005), the number of TatA monomers governs the pore diameter. The alternative hypothesis is that TatA will help to weaken or remodel the lipid bilayer by the polymerization of membrane-active APHs (Cline and McCaffery, 2007). A third model posits that a ring of APHs inserted into the cytoplasmic membrane where the hydrophobic TMHs of TatA and the polar surface of APHs and C-tails adapt a perpendicular orientation for the forming of hydrophilic pores (Walther *et al*., 2013). However, a recent structural study favours a model in which TatA polymerization thins and disorders the membrane to produce transient rupture (Rodriguez *et al*., 2013). Three different topologies of TatA are shown in Fig. 1.14. Unlike the chaperone SecB or SRP in the Sec pathway, there is no similar enzyme which is specific to the signal sequence involved in the quality control of the TAT system and it is believed that the general chaperone like DnaK or SlyD might mediate the proofreading of the TAT substrate (Graubner *et al*., 2007; Holzapfel *et al*., 2009; Jong *et al*., 2004). However, some substrate-specific chaperones were found to dedicate to the maturation of the corresponding TAT substrates, for example, TorD is a twin-arginine motif binding, proofreading and cofactor-insertion mediating chaperone only involved in the maturation of the TMAO reductase (TorA) (Hatzixanthis *et al*., 2005; Jack *et al*., 2004; Pommier *et al*., 1998).

The TAT pathway is also found in *C. jejuni* which encodes homologues of *tatA/E* (*cj1176c*), *tatB* (*cj0579c*), *tatC* (*cj0578c*) and *tatD* (*cj0644*) (Parkhill *et al*., 2000), and a number of proteins display putative N-terminal TAT signal sequences, the majority of which are involved in respiratory electron transport (Parkhill *et al*., 2000). In *C. jejuni*, alkaline phosphatase (Cj0145) and the nitrate reductase NapA subunit were the first proteins shown to be TAT-dependent substrates (in strain 81116; van Mourik *et al*., 2008). In a previous study from the Kelly lab (Hitchcock *et al*., 2010), proteomics and activity measurements with an isogenic *tatC* mutant and a complemented strain were used to experimentally verify the TAT dependence of NapA and the majority of the other proteins that are predicted to be exported via the TAT pathway in strain NCTC 11168. A study of the TAT system in *C. jejuni* 81-176 (Rajashekara *et al*., 2009) showed that a *tatC* null mutant was more sensitive to antimicrobials, defective in biofilm formation, motility, flagellation, survival under osmotic shock, oxidative and nutrient stress, although many of these phenotypes are likely to be due to indirect effects of the mutation. These wide-ranging phenotypes do however highlight the importance of the TAT system in general fitness and bacterial pathogenesis.

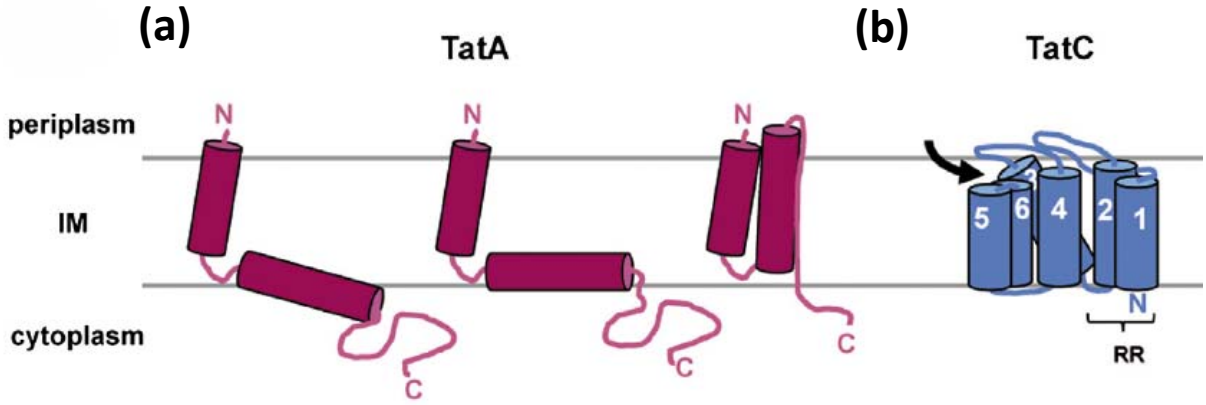

Figure 1.14 Three different topologies of TatA and the structure of TatC. (a) Left, NMR structire of an N-terminal fragment of *B. subtilis* $TatA_d$ reconstituted into planer bicells (Walther *et al*., 2010). The N-terminal TMH is followed by a partially membrane-embedded APH. Middle, full immersion of the APH of TatA that could cause destabilising of the bilayer. Right, flipping of the APH into the membrane to form a hydrophilic channel from a ring of TatA promoters. (b) The arrow indicates access from the periplasm to the concave face of the molecule and the bracket encompassed the RR twin-arginine motif binding site (N-terminus and first cytosolic loop of TatC). Figure revised from Kudva *et al*., 2013.

1.9 Aims

The genome sequences of *C. jejuni* NCTC 11168 reveal a large number of genes encoding proteins with predicted roles in electron transport chains which allow growth at the low oxygen concentrations found in human and animal guts. However, there are still many electron transport proteins with unknown functions, particularly novel *c*-type cytochromes; these are usually periplasmic or periplasmic-facing membrane bound proteins that may be crucial either as electron conducting components or as part of an electron input or output enzymes. This research will investigate the composition, physiology, biochemistry and regulation of the *c*-type cytochromes in electron transport systems of *C. jejuni*. Several putative genes encoding *c*-type cytochromes have been identified; they are *cj1153*, *cj1020c*, *cj0158c*, *cj0037c*, *cj0854c* and *cj0874c*. It is important to elucidate the electron transfer mechanism between these *c*-type cytochromes and terminal oxidases or reductases, which may transfer electrons in a sequential or in a parallel manner. In addition the physiological role, the biogenesis of *c*-type cytochromes will be further elucidated, although the knowledge of the Ccs system in *C. jejuni* is still very limited to date.

The TAT pathway will also be emphasized in this study since it is important for the enzyme activity involved in the electron transport chains. The role of two *tatA* homologues *cj1176c* and *cj0786* that are present in the genome of *C. jejuni* NCTC 11168 will be investigated in this work. The Cj1176c protein has similar structure to the TatA in *E. coli*, whereas Cj0786 is encoded in the *nap* operon with a shorter C-terminus.

Taken together, the aim of this study is to produce a more complete picture of the role of the electron transport pathways in cell growth and host colonization.

Chapter 2 Materials and Methods

2.1 Materials

Chemicals used in this study were purchased from Fisher, Life Technologies, Oxoid, Sigma-Aldrich and VWR international. Antibiotics were obtained from Melford Laboratories Ltd. Gases were supplied by BOC.

2.2 Organisms and growth media

2.2.1 Organisms used in this study

All bacterial strains used in this study are listed in table 2.1. *C. jejuni* was preserved at – 70^{o}C in Brain-Heart Infusion (BHI) broth with 15% (v/v) glycerol as cryoprotectants and *Escherichia coli* strains were stored at – 70^{o}C in Luria-Bertani (LB) broth containing 20% (v/v) glycerol.

Table 2.1 *Campylobacter jejuni* strains used in this study

Campylobacter jejuni	Description	Source
NCTC 11168	Clinical isolate used in genome sequencing	Parkhill *et al*., 2000
81116	Genetically stable strain, amenable to genetic manipulation, and infective for chickens	M.M.S.M. Wösten, Utrecht University, The Netherlands
Strains used in chapter 3		
c8j_0815^{-} (*cjtsdA*$^{-}$)	81116 *c8j_0815*::*kan*	This study
c8j_0815$^{+/-}$ (*cjtsdA*$^{+/-}$)	81116 *c8j_0815*::*kan* complemented with WT copy of *cjtsdA*	This study
c8j_0040^{-}	81116 *c8j_0040*::*kan*	This study
c8j_0040$^{+/-}$	81116 *c8j_0040*::*kan* complemented with WT copy of *c8j_0040*	This study
Strains used in chapter 4		
cj1176^{-} (*tatA1*$^{-}$)	11168 *cj1176*::*kan*	This study
cj1176$^{+/-}$ (*tatA1*$^{+/-}$)	11168 *cj1176*::*kan* complemented with WT copy of *cj1176*	This study
cj0786c^{-} (*tatA2*$^{-}$)	11168 *cj0786c*::*cat*	This study

cj0786c$^{+/-}$ (*tatA2*$^{+/-}$)	11168 *cj0786c*::*cat* complemented with WT copy of *cj0786c*	This study
cj1176^{-} *cj0786c*$^{-}$ (*tatA1*$^{-}$*tatA2*$^{-}$)	11168 *cj1176*::*kan cj0786c*::cat double mutant	This study
Strains used in chapter 5		
cj1153^{-}	11168 *cj1153*::*kan*	This study
cj1020c^{-}	11168 *cj1020c*::*cat*	This study
cj0037c^{-}	11168 *cj0037c*::*kan*	This study
cj0158c^{-}	11168 *cj0158c*::*kan* (insertion)	This study
pccj1153$^{+/-}$	11168 *cj1153*::*kan* complemented with WT copy of *cj1153* with its native promoter	This study
fdxA1153$^{+/-}$	11168 *cj1153*::*kan* complemented with WT copy of *cj1153* with *fdxA* promoter	This study
cj1020c$^{+/-}$	11168 *cj1020c*::*cat* complemented with WT copy of *cj1020c*	This study
cj0037c$^{+/-}$	11168 *cj0037c*::*kan* complemented with WT copy of *cj0037c*	This study
H33A	11168 *cj1153*::*kan* complemented with point mutated *cj1153* (H_{33} to A)	This study
H95A	11168 *cj1153*::*kan* complemented with point mutated *cj1153* (H_{95} to A)	This study
ccoN^{-}	11168 *cj1490c*::*kan*	This study
ccoNOQP^{-}	11168 *cj1490c - cj1487c*::*kan*	This study
cioAB^{-}	11168 *cioAB*::*apr* (*cj0081 - cj0082*:: apr)	This study
cioAB^{-} *cj1153*$^{+/-}$	11168 *cioAB*::apr *cj1153*::*kan* complemented with WT copy of *cj1153* plus *fdxA* promoter	This study
cioAB^{-} *cj1020c*$^{-}$	11168 *cioAB*::apr *cj1020c*::*cat* double mutant	This study
cioAB^{-} *cj0037c*$^{-}$	11168 *cioAB*::apr *cj0037c*::*kan* double mutant	This study
cioAB^{-} *cj1020c*$^{+/-}$	11168 *cioAB*::apr *cj1020c*::*cat* complemented with WT copy of *cj1020c*	This study

cioAB^{-} *cj0037c*$^{+/-}$	11168 *cioAB*::apr *cj0037c*::*kan* complemented with WT copy of *cj0037c*	This study
dsbD^{-}	11168 *cj0603c*::*kan*	This study
cj1207c^{-}	11168 *cj1207c*::*kan*	This study
cj1664^{-}	11168 *cj1664*::*kan*	This study
cj1665^{-}	11168 *cj1665*::*kan*	This study
cj1664^{-} *cj1665*$^{-}$	11168 *cj1664* - cj1665::*kan*	This study
racR^{-}	11168 *cj1261*::*kan*	This study
racS^{-}	11168 *cj1262*::*kan*	This study
racRS^{-}	11168 *cj1261* - *cj1262*::*kan*	This study
cj1153$^{+/-}$*-His*	11168 *cj1153*::*kan* complemented with his-tagged copy of *cj1153* with *fdxA* promoter	This study

Table 2.2 Strains of *Escherichia coli* used in this study

Escherichia coli	Genotype	Source
DH5α™	F– Φ80*lac*ZΔM15 Δ(*lac*ZYA^{-}*arg*F) U169 *rec*A1 *end*A1 *hsd*R17 (rK–, mK+) *pho*A *sup*E44 λ– *thi*$^{-}$1 *gyr*A96 *rel*A1	Invitrogen
BL21 (DE3)	F– *omp*T *hsd*SB(rB–, mB–) *gal dcm* (DE3)	Invitrogen

2.2.2 Media preparation and antibiotics

All media were prepared with distilled water (dH_2O) according to manufacturer's instruction and sterilized by standard autoclaving condition (121 ^{o}C, 15 min, 15 psi). Solid media could be stored at 4 ^{o}C for up to a month. For microaerobic growth of *C. jejuni*, liquid media were equilibrated by storage in the relevant gas atmosphere.

Antibiotics were prepared in distilled water and filter-sterilised (0.22 μm), except for chloramphenicol and erythromycin which needed ethanol as solvent. All antibiotic stocks were stored at 4 ^{o}C after preparation and listed in table 2.3.

Table 2.3 Antibiotics used in this study. Final concentration refers to the concentration of antibiotics once added into media.

Antibiotic	Function	Solvent	Final concentration
Amphotericin B	Antifungal	Sterile dH_2O*	10 μg/ml
Vancomycin	Anti-G(+) bacteria	Sterile dH_2O	10 μg/ml
Carbenicillin	Selective	Sterile dH_2O	50 μg/ml
Kanamycin	Selective	Sterile dH_2O	50 μg/ml
Chloramphenicol	Selective	EtOH	30-50 μg/ml
Apramycin	Selective	Sterile dH_2O	*E. coli*: 50 μg/ml *C. jejuni*: 60 μg/ml
Erythromycin	Selective	EtOH	*E. coli*: 100 μg/ml *C. jejuni*: 15 μg/ml

**Requires drop-wise addition of 10M NaOH to dissolve*

2.2.3 Growth media of *C. jejuni*

For the growth of *C. jejuni* on solid media, blood agar was prepared from autoclaved Columbia agar base (Oxoid) supplemented (when cooled to 80 ^{o}C) with 5% (v/v) lysed sterile horse blood (VWR international). Amphotericin B, vancomycin and selective antibiotic (where required) were added when media had cooled to approximately 50 ^{o}C. Plates were stored at 4 ^{o}C for up to one month. For some experimental purposes, Muller-Hinton (MH) agar was used occasionally to grow *C. jejuni*.

Liquid cultures of *C. jejuni* were routinely grown using Muller-Hinton (Oxoid) broth with 20 mM L-serine (MHS) and BHI (brain-heart infusion) broth. Media was sterilised by autoclaving and allowed to cool down to room temperature for storage. For alkaline phosphatase induction, sterilised phosphate-free DMEM (Life technologies) was used as basal medium supplemented with filter-sterilised 20 mM L-serine, 25 mM HEPES, 1.6 and 0.08 mM KH_2PO_4 for cell equilibration and induction respectively, with appropriate antibiotics.

2.2.4 Growth of *C. jejuni* in batch culture

C. jejuni was routinely maintained on blood agar at 37^{o}C under microaerobic conditions (5% O_2, 10% CO_2 and 85% N_2) generated in a MACS-VA500 Microaerobic Workstation (Don Whitley Scientific Ltd), and were subcultured onto fresh media every 48 to 72 hours to maintain viability. Liquid cultures were routinely grown at 37 ^{o}C in BHI, MHS broth or DMEM under different experimental conditions: (i) standard

microaerobic conditions (gas concentrations as described previously): 25 or 100 ml media in 100 or 250 ml conical flasks respectively were maintained shaking at 180 r.p.m. continuously; or (ii) oxygen-limited condition: the gas composition was identical to that in (i) but the media was filled to the top of 250 or 500 ml conical flasks to restrict oxygen diffusion, without shaking. Where required, various electron donors or acceptors were added from filter-sterilised stock solutions to a final concentration of 20 or 30 mM. Media was pre-equilibrated in the microaerobic growth cabinet for 16 to 18 hours prior to inoculation where the ideal starting optical density at 600 nm [OD_{600}] was about 0.1 and measured by an Ultraspec 2000 spectrophotometer (Janway). Two main sources of starting culture were microaerobically grown overnight liquid cultures or 24 hr old plate grown cells. The growth of bacteria was monitored by measuring OD_{600} hourly in microaerobic condition and the measurement was done for every two hours in oxygen-limited growth curve, where the media only was taken as blank.

For the induction of alkaline phosphatase (AP), the overnight grown culture in 25 ml phosphate-free DMEM with 1.6 mM KH_2PO_4 was collected and washed by TBS twice to remove excess phosphate in previous medium. Then the cells were resuspended in the basal medium with 0.08 mM KH_2PO_4 for AP induction. The overnight culture was taken as sample for the AP assay and the activity was measured according to section 2.8.2.6.

2.2.5 Growth of *E.coli*

Luria-Bertani (LB, Melford) broth and agar, dYT broth and NZCYM (Amresco) broth were used in the growth of *E. coli*. All were prepared according to manufacturer's instruction and sterilised by autoclaving and then supplemented with appropriate antibiotics after cooling down to room temperature. Liquid culture was grown aerobically at 37^{o}C with shaking at 250 r.p.m.

2.3 DNA preparation and manipulation

All molecular biology grade reagents were purchased from Bioline, Fisher, New England Biolabs (NEB), Promega and Life Technologies. Basic DNA manipulative procedures and protocols were according to Sambrook and Russell (Sambrook and Russell, 2001) with slightly modifications. To minimise any interference from

chemicals in the buffer solution during manipulation, all nucleotides were dissolved in sterilised ddH_2O.

2.3.1 Plasmid used in this study

All plasmids used in this study are listed in Table 2.4.

Table 2.4 Plasmids used in this study

Plasmid	Description	Resistance marker(s)	Source
pGEM®3Zf(-)	Cloning vector with T7 and SP6 promoters flanking a multiple cloning site with the α-peptide coding region of β-galactosidase	Amp	Promega
pJMK30	Cloning vector harbouring a 784 bp kanamycin resistance encoding gene	Amp Kan	Ketley *et al*., 1997
pAV35	Cloning vector harbouring a 850 bp chloramphenicol resistance encoding gene	Amp Cm	van Vliet *et al*., 1998
pAC1A	pGEM®-T ligated to *aac*(3)IV amplified *aac*-targeted primers	Amp Apr	Cameron and Gaynor, 2014
pEC86	Contain the *E. coli* cytochrome *c* maturation (ccm) genes with constitutive expression by the tetracycline promoter	Cm	Arslan *et al*., 1998
pC46	Cloning vector harbouring *C. jejuni* pseudogene *cj0046* and *cat* gene used for gene complementation	Cm	Duncan Gaskin, IFR, UK
pK*metK*	Cloning vector harbouring *C. jejuni* pseudogene *cj0046*, *kan* gene and *metK* promoter, used for gene complementation	Kan	Duncan Gaskin, IFR, UK
pC*metK*	Cloning vector harbouring *C. jejuni* pseudogene *cj0046*, *cat* gene and *metK* promoter, used for gene complementation	Cm	Duncan Gaskin, IFR, UK
pK*fdxA*	Cloning vector harbouring *C. jejuni* pseudogene *cj0046*, *kan* gene and *fdxA* promoter, used for gene complementation	Kan	Duncan Gaskin, IFR, UK

pC*fdxA*	Cloning vector harbouring *C. jejuni* pseudogene *cj0046*, *cat* gene and *fdxA* promoter, used for gene complementation	Cm	Duncan Gaskin, IFR, UK
pPR-IBApelBJ	Used for over-expression of proteins with C-terminal Strep-tag under control of IPTG inducible T7 promoter	Amp	Grein *et al*., 2010
pET21a(+)	Used for over-expression of proteins with C-terminal His-tag under control of IPTG inducible T7 promoter	Amp	Novagen
pGEM1153kan	pGEM3Zf(-) containing the first 20 and last 20 bp of *cj1153* (plus flanking DNA) with the *kan* cassette inserted in place of the deleted sequence	Amp Kan	This study
pGEM1020Cat	pGEM3Zf(-) containing the first 31 and last 9 bp of *cj1020c* (plus flanking DNA) with the *cat* cassette inserted in place of the deleted sequence	Amp Cm	This study
pGEM0037kan	pGEM3Zf(-) containing the first 21 and last 10 bp of *cj0037c* (plus flanking DNA) with the *kan* cassette inserted in place of the deleted sequence	Amp Kan	This study
pGEM0158kan	pGEM3Zf(-) containing *cj0158c* and flanking DNA with the *cj0158c* ORF interrupted with the *kan* cassette	Amp Kan	This study
pGEM0854kan	pGEM3Zf(-) containing the first 20 and last 15 bp of *cj0854c* (plus flanking DNA) with the *kan* cassette inserted in place of the deleted sequence	Amp Kan	This study
pGEM0815kan	pGEM3Zf(-) containing the first 9 and last 20 bp of *c8j_0815* (plus flanking DNA) with the *kan* cassette inserted in place if the deleted sequence	Amp Kan	This study
pGEM0040kan	pGEM3Zf(-) containing *c8j_0040* and flanking DNA with the *c8j_0040* ORF interrupted with the *kan* cassette	Amp Kan	This study

pGEM1176kan	pGEM3Zf(-) containing the first 13 and last 6 bp of *cj1176* (plus flanking DNA) with the *kan* cassette inserted in place of the deleted sequence	Amp Kan	This study
pGEM0786Cat	pGEM3Zf(-) containing the first 17 and last 12 bp of *cj0786c* (plus flanking DNA) with the *cat* cassette inserted in place of the deleted sequence	Amp Cm	This study
pGEM1490kan	pGEM3Zf(-) containing the first 31 and last 10 bp of *cj1490c* (plus flanking DNA) with the *kan* cassette inserted in place of the deleted sequence	Amp Kan	This study
pGEM149087kan	pGEM3Zf(-) containing the first 31 bp of *cj1490c* and last 9 bp of *cj1487c* (plus flanking DNA) with the *kan* cassette inserted in place of the deleted sequence	Amp Kan	This study
pGEMcioABApr	pGEM3Zf(-) containing the first 22 bp of *cj0081* and last 19 bp of *cj0082* (plus flanking DNA) with the *apr* cassette inserted in place of the deleted sequence	Amp Apr	This study
pGEM0603kan	pGEM3Zf(-) containing the first 22 and last 46 bp of *cj0603c* (plus flanking DNA) with the kan cassette inserted in place of the deleted sequence	Amp Kan	This study
pGEM1000kan	pGEM3Zf(-) containing the first 2 and last 8 bp of *c1000* (plus flanking DNA) with the kan cassette inserted in place if the deleted sequence	Amp Kan	This study
pGEM1013kan	pGEM3Zf(-) containing the first 47 and last 29 bp of *cj1013c* (plus flanking DNA) with the kan cassette inserted in place of the deleted sequence	Amp Kan	This study
pGEM1207kan	pGEM3Zf(-) containing the first 3 and last 12 bp of *cj1207c* (plus flanking DNA) with the kan cassette inserted in place of the deleted sequence	Amp Kan	This study

pGEM1664kan	pGEM3Zf(-) containing the first 30 and last 38 bp of *cj1664* (plus flanking DNA) with the kan cassette inserted in place of the deleted sequence	Amp Kan	This study
pGEM1665kan	pGEM3Zf(-) containing the first 32 and last 49 bp of *cj1665* (plus flanking DNA) with the kan cassette inserted in place of the deleted sequence	Amp Kan	This study
pGEM166465kan	pGEM3Zf(-) containing the first 30 of *cj1664* and last 49 bp of *cj1665* (plus flanking DNA) with the kan cassette inserted in place of the deleted sequence	Amp Kan	This study
pGEM1261kan	pGEM3Zf(-) containing the first 18 and last 7 bp of *cj1261* (plus flanking DNA) with the kan cassette inserted in place of the deleted sequence	Amp Kan	This study
pGEM1262kan	pGEM3Zf(-) containing the first 12 and last 9 bp of *cj1262* (plus flanking DNA) with the kan cassette inserted in place of the deleted sequence	Amp Kan	This study
pGEM126162kan	pGEM3Zf(-) containing the first 18 bp of *cj1261* and last 9 bp of *cj1262* (plus flanking DNA) with the kan cassette inserted in place of the deleted sequence	Amp Kan	This study
pC1153	Plasmid construct of pC46 inserted with *cj1153* gene and upstream promoter region via *BsmB*I site	Cm	This study
pC*fdxA*1153	pC*fdxA* with *cj1153* inserted into *BsmB*I site under the control of the *fdxA* promoter	Cm	This study
pC*fdxA*1153 -H33A	As pC*fdxA*1153 but with nucleotide sequence changed so amino acid at position 33 (in full length protein) changed from His to Ala	Cm	This study
pC*fdxA*1153 -H95A	As pC*fdxA*1153 but with nucleotide sequence changed so amino acid at position 95 (in full length protein) changed from His to Ala	Cm	This study
pC*fdxA*1153His	pC*fdxA* with *cj1153* plus 5X His-tag inserted into *BsmB*I site under the control of the *fdxA* promoter	Cm	This study

pK*metK*1020	pK*metK* with *cj1020c* inserted into *BsmB*I site under the control of the *metK* promoter	Kan	This study
pK*fdxA*1020	pK*metK* with *cj1020c* inserted into *BsmB*I site under the control of the *metK* promoter	Kan	This study
pC*fdxA*0037	pC*fdxA* with *cj0037c* inserted into *BsmB*I site under the control of the *fdxA* promoter	Cm	This study
pC*metK*1176	pC*metK* with *cj1176* inserted into *BsmB*I site under the control of the *metK* promoter	Cm	This study
pK*metK*0786	pK*metK* with *cj0786c* inserted into *BsmB*I site under the control of the *metK* promoter	Kan	This study
pCtsdA	Plasmid construct of pC46 inserted with *c8j_0815* gene and upstream promoter region via *BsmB*I site	Cm	This study
pC0040	Plasmid construct of pC46 inserted with *c8j_0040* gene and upstream promoter region via *BsmB*I site	Cm	This study
pEtsdA	pPR-IBApelBJ containing *c8j_0815* gene minus start and stop codons cloned into *Nde*I/*EcoR*V restriction sites	Amp	This study
pEcj40	pPR-IBApelBJ containing *c8j_0040* gene minus start and stop codons cloned into NdeI/Eco47III restriction sites	Amp	This study
pET1153	pET21a(+) containing *cj1153* gene minus start and stop codons cloned into *Nde*I/*Xho*I restriction sites	Amp	This study
pET1020	pET21a(+) containing *cj1020c* gene minus start and stop codons cloned into *Nde*I/*Xho*I restriction sites	Amp	This study
pET0037	pET21a(+) containing *cj0037c* gene minus start and stop codons cloned into *Nde*I/*Xho*I restriction sites	Amp	This study

2.3.2 Genomic DNA (gDNA) extraction

The genomic DNA was isolated from *C. jejuni* strains NCTC 11168 and 81116 by using Wizard® genomic DNA kit (Promega) according to manufacturer's instruction. The gDNA concentration was measured (section 2.3.5) and diluted as appropriate for routine use in PCR (section 2.3.5) and stored in -20 ^{o}C.

2.3.3 Isolation of plasmid DNA

Plasmid DNA was isolated from *E. coli* strain DH5α using Qiaprep® Spin Miniprep kits (Qiagen) and Wizard® Plus Midiprep kit (Promega). The procedures were following manufacturer's instructions and resulting in RNA-free plasmid DNA.

2.3.4 Determination of nucleotide concentration

The concentration of DNA and RNA samples in this study was measured by BioPhotometer (Eppendorf) and Genova nano micro-volume spectrophotometer (Jenway) against ddH_2O only as the blank. The concentration was determined according to manufacturers' instruction. For high-quality DNA and RNA samples, the ratio of A_{260}/A_{280} should be above 1.8 and 2.0 respectively (double-stranded DNA with an A_{260} of 1.0 is 50 ng μl^{-1}; RNA with an A_{260} of 1.0 is 40 ng μl^{-1}).

2.3.5 Polymerase Chain Reaction (PCR)

The DNA polymerases used in this study include Accuzyme DNA polymerases, MyTaq (Both from Bioline), Phusion DNA polymerase (Fisher) and Q5® DNA polymerase (New England Biolabs). The final volume per reaction was 12.5 µL in 0.5 or 0.2 ml PCR tubes. Each reaction was prepared of the following:

DNA template	5 µL (not over 50 ng DNA)
dNTPs mix 1.25mM each stock	1 µL
10 x reaction buffer (containing Mg^{2+})	1.25 µL
5 nM forward primer	0.5 µL
5 nM reverase primer	0.5 µL
DNA polymerase	0.05 µL
Milli-Q water	4.2 µL
Total volume	12.5 µL

The PCR was performed in a Techgene thermal cycler (Techne). The initial denaturation was carried out at 95 or 98 ^{o}C for 3 minutes, and then the reaction continued for 30 cycles of amplification: denaturing for 10 seconds at 94 or 98 ^{o}C, annealing for 15 seconds at specific temperature calculated from T_m value of forward and reverse primers, and the extension time was from 10 seconds to 2 minutes (according to the manufacturers' instructions of different enzymes, usually was 30 seconds per 1 kb) at 72 ^{o}C. The final extension was 5 minutes at 72 ^{o}C. Then the amplified DNA product was visualised by horizontal agarose gel electrophoresis and purified by QIAquick PCR purification kit (Qiagen).

Colony-PCR was carried out for quick screening of the correct clones of *E.coli* and *C. jejuni*. Tiny amount of cells were transferred by sterilised toothpick and resuspended in ddH_2O in a PCR tube for further PCR amplification, which was carried out by the 2X MyTaq polymerase (Bioline) with specific primers. Also, in order to confirm the correct construction of plasmids prior to transformation into *E.coli* and *C. jejuni*, a PCR was performed by the same polymerase using ddH_2O-diluted plasmids as templates.

2.3.6 DNA oligonucleotides

All primers (Table 2.5) synthesized from Sigma-Aldrich were used in mutants and complemented strains construction of *C. jejuni* and recombinant protein expression in *E. coli*.

Table 2.5 Primers used in this study

Name	Sequence (5' to 3')
M13 forward	TGTAAAACGACGGCCAGT
M13 reverse	CAGGAAACAGCTATGACC
3zf-F	GCCAGTGAATTGTAATACGACTC
3zf-R	ACGCCAAGCTATTTAGGTGACAC
pGEM1153 5F	GAGCTCGGTACCCGGGGATCCTCTAGAGTCACCTTCTAAATGCGGACAAT
Kan1153 5R	AAGCTGTCAAACATGAGAACCAAGGAGAATACTACTAATAATTTTTTCAT
Kan1153 3F	GAATTGTTTTAGTACCTAGCCAAGGTGTGCAAAATAATTTCTAAAAAAGG
pGEM1153 3R	AGAATACTCAAGCTTGCATGCCTGCAGGTCCTTTAAAAAAAGCCATCAAA
pGEM1020 5F	GAGCTCGGTACCCGGGGATCCTCTAGAGTCAAAACAAAGCAAGGTTTTAG
ISACat1020 5R	AAGCTGTCAAACATGAGAACCAAGGAGAATTTGAACTAATAAACAACCAG
ISACat1020 3F	GAATTGTTTTAGTACCTAGCCAAGGTGTGCCTAAAATAAAATGTAAAAAC

pGEM1020 3R	AGAATACTCAAGCTTGCATGCCTGCAGGTCAAACTCTACTTGCATATTTC
pGEM0158 5F	GAGCTCGGTACCCGGGGATCCTCTAGAGTCATTGATAGTTTTGATCATGC
Kan0158 5R	AAGCTGTCAAACATGAGAACCAAGGAGAATGACTTCATGTTCATCATTTG
Kan0158 3F	GAATTGTTTTAGTACCTAGCCAAGGTGTGCAATCCTAGTATTATCAACTC
pGEM0158 3R	AGAATACTCAAGCTTGCATGCCTGCAGGTCACAACTAATCCATCTAAAAG
pGEM0854 5F	GAGCTCGGTACCCGGGGATCCTCTAGAGTCTCTTTACAAATATGATCAGG
Kan0854 5R	AAGCTGTCAAACATGAGAACCAAGGAGAATCATTAAAACAATTTTCAAAG
Kan0854 3F	GAATTGTTTTAGTACCTAGCCAAGGTGTGCAAGGAAGAAAAATGACAAAC
pGEM0854 3R	AGAATACTCAAGCTTGCATGCCTGCAGGTCCGAATAGCACTCATGGTTGC
pGEM0037 5F	GAGCTCGGTACCCGGGGATCCTCTAGAGTCGCTTTTTTTGCGGAATTTTG
Kan0037 5R	AAGCTGTCAAACATGAGAACCAAGGAGAATCAATAAAATGTGTTTTTTCA
Kan0037 3F	GAATTGTTTTAGTACCTAGCCAAGGTGTGCAGGAGAATGATTAATTTTGG
pGEM0037 3R	AGAATACTCAAGCTTGCATGCCTGCAGGTCATCACAAAGACTATGCCAAA
pGEM0815 5F	GAGCTCGGTACCCGGGGATCCTCTAGAGTCTTATCCAATCACCTTCTTTT
Kan0815 5R	AAGCTGTCAAACATGAGAACCAAGGAGAATTTTATTCATCAATTTTCCTC
Kan0815 3F	GAATTGTTTTAGTACCTAGCCAAGGTGTGCCAAATATGATCAAAAAATAA
pGEM0815 3R	AGAATACTCAAGCTTGCATGCCTGCAGGTCCAAAGATGAGCAAAATGGTA
pGEM0040 5F	GAGCTCGGTACCCGGGGATCCTCTAGAGTCCTAAAATCAATTTGAACTGC
Kan0040 5R	AAGCTGTCAAACATGAGAACCAAGGAGAATTTCTTTTAGCCATTTAAAAT
Kan0040 3F	GAATTGTTTTAGTACCTAGCCAAGGTGTGCGCTTATGGTATTAAAGACGG
pGEM0040 3R	AGAATACTCAAGCTTGCATGCCTGCAGGTCCGAAGAAGGGATTAAAAGTC
pGEM1176 5F	GAGCTCGGTACCCGGGGATCCTCTAGAGTCTTTAGAATGGGCTAGAGTGC
Kan1176 5R	AAGCTGTCAAACATGAGAACCAAGGAGAATACCAACCACCCATTTTATTC
Kan1176 3F	GAATTGTTTTAGTACCTAGCCAAGGTGTGCGCTTAAGGTTTAGTCTTTTG
pGEM1176 3R	AGAATACTCAAGCTTGCATGCCTGCAGGTCTACCCGCATCATTGACATAG
pGEM0786 5F	GAGCTCGGTACCCGGGGATCCTCTAGAGTCCACAAGTGATTTTAAGCCTG
ISACat0786 5R	AAGCTGTCAAACATGAGAACCAAGGAGAATCATATACTTTACACTTTAAG
ISACat0786 3F	GAATTGTTTTAGTACCTAGCCAAGGTGTGCAAAACAAAATAGGCATTAAA
pGEM0786 3R	AGAATACTCAAGCTTGCATGCCTGCAGGTCTTTTATCTTCTAAGTCTTGC
pGEM1490 5F	GAGCTCGGTACCCGGGGATCCTCTAGAGTCTCTGATAGGTGAAAAAATTG
Kan1490 5R	AAGCTGTCAAACATGAGAACCAAGGAGAATAGTCGTAATTTAATACATTA
Kan1490 3F	GAATTGTTTTAGTACCTAGCCAAGGTGTGCGGCAGCATAAAAAGGAGAAA
pGEM1490 3R	AGAATACTCAAGCTTGCATGCCTGCAGGTCTCATAAGGAACATTGAAAAC
Kan1487 3F	GAATTGTTTTAGTACCTAGCCAAGGTGTGCGGTGAATGATGGAAAATAAT
pGEM1487 3R	AGAATACTCAAGCTTGCATGCCTGCAGGTCATCTCGTTACTTACTTTTTG
pGEM0081 5F	GAGCTCGGTACCCGGGGATCCTCTAGAGTCTTCAAATTCTCCAAATGAAC

Apr0081 5R	TTATTCCTCCTAGTTAGTCACAACGCTACTAAGTTCGTTC
Apr0082 3F	TACCTGGAGGGAATAATGACGATGATCACGCATATTAAGG
pGEM0082 3R	AGAATACTCAAGCTTGCATGCCTGCAGGTCTAAAAAAATGCTGATTGAAG
pGEM0603 5F	GAGCTCGGTACCCGGGGATCCTCTAGAGTCGTTGCGGTGTACAAAAACCC
Kan0603 5R	AAGCTGTCAAACATGAGAACCAAGGAGAATAAATAATACCAAAAATACGC
Kan0603 3F	GAATTGTTTTAGTACCTAGCCAAGGTGTGCGGGTTTTATCAGTGCTGATG
pGEM0603 3R	AGAATACTCAAGCTTGCATGCCTGCAGGTCAGTTGATTGAGTTCAAATAC
pGEM1000 5F	GAGCTCGGTACCCGGGGATCCTCTAGAGTCGCATAGAAGTTTCTTTATCG
Kan1000 5R	AAGCTGTCAAACATGAGAACCAAGGAGAATATGAGTGATTCCTTTATTTA
Kan1000 3F	GAATTGTTTTAGTACCTAGCCAAGGTGTGCAATCATAAACATAATAACCG
pGEM1000 3R	AGAATACTCAAGCTTGCATGCCTGCAGGTCTCTTAAATACATACGAACAG
pGEM1013 5F	AGAATACTCAAGCTTGCATGCCTGCAGGTCCGAATCCTCTTGAGCGCACC
Kan1013 5R	GAATTGTTTTAGTACCTAGCCAAGGTGTGCGGAAGCGAAATTTTGTGGGC
Kan1013 3F	AAGCTGTCAAACATGAGAACCAAGGAGAATACAACCGAAACTCTTAAATC
pGEM1013 3R	GAGCTCGGTACCCGGGGATCCTCTAGAGTCGGTTAATTTCTTAGGTTATG
pGEM1207 5F	GAGCTCGGTACCCGGGGATCCTCTAGAGTCTTTATCGACGCCAATTACAG
Kan1207 5R	AAGCTGTCAAACATGAGAACCAAGGAGAATCATTATTTATCAATCCTTTA
Kan1207 3F	GAATTGTTTTAGTACCTAGCCAAGGTGTGCGCTATACTTTAATGTTTAAT
pGEM1207 3R	AGAATACTCAAGCTTGCATGCCTGCAGGTCATCAAAAGTAACCGCTGAAG
pGEM1664 5F	GAGCTCGGTACCCGGGGATCCTCTAGAGTCATATCTTGGATAATGAAAAC
Kan1664 5R	AAGCTGTCAAACATGAGAACCAAGGAGAATAATGCTTAAGATTAAAAGGC
Kan1664 3F	GAATTGTTTTAGTACCTAGCCAAGGTGTGCGGGAATTTTTCGAATCCAAG
pGEM1664 3R	AGAATACTCAAGCTTGCATGCCTGCAGGTCATGCTATAAGGAGTTAAGCC
pGEM1665 5F	AGAATACTCAAGCTTGCATGCCTGCAGGTCCAAATTTATGAAAGTCCTAC
Kan1665 5R	GAATTGTTTTAGTACCTAGCCAAGGTGTGCAACTCCTTATAGCATACTTG
Kan1665 3F	AAGCTGTCAAACATGAGAACCAAGGAGAATAAGAAATAAGCTTGGATTCG
pGEM1665 3R	GAGCTCGGTACCCGGGGATCCTCTAGAGTCGCCAAATTCGCAGATCGAAC
pGEM1261 5F	GAGCTCGGTACCCGGGGATCCTCTAGAGTCATCTCCTAAATCCTCAAAAC
Kan1261 5R	AAGCTGTCAAACATGAGAACCAAGGAGAATCATCAACACATTAATCATTC
Kan1261 3F	GAATTGTTTTAGTACCTAGCCAAGGTGTGCAGGATGACAAAAAATTATTC
pGEM1261 3R	AGAATACTCAAGCTTGCATGCCTGCAGGTCTCATACAAGCCATCAAAATC
pGEM1262 5F	GAGCTCGGTACCCGGGGATCCTCTAGAGTCACCTGGAATTGATGGTCTTG
Kan1262 5R	AAGCTGTCAAACATGAGAACCAAGGAGAATATTTTTTGTCATCCTATCAG
Kan1262 3F	GAATTGTTTTAGTACCTAGCCAAGGTGTGCGAAAAATAATGGTAAAAGGC
pGEM1262 3R	AGAATACTCAAGCTTGCATGCCTGCAGGTCAAAAAAGATGGTTGCATCAG
1153com-F	TAAA**CGTCTC**ACATGCATTATCTTTAATTTCTTAAGATTT

fdxA-1153-F	AGGA**CGTCTC**ACATGAAAAAATTATTAGTAGTTTCTGCTTTGGC
1153com-R	AAAA**CGTCTC**ACATGTTATTATTTTAAAGTTTCAATATGAGCTT
1153com5XHis-R	CT**CGTCTC**ACATGTTAATGATGATGATGATGTTTTAAAGTTTCAATATGA
H33A forward	GCAGTATGCGCGGGTGCAAAT
H33A reverse	ATTTGCACCCGCGCATACTGC
1153comR H95A	AAAA**CGTCTC**ACATGTTATTATTTTAAAGTTTCAATCGCAGCTTCGATAG
metK-1020-F	ATGC**CGTCTC**ACATGATTGCACGCTGGTTGTTTATTAG
1020com-R	AATT**CGTCTC**ACATGTTATTATTTTAGAAATATATTAT
fdxA-0037-F	AGGA**CGTCTC**ACATGAAAAAACACATTTTATTGCTTG
0037com-R	GAAT**CGTCTC**ACATGTCATTCTCCTGGGAAGTGATTTGG
1176c-F	GAAGG**CGTCTCACATG**GGTGGTTGGTCAAGTCCAAG
1176c-R	TCAA**CGTCTCACATG**TTAAGCTTTTTTTGTTTCGTCTATACTTG
0786c-F	CTTAAAGTG**CGTCTCACATG**GTATTTTTAATCCCATTGC
0786c-R	TATG**CGTCTCACATG**CTATTTTGTTTTAAACAATTTTTC
0815c-F	CTTT**CGTCTC**ACATGAAGATTTTATTATAGCGAAAAAAC
0815c-R	CCAA**CGTCTC**ACATGTTATTTTTTGATCATATTTGTATAAG
0040com-F	CTAT**CGTCTC**ACATGACATAAAGTTAATATCATAAAA
0040com-R	TAAC**CGTCTC**ACATGTCATTCTCCTGGGAAGTGATTTG
Cam.je_fw	GGAGGAAAA***CATATG***AATAAATTTTC
Cam.je_rev	AATTGCCTTA***GATATC***TTTTTTGATC
Cj40_fw	AGGAAA***CATATG***AAAAAACACATTTTATTGCTTGG
Cj40_rev	CAAAAT***GATATC***TTCTCCTGGGAAGTG
NdeI1153-F	GCG***CATATG***AAAAAATTATTAGTAGTTTC
XhoIHis1153-R	CGG***CTCGAG***TTTTAAAGTTTCAATATG
NdeI1020-F	GCG***CATATG***ATTGCACGCTGGTTGTTTATTAG
XhoIHis1020-R	CGG***CTCGAG***TTTTAGAAATATATTATG
NdeI0037-F	GCG***CATATG***AAAAAACACATTTTATTGCTTGG
XhoIHis0037-R	CGG***CTCGAG***TTCTCCTGGGAAGTGATTTGG
Kan-F	ATTCTCCTTGGTTCTCATGTTTGACAGCTTAT
Kan-R	GCACACCTTGGCTAGGTACTAAAACAATTCAT
ISACAT-F	ATTCTCCTTGGTTCTCATGTTTGACAGCTTGAATTCCTGCAGCCCGGGGG
ISACAT-R	GCACACCTTGGCTAGGTACTAAAACAATTCACTAGTGGATCCCGGGTACC
Apr-F	TGACTAACTAGGAGGAATAAATGCAATACGAATGGCGAAAAG
Apr-R	GTCATTATTCCCTCCAGGTATCAGCCAATCGACTGGCGAGCG
cj0046-F	GAGCCAATCCTATTTCATCAGCTATG
cj0046-R	CCAGCCCATAAAAGTAAAAGCGAGAC

1176semi-F	GAATGAAGGAGAATAAAATGG
1176semi-R	CTTAAGCTTTTTTTGTTTCGTC
0786semi-F	AAAATGAAAATGCTGAGAATG
0786semi-R	TGATTTTTAATGCCTATTTTG
gyrAsemi-F	GTTATTATAGGTCGTGCTTTG
gyrAsemi-R	CAAAGTTGCCTTGTCCTGTAA
1153 RT-F	TCTTGGTGTTTCTGCTTTTG
1153 RT-R	TTGAAGTCTTTCAGCAGAAG
0037 RT-F	CTTATGTCTTAGTTTGAGTC
0037 RT-R	ATTCTTGCACAGGTCTTTTG
1020 RT-F	ATACCTTTGATGCAAATAAG
1020 RT-R	AATTCTAGATCCTATAACAC
sorA RT-F	CTGATACAGGATTGATTATC
sorA RT-R	TCTTGCATCCATCTTATAGC
napB RT-F	TTCTTATGAAAATGCACCAC
napB RT-R	ATAATGACTAGCAGGAAGTG
petCRT-F	GATTTTGCTAAGGGTGATGC
petC RT-R	CTAAGATCAGGTGGTATTAC
ccoP RT-F	ATCTTTAATTGGAGCTATTC
ccoP RT-R	TTATACTCTCCTATTCCATC
cioA RT-F	TGGCGGTTGAAGGTATTATG
cioA RT-R	CCAAAAAGCAGAAAGATTAC
cioB RT-F	TTATGGCTCTAAAACCTATG
cioB RT-R	AAAGGATTTTGCCAAGAAAC

*Esp3*I sites are underlined in bold, other restriction sites used for cloning such as *Nde*I (CATATG) *Xho*I (CTCGAG) and *EcoR*V (GATATC) sites are shown in bold and italic. Red sequence shows the position of mismatches in site-directed mutagenesis primers.

2.3.7 DNA gel electrophoresis

Horizontal agarose gel electrophoresis was used to analyse DNA fragments. The agarose powder (0.8 to 1.2% [w/v]) was dissolved in 1X TAE buffer and melted completely by heating in a microwave oven, and then ethidium bromide was added to a final concentration of 200 ng ml^{-1}. The cooled gel solution was poured into a cast and allowed to set with comb in place. DNA samples were mixed with 6X loading buffer and loaded into the wells alongside 1kb Hyperladder (Bioline). The electrophoresis was

carried out in 1X TAE buffer at a constant voltage of 150 volts until significant migration had occurred. The gel was visualized under an ultraviolet (UV) light source and the pattern was analysed by a Gene Flash Gel Doc system (Syngene).

2.3.8 Isolation DNA from agarose gel

DNA needed for further experiments was extracted, purified by QIAquick Gel Extraction Kit (Qiagen) and dissolved in an appropriate volume of ddH_2O.

2.3.9 Restriction enzyme digestion of DNA

The enzyme digestion of DNA was carried out for 1 hour or overnight in the presence of 10-50 units of enzymes with the final volume 10, 50 or 100 µl. According to the manufacturers' guidelines (NEB or Fisher), the buffer systems, reactive temperature and the demand of BSA varied with different restriction enzymes. In the case of double digestion with two enzymes, a compatible reaction buffer was chosen or the sequential digestion would be performed. The digested fragment was purified by QIAquick® PCR purification Kit (Qiagen) to remove residual enzyme and buffer.

2.3.10 Alkaline phosphatase treatment of DNA

In order to decrease self-ligation of vectors which could lead to high background while cloning, the linear plasmid DNA was treated with alkaline phosphatase which could remove 5´ phosphate of digested DNA. The reaction was carried out in a total volume of 50 µl containing 1 µl Antarctic Phosphatase (NEB) and 5 µl 10X reaction buffer. Then the mixture was incubated at 37^{o}C for 30 minutes then heat-inactivated at 65^{o}C for 5 minutes.

2.3.11 DNA Ligation

The concentration of both linearised plasmid and insert DNA was determined by a spectrophotometer (section 2.3.4). The molar ratio used the most of the insert to vector was 3:1 in ordinary ligation and 100 - 120 ng of vector DNA was always used per reaction. The insert DNA used per ligation was calculated by the following equation:

ng of vector × kb size of insert / kb size of vector × molar ratio of insert: vector (3:1)

= ng of insert

The volume of every component per one ligation could be calculated by computerised calculators which were available on the internet like Gibthon ligation ratio calculator (http://django.gibthon.org/tools/ligcalc/). The reaction was carried out in a total volume of 20 µl containing each DNA fragment, 2 µl of 10X ligation buffer, 1 µl T4 DNA ligase (NEB) and the Milli-Q water was compensated to 20 µl. The mixture was incubated at room temperature for 30 minutes for sticky ends or 2 hours for blunt ends ligation according to the manufacturer's manual (NEB). Then the ligation product was used directly in the transformation of chemically competent *E.coli* cells (section 2.5.1).

2.3.12 Isothermal assembly reaction (ISA)

The method of isothermal assembly reaction (ISA) was first introduced by Gibson in 2009 (Gibson *et al*., 2009). Three commercial enzymes were utilised to join several long DNA fragments in only one reaction and complicated cloning steps were avoided (Fig. 2.1). The ISA method was used to construct all insertion and knockout *C. jejuni* mutants in this study.

The mastermix was prepared by mixing ISA buffer (see appendix I) with T5 exonuclease (0.125 U, Epicenter), Phusion DNA polymerase (0.5U, Fisher) and *Taq* DNA ligase (4U, NEB) and 15 µl aliquots were made per one reaction in PCR tubes. The mastermix could be stored at -20 ^{o}C for at least 3 months without any loss of enzyme activities. The main backbone DNA used in the ISA reaction in this study was pGEM3Zf (-) (Promega). It was digested by *Hinc*II overnight and purified with ddH_2O. The other three assembly partners are an antibiotic cassette, 5' and 3' flanking regions of the target gene with two adaptors between them: the left and right linkers (LL and RL, Fig. 2.1 step 2). The length of each primer used in the PCR for ISA was 50 bp and included two parts: a linker with 30 bp in length and a 20 bp long fragment complemented to flanking DNA of the gene of interest or a specific antibiotic cassette. Furthermore, the first 30 bp of extreme primers (the forward primer of 5' flanking and the reverse primer of 3' flanking region) were complemented to pGEM3Zf (-) and the design of LL and RL allowed the adjacent DNA fragments to be joined, which shared the overlap of a single stranded terminal sequence and the antibiotic cassette would be in the middle of two flanking regions (Fig. 2.1 step 2). The kanamycin, chloramphenicol or apramycin cassettes were amplified by Kan, ISACAT and Apr primer sets with Phusion polymerase and purified by QIAquick gel extraction in order to avoid any false positive colonies forming when screening. The concentration of all four ISA fragments

were measured (see section 2.3.5) and combined in equimolar concentrations (15 – 150 ng of each, see section 2.3.11) in a total volume which did not exceed 5 µl (or compensated to 5 µl by ddH_2O). This DNA mixture was added in 15 µl ISA mastermix (thawed on ice). The ISA reaction was allowed to proceed at 50^oC for at least 2 hours in the Techgene thermal cycler (Techne) then the mixture was cooled down to room temperature. The ISA product (10 µl) was used to transform competent *E.coli* DH5α cells directly without any purification and the transformants were screened on LB agar plates containing appropriate antibiotics. Colony PCR was performed with M13 or 3zf primer sets (Table 2.5) to confirm clones with the correct assembling size. The plasmid-based PCR with different primer sets was also carried out when required after plasmid isolation. The plasmid with correct size of insertion was subsequently sequenced by automated DNA sequencing using 3zf primers (Core Genomic Facility, University of Sheffield Medical School, UK) and transformed into competent *C. jejuni* cells.

2.3.13 Site directed mutagenesis

Site directed mutagenesis was applied to modify nucleotides corresponding to specific codons and the variant recombinant proteins were then expressed. This was achieved by the combination of primer design and overlap extension PCR. The gene of interest was cloned into an appropriate expression vector by designed primers, which contained the required nucleotide differences to the native gene. Standard PCR was then performed by proofreading Phusion or Q5 polymerase and the product was purified. Then overlap extension PCR was performed according to the following:

Overlapping fragment 1 (purified)	4 µl (150~200 ng DNA)
Overlapping fragment 2 (purified)	4 µl (150~200 ng DNA)
dNTPs mix 1.25mM each stock	8 µl
10 x reaction buffer (containing Mg^{2+})	10 µl
5 nM forward primer	4 µl
5 nM reverase primer	4 µl
DNA polymerase (2U /µl)	1 µl
Milli-Q water	65 µl
Total volume	100 µl

The product of the overlap extension PCR was analysed by agarose gel electrophoresis and purified by QIAquick PCR purification kit. Then the purified fragment was cloned

into the appropriate expression vector with available restriction sites. The process of screening and sequencing was described in 2.3.12.

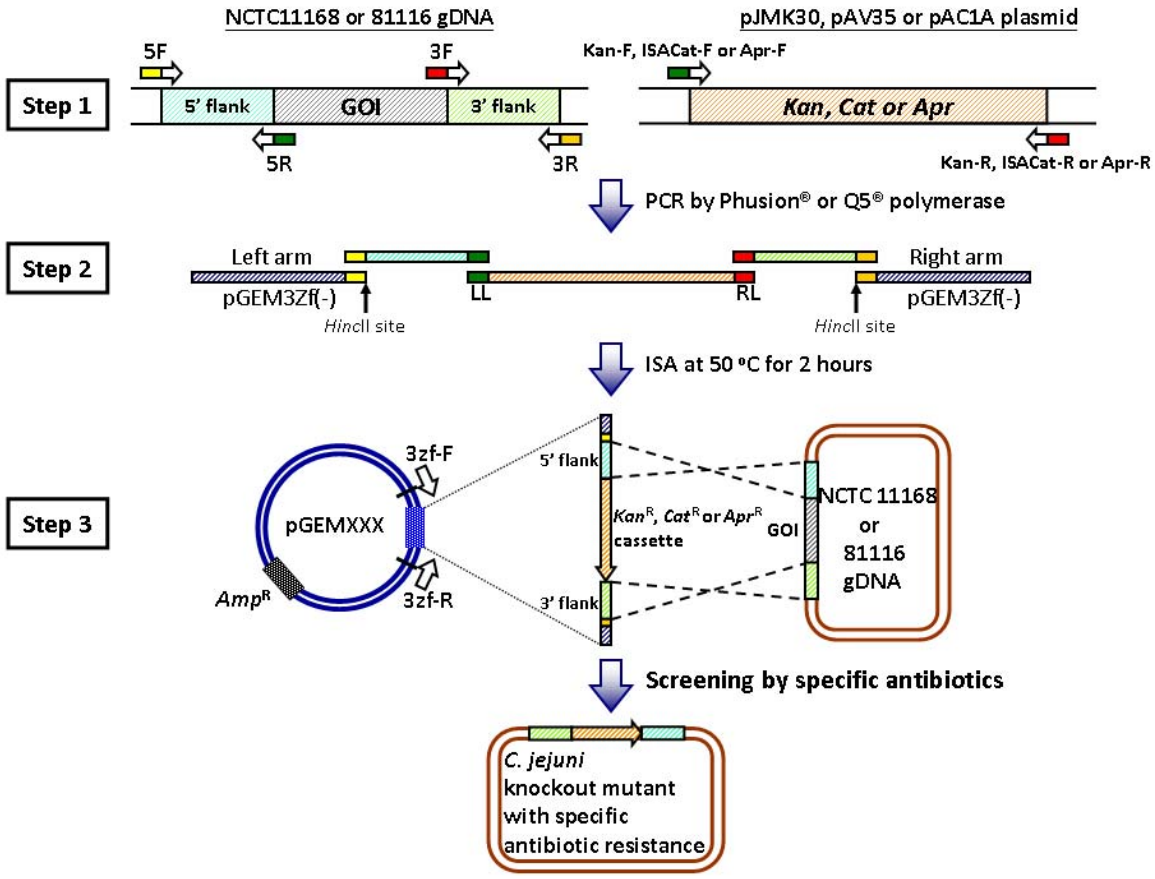

Figure 2.1 Method of gene-specific knockout mutations in *C. jejuni* by using isothermal assembly reaction (ISA). Step1: The 5' and 3' flanking regions of gene of interest (GOI) and an antibiotic cassette are amplified by three sets of primers containing complemented linkers respectively. **Step 2**: The purified fragments are mixed with the ISA buffer and incubated at 50°C for at least 2 hours. The ISA reaction will be carried out by T5 exonuclease, Phusion® DNA polymerase and *Taq* DNA ligase, which results in a plasmid containing each fragment. Correct constructs will be amplified in *E. coli* and further transformed into *C jejuni* competent cells via electroporation. **Step 3**: The homologous recombination occurs between the plasmid and the genomic DNA of *C. jejuni* where the target gene will be replaced by an antibiotic cassette and the successful transformant will be able to survive on plates

2.4 RNA preparation and manipulation

2.4.1 Total RNA isolation from *C. jejuni*

The overnight culture of *C. jejuni* in MHS (10 ml) was harvest at 8,000 r.p.m. and 4°C for 15 minutes then the pellet was resuspended in 1ml TRI Reagent® (Sigma). The RNA extraction protocol was according to the manufacturer's instruction with a few

modifications: The cell suspension was incubated at room temperature for 5 minutes and 200 µl of chloroform was added. The sample was shaken vigorously for 30 seconds and allowed to stand on ice for 10 minutes, then centrifuged at 13,000 r.p.m. and 4^{o}C for 15 minutes. The clear aqueous layer containing RNA was transferred to a clear and RNase-free tube which contained 700 µl ice-cold isopropanol. The mixture was gently inverted for 15 seconds then incubated at -20^{o}C for 60 minutes. The RNA sample was centrifuged at 13,000 r.p.m. and 4^{o}C for 20 minutes and the supernatant was decanted carefully. The pellet was washed by 750 µl ice-cold 75% ethanol and centrifuged by the same condition for 5 minutes. The clean pallet was air-dried for 15 minutes and resuspended in 50 µl nuclease-free ddH_2O. Total RNA preparations were DNase treated using the Turbo DNA-free™ Kit (Ambion) according to the manufacturer's instructions. The RNA concentration and purity was measured (section 2.3.5) and all RNA samples were stored at −80 ˚C.

2.4.2 Synthesis of complementary DNA (cDNA)

The cDNA was synthesized from 5 µg of total RNA by using SuperScript III Reverse Transcriptase (Invitrogen) according to the manufacturer's instructions. The final reaction volume was 20 µl.

2.4.3 Semi-quantitative reverse-transcription PCR (RT-PCR)

According to the instructions used in 2.4.2, the synthesized cDNA product could be used for PCR directly with no purification. The mastermix was made with 2 µl of cDNA, 5 nM forward and reverse primers (final concentration) and 2X Mytaq (Bioline, UK) to a final volume of 50 µl which then was divided into 8 µl aliquot in six PCR tubes and the reaction was carried out with Techgene thermal cycler (Techne). The sampling was achieved by removing tubes from the thermal cycler at cycle number 10, 15, 20, 25, 30 and 35 and all tubes were allowed to stand on ice until the final extension at 72^{o}C for all tubes for 5 minutes. The amplified fragments were separated on 1.3% agarose gels and the density of each band was analysed by the ImageJ program (http://imagej.nih.gov/ij/).

2.4.4 Real-Time PCR (qRT-PCR)

The gene-specific primers (20 bp in length) were designed to amplify 100 to 150 nucleotide fragments of target genes and *gyrA* (DNA gyrase subunit A) is an internal control. The specificity of primer sets was confirmed by ordinary PCR of a single band using total genomic DNA of *C. jejuni* NCTC 11168 as a template. The cDNA samples were prepared according to section 2.4.2. The qRT-PCR was performed in 96-well optical reaction plates (Applied Biosystems) and each well contained 20 µl following mixture:

cDNA (RT product from 5 µg total RNA)	1 µl
5 nM forward primer	1 µl
5 nM reverse primer	1 µl
ddH_2O	7 µl
SensiMix SYBR® Low-ROX Kit (Bioline)	10 µl
Total volume	20 µl

The QRT-PCR was carried out with in a MX3005P thermal cycler (Stratagene, UK) and the thermal cycling conditions were as follows: 95^{o}C for 10 mins; 40 cycles of (95^{o}C/15 sec) (55^{o}C 15sec) (72^{o}C 15sec). The data was analysed by the MxPro program (Agilent Technologies) where the threshold and the Ct value were determined with downstream data analysis performed with Microsoft EXCEL. No template reactions were taken as negative controls and the standard curve of each target gene was established using genomic DNA to compensate for variation in priming efficiency between different primer pairs. The protocol for the Standard Curve Method in the *User Bullitin #2* (*ABI Prism 7700 Sequence Detection System*, Subject: Relative Quantification of Gene Expression; Applied Biosystems) was used to calculate the transcriptional level of target genes. The expression of target genes was normalised to *gyrA* expression, which is constitutive in *C. jejuni*.

2.5 Preparation and transformation of competent cells

2.5.1 Preparation of Competent *E.coli* cells

The protocol for making competent *E. coli* cells was according to the Hanahan method (Hanahan, 1983). *E. coli* cultures were grown in 100 ml LB broth at 37^{o}C and 250 r.p.m. with initial OD_{600} = 0.1. The OD_{600} would reach 0.5 to 0.6 after 90 to 120 minutes incubation and cells were chilled on ice for 15 minutes then harvested by centrifugation at 10000 x *g* for 15 minutes at 4^{o}C. Supernatants were removed and the pellet was resuspended in 50 ml filter-sterilised RF1 then the cell solution was kept on ice for 15 minutes. Chilled cells were collected by centrifugation as the same condition and resuspended in 8 ml sterilised RF2. Competent *E. coli* cells were incubated on ice for another 20 minutes, aliquoted into pre-chilled microcentrifuge tube and stored at -80^{o}C. The viability and transformation efficiency were tested by the competent cell only or the transformation with intact vectors.

2.5.2 Transformation of competent *E. coli* by heat shock method

The competent *E. coli* cells (100 µl aliquot) were freshly thawed on ice for transformation. Plasmid DNA (10 to 20 ng) or ligation products (10 out of 20 µl reaction) were added into cells and mixed gently by swirling with a tip. The tube containing mixture was moved on ice for 3 minutes, transferred to 42 ^{o}C waterbath and incubated for 90 seconds (heat shock). Then the tube was kept on ice for 5 minutes incubation. For the recovery of transformant, 500 µl dYT was added and the cell was incubated at 37 ^{o}C for 1 hour with shaking at 250 r.p.m. Cells with the volume of 100, 200 and 300 µl were plated onto LB solid media containing specific antibiotics. Plates were incubated overnight at 37^{o}C until the size of colonies was large enough for performing colony-PCR.

2.5.3 Preparation and transformation of competent *C. jejuni*

Fresh *C. jejuni* cells were collected from one blood agar plate and resuspended in 750 µl BHI broth. Cells were pelleted by centrifugation at 11000 r.p.m. for 5 minutes at 4^{o}C and resuspended in 1 ml ice-cold washing buffer and centrifuged again. This step was repeated three times and cells were finally resuspended in 200 µl washing buffer. Plasmid DNA (200 to 400 ng) was added into a 100 µl aliquot cells and incubated on ice for 15 minutes. Then the mixture was transferred into a pre-chilled electroporation

cuvette (VWR international) which was immediately placed in *E.coli* Gene Pulser chamber (Bio-rad Laboratories) and electroporated with a pulse of 25 F, 2.5 kV and 200Ω for 4 milliseconds. BHI broth (100 µl) was added to the electroporated cells and plated onto two non-selective blood agar plates. After microaerobic incubation at 37 ^{o}C for 24 hours, cells grown on the plate were collected into 750 µl BHI, centrifuged (11,000 r.p.m. for 5 min, RT), resuspended in 400 µl BHI and plated onto selective blood agar in duplicate (200 µl per plate). Plates were incubated microaerobically at 37^{o}C until single colonies formed apparently by correct transformants which were checked by colony-PCR with the forward primer of the antibiotic cassette and the reverse primer of 3' flanking region.

2.6 Preparation of *C. jejuni* cell fractions

2.6.1 Cell free extracts (CFE)

An overnight liquid culture (50 ml) of *C. jejuni* strain NCTC 11168 in MHS or 81116 in BHI was collected by centrifugation at 10,000 x *g* for 15 min at 4 ºC. The pellet was washed by 20 mM phosphate buffer pH 7.4 (appendix A) and spun down by the same condition above. The pellet was resuspended in 1 ml phosphate buffer and the cell solution was sonicated for 2 × 30 seconds pulses at a frequency of 16 amplitude microns using a Soniprep 150 ultrasonic disintegrator (SANYO) and the cell debris or unbroken cells were removed by centrifugation (16,000 *x g* for 30 min, 4 ^{o}C). The supernatant was collected as the cell free extract and used freshly or stored at -20 ^{o}C.

2.6.2 Periplasm preparation by osmotic shock method

For periplasm preparation, 200 ml of mid-log phase cultures of *C.jejuni* in MHS or BHI were harvested by centrifugation at 9,500 r.p.m. for 15 minutes at room temperature, resuspended gently by pipetting in 5 ml STE buffer and incubated at room temperature with gentle shaking for 30 minutes. Cells were collected at 10000 x *g* for 10 minutes at room temperature and the supernatant was removed. Then, the pellet was resuspended in 2 ml of ice-cold 10 mM Tris-HCl (*p*H 8.0), incubated at 4^{o}C for 2 hours with gentle shaking at 20 r.p.m. and centrifuged at 11000 r.p.m. for 20 minutes at 4^{o}C. The supernatant was collected as periplasmic fractions and used immediately or stored at -20 ^{o}C for further experiments. The pellet left was used in membrane protein preparation.

2.6.3 Membrane protein preparation

In order to minimise contamination with periplasmic proteins, the membrane protein fraction was prepared from the residual plasmolysed cell pellet in the periplasm preparation. The pellet was resuspended in 8 ml of 20 mM Tris-HCl *p*H 8.0 and sonicated for 4 × 30 seconds pulses at a frequency of 16 amplitude microns. CFE was separated from cell debris by centrifugation at 16,000 x *g* for 30 min at 4 ºC and the supernatant was transferred into a 10 ml ultracentrifugation tube. The top space of the tube was filled with 20 mM Tris-HCl *p*H 8.0 and the membranes were collected by further ultracentrifugation at 40,000 x *g* for 2 hr at 4 ^{o}C. The supernatant was discarded carefully and the pellet containing membrane proteins was resuspended in 1 ml of 20 mM Tris-HCl *p*H 8.0 and stored in -20^{o}C for further analysis.

2.7 Protein manipulation

2.7.1 Determination of protein concentration by Bradford assay

Two major assays were used to determine the concentration of protein solutions; they were the Bradford assay (soluble protein only; Bradford, 1976) and the Lowry assay (intact cells and membranes; Markwell *et al*., 1978). The volume of reagents in both assays used in this study was scaled down to fit in the volume of a 96-well plate. The Bradford assay was carried out according to the original paper with slight modifications. Dye solution (Bio-Rad) was 4X diluted with ddH_2O and 200 µl diluted dye was added into 50 µl of protein standards with series of concentration (0 to 100 µg/ml, diluted from 1 mg/ml HPLC-grade BSA; Sigma) and appropriately diluted samples by a multi-channel pipette respectively. The plate was incubated at room temperature for 10 min and the OD_{595} was measured by a plate reader (VICTOR®X3 Multilabel Plate Reader made by PerkinElmer). The protein concentration of unknown samples was calculated by reference to the standard curve determined from protein standards.

2.7.2 Lowry assay

The assay for determining the protein concentration of whole cells and membrane fractions was modified from the Lowry method (Markwell *et al*., 1978). The solution C was made freshly before use by mixing solution A and B in a 100:1 ratio (v/v) and 150 µl of solution C was added into 50 µl of protein standards with series of concentration (0 to 200 µg/ml BSA, Sigma) and diluted samples respectively in a 96-well plate. The

plate was incubated at room temperature for 1 hour. Afterward 15 ul of 1X Folin-Ciocalteau's phenol solution (Sigma) was added into each well and mixed entirely. The mixture was incubated for another 45 minutes at room temperature and the OD_{600} was measure by the plate reader (PerkinElmer). The protein concentration of each sample was calculated by same way described in the Bradford assay.

2.7.3 Protein gel electrophoresis

The protein gel electrophoresis system used in this study is based on vertically run gels. According to the different composition of the gel and buffer solutions, two acrylamide-based systems used in the separation of protein samples are sodium dodecyl sulphate - polyacrylamide gel electrophoresis (SDS-PAGE) and Tricine-PAGE. SDS-PAGE is used in routine separation of protein mixtures (from 20 to 300 kD) for confirming the purity of protein samples or for further Western analysis while the Tricine-PAGE is able to give a better resolution in the separation of proteins with lower molecular weight (5 to 30 kD).

2.7.3.1 SDS-PAGE

The standard procedures of SDS-PAGE were according to Sambrook and Russell (Sambrook and Russell, 2001) with a few modifications and the electrophoresis was performed using the Mini-PROTEAN® 3 system (Bio-rad). Glass plates were rinsed entirely with dH_2O and cleaned with 75 % ethanol prior to use. Both separating and stacking gel solution were prepared according to Table 2.6 in 25 ml universal containers and APS was added at last to initiate the polymerisation. The separating gel solution was made first and pipetted into two assembled gel casts and the gel mixture was overlaid with pure ethanol and allowed to set. The top of polymerised gels was washed thoroughly with dH_2O to remove excess ethanol and residual water was also blotted from the gel with 3 mm filter papers (Sartorius). Then the stacking gel solution was made as above with a lower concentration of acrylamide and poured on top of the separating gel with a 10-well comb inserted. The comb was removed from the set gel and every well was rinsed entirely with ddH_2O to remove residual gel. The entire module with two set gels (or one set gel and a buffer dam) was placed in a tank containing 1X running buffer.

Protein samples (less than 25µl) were mixed with 5X SDS sample buffer in a 5:1 ratio (v/v) before boiling for 5 minutes and the mixture was allowed to incubate on ice for 5 minutes for cooling down. Samples were loaded onto the gel along with PageRuler® Prestained Protein Ladder (Thermo Scientific) molecular weight standard. The gel module was filled with 1X running buffer to the top and connected to a power supply (Bio-rad). Lower voltage was applied for the sample stacking (50 or 75 V), then the constant voltage (150 V) was applied until the bromophenol blue tracking dye reached the bottom of the gel. Gels were stained with Coomassie brilliant blue R (Sigma) for 30 minutes at room temperature and de-stained until individual protein bands were visible.

2.7.3.2 BN-PAGE (first dimension)

The protocol of BN-PAGE is based on the method described by Wittig *et al*., (2006). The cathode buffer of the first dimension electrophoresis is comprised of Tricine, imidazole and coomassie blue G-250, which is able to maintain the integrity of protein complexes. The composition and the concentration of separating and stacking gels are listed in Table 2.7. The first dimension electrophoresis was carried out in a cold room with chilled buffer and the blue gel strip of first dimension BN-PAGE was then cut off and placed perpendicularly on the top of the second dimension gel (Tricine-PAGE or SDS-PAGE) for further separation.

2.7.3.3 Tricine-PAGE

The standard Tricine-PAGE method is according to the original paper (Schägger, 2006). The procedures are similar to SDS-PAGE but the buffer system is discontinuous: Tricine in the cathode buffer (see appendix A) has higher pI (8.3) than glycine (6.9) used in the running buffer of SDS-PAGE, which leads to different protein mobilities in the gel. Tricine-PAGE gives a better resolution for separating protein samples with molecular weight less than 10 kD. The composition and the concentration of separating and stacking gels are listed in Table 2.8.

For the purpose of separating *c*-type cytochromes with small molecular weight and further haem blots, reducing agents such as β-mercaptoethanol or dithiothreitol are not added in the sample buffer to avoid the dissociation of haem molecules. Protein samples were mixed with the non-reducing sample buffer and incubated at 42^{o}C for one hour then the mixture was loaded onto the gel along with the marker (Thermo Scientific).

The starting voltage was set as 50 V for 30 minutes stacking then increased to 100 V until the run ended.

Table 2.6 SDS-PAGE gel composition and polymerization conditions; unit: ml.

Solution	Separating gel				Stacking gel
	8 %	10 %	12 %	15 %	4.2 %
A*	2.7	3.4	4.0	5.0	1.4
B*	2.5	2.5	2.5	2.5	—
C*	—	—	—	—	2.5
ddH_2O	4.55	3.85	3.25	2.25	7.9
10 % SDS	0.1				0.1
10% APS**	0.15				0.1
Total Volume	10				10

* See appendix A
** Ammonium persulfate

Table 2.7 BN-PAGE (first dimension) gel composition; unit: ml.

Solution	Separating gel			Stacking gel
	8 %	10 %	12%	4 %
50% acrylamide/bis	1.6	2	2.4	0.8
3X Gel buffer*	3.34			3.34
Glycerol	1.0			—
ddH_2O	3.9	3.5	3.1	5.61
10 % APS	0.15	0.15	0.1	0.15
TEMED**	0.015			0.01
Total Volume	10			10

* See appendix A
** *N, N, N′, N′* - tetramethylethylenediamine

Table 2.8 Tricine PAGE gel composition and polymerization conditions; unit: ml.

Solution	Separating gel			Stacking gel
	8 %	10 %	12%	4 %
50% acrylamide/bis	1.6	2	2.4	0.8
3X Gel buffer*	3.34			3.34
Glycerol	1.0			—
ddH_2O	3.9	3.5	3.1	5.61
10 % APS	0.15	0.15	0.1	0.15
TEMED	0.015			0.01
Total Volume	10			10

* See appendix A

2.7.4 The expression of recombinant proteins in *E. coli*

2.7.4.1 Over-expression of recombinant *c*-type cytochromes in *E. coli*

The pET21a(+) (Novagen) and pEC86 vectors were used to over-express recombinant *c*-type cytochromes in *E. coil* strain BL21 (DE3). The pET21a(+) plasmid harbours an IPTG-inducible T7 promoter upstream of the multiple cloning site and also allows translational products carrying a hexa-histidine tag at the C-terminal sequence. The pEC86 plasmid is comprised of a *ccm* (cytochrome *c* maturation) operon, which is necessary for the maturation and expression of *c*-type cytochromes in *E. coli*. The gene of interest was amplified by PCR with specific primers carrying an *Nde*I site at the 5' end and *Xho*I site at 3' end (minus stop codon) and cloned into pET21a(+). The resulting vector was named pETXXXX (where XXXX corresponds to the gene number). The insert DNA was sequenced (Core Genomic Facility, University of Sheffield Medical School, UK) to be confirmed as correct and in frame with the histidine-tag. Then pETXXXX and pEC86 were co-transformed into *E.coli* strain BL21 (DE3) by heat shock and the transformants were screened by plating on LB agar containing carbenicillin (50 μg/ml) and chloramphenicol (30 μg/ml). The level of expression and solubility were tested by inoculating a single colony of transformant in 100 ml LB broth at different temperatures. The overnight culture was collected, resuspended in 2 ml PBS, broken by sonication (4 x 15 sec pulses at a frequency of 16 amplitude microns in a Soniprep150 ultrasonic disintegrator, SANYO) and centrifuged (13,000 r.p.m., 20 minutes, 4^{o}C). Then 10 μl supernatants were analysed by Tricine-PAGE and haem blot.

For the litre-scale protein over-expression and purification, the starting 5 ml overnight culture was inoculated in 1 litre LB broth with carbenicillin and chloramphenicol. Cells were grown at 37^{o}C with shaking at 200 r.p.m. for 16 to 18 hours and harvested by centrifugation at 9,500 r.p.m. for 15 minutes at 4^{o}C. The pellet was resuspended in 10 ml per gram cell paste of binding buffer and broker by sonication (8 x 15 sec pulses with the same condition as above) on ice. The cell debris was spun down as the same condition above and the supernatant containing recombinant *c*-type cytochrome was collected for further purification.

2.7.4.2 Over-expression of recombinant C8j_0040, CjTsdA and AvTsdA in *E. coli*

Single colonies of *E. coli* BL21(DE3) cells containing pEtsdA or pEcj40 with pEC86 were respectively inoculated in 5 ml NZCYM medium (Amresco) for 16 to 18 hours as the starting culture, which were poured into 500 ml NZCYM medium containing 50 μg/ml carbenicillin and 50 μg/ml chloramphenicol. Cells were grown at 37°C and 180 r.p.m. until reaching OD_{600} of 0.6, then the culture was switched to 25°C and the cells were harvested after incubation for 16 hours (no later than 20 hours). Cells were collected by centrifugation, resuspended in buffer W (100 mM Tris-HCl, 150 mM NaCl, pH 8.0) and lysed by sonication (8 x 15 sec pulses with the same condition as above). After removing insoluble cell materials by centrifugation (16,000 *x*g for 30 min at 4°C), recombinant CjTsdA and C8j_0040 proteins were collected form the supernatant for further purification.

2.7.5 Protein purification

For the purification of histidine-tagged recombinant proteins, the procedures were performed on an Akta Prime plus purification system (GE Healthcare).

2.7.5.1 Nickel affinity chromatography

The purification procedure of histidine-tagged recombinant proteins was carried out by using 5 ml HisTrap^{TM} HP columns (GE Healthcare, UK), following the manufacturer's guidelines. Proteins were typically applied to the column in the binding buffer, and then 100 to 150 ml binding buffer was allowed to pass through the column until the UV signal from the Akta Prime was totally flat. Linear gradient of 20 to 500 mM imidazole in elution buffer was performed for eluting purpose. Protein containing fractions were pooled, stored on ice and analysed for purity by SDS-PAGE.

2.7.5.2 Buffer exchange and protein concentration

Fractions containing recombinant proteins were pooled and applied into a dialysis bag (Sigma-Aldrich, 8,000 MWCO) with clamps on both ends. Then the dialysis bag was placed into 2 litres ice-cold phosphate buffer (pH 7.4) with gentle stirring at 4^{o}C. The phosphate buffer was replaced twice for every 6 hours until the dialysis ended. The de-salting sample was pooled again and applied into Vivaspin columns (Sartorius, UK)

with an appropriate molecular weight cut-off (MWCO), which were used to concentrate protein. When necessary, the Vivaspin column is also suitable for the buffer exchange with small-volume samples.

2.7.5.3 Ion-exchange chromatography

The recombinant protein used for ion-exchange chromatography was dialysed against to 50 mM Tris-HCl pH 8.0 overnight and concentrated to 1.5 to 2 ml. The sample was applied to a 5 ml HiTrap™ DEAE FF column (GE Healthcare, UK) and protein was eluted with a gradient of 0 to 1 M NaCl in the same buffer over 50 ml. Peak UV absorbing fractions were analysed by SDS-PAGE.

2.7.5.4 Purification of recombinant C8j_0040, CjTsdA and AvTsdA

The purification protocols were according to the manufacturer's instruction with modification. The Strep-Tactin resin (1 to 1.5 ml; IBA GmbH, Göttingen, Germany) was packed in a disposable plastic column (Thermo) by gravity, and then a porous pad was place on the top of resin. The cell free extract was applied to the column and allowed to flow through the resin by gravity and the resin was washed by 15 ml buffer W. Then the recombinant protein was eluted by buffer E containing D-desthiobiotin and the eluent with brown colour was pooled and analysed by SDS-PAGE. The resin had to be regenerated after use by buffer R containing 2-(4-hydroxyphenylazo) benzoic acid (HABA).

2.7.6 Western blotting

Cell-free extracts or periplasmic protein samples were separated by SDS-PAGE (section 2.7.3.1) and the gel was rinsed by chilled 1X transfer buffer (see Appendix A) for five minutes. The electroblotting was performed using Mini Trans-Blot® Electrophoretic Cell (Bio-Rad) and the transfer sandwich was assembled according to the manufacturer's instruction. The protein samples were transferred onto a nitrocellulose membrane (Hybond-C extra, GE Healthcare UK) at a constant current 400 mA for 1 hour in ice-cold 1X transfer buffer. When necessary, the electroblotted membrane could be kept in 6M urea-PBST overnight at 4^{o}C for the further reactions on the next day.

All immuno-detection steps were carried out at RT with constant agitation. PBST buffer was used as a base for urea-PBST, ECI buffer and for membrane washing (three times for 5 min each with 20 ml of PBST). ECI buffer was used in the dilution of anti-MfrA serum (from rat, BioServ UK Ltd, University of Sheffield, UK), anti-GroEL (from rabbit) and horse-raddish peroxidase (HRP) conjugated secondary antibodies (Anti-Rat IgG, Sigma-Aldrich; Anti-rabbit IgG, NEB).

The blocking was carried out with Gelatin-NET solution for 1 hour. After washing in PBST, the primary antibodies were diluted appropriately with ECI and applied to the membrane. The membrane was allowed to react with the primary antibodies for approximately 1 hr and washed in PBST. Then, the secondary antibodies in ECI were applied to the membrane and the incubation was carried out for another hour. After the final wash step in PBST, the antibody binding was visualised by means of enhanced chemiluminescence (ECL Kit, GE Healthcare) according to manufacturer's instructions. Exposure time was varied as necessary.

2.8 Biochemical analysis

2.8.1 Detection of *c*-type cytochromes by enhanced chemiluminescence (Haem blot)

The protocol was according to the original paper published by Vargas (Vargas *et al*., 1993) with modifications: protein samples were electroblotted from the gel of Tricine-PAGE to a nitrocellulose membrane (see section 2.7.6). Then, the membrane was washed by 1X PBS for five minutes at room temperature to remove excess SDS and methanol and transferred into a exposure cassette (Amersham Biotech). The pre-mixed solution A and B of the enhanced chemiluminescence kit (ECL, GE healthcare) was added onto the membrane and incubated with the membrane for one minute. In a dark room with a safety light, autoradiography film was placed on top of the membrane wrapped in saran wrap and exposed for different time intervals until the signal could be visualised easily. The X-ray film was developed in developing solution (Kodak), rinsed thoroughly in water, immersed in fixer (Kodak) and allowed to dry.

2.8.2 Enzyme assays

Unless otherwise stated, two major types of assays for measuring enzyme activity were performed in this study. The first method was based on measuring the absorbance change of methyl- or benzyl viologen at 37 ^{o}C using a Shimadzu UV-2401PC spectrophotometer while the other was monitoring the oxygen consumption rate in an airtight chamber at 37 ^{o}C using a Clark-type oxygen electrode linked to a chart recorder. Typically triplicates of 50 ml MHS cultures were grown microaerobically at 37^{o}C for 16 to 18 hours. Cells were harvested by centrifugation at 6,000 r.p.m. for 10 mins at 4^{o}C and washed by ice-cold suitable buffer twice to remove endogenous substrate. The pellet was resuspended in 1 to 2 ml of buffer and stored on ice. Cell free extracts (CFE), membranes and periplasmic fractions were prepared as described in section 2.6 and the protein concentration was determined according to section 2.7.1 and 2.7.2.

2.8.2.1 Viologen-linked assays

Methyl- or benzyl viologen linked reductase assays were performed with intact cells or periplasmic fractions in a 1 ml assay mixture contained in a screw top glass cuvette with a 10 mm light path (Hellma®) and a silicon seal was placed to prevent gas exchange during measurements. All buffers and the substrate solution were made anaerobically by sparging with oxygen-free argon for at least 30 mins. There were two major buffer systems used in this assay: 25 mM sodium phosphate buffer pH 7.4 (whole cells and nitrate reductase in the periplasm) and 10 mM Tris-HCl buffer pH 7.4 (periplasm) with 1 mM methyl viologen (nitrate and TMAO reduction) or benzyl viologen (fumarate reduction). The final concentration of electron acceptors was 5 mM (TMAO and sodium nitrate) and 10 mM (sodium fumarate). Cells or periplasmic fractions were added to the buffer and viologen mixture to the volume of 990 µl, and sparged with oxygen-free argon. Then, aliquots of freshly prepared sodium dithionite solution were injected into the cuvette until a steady absorbance at 585 or 578 nm was achieved (for methyl- or benzyl viologen respectively) and 10 µl of anaerobic solution of electron acceptors was injected into the cuvette to initiate the assay. The decreasing of absorbance was recorded in 6 minutes and the specific activities for all substrate were calculated using an extinction coefficient for methyl viologen of 11.8 mM^{-1} cm^{-1} at 585 nm and for benzyl viologen of 8.6 mM^{-1} cm^{-1} at 578 nm.

2.8.2.2 Measurement of tetrathionate reductase activity

Methyl viologen-linked tetrathionate reductase assays were carried out with recombinant *C. jejuni* or *A. vinosum* TsdA and C8j_0040 proteins in a 1 ml assay mixture containing oxygen-free 100 mM ammonium acetate buffer, pH 5, 0.3 mM methyl viologen and a series of final concentrations of sodium tetrathionate solution (from 0 to 4 mM) in a screw top glass cuvette with a silicone seal to prevent gas exchange at 30°C (AvTsdA) or 42°C (CjTsdA and C8j_0040). Concentrations of methyl viologen above 0.2 mM gave no further increase in rates. Recombinant proteins were added to the buffer plus methyl viologen mixture, sparged with argon for 6 min and aliquots of 2% titanium (III) citrate oxygen scavenger solution (Zehnder and Wuhrmann, 1976) was injected into the cuvette until a stable absorbance at 585 nm was achieved (above 2.0). The assay was initiated by the injection of an anaerobic tetrathionate solution and the absorbance decrease in the first 40 seconds was recorded. Controls without enzyme were used to correct where necessary for the chemical reduction of tetrathionate by the viologen. Activity is expressed as μmol tetrathionate reduced min^{-1} mg $protein^{-1}$ on the basis of a 1:2 molar ratio of tetrathionate reduced to viologen oxidized.

2.8.2.3 Assay of thiosulphate: ferricyanide reductase activity

For assay of electron transfer from thiosulphate to the artificial acceptor ferricyanide in cell-free extracts, cells were resuspended in 100 mM Tris-HCl buffer pH 7.5 and cell-free extracts were prepared by sonication as described in section 2.6.1. The assay mixture (1 ml final volume) contained 25 mM phosphate buffer (pH 7.4) or 25 mM ammonium acetate buffer (pH 5.5), 1 mM potassium ferricyanide and 8 mM sodium thiosulphate. The assay was started by addition of cell-free extract and ferricyanide reduction followed at 420 nm was recorded by the Shimadzu UV-2401PC spectrophotometer. An extinction coefficient for ferricyanide of 1.09 mM^{-1} cm^{-1} at 420 nm was used for rate calculations. Activity of the recombinant purified CjTsdA was measured in a similar way using 100 mM acetate buffer pH 4.0, 1 mM ferricyanide as electron donor and 8 mM thiosulphate as substrate. Measurements were started by adding enzyme and ferricyanide reduction followed at 420 nm was described as above.

2.8.2.4 Measurement of respiration rate by oxygen consumption

Substrate-dependent respiration rate was determined by measuring the change of dissolved oxygen concentration of cell suspensions in a Clark-type oxygen electrode (Rank Brothers), which is linked to a chart recorder and calibrated with air-saturated 25 mM phosphate buffer, pH 7.4 (220 nmol dissolved O_2 ml^{-1} at 37 ^oC) or 25 mM ammonium acetate buffer (pH 5.5). The sample of intact cells was prepared according to section 2.8.2. A zero oxygen baseline was measured by adding sodium dithionite. The volume of assay mixture was 2 ml, which contained appropriate volume of cell suspension and air-saturated 25 mM phosphate buffer (pH 7.4) in the electrode chamber. The cell suspension was maintained at 37^oC and stirred at a constant rate. Substrates (10 mM sodium fumarate, 1 mM sodium sulphite, 5 mM sodium thiosulphate and 0.25 mM *N,N,N',N'*- tetramethyl-*p*-phenylenediamine (TMPD) plus 1 mM ascorbic acid) were added by injection through a fine central pore in the airtight plug. The rate was expressed in nmol O_2 per min^{-1} mg $protein^{-1}$.

2.8.2.5 Measurement of tetrathionate reduction rates in intact cells

Rates of tetrathionate reduction by cell suspensions were measured by adding washed cells to 25 mM phosphate buffer (pH 7.4) containing 20 mM sodium formate to the final volume of 14.5 ml. The mixture was incubated at 37 ^oC for 10 minutes to allow all of the dissolved oxygen to be consumed. Then, 0.5 ml of 60 mM sodium tetrathionate was added to make 2 mM final concentration and 0.5 ml of samples was taken every 2 minutes. The cells were immediately removed by centrifugation (13,000 r.p.m., 3 mins at room temperature) and the tetrathionate concentration in the supernatants was measured as described in section 2.8.3.

2.8.2.6 Phenoloxidase assays

Phenoloxidase assays were carried out with whole cells as described by Hall *et al,* (Hall *et al.,* 2008). The 1 ml assay mixture contained 100 µl of cells and 25 mM sodium acetate buffer (pH 5.7). The chromogenic substrate *p*-phenylenediamine (*p*-PD) was used to initiate assays with the final concentration of 10 mM and the rate was recorded at 487 nm. The negative control without cells was performed to adjust rates for endogenous background oxidation of *p*-PD. Specific activities were calculated using an extinction coefficient for *p*-PD of 14.7 mM^{-1} cm^{-1} at 487 nm.

2.8.2.7 Alkaline phosphatase (PhoX) assays

For the purpose of measuring alkaline phosphatase activity, the cells were grown under conditions described in section 2.2.3. The enzyme assay was modified from van Mourik *et al* (van Mourik *et al*., 2008). The OD_{600} of overnight DMEM cultures with 0.08 mM [Pi] was measured and cells were harvested and resuspended in 0.9 ml 1M Tris-HCl, pH 8.5. Then, 0.1 ml of 10.75 mM *p*-nitrophenyl phosphate (Sigma) was added and the reaction was maintained at 37 ^{o}C for 5 to 10 min. To stop phosphatase activity, the reaction tube was chilled on ice, then 0.1 ml ice-cold 1M K_2HPO_4 was added and the cells were microfuged at 13,000 x *g* for 5 min. The supernatant was collected and the A_{550} and A_{420} were measured immediately. The units of alkaline phosphatase were calculated by the formula: $10^3 \times [A_{420} - (1.75 \times A_{550})] / t \times OD_{600} \times V$ where t is incubation time (minutes) and V is cell volume (ml).

2.8.3 Determination of thiosulphate and tetrathionate concentration in culture supernatants

BHI was the basal medium used for growing *C. jejuni* strain 81116 and derived mutants. 2 mM sodium thiosulphate ($Na_2S_2O_3$; Sigma Aldrich) or 4 mM sodium tetrathionate ($Na_2S_4O_6$; Sigma Aldrich) were added in starting cultures under microaerobic conditions. For the measurement of anaerobic growth, only 4 mM sodium tetrathionate was used as an artificial electron acceptor. Growth was monitored at specific time points by measurement of the OD_{600} and the supernatant was collected by centrifugation (13,000 r.p.m. for 5 min at 4 ^{o}C). Both methods are based on conversion to thiocyanate, followed by determination as the red iron complex after addition of ferric nitrate reagent ($Fe(NO_3)_3$; see Appendix I) and measurement of absorbance at 460 nm by reference to a standard curve. The concentration of thiosulphate in culture supernatants was measured by the method described by Urban (1961) with modifications. Firstly, 50 µl of the supernatant was diluted in 600 µl ddH_2O. Then, sodium acetate (200 µl), 50 µl of 200 mM KCN and 50 µl of 40 mM $CuCl_2$ were added sequentially to the sample and mixed well. 50 µl of $Fe(NO_3)_3$ was then added and the OD_{460} was measured immediately. The concentration of tetrathionate was also determined by modification of the method described by Kelly *et al* (1969). Supernatant (50 µl) was mixed with 450 µl ddH_2O, then 50 µl of 1M Tris acetate and 50 µl 200 mM KCN were added. Following through mixing and incubation for 5 min at room temperature, 50 µl of $Fe(NO_3)_3$ was then added and the OD_{460} was immediately measured against a blank containing 50 µl

ddH_2O in place of supernatant. The concentration of each compound in the sample was calculated respectively by reference to its standard curve.

2.8.4 Differential cytochrome *c* spectroscopy

In order to determine the content of *c*-type cytochromes in the periplasm, dithionite-reduced *minus* air-oxidised difference spectroscopy was performed. The concentration of periplasm was 1 mg/ml with the volume of 1 ml per quartz cuvette. Spectra were measured at room temperature by using a Shimadzu UV-2401 dual wavelength scanning spectrophotometer (Shimadzu). Reduced *minus* oxidised scans were carried out from 400 to 700 nm after the addition of sodium dithionite to the sample cuvette.

2.8.5 Analysis of enzyme rate data of TsdA

Primary plots of initial rate against substrate concentration fit to the generalised Hill equation provide the best way to extract the relevant kinetic parameters with enzymes like TsdA that use two molecules of the same substrate (Segel, 1993; Hensen et al., 2006) and were analysed by non-linear regression using Graph Pad Prism (version 6; Graph Pad Inc.).

Chapter 3

Identification of a novel type of bi-functional tetrathionate reductase (TsdA) in *C. jejuni* strain 81116

3.1 Introduction

The two-electron reduction of tetrathionate to thiosulphate (E_{M7} = +24 mV; Thauer *et al*., 1977) is a reaction that some bacteria can use to support growth under anaerobic conditions. Tetrathionate reduction has previously been associated with two types of unrelated electron transport enzymes; the three-component molybdoenzyme TtrABC typified by that characterized from *Salmonella typhimurium* (Hinojosa-Leon *et al*., 1986; Hensel *et al*., 1999) and the octahaem Otr enzyme found in *Shewanella* (Mowat *et al*., 2004). The active site of the highly specific Ttr enzyme contains a molybdopterin guanine dinucleotide (MGD) cofactor that is bound to TtrA (localized in the periplasm) and carries out the reductive cleavage of the sulphane-sulphur bond of tetrathionate. Electron transfer to TtrA is mediated by four [4Fe-4S] clusters in the periplasmic TtrB subunit, while the membrane bound TtrC subunit receives electrons from the menaquinol pool and transfers them to TtrB (Hensel *et al*., 1999). In contrast, the soluble periplasmic Otr enzyme can also reduce nitrite and hydroxylamine (Atkinson *et al*., 2007) and contains an active site haem with an unusual lysine ligation (Mowat *et al*., 2004).

The role of tetrathionate as a bacterial electron acceptor has gained increasing attention in recent years after it was proposed that *S. typhimurium* induces host-driven formation of tetrathionate from thiosulphate via the reactive oxygen species produced during inflammation (Winter *et al*., 2010). The tetrathionate is then used as a terminal electron acceptor via TtrABC, giving the bacteria a growth advantage compared to the majority of the commensal flora, which lack this enzyme. Tetrathionate respiration also allows the utilization of specific non-fermentable carbon sources such as ethanolamine, which also contributes to the competitiveness of *S. typhimurium* in the gut (Thiennimitr *et al*., 2011). This has provided an explanation for the *in vivo* function of Ttr and the role of tetrathionate, which has long been used to enrich for Salmonellae (Rappaport *et al*., 1956). Some other enteric pathogens like *Citrobacter* and *Proteus* can also respire tetrathionate and their genome sequences harbour Ttr homologues, although this ability has been less well studied (Oltman *et al*., 1979).

In *C. jejuni*, pathways to a variety of alternative electron acceptors have been identified, including fumarate (Sellars *et al*., 2002; Weingarten *et al*., 2009; Guccione *et al*., 2010), nitrate and nitrite (Pittman *et al*., 2007), trimethylamine *N*-oxide (TMAO) and dimethylsulphoxide (DMSO) (Sellars *et al*., 2002). However, inspection of the available genome sequences shows that neither Ttr nor Otr homologues are present, and it would be assumed that *C. jejuni* is unable to use tetrathionate as an electron acceptor. In this Chapter, it is demonstrated that, contrary to expectations, some strains of *C. jejuni* are capable of tetrathionate reduction and this can stimulate growth under oxygen-limited conditions. The enzyme responsible for this activity has been identified as a homologue of TsdA, a novel dihaem cytochrome c, first characterized in *Allochromatium vinosum*, a phototrophic sulphur oxidizing bacterium, as a thiosulphate dehydrogenase (Hensen *et al*., 2006; Denkmann *et al*., 2012). The physiological role in growth and the biochemistry of *C. jejuni* TsdA will be characterised. Also, the enzyme kinetics of the two TsdA enzymes from *A. vinosum* (AvTsdA) and *C. jejuni* (CjTsdA) will be compared, to elucidate their distinct roles in two species surviving in totally different environments. Finally, a possible model of TsdA in *C. jejuni* is depicted which indicates the role of TsdA in the electron transport chains of *C. jejuni* and its role under microaerobic and anaerobic conditions to maintain cell growth and survival.

The work described in this chapter has been published (Liu *et al*., 2013) and some of it was done in collaboration with Dr Christiane Dahl and Dr Kevin Denkmann, University of Bonn. Their experimental contributions and provision of data are explicitly acknowledged in the text and figure legends where appropriate.

3.2 Results

3.2.1. Tetrathionate stimulates the growth of *C. jejuni* strain 81116 under oxygen-limited conditions

The ability of tetrathionate to stimulate oxygen-limited growth of strain 81116 was first examined. Cultures of *C. jejuni* were incubated at 37°C in almost completely filled 500 ml shake flasks containing BHI medium plus 20 mM sodium formate as an artificial donor. Then cultures above were supplemented with or incubated without 10 mM tetrathionate as an electron acceptor. Under oxygen-limitation conditions, tetrathionate did support the growth of strain 81116 (Fig. 3.1 A, B). No increase in optical density was apparent in the absence of an added electron acceptor (Fig. 3.1 A), and the cells slowly lost viability (Fig. 3.1 B), consistent with previous studies (Sellars *et al*., 2002; Guccione *et al*., 2010). A rapid initial rise in optical density occurred in the presence of 10 mM tetrathionate (Fig. 3.1 A), accompanied by an increase in cell numbers (Fig. 3.1 B), indicating a short period of growth stimulation. Tetrathionate was depleted within 5 hours after inoculation and converted into thiosulphate with the expected 1:2 molar stoichiometry (Fig. 3.1 C). Although the tetrathionate-dependent stimulation in growth is not large, it is similar to those observed in previous studies with other alternative electron acceptors such as fumarate, nitrate, nitrite, DMSO and TMAO (Sellars *et al*., 2002; Smart *et al*., 2009; Hitchcock *et al*., 2010).

3.2.2. Identification of *tsdA* as a novel candidate tetrathionate reductase gene in *C. jejuni*

To confirm the tetrathionate reductase activity in *C. jejuni* was not contributed by enzymes like TtrABC or Otr (Hinojosa-Leon *et al*., 1986; Hensel *et al*., 1999, Atkinson *et al*., 2007), BLAST analysis was carried out and the results indicated that none of these proteins are encoded in the genome of strain 81116. Recently, the gene *Alvin_0091* (*tsdA*) from the purple sulphur bacterium *A. vinosum* which encodes a monomeric dihaem cytochrome *c* thiosulphate dehydrogenase was identified as the prototype of a family that, with the exception of the zeta-Proteobacteria (Emerson *et al*., 2007), was widespread among all other branches of the Proteobacteria, and was also found in Gram-positive bacteria (Denkmann *et al*., 2012). A *tsdA* homologue is also found in the genome sequences of several *C. jejuni* strains, suggesting that this pathogen may be able to utilise thiosulphate as an electron donor. We therefore hypothesized that

the TsdA enzyme might also be responsible for tetrathionate respiration by catalysing the reverse reductive cleavage reaction.

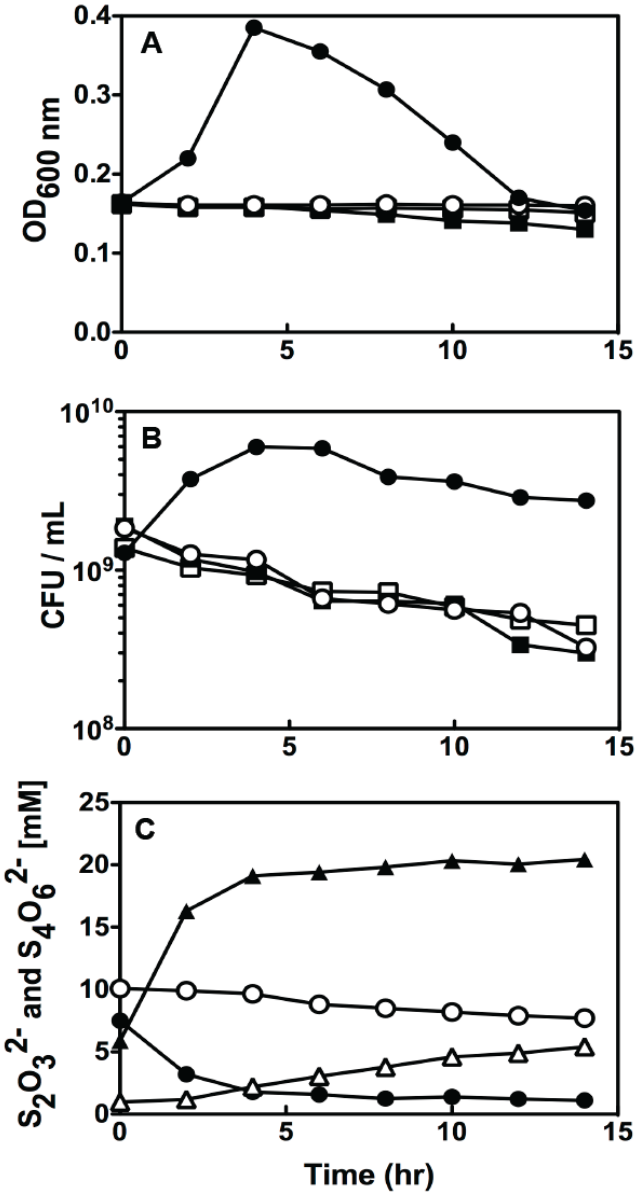

Figure 3.1 Tetrathionate supports the growth of *C. jejuni* under oxygen-limited conditions. (A) The optical density at 600 nm of the wild-type 81116 strain (closed symbols) is compared with that of a 81116 *tsdA* mutant (open symbols). In the absence of added tetrathionate (squares), no growth of either strain occurred. In the presence of 10 mM initial tetrathionate (circles), a rapid optical density increase of the wild-type but not the mutant was observed, followed by a decrease. This was correlated with the viable count measured in (B), by serial dilution and plating onto blood agar medium with microaerobic incubation. In (C), the period of wild-type cell growth was correlated with rapid tetrathionate consumption (closed circles) and concomitant thiosulphate accumulation (closed triangles), whereas in the *tsdA* mutant culture, tetrathionate decreased (open circles) and thiosulphate accumulated (open triangles) much more slowly. The data shown are from a single growth experiment, which was repeated three times with similar results.

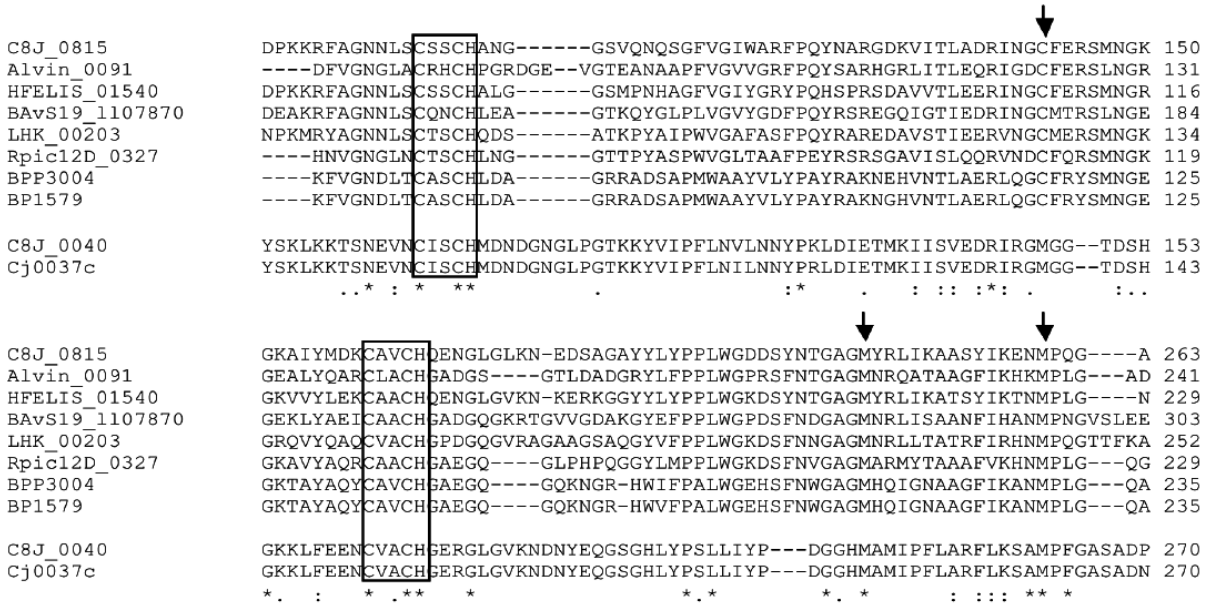

Figure 3.2. Sequence alignments of TsdA homologues. Haem binding motifs are indicated by boxes, putative distal haem ligands are marked with arrows. Strictly conserved residues are marked with asterisks. Species: *Campylobacter jejuni 81116 (ε-Proteobacterium, C8J_0815 and C8J_0040), Allochromatium vinosum DSM 180T (γ-Proteobacterium, Alvin_0091), Helicobacter felis (ε-Proteobacterium; HFELIS_01540), Brucella abortus S19 (α- Proteobacterium; BAvS19_II07870), Laribacter hongkongensis (β-Proteobacterium, LHK_00203), Ralstonia pickettii 12D (β-Proteobacterium; Rpic12D_0327), Bordetella parapertussis (β-Proteobacterium, BPP3004), Bordetella pertussis (β-Proteobacterium, BP1579), Campylobacter jejuni NCTC 11168 (ε-Proteobacterium; Cj0037).*

In *C. jejuni* strain 81116 the *tsdA* homologue is *c8j_0815*. Amino acid sequence analysis indicated C8j_0815 was very similar to the thiosulphate dehydrogenase identified by Denkmann *et al*., (2012) because of the following features (Fig. 3.2): Two -CXXCH- haem *c*-binding motifs, one conserved cysteine residue in the motif $ArgX_3Cys$ and two conserved methionines. In addition, a second *tsdA*-like gene is present in the *C. jejuni* 81116 genome, namely *c8j_0040*. However, its amino acid sequence is different in one major respect from that of the *c8j_0815* encoded protein: The strictly conserved cysteine residue present in C8j_0815 is replaced by a methionine in C8j_0040 (Fig. 3.2). This feature is significant, as site-directed mutagenesis has shown that this conserved cysteine is a haem ligand and is absolutely essential for enzyme activity as a tetrathionate-forming thiosulphate dehydrogenase for the characterized purple bacterial TsdA (Denkmann *et al*., 2012).

Comparative sequence alignment with *C. jejuni* subsp. *jejuni* NCTC 11168 showed that *cj0037c* in this strain encoded a protein identical in amino acid sequence to C8j_0040 (Fig. 3.1). However, the intact corresponding gene of *c8j_0815* does not exist in strain NCTC 11168. Its genome sequence revealed the presence of probable pseudogenes (*cj0873c*, *cj0874c* and *cj0876c*) together making a complete *tsdA* gene, where *cj0874c* encodes the haem binding sites and the active-site cysteine (Fig. 3.3). Thus, strain NCTC 11168 contains corrupted *tsdA*-like gene fragments, from which synthesis of a functional protein seems impossible. Furthermore, tetrathionate was unable to stimulate the growth of strain NCTC 11168 when incubated in media under oxygen-limited conditions (data not shown) and this is consistent with the interpretation above.

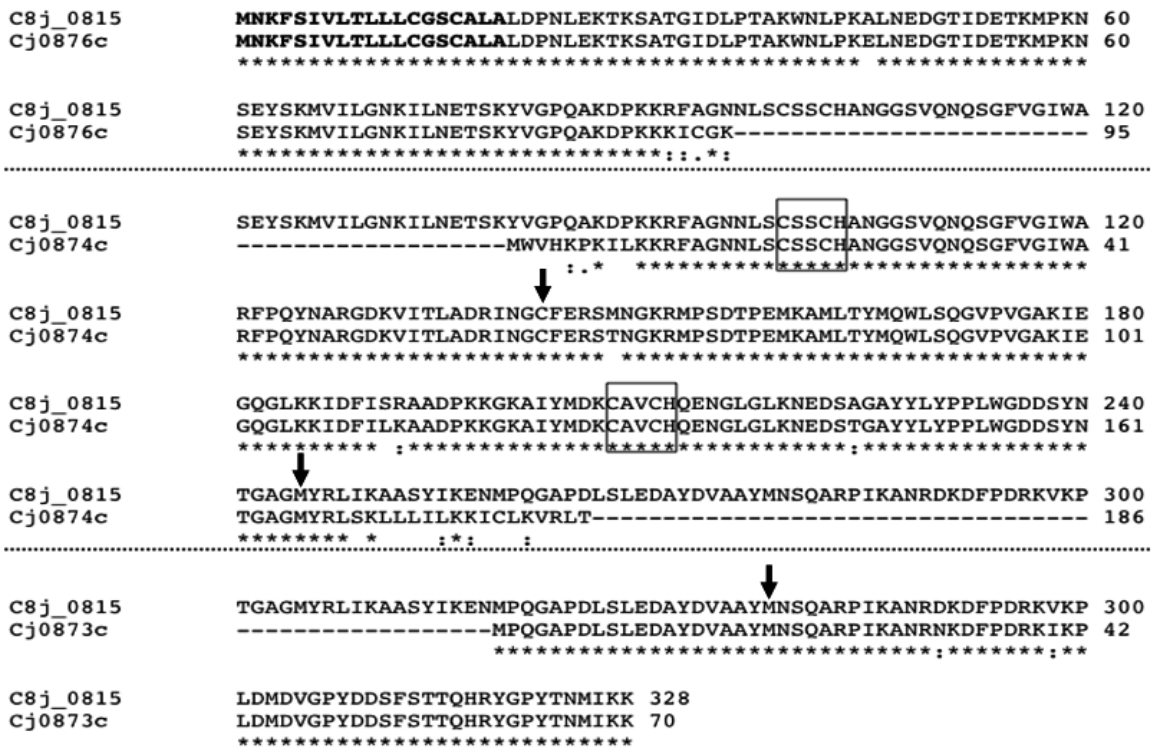

Figure 3.3. Alignment of the intact C8j_0815 (*tsdA*) gene encoding thiosulphate dehydrogenase in *C. jejuni* strain 81116 with three pseudogene fragments (*cj0874c-cj0876c*) in strain NCTC 11168. The N-terminal signal sequences are shown in bold. Boxes indicate the conserved haem binding CXXCH motifs. Arrows indicate the putative distal haem ligands. Asterisks indicate identical residues, colons indicate similar residues.

3.2.3. Construction of a *tsdA*⁻ mutant in strain 81116

The cloning strategy for creating a *tsdA* (*C8J_0815*) knockout mutant uses homologous recombination, where the target gene is replaced by an antibiotic cassette *in vivo* (Fig. 3.4). Two flanking regions containing linkers were amplified by two sets of primers (pGEM0815 5F / Kan0815 5R and Kan0815 3F / pGEM0815 3R) using 81116 genomic DNA as the template. The kanamycin resistant cassette (*kan*) with linkers was amplified from the vector pJMK30 by Kan-F and Kan-R. The backbone plasmid DNA pGEM3zf(-) was linearized by *Hinc*II then isothermal assembly (ISA) was carried out with the four fragments above. The ISA product pGEM0815kan was then transformed into *E.coli* strain DH5α and the transformants were screened by colony PCR by the primer sets of M13-F / M13-R and Kan-F / pGEM0815 3R to confirm the *kan* cassette was positioned between the two flanking regions with the correct orientation.

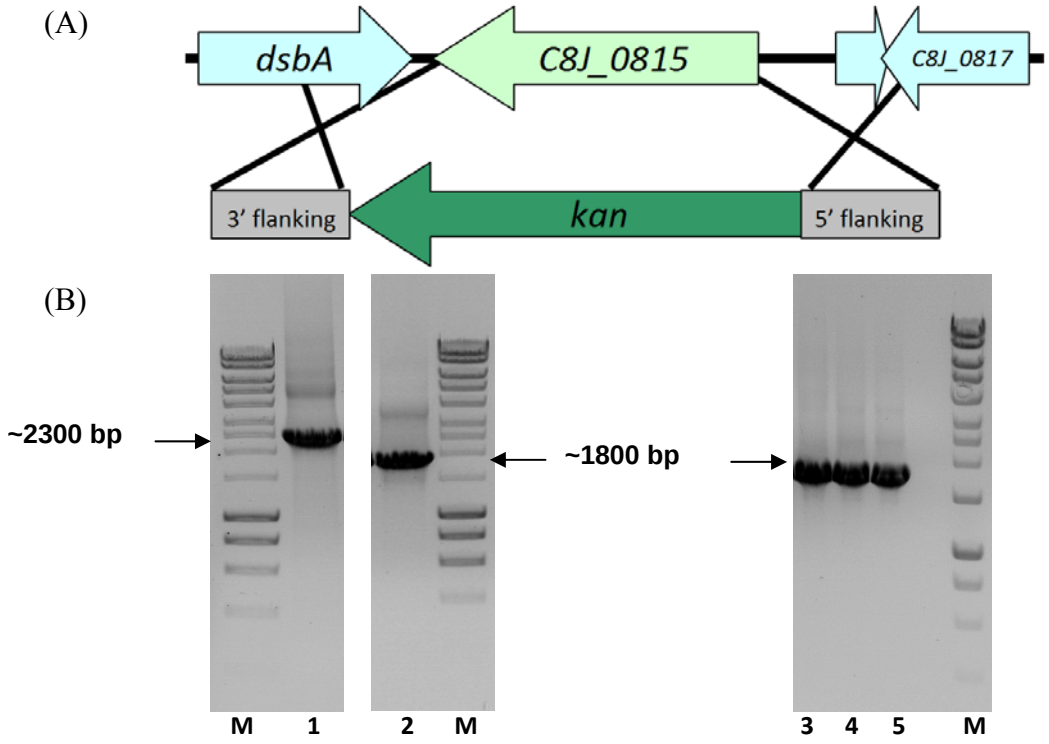

Figure 3.4. Constructions of pGEM0815kan and verification of *tsdA C. jejuni* strains. (A) The *tsdA* mutant was generated by the replacement of a *kan* cassette in the *C8J_0815* (*tsdA*) gene. **(B)** Agarose gel electrophoresis confirmation of pGEM0815kan constructs and *tsdA* mutants. Lane 1 and 2 show the PCR product obtained with the pGEM0815kan plasmid with specific primers and lane 3 ~ 5 were from *tsdA C. jejuni* transformants; lane 1: M13 primers; lane 2: Kan-F / pGEM0815-3R; lane 3~5: Kan-F / pGEM0815-3R; lane M: HyperLadder™ 1kb molecular weight marker (Bioline).

The pGEM0815kan vector was then transformed into *C. jejuni* strain 81116 by the electroporation method and the transformants screened on blood agar plates supplemented with kanamycin (50 μg/ml). The *tsdA* mutant was confirmed by colony PCR with Kan-F / pGEM0815-3R primers. The phenotype would also be confirmed by growth curve and biochemical analysis (section 3.2.2, 3.2.3 and 3.2.5).

3.2.4 Complementation of the *tsdA* gene in the *tsdA* mutant

The complementation of the *tsdA* gene was carried out by using the pC46 plasmid (Duncan and Gaskin, IFR, UK), which contains two flanking regions of the *cj0046* pseudogene and a *Esp3*I restriction site followed by a chloramphenicol resistance (Cm) cassette between *cj0046F* and *cj0046R*. The ORF of *tsdA* plus the upstream promoter region and ribosome-binding site (987 + ~200 bp) was PCR-amplified using the primers 0815c-F and 0815c-R. The resulting fragment was *Esp*3I-digested and cloned into the *Esp3*I site of alkaline phosphatase treated pC46 vector to create pCtsdA (Fig. 3.5 A). The construct was then transformed into *tsdA* mutant by the electroporation method and the insert in pC*tsdA* integrated the intact *tsdA* gene at the *cj0046* pseudogene locus, which was confirmed by colony PCR using primers 0815c-F and cj0046-R (Fig. 3.5 B).

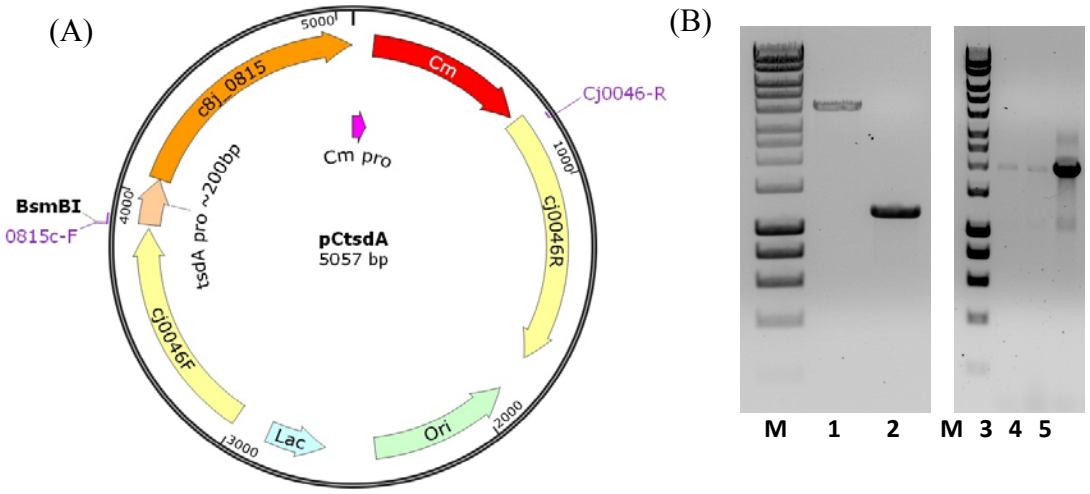

Figure 3.5 Constructions of pCtsdA and verification of *tsdA*$^+$ *C. jejuni* strains. (A) The map of pCtsdA. The *tsdA* gene (*c8j_0815*) plus 200 bp upstream fragment was cloned into pC46 vector. **(B)** Agarose gel electrophoresis confirmation of gene products. Lane 1: Linearized pC46 vectors; lane 2: PCR product of *tsdA* plus 200 upstream fragmants; lane 3~5: The colony PCR product obtained from *tsdA*/*tsdA*$^+$ *C. jejuni* transformants amplified by 0815c / cj0046-R primers; lane M: HyperLadder^{TM} 1kb molecular weight marker (Bioline).

3.2.5 Mutation of *tsdA* abolishes formate-dependent tetrathionate reduction in a short-term cell incubation assay and negates tetrathionate stimulated growth

For an assessment of the *in vivo* role of *tsdA* gene in the strain 81116, the *tsdA* mutant and the complemented merodiploid strain were compared with the wild-type parent. The periplasmic fractions of each strain above were prepared by a cold osmotic shock method (section 2.6.2) and analysed by 10% Tricine-PAGE. The haem blot was also performed with identical amount of sample (20 μg periplasm per lane). In the periplasm of the *tsdA* mutant, a specific ~36 kD periplasmic *c*-type cytochrome was absent which corresponded to the correct size of mature TsdA (Fig. 3.6 A). TsdA is present in both wild-type and complemented strains, as shown by haem blots of periplasmic proteins (Fig. 3.6 A). However, TsdA is not highly abundant according to the Coomassie blue staining but still could be detected by haem blots. In order to compare rates of tetrathionate reduction in 81116 wild-type, *tsdA* mutant and complemented strains, an anaerobic cell incubation assay was carried out. The physiological electron donor used in this assay was 20 mM formate and the cells were allowed to respire all of oxygen present before tetrathionate was added as an electron acceptor. The initial rate of reduction was measured as described in the section 2.8.2.5. Strain 81116 wild-type cells reduced tetrathionate rapidly under these conditions, while no rate was detectable with the *tsdA* mutant (Fig. 3.6 B). The complemented merodiploid mutant strain showed a restoration of activity to ~60% of the wild-type, presumably reflecting lower than wild-type expression of the integrated ectopic copy of *tsdA* (Fig. 3.6 B). These data clearly indicate that TsdA is able to act as a tetrathionate reductase in strain 81116. Accordingly, the observation of tetrathionate reduction *in vivo* supports the anaerobic growth results of wild-type 81116 and *tsdA* strains (Fig. 3.1). The *tsdA* mutant failed to show the rapid burst of tetrathionate stimulated growth under oxygen-limited conditions seen with the wild-type parent strain (Fig. 3.1 A) and lost viability over the course of the experiment as the same rate as the wild-type in the absence of an electron acceptor (Fig. 3.1 B). According to the Figure 3.1 panel A and B, the *tsdA* mutant was unable to utilise tetrathionate as an electron acceptor under anaerobic condition. However, the concentration of tetrathionate in *tsdA* cultures still dropped with time until the end of growth and was accompanied by the increase of thiosulphate (Fig. 3.1 C) but a similar phenomenon was not observed in control incubations (BHI-S plus formate and tetrathionate without cells, data not shown). It is suggested that there might be another enzyme able to slowly reduce tetrathionate to thiosulphate.

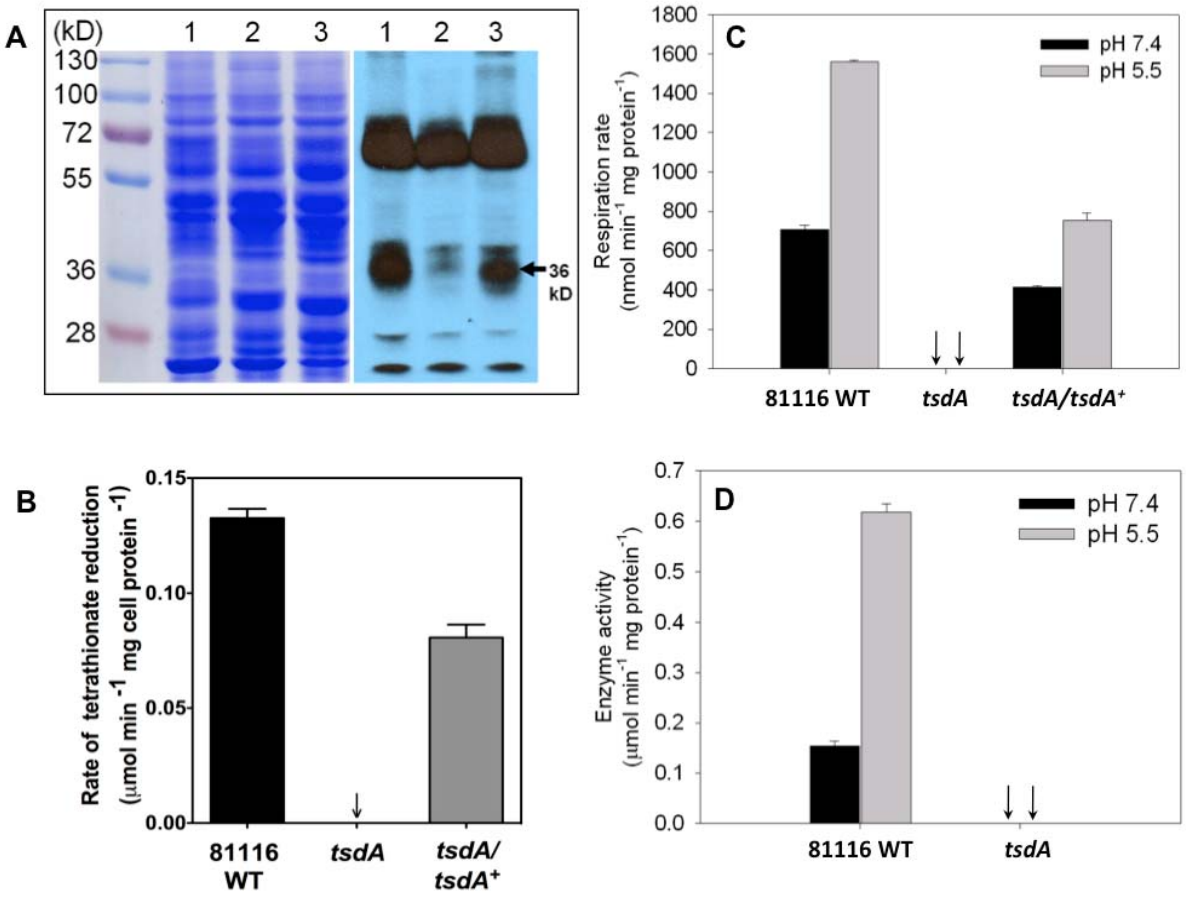

Figure 3.6 Periplasmic cytochrome *c* profiles, tetrathionate reduction and thiosulphate oxidation in 81116 wild-type, mutant and complemented strains.

(A) 10% Tricine-PAGE gel and haem blot of periplasmic proteins. Left panel; CBR stained gel of periplasmic proteins, 20 µg per lane. Right panel; haem blot of an identical gel. Lane 1: wild-type 81116 strain. Lane 2: *tsdA::kan* mutant. Lane 3: Complemented *tsdA/tsdA*$^{+}$ merodiploid strain. Arrow indicates the TsdA cytochrome *c* of ~ 36 kD present in the wild-type and complemented strains but missing in the mutant strain. Marker: Pageruler^{TM} Plus Prestained Protein Ladder (Fermentas)

(B) Rates of formate-dependent tetrathionate reduction in anaerobic cell suspensions. The rate was measured as described in section 2.8.2.5. The rates are averages from three independent cultures, with error bars showing standard deviation from the mean.

(C) Thiosulphate-dependent respiration is stimulated at low pH and is abolished in the *tsdA* mutant. Rates of oxygen consumption were measured in intact cells from three independent cultures, as described in section 2.8.2.4, after the addition of 5 mM sodium thiosulphate. The rates are averages with error bars showing standard deviation from the mean.

(D) Thiosulphate:ferricyanide reductase activity in cell-free extracts of wild-type and *tsdA* mutant strains. The thiosulphate-dependent reduction of ferricyanide was followed spectrophotometrically at 420 nm. Cell-free extracts were prepared from three independent cultures of each strain and the mean rates and standard deviations are shown.

3.2.6 TsdA mediates thiosulphate-dependent oxygen respiration in intact cells and thiosulphate: ferricyanide reductase activity in cell-free extracts

The wild-type *C. jejuni* 81116 showed significant thiosulphate-dependent oxygen consumption when assayed at neutral pH (Fig. 3.6 C). However, the rate was increased by ~200% when the assay was carried out at pH 5.5. The cell viability dropped rapidly below pH 5.5 and the activity of thiosulphate dehydrogenase could not be detected like the TsdA in *A. vinosum* at pH 4.0 (data not shown; Denkmann *et al*., 2012). At either pH 5.5 or 7.4, no activity could be detected with *tsdA* mutant cells, whereas the complemented *tsdA/tsdA*$^{+}$ merodiploid strain showed a restoration of activity to ~60% of wild-type rates at pH 7.4 and ~50% at pH 5.5 (Fig. 3.6 C). In the thiosulphate: ferricyanide reductase assay, ferricyanide acted as an artificial electron acceptor for TsdA enzyme in cell free extracts. The measurement of thiosulphate: ferricyanide reductase activity in such extracts of the wild-type strain showed the same low pH stimulation as with intact cells respiration (Fig. 3.6 D). This activity was totally abolished in cell-free extracts of the *tsdA* mutant (Fig. 3.6 D). Furthermore, there was no evidence showed that thiosulphate or tetrathionate could mediate induction of TsdA, as wild-type 81116 cells grown with or without thiosulphate or tetrathionate showed similar rates of thiosulphate-dependent respiration and tetrathionate reduction (data not shown). Taken together; these data indicate that TsdA can couple thiosulphate oxidation to electron transport to oxygen. Also, the strain NCTC 11168 did not show any oxygen consumption rate in the thiosulphate-dependent respiration test, consistent with the pseudogene status of *tsdA* in this strain.

3.2.7 Thiosulphate oxidation and tetrathionate reduction kinetics of wild-type and *tsdA* mutant strains during microaerobic growth

The microaerobic growth curve of wild-type 81116 and *tsdA* mutant was carried out in 100 mL MH-S broth at pH 7 supplemented with 4 mM thiosulphate or 2 mM tetrathionate respectively. The OD_{600} of initial culture was ~0.1 and the turbidity was monitored hourly. Also, the supernatant was taken by centrifugation and the concentration of thiosulphate and tetrathionate was determined according to the section 2.8.3. The ability of TsdA to act bi-directionally in different stages of a single batch culture is demonstrated in Fig. 3.7. Panel A (wild-type 81116 strain) and D (isogenic *tsdA* mutant) show the growth kinetics which are correlated with the oxidation of

thiosulphate (panel B and E) and the accumulation of tetrathionate (panel C and F) in the culture supernatants. In wild-type cells grown with thiosulphate, oxidation began immediately after inoculation and proceeded rapidly (Fig. 3.7 B); with 4 mM initial thiosulphate, the concentration approached zero within 3 h (initial rate of ~ 3 mM h^{-1}). Tetrathionate accumulated in parallel to thiosulphate depletion (Fig. 3.7 C) and reached the expected stoichiometric ratio of 1 mole tetrathionate: 2 moles initial thiosulphate by 3 h (early exponential phase). After a short lag period from 3 to 4 h, the accumulated tetrathionate was rapidly reduced back to thiosulphate, which accumulated in the culture supernatant to ~ 4 mM, equivalent to the starting concentration, by 7 h after inoculation (mid- exponential phase). There then followed a longer lag period from 7 to 12 h in the growth curve, up to the end of the exponential growth phase, where the thiosulphate concentration did not change significantly. The culture entered stationary phase after 12 h growth and this was correlated with another round of thiosulphate oxidation and accumulation of tetrathionate, which lasted until the end of the experiment 30 h. The rate of this second phase of thiosulphate oxidation (~ 0.22 mM h^{-1}) was much slower than the initial rate (Fig. 3.7 B), presumably reflecting much slower oxygen availability and/or an altered physiological state of the cells in stationary phase. However, the concentration change of thiosulphate and tetrathionate in the culture of *tsdA* mutant was not as complicated as that in wild-type 81116. The *tsdA* mutant grown with thiosulphate did not show any activity for thiosulphate oxidation over a 30 h period (Fig. 3.7 E) and tetrathionate was not detectable above background at any point (Fig. 3.7 F).

When a culture of strain 81116 wild-type cells was grown with a starting concentration of 2 mM sodium tetrathionate solely, there was a lag period of about 4 h, before the tetrathionate started to be reduced (Fig. 3.7 C). Thereafter, the kinetics and pattern of thiosulphate accumulation and its subsequent slow oxidation in stationary phase were similar to cultures to which thiosulphate was initially added. Cultures of the *tsdA* mutant showed similar lag period to convert tetrathionate to thiosulphate, but a much slower rate than the wild-type (Fig. 3.7 E and F) and did not give any re-oxidation of the thiosulphate in the stationary phase. Furthermore, the similar kinetics of converting tetrathionate to thiosulphate in the *tsdA* mutant was found in cultures of strain NCTC 11168 which was incubated microaerobically with an initial concentration of 2 mM tetrathionate (data not shown).

Finally, cultures of both *tsdA* mutant and 81116 strain wild-type to which either thiosulphate or tetrathionate were added, showed a slightly higher growth rate from mid-late exponential phase compared with those without any additions (Fig. 3.7 A and D). This effect was not apparent until after thiosulphate was exhausted, and corresponded exactly with the phase of tetrathionate reduction, consistent with an increased energy gain from this reaction.

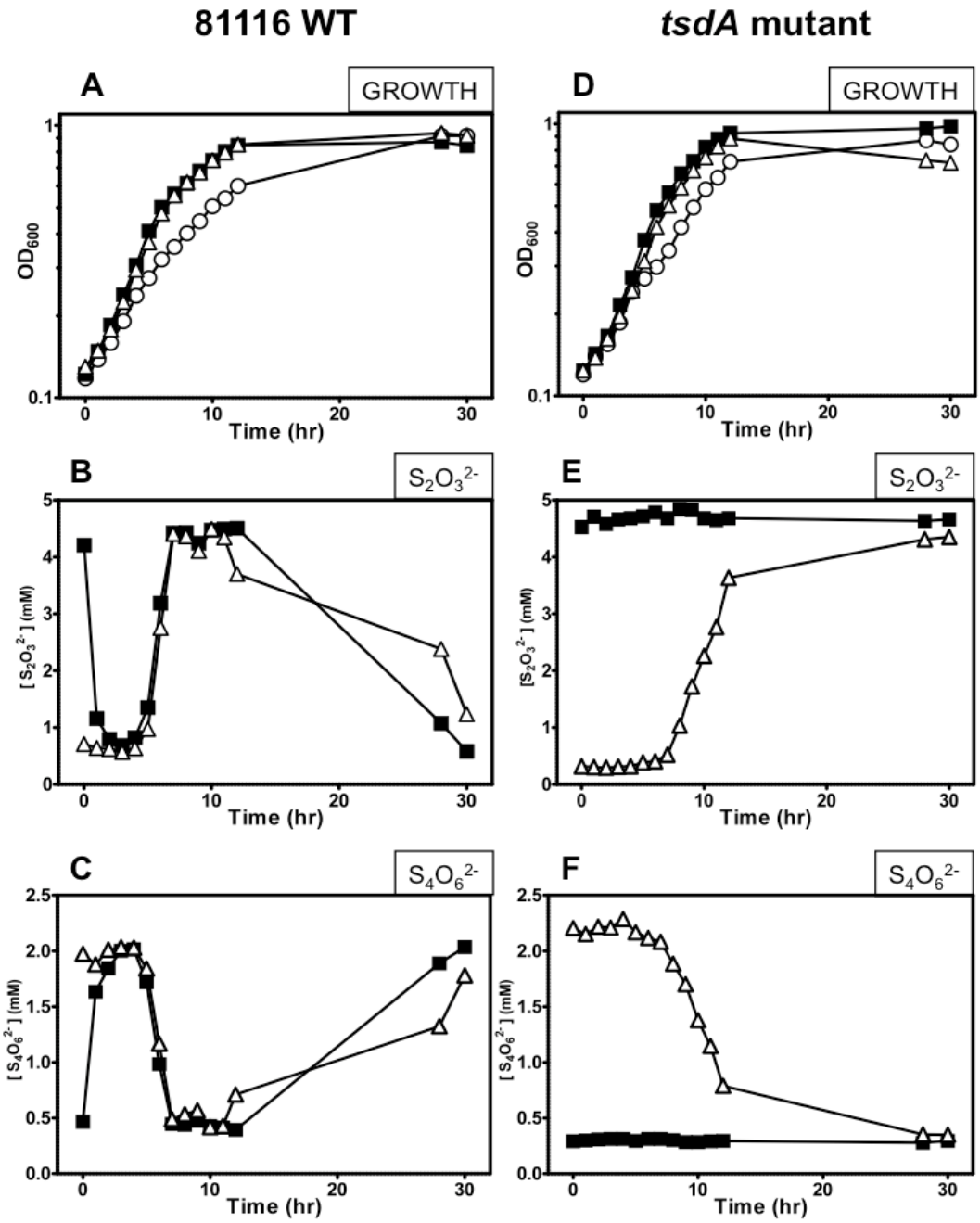

Figure 3.7 Kinetics of growth, thiosulphate oxidation and tetrathionate reduction in microaerobically grown cultures of *C. jejuni*. Cultures of wild-type 81116 (A–C) or the *tsdA* mutant (D–F) were grown under microaerobic conditions at 37°C in unsupplemented MH-S medium (open circles) or in MH-S medium + 4 mM sodium thiosulphate (filled squares) or MH-S medium + 2 mM sodium tetrathionate (open triangles). Panels (A) and (D) show the growth of these cultures as measured by OD at 600 nm. Panels (B) and (E) show the concentration of thiosulphate and (C) and (F) show the concentration of tetrathionate, in each of the culture supernatants at each time point corresponding to the growth curves in (A) and (D). Supernatants were prepared by centrifugation (10,000 x*g*, 5 min) and thiosulphate and tetrathionate were determined as described in section 2.8.3. Data shown are from a single representative experiment. The experiment was repeated twice with similar results.

3.2.8 Spectroscopic characterization and thiosulphate dehydrogenase activity of purified recombinant *C. jejuni* TsdA (CjTsdA)

In order to characterize TsdA proteins, recombinant CjTsdA, AvtsdA with Strep-tags were expressed in *E.coli* strain BL21 (DE3) according to the section 2.7.4.2, which involved coexpression of the *E.coli* cytochrome *c* maturation (*ccm*) genes from pEC86 (Arslan *et al*., 1998). The recombinant proteins were purified by Strep-Tactin affinity chromatography and the purities were also confirmed by 10% Tricine-PAGE (Fig. 3.8 A).

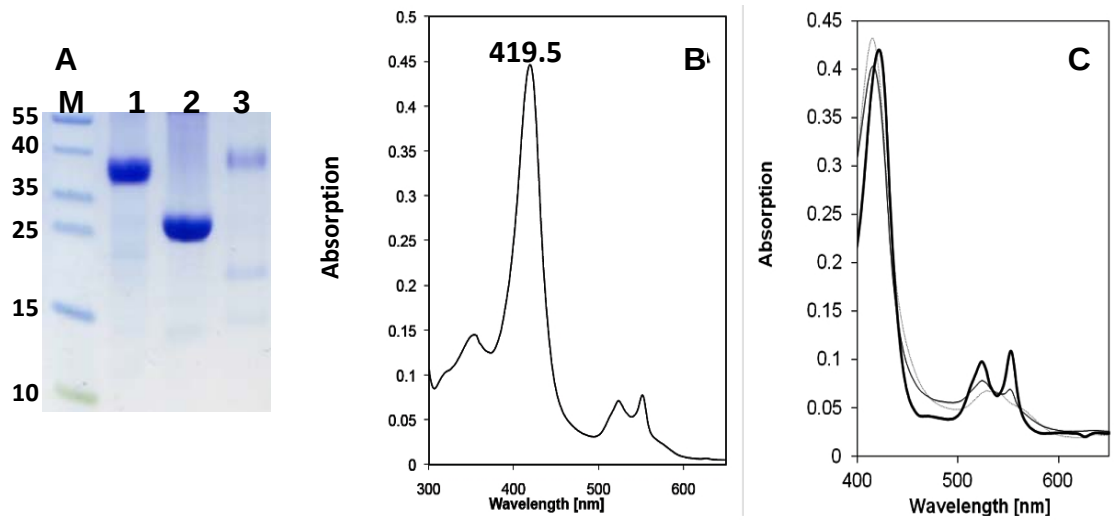

Figure 3.8 Purified recombinant TsdA and C8j_0040 and spectral analysis of recombinant CjTsdA at pH 8.0 (20 mM Tris-HCl, 42 ºC) in different redox states. **(A)** Recombinant TsdA and C8j_0040 protein was analysed by 10% Tricine-PAGE where the corresponding molecular weights were indicated: Lane 1: 20 µg CjTsdA (~36 kD); Lane 2: 20 µg AvtsdA (~ 26 kD), Lane 3: 5 µg C8j_0040 (~ 39 kD); Lane M: Fermentas PageRuler Prestained Protein Ladder 26616. **(B)** Protein "as isolated", the Soret peak appears at 419.5 nm. **(C)** Spectrum in the range 400 to 650 nm. Protein oxidized with ferricyanide (dotted line), after addition of 2 mM thiosulfate (thin solid line) and the dithionite reduced form (bold solid line) are shown. Protein concentration: 280 µg ml^{-1}. The spectra were obtained by Kevin Denkmann and Christiane Dahl.

The UV-Vis electronic absorption spectrum of the purified recombinant CjTsdA in the "as isolated" state is shown in Fig. 3.8 panel B (data in Fig. 3.8 and Fig. 3.9 were obtained by our collaborator Dr Kevin Denkmann). The spectrum is dominated by the intense Soret peak at 419.5 nm, α- and β-peaks are also observed at 552 and 523.5 nm respectively. When ferricyanide was added, it totally oxidized the protein resulting in a

Soret peak with a maximum at 414.5 nm (dotted line in Fig. 3.8 C). In the oxidized state, both α- and β-bands are red-shifted and characteristically broad. A shoulder is apparent at 570 nm (Fig. 3.8 C and 3.9). Partial reduction of the protein was observed upon addition of 2 mM thiosulphate (thin solid line in Fig. 3.8 C). In this state, the ratio of the α-peak to the β-peak was lower than in the completely reduced state, which was achieved by addition of sodium dithionite (bold solid line in Fig. 3.8 C). The Soret band is red-shifted to 421.5 nm in the completely reduced state. The ratio of α- (554 nm) and β-peak (524 nm) in the fully reduced state is α/β = 1.1 (Fig. 3.8 C). A very low intensity band at around 625 nm was apparent in the oxidized state, which was completely bleached in the protein reduced with dithionite (Fig. 3.9). This band was assigned to the iron high-spin state (Miles *et al*., 1993). The very low absorbance of this high-spin marker indicates that only a small amount of haem exists in 5-coordination or with a weak-field ligand at the sixth coordination site under these conditions (42 °C, pH 8.0). In summary, the spectral features of recombinant CjTsdA are very similar to those obtained for the prototype of the haem *c*-containing thiosulphate dehydrogenases, the enzyme from *A. vinosum* (Denkmann *et al*., 2012).

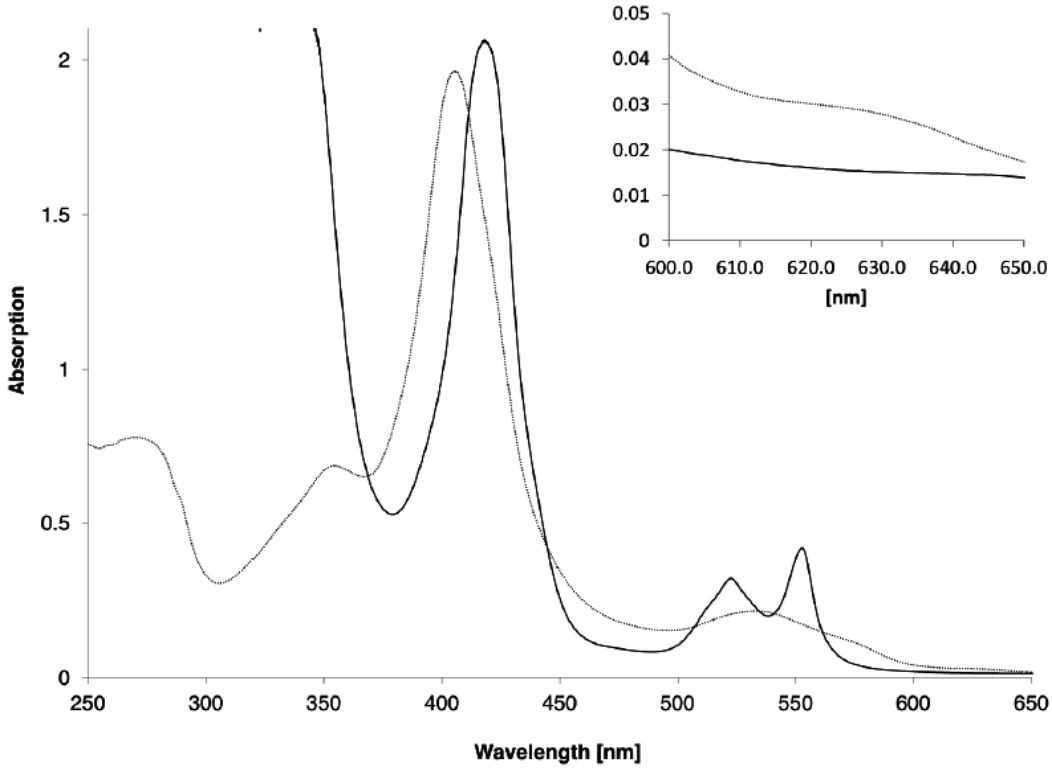

Figure 3.9 Absorption spectra of concentrated CjTsdA (~ 1.5 mg ml^{-1}) in the oxidised form (dotted line) or fully reduced with sodium dithionite (solid black line). The inset shows a weak feature at 630 nm which is bleached by dithionite, indicative of iron in the high spin state. These spectra were obtained by Kevin Denkmann and Christiane Dahl.

The purified CjTsdA protein catalysed thiosulphate-dependent reduction of ferricyanide, which was used as an artificial electron acceptor (Em +430 mV; Fultz and Durst, 1982), and it converted thiosulphate into tetrathionate stoichiometrically with the expected 2:1 ratio (Kevin Denkmann, personal communication). The following kinetic characterization of the thiosulphate oxidation reaction was carried out by our collaborator, Dr Kevin Denkmann, University of Bonn. The assay was carried out in triplicate with the electrophoretically pure CjTsdA, with varied concentrations of thiosulphate and saturated ferricyanide (1mM). The $S_{0.5}$ value for ferricyanide was 0.18 mM; no further increase in rate was found above 1 mM so this was used as the standard concentration for further assays. The optimal pH of CjTsdA with 1 mM ferricyanide and 8 mM thiosulphate was found to be 4.0 at 42°C. The enzyme activity reached a maximum at 45°C (pH 4.0; 1 mM ferricyanide; 8 mM thiosulphate) and stayed at the same level up to 55°C correlating well with the optimum growth temperature for *C. jejuni* of 42°C (Kevin Denkmann, personal communication). An analysis of the kinetics of thiosulphate oxidation with ferricyanide as an electron acceptor showed that the $S_{0.5}$ value for thiosulphate was 2.0 mM, while the V_{max} was 990 ± 42 U mg^{-1} with thiosulphate as the varied substrate. The corresponding k_{cat} is > 20-fold lower than that for the *A. vinosum* enzyme (Denkmann *et al*., 2012) and the k_{cat} / $S_{0.5}$ ratio is > 40-fold lower (summarized in Table 3.1), indicating that the *C. jejuni* enzyme is a much less efficient thiosulphate dehydrogenase than the *A. vinosum* enzyme.

3.2.9 Thiosulphate-dependent reduction of cytochrome *c* by CjTsdA and AvTsdA

In the chemotroph *Thiomonas intermedia*, a dihaem cytochrome *c* (TsdB) acts as the natural electron acceptor for the TsdA of this bacterium (Denkmann *et al*., 2012). This TsdB can also serve as a heterologous electron acceptor *in vitro* for TsdA from the phototroph *A. vinosum* (Denkmann *et al*., 2012). There is no TsdB homologue in *C. jejuni* strain 81116, and no other dihaem cytochromes apart from TsdA and C8j_0040. However, several possible candidate monohaem *c*-type cytochromes encoded in the 81116 genome might be physiological redox partners for CjTsdA. The following work on TsdA electron acceptors in this section (3.2.9) was carried out by our collaborator, Dr Kevin Denkmann at the University of Bonn.

Table 3.1 Summary of thiosulphate dehydrogenase and tetrathionate reductase kinetic parameters for purified CjTsdA and AvTsdA.

Reaction	**Thiosulphate →ferricyanide**				**Methyl viologen→tetrathionate**			
Parameter	V_{max}	k_{cat}	$S_{0.5}$	$k_{cat}/S_{0.5}$	V_{max}	k_{cat}	$S_{0.5}$	$k_{cat}/S_{0.5}$
Units	U mg^{-1}	s^{-1}	mM	mM^{-1} s^{-1}	U mg^{-1}	s^{-1}	mM	mM^{-1} s^{-1}
CjTsdA	990±42	604	2.0	**302**	64±1.1	40	0.01	**4,000**
AvTsdA	28,600±890(1)	14,000(1)	1.1(1)	**12,727**	22±0.7	14	0.50	**28**

(1) Values taken from Denkmann et al. (2012). The units for Vmax are µmol min^{-1} mg protein^{-1}. Figures in bold emphasize the differences between the specificity constants for CjTsdA and AvTsdA.

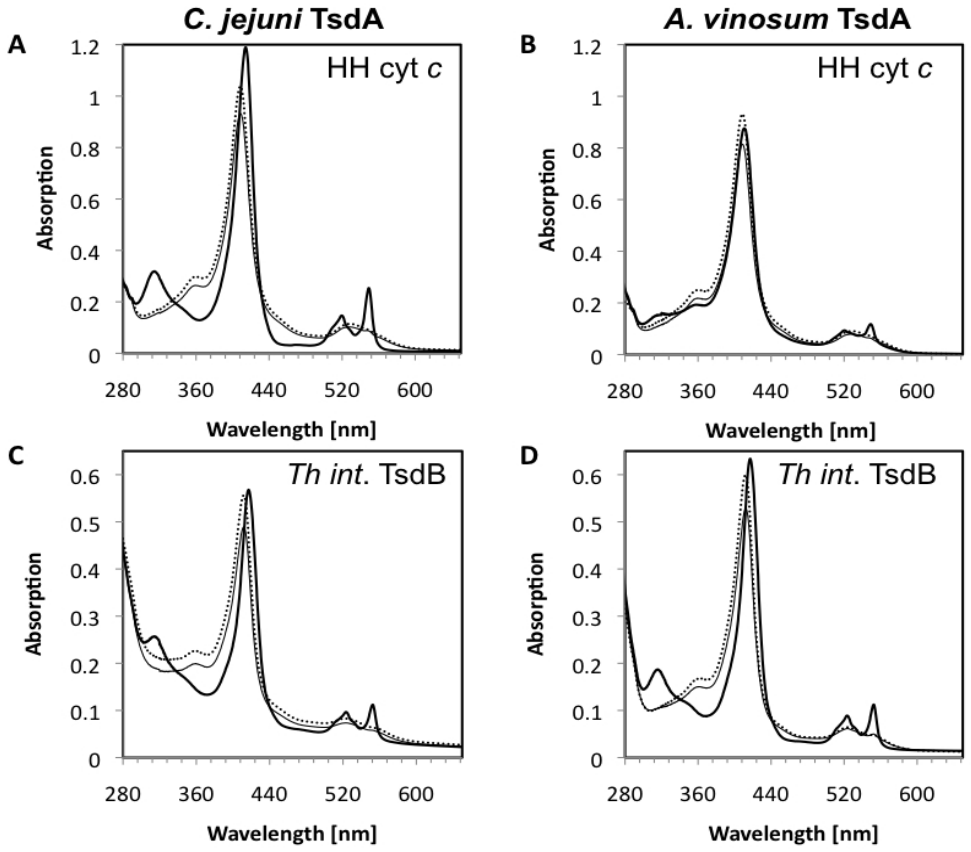

Figure 3.10 *c*-type cytochromes as electron acceptors for TsdA from *Campylobacter jejuni* and *Allochromatium vinosum*. UV-Vis spectra of the monohaem cytochrome *c* from horse heart (7.5 mM, A and B) and the dihaem cytochrome *c* TsdB from *Thiomonas intermedia* (3 mM, C and D) in 100 mM ammonium acetate buffer, pH 6.0 were recorded from 280 to 650 nm. Sequential spectra obtained for the oxidized protein (dotted line), after addition of 8 mM thiosulphate (thin solid line) and after addition of 74 nM *C. jejuni* TsdA (bold solid lines in A and C) or 102 nM *A. vinosum* TsdA (bold solid lines in B and D) are shown. These spectra were obtained by Kevin Denkmann and Christiane Dahl.

TsdA was found to be able to reduce the monoheam cytochrome *c* from horse heart (Em +248 mV; Pande and Myer, 1978; Myer *et al*., 1979) strongly in the presence of thiosulphate (Fig. 3.10 A). To determine optimal pH, a series of buffers with different pH were tested and the reaction was monitored at 550 nm. The CjTsdA showed highest reducing activity at pH 7, higher than the more acidic pH optimum seen with ferricyanide (Fig. 3.11). Analysis of primary *v* versus [thiosulphate] plots of initial rates of the CjTsdA and thiosulphate-dependent reduction of horse heart cytochrome *c* at pH 7 gave an $S_{0.5}$ of 70 ± 20 mM, with a V_{max} of 425 ± 57 U mg protein^{-1}. In contrast, the reduction of horse heart cytochrome *c* by the purified *A. vinosum* TsdA enzyme (Fig. 3.10 B) was clearly incomplete under the same conditions as in Fig. 3.10 A. However, although the dihaem cytochrome *c* TsdB from *T. intermedia* (redox potential unknown) could be reduced to some extent by *C. jejuni* TsdA (Fig. 4 C), this was incomplete compared with the reaction with the *A. vinosum* TsdA (Fig. 4 D). Overall, these findings are consistent with the view that a monohaem *c*-type cytochrome is the most likely *in vivo* redox partner for CjTsdA.

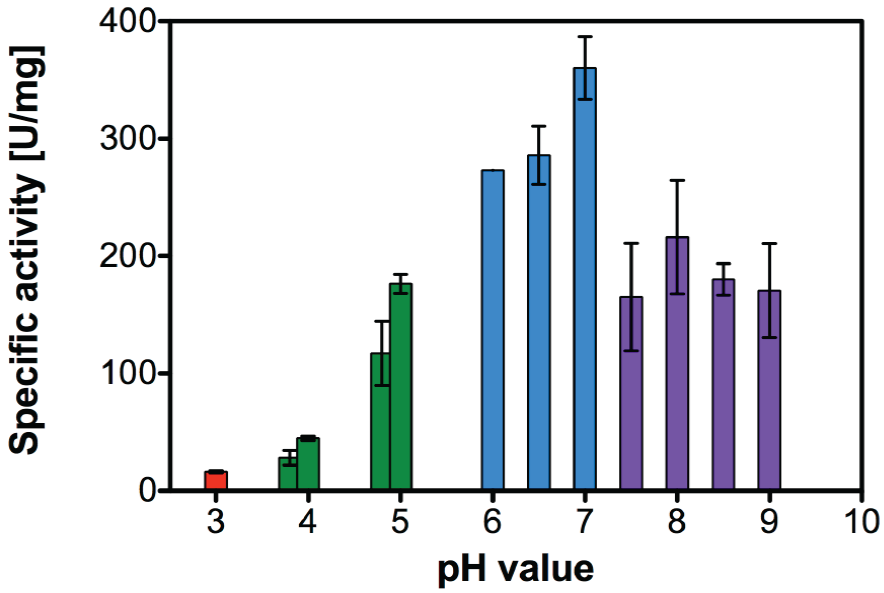

Figure 3.11 pH dependency of the reduction of horse heart cytochrome *c* by CjTsdA. Assay mixtures contained 80 µM cytochrome c, 82 nmol purified CjTsdA and 8 mM sodium thiosulphate in 100 mM of the appropriate buffer (Red: citrate buffer; Green: acetate buffer; Blue: bis-Tris buffer; Purple: Tris- HCl buffer). Reactions were performed as triplicate at 42 ºC, started by addition of the enzyme and followed by the increase of absorbance at 550 nm. Activity was expressed as µmol cytochrome *c* reduced per min and mg protein on the basis of a molar extinction coefficient at 550 nm of 21.1 mM^{-1} cm^{-1}. Means are showed in bars and the standard deviation was indicated. These data were obtained by Kevin Denkmann.

3.2.10 Kinetics of tetrathionate reduction catalysed by CjTsdA and AvTsdA

In order to demonstrate tetrathionate reductase activities of CjTsdA and AvTsdA *in vitro*, the assay was carried out under strictly anaerobic conditions with the electrophoretically pure recombinant proteins, different concentrations of tetrathionate and 0.3 mM reduced methyl viologen as an electron donor (E_m = -440 mV). Rates of tetrathionate-dependent methyl viologen oxidation were optimal at pH 5-6 for both enzymes, so an assay pH of 5 was routinely performed. Figure 3.12 shows the comparison of the kinetics of tetrathionate-dependent methyl viologen oxidation for CjTsdA or AvtsdA. Strikingly, the CjTsdA enzyme showed a much lower tetrathionate $S_{0.5}$ value (0.01 ± 0.005 mM) compared with that for the AvTsdA enzyme (0.5 ± 0.05 mM). In addition, the k_{cat} value for CjTsdA was larger than that for AvTsdA (Table 3.1). Consequently, the $k_{cat}/S_{0.5}$ values for the two enzymes in the direction of tetrathionate reduction differ by over 140-fold (Table 1). Taken together with the differences in kinetics for thiosulphate oxidation, the data support a physiological role for CjTsdA as a tetrathionate reductase while the AvTsdA more likely acts *in vivo* as a thiosulphate dehydrogenase.

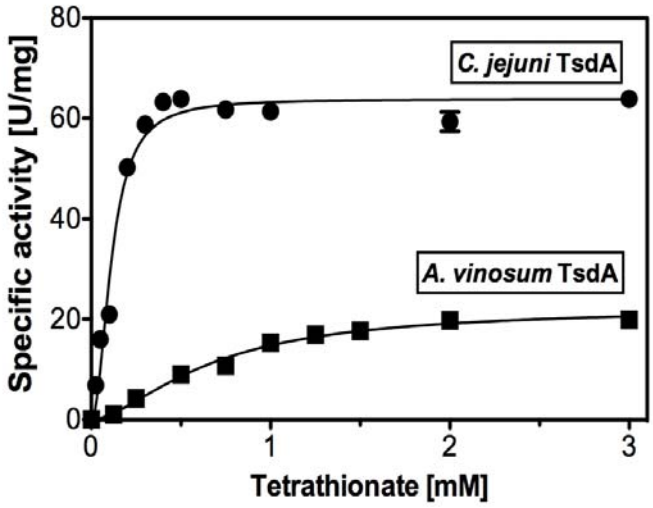

Figure 3.12 Comparison of kinetics of tetrathionate reduction by purified *C. jejuni* and *A. vinosum* TsdA enzymes. Assay mixtures contained 300 µM methyl viologen which had been pre-reduced with a small excess of titanium citrate, 100 mM ammonium acetate buffer, pH 5.0 and varying concentrations of tetrathionate. Assays for CjTsdA contained 0.15 µM protein or 1.5 µM for AvTsdA. The specific activity is expressed as µmol tetrathionate reduced min^{-1} mg $protein^{-1}$. Each data point is the mean ± standard deviation of three assays on the same batch of protein, but in most cases the error bars are too small to be seen. The solid line through the data points is the fit to the Hill equation using non-linear regression as described in the section 2.8.6.

3.2.11 C8j_0040 has low levels of both thiosulphate dehydrogenase and tetrathionate reductase activity

According to the sequence similarity between C8j_0815 (CjTsdA) and C8j_0040 (Fig. 3.1), the C8j_0040 protein might also be able to oxidise thiosulphate and reduce tetrathionate like the bi-functional CjTsdA. Recombinant C8j_0040 was overexpressed in *E.coli* strain BL21(DE3) with the same strategy as applied for CjTsdA. The molecular weight of electrophoretically pure C8j_0040 (including Strep-tag and two haems) was 39.3 kD (Fig. 3.8 A). It also reacted positive in a haem stain and exhibited a spectrum typical for a *c*-type cytochrome with α-, β- and γ-peaks at 554, 524 and 423 nm in the reduced state respectively (Kevin Denkmann, personal communication). Thiosulphate-dependent activity with either ferricyanide or the monohaem cytochrome *c* from horse heart as electron acceptor was measured by Dr Kevin Denkmann, but in contrast to the highly active CjTsdA, the rates exhibited by this protein were very low (maximum specific activity measured with 8 mM thiosulphate and 1 mM ferricyanide; 19 U mg protein^{-1}). The tetrathionate reductase activity of C8j_0040 was also demonstrated using 1mM tetrathionate and reduced methyl viologen as electron donor, but again the specific activity was extremely low (1.5 U mg protein^{-1}). Perhaps the occurrence of methionine rather than cysteine as the putative active-site haem ligand in C8j_0040 (Fig. 3.1), still allows for some TsdA-like enzymatic function in this position. To examine the hypothesis that C8j_0040 might serve the electron acceptor for CjTsdA, UV-Vis difference spectra were performed by Dr Kevin Denkmann. The addition of 8 mM thiosulphate alone led to a small degree of reduction of this *c*-type cytochrome at pH 5.0. This reduction was only slightly increased upon addition of catalytic amounts of CjTsdA. Prolonged incubation time of up to 5 min did not increase the level of reduction of C8j_0040, which never reached completion. This finding precludes a function of C8j_0040 as the natural electron acceptor of CjTsdA.

A *c8j_0040* null mutant was constructed in strain 81116, and intact cells tested for both thiosulphate oxidation in the oxygen electrode and tetrathionate reduction in short term incubation assays with formate as an electron donor. Both activities were detected but with reduced rates compared with the wild-type parent strain (thiosulphate-dependent oxygen consumption rates of ~ 0.7 μmol min^{-1} mg protein^{-1} for wild-type and ~ 0.55 μmol min^{-1} mg protein^{-1} for mutant; tetrathionate reduction rates of ~ 0.13 μmol min^{-1} mg protein^{-1} for wild-type and 0.07 μmol min^{-1} mg protein^{-1} for mutant). However, the growth of this mutant on tetrathionate under oxygen-limited conditions was

indistinguishable from that of the parent strain, and the kinetics of tetrathionate reduction and thiosulphate accumulation in such cultures were also very similar to the wild-type (data not shown). These data do not provide any evidence that the low activities exhibited by C8j_0040 are physiologically relevant.

3.3 Discussion

There is emerging evidence showing that inorganic sulphur compounds play an important but underestimated role during the infection process of microorganisms in the human intestine (Blachier *et al*., 2010). Enteric pathogens are able to utilise these compounds in energy conserving pathways that may have both direct and indirect effects on pathogenicity and invasiveness or may provide a growth advantage over competing microorganisms in gut flora (Winter *et al*., 2010; Tareen *et al*., 2011). The work described in this study reveals that tetrathionate can be used by *C. jejuni* as a terminal electron acceptor, which adds to the increasing evidence of the metabolic versatility of this pathogen. However, none of known types of tetrathionate reductase genes was found in *C. jejuni* genome sequences indicating the dihaem *c*-type cytochrome encoded by gene *c8j_0815*, which is able to reduce tetrathionate, is a novel type of tetrathionate reductase. Since TsdA was first found in the phototrophic *A. vinosum* acting as a thiosulphate dehydrogenase, taken together with the data above, it seems that TsdA in fact is a bi-functional enzyme that can support growth of *C. jejuni* with tetrathionate under oxygen-limited conditions. TsdA is thus a previously unrecognized but simpler type of tetrathionate reductase than either the multi-subunit molybdoenzyme Ttr or the non-specific multi-haem Otr (Hinojosa-Leon *et al*., 1986; Hensel *et al*., 1999 and Atkinson *et al*., 2007). Genes homologous to *tsdA* are present in a number of known pathogens from the α-, β-, γ- and ε-proteobacteria, and include other gastrointestinal mucosal pathogens such as *Campylobacter curvus*, *Helicobacter felis*, *Arcobacter butzleri* and *Laribacter hongkongensis* (Fig. 3.1), which thus have the potential for tetrathionate respiration. Interestingly, however, the homology searches have also revealed that TsdA-like genes are present in many strains and species of *Brucella* (zoonotic pathogens that are fastidious intracellular parasites) and *Bordetella* (host-adapted respiratory pathogens; Fig. 3.1), which raises the possibility that TsdA mediated tetrathionate reduction and/or thiosulphate respiration could be important in tissues other than the intestinal mucosa.

The comparisons of the growth of wild-type 81116, *tsdA* and *tsdA/tsdA*$^+$ demonstrate the physiological role of TsdA as a tetrathionate reductase in *C. jejuni*. Under anaerobic conditions, the cell suspension of wild-type showed a small burst of growth when provided with tetrathionate, plus formate (E_m -420mV) as electron donor. The periplasmic location of TsdA indicates that electron transport from cytochrome *c* to tetrathionate will not be electrogenic, but the overall respiration chain from formate to tetrathionate will be energy conserving due to the electrogenic nature of the formate dehydrogenase and cytochrome bc_1 complex (Fig. 3.13). This is clearly sufficient to support limited growth, as is also the case with other systems that terminate in non-electrogenic periplasmic reductases, for example those for nitrate, nitrite, TMAO and DMSO (Sellars *et al*., 2002; Kelly, 2008).

In addition, TsdA can also act physiologically as a thiosulphate dehydrogenase, which is confirmed by the comparison of oxygen consumption rate in wild-type, *tsdA* mutant and complemented strains incubated with excess thiosulphate and oxygen. Further insight into the ability of TsdA to switch between dehydrogenase and reductase activities *in vivo* was obtained in experiments where thiosulphate and tetrathionate were quantified during microaerobic growth with thiosulphate as an electron donor (Fig. 3.7). At the start, when thiosulphate and oxygen are in excess, TsdA is acting as a dehydrogenase and thiosulphate was rapidly oxidised to tetrathionate, which accumulated. Tetrathionate only started to be reduced after the exhaustion of the initial thiosulphate present and once the cell density had increased significantly, by mid-exponential phase. Presumably, increasing cell density will lead to progressive oxygen limitation, which will result in an increase in the reduction state of the menaquinone (MK) pool (i.e. higher MKH_2/MK ratio). Electron flux from MKH_2 to tetrathionate will only then start to become significant, allowing TsdA to act in reverse on the accumulated tetrathionate. Interestingly, the growth experiments in figures 3.4 and 3.6 revealed that the strain 81116 *tsdA* mutant was nevertheless capable of very slow tetrathionate reduction, suggesting the existence of an additional tetrathionate reductase activity. This point is further discussed below in relation to the C8j_0040 protein.

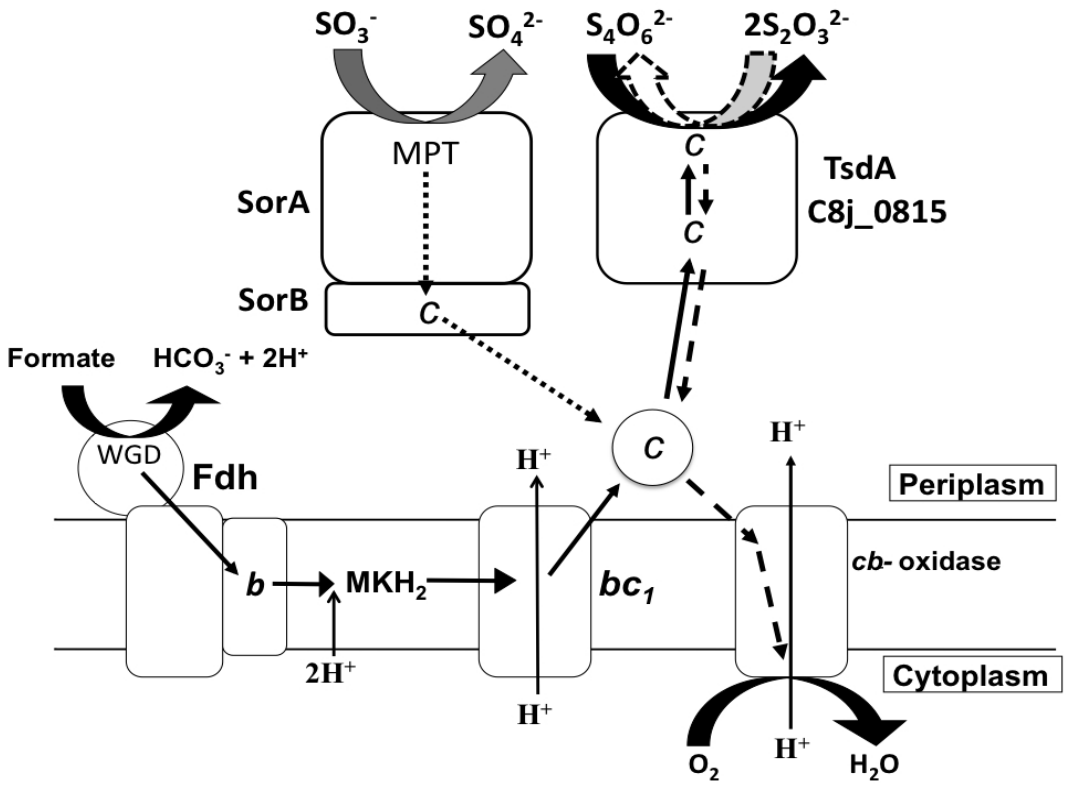

Figure 3.13 Model for bi-directional electron transfer *in vivo* between tetrathionate and thiosulphate catalysed by *C. jejuni* TsdA. Solid thin arrows show the route of electron transfer from formate as a typical low potential electron donor via the formate dehydrogenase (Fdh) which is thought to have a tungstopterin guanine dinucleotide (WGD) cofactor (Smart *et al*., 2009) to tetrathionate, via the menaquinol pool (MKH_2), the cytochrome bc_1 complex (bc_1) and periplasmic cytochrome *c*. Dashed arrows indicate electron transfer from thiosulphate to oxygen via TsdA, periplasmic cytochrome *c* and the *cb*-type oxidase. For comparison with thiosulphate oxidation, the previously identified sulphite:cytochrome *c* dehydrogenase (SorAB; Myers and Kelly, 2005) with its molybdopterin (MPT) cofactor is also shown, with electron transfer to cytochrome *c* indicated by dotted arrows. Note that the Fdh, bc_1 and *cb*-oxidase complexes are electrogenic, while TsdA and SorAB are not.

In fact, the redox potential of the thiosulphate/tetrathionate couple is relatively high for thiosulphate to be a good electron donor (E_m +24 mV) and the only *C. jejuni* quinones are menaquinone (E_m -75 mV) and methylmenaquinone (E_m -124 mV; Juhnke *et al*., 2009; Guccione *et al*., 2010). The electrons from the oxidation of thiosulphate to tetrathionate can therefore only couple at the high potential end of the respiratory chain (Fig. 3.13). The most likely route for the electrons from TsdA to terminal oxidases

would be from TsdA to a high potential monohaem *c*-type cytochrome, which *in vivo* would feed electrons directly into the *cb*-type cytochrome *c* oxidase (Fig. 3.13). Thus, thiosulphate is only a useful electron donor when there is sufficient oxygen available to allow turnover of the cytochrome *c* oxidase. This is clearly seen in the growth experiments where thiosulphate was most rapidly oxidized at low cell density in early exponential phase, in contrast with a much slower rate in oxygen-limited stationary-phase cultures (Fig. 3.7). In the intestinal mucosal niche occupied by *C. jejuni*, oxygen availability will vary greatly, as there will be a steep oxygen gradient between the underlying epithelial cell layer (microaerobic) and the lumen (anaerobic). Similar considerations apply to the use of sulphite as an electron donor (also shown in Fig. 3.13), where electrons from periplasmic oxidation by SorA flow via the *c*-type cytochrome, SorB, to the *cb*-oxidase (Myers and Kelly, 2005).

The biochemical analysis with the purified *C. jejuni* TsdA enzyme clearly confirmed its bi-functionality. As a thiosulphate dehydrogenase, the enzyme showed a low pH optimum when using ferricyanide as electron acceptor, as found in AvTsdA as well (Denkmann *et al*., 2012). Nevertheless, both thiosulphate-dependent oxygen consumption in cell suspensions and the initial rate of thiosulphate oxidation in growing cultures was significant at neutral pH values. This presumably reflects the greater efficiency of electron transfer to the natural *in vivo* electron acceptor compared with ferricyanide. Also, *in vitro* studies with horse heart cytochrome *c* as electron acceptor showed a pH optimum of 7, as well as a much lower $S_{0.5}$ value for thiosulphate. Tetrathionate reduction could be driven by reduced methyl viologen as electron donor and these assays revealed a much higher tetrathionate affinity and higher V_{max} and k_{cat} compared with the AvTsdA enzyme. The enzyme kinetic studies reveal the fact of a marked difference in the catalytic properties of both the forward and reverse reactions of CjTsdA compared with AvTsdA (summarized in Table 3.1). The $k_{cat}/S_{0.5}$ ratio for thiosulphate oxidation with ferricyanide is over 40 times higher for AvTsdA than for CjTsdA, while for tetrathionate reduction, the ratio is over 140 times higher for CjTsdA compared with AvTsdA, largely due to the ~ 50-fold higher affinity of CjTsdA for tetrathionate. In short, the data show that *C. jejuni* TsdA is well adapted for tetrathionate reduction while the *A. vinosum* enzyme is a very poor tetrathionate reductase but an excellent thiosulphate dehydrogenase, in keeping with its known physiological role in the latter bacterium. The general conclusion is that TsdA enzymes may not have the same role in different bacteria, but that they are optimized for thiosulphate oxidation or

tetrathionate reduction according to the physiological requirements and lifestyle of the particular bacteria concerned.

The spectral features of recombinant *C. jejuni* TsdA (characterised in the laboratory of our collaborator Dr Christiane Dahl by Dr Kevin Denkmann) are dominated by hexa-coordinated low-spin *c*-type haem with small contributions from high-spin haem. The latter presumably arise from the His-Cys coordinated active-site haem with the former arising from the additional methionine ligated haem, which has an electron-transferring role. These features are very similar to those of the only other fully characterized TsdA, from *A. vinosum* (Denkmann *et al*., 2012). Since bidirectional catalysis has now been demonstrated for TsdA, it could be anticipated that the active-site haem has a reduction potential in the vicinity of the substrate/product couple, i.e. E_m at least ~ +24 mV. If confirmed, this would represent the most positive midpoint potential reported to date for such a His–Cys ligated haem centre. In the trihaem SoxAX enzymes the His–Cys and His–$CysS^-$ (persulphide) ligated haems have an Em ± -400 mV (Reijerse *et al*., 2007). SoxAX is the key component of the thiosulphate oxidizing Sox multi-enzyme complex and catalyses a reaction analogous to that of TsdA: instead of oxidative linkage of the sulphane sulphur atoms of two thiosulphate molecules as catalysed by TsdA, SoxA oxidatively links thiosulphate with the thiolate of a cysteine residue at the carboxy-terminus of the SoxY subunit of the SoxYZ protein (Friedrich *et al*., 2001), with two electrons transferred to cytochrome *c*. The mechanism is widely assumed to involve thiosulphate binding to the $CysS^-$ ligand of the SoxAX active-site haem (Bamford *et al*., 2002; Dambe *et al*., 2005). Interestingly, the amino acid sequence of the active-site haem-binding region and that harbouring the conserved cysteine in SoxA from *Starkeya novella* and other SoxAX-containing bacteria is very similar to the corresponding region in *A. vinosum* and related TsdA proteins (Denkmann *et al*., 2012). The exact nature of the thiolate haem ligand in TsdA remains to be determined, but the simplicity of the TsdA class of enzyme with just two (differently ligated) haems, should allow detailed spectroscopic and kinetic studies of the forward and reverse reaction mechanisms to be made, and might also shed light on the factors that determine conversion of thiosulphate to tetrathionate as opposed to sulphate. In view of the fact that the as-isolated CjTsdA protein was partially reduced, it is assumed that the His–Met ligated haem must have a very positive redox potential. This is also true of SoxAX (Cheesman *et al*., 2001), where the His–Met ligated haem has been established to have an Em ~ +190 mV (Reijerse *et al*., 2007).

Intriguingly, another TsdA homologue was also found in *C. jejuni*, the C8j_0040 protein (Cj0037 in strain NCTC 11168, see chapter 5). The C8j_0040 protein was characterized for thiosulphate dehydrogenase and tetrathionate reductase activity and for the role of possible electron acceptor of TsdA. The latter result was negative but we have since obtained some evidence that the homologue of this protein in strain NCTC 11168 (Cj0037) is involved in electron transfer from the bc_1 complex to the terminal *cb*-oxidase and this will be further discussed in Chapter 5. The C8j_0040 was found to catalyse very low levels of thiosulphate oxidation and tetrathionate reduction, which was surprising in the light of the replacement of the active-site cysteine with a methionine as a putative haem-binding ligand and the known essentiality of this residue for catalysis in the AvTsdA protein (Denkmann *et al*., 2012). It thus seems possible that a minor activity can be maintained by a haem in which the axial cysteine ligand is missing or replaced as is the case for the C8j_0040 protein. This low catalytic activity does not contribute to physiological thiosulphate oxidation (which was completely abolished in the *tsdA* mutant) or to the residual tetrathionate reduction in the *tsdA* mutant, but the origin of this requires further investigation.

3.4 Conclusions

Two TsdA homologues were found in *C. jejuni* strain 81116: C8j_0815 and C8j_0040; the former showed an excellent enzyme activity for reducing tetrathionate under anaerobic conditions but less efficient thiosulphate dehydrogenase activity compared with the TsdA from *A. vinosum*. The role of C8j_0040 in the electron transport chain of *C. jejuni* is still unclear though it still showed very low levels of both enzyme activities, which is due to the replacement of a single amino acid in its haem-binding region. The growth experiments revealed the bi-functionality of TsdA allowing the cells of strain 81116 to utilise thiosulphate and tetrathionate under different atmospheric conditions to support its viability. The utilisation of both sulphur compounds not only proves the complexity and the flexibility of the respiration chain in *C. jejuni* but offers a potential advantage to survive in the highly-competitive environment like the human intestine, where the infectious dose is as low as a cell number of 500 (Robinson, 1981).

Compared to TtrABC in *S. typhimurium* or muitlhaem Otr in *Shewanella frigidimarina*, TsdA is much simpler according to its amino acid composition and also the first tetrathionate reductase composed of a di-haem *c*-type cytochrome to date. It is worth

noting that only a few other examples of bacteria that can both oxidize thiosulphate and reduce tetrathionate have so far been reported, for example certain *Pseudomonas* strains (Trudinger, 1967; Tuttle, 1980). A cytochrome *c*-containing thiosulphate oxidase preparation enriched from the soluble fraction of aerobically grown 'marine pseudomonad 16B' was found to catalyse tetrathionate reduction (Whited and Tuttle, 1983) and the authors concluded that thiosulphate oxidase and tetrathionate reductase were reversible activities of the same enzyme. According to the data above, this chapter unambiguously demonstrates that the dihaem cytochrome *c* TsdA is reversible. Given the widespread distribution of TsdA, it may now be the case that, like *C. jejuni*, many more bacteria than previously thought are capable of growth on tetrathionate, in addition to being able to use thiosulphate as an electron donor.

Chapter 4

Two TatA paralogues are involved in the translocation of twin-arginine translocase substrates in *Campylobacter jejuni*

4.1 Induction

The twin-arginine translocase (TAT) system is one of the major pathways for protein translocation across the cytoplasmic membrane in *C. jejuni* and it is capable of transferring fully folded proteins through the lipid bilayer. The major components involved in the TAT system are TatA, TatB and TatC where TatA is considered as pore forming or structure weakening of the cytoplasmic membrane. TatB and TatC always form a TatBC complex which is responsible for signal peptide recognition, substrate recruiting and feeding to TatA homo-oligomers which facilitates the protein translocating process (Bolhuis *et al*., 2001; Tarry *et al*., 2009). TAT-dependent substrates share a common feature: bearing a signal peptide at the N-terminal sequence which has a highly conserved twin-arginine motif S/T-R-R-x-F-L-K (where x is a polar amino acid). There are at least fifteen enzymes in *C. jejuni* predicted / considered as TAT-dependent (Table 4.1, adopted from Hitchcock *et al*., 2010) and most of them are involved in the electron transport chain.

Although TatA is an essential component in the formation of the TatAC or TatABC complex and also accounts for the translocation mechanism (e.g. pore forming or membrane weakening), the second homologue (TatE, TatA2 or TatAx where x is a number or letter), in diverse bacteria, plays an important role in transportation under certain growth conditions (Brüser, 2007). The Gram-positive bacterium *B. subtilis* contains three *tatA* genes, denoted *tatAd*, *tatAy* and *tatAc*, and two *tatC* genes denoted *tatCd* and *tatCy*. The *tatAd-tatCd* and *tatAy-tatCy* genes are organised in operons at separate genomic loci (Jongbloed *et al*., 2000). Two TatAC-type systems, TatAdCd and TatAyCy, operate in parallel with different substrate specificities but recognize similar elements of the signal peptide. The environmental conditions, such as salinity, can determine the specificity and need for the secretion of a Tat substrate in *B. subtilis*, although the third *tatA* gene *tatAc* shows no demonstrable role in Tat-dependent protein transport (van der Ploeg *et al*., 2011; Jongbloed *et al*., 2004). TatE is another well-known TatA homologue found in Gram-negative bacterium *E. coli*, which is independent of the *tatABCD* operon and encoded by a monocistronic *tatE* gene. The *E.*

coli tatE gene encodes a 67-amino acid predicted membrane protein that exhibits greater than 50% sequence identity with TatA. Overexpression of TatE results in complementation of a *tatA* mutant, indicating a similar role (Sargent *et al*., 1999). It has been suggested the assembly mechanism of TatE is similar to that of TatA and a recent study suggests that solubilised/ purified recombinant TatE is likely to reflect the natural TatA-similar state of the complex although with a smaller size (Baglieri *et al*., 2012). In addition to *B. subtilis* and *E. coli*, recently TatA homologues have been found in other bacteria such as *Pseudomonas stutzeri*, *Bdellovibrio bacteriovorus* and *Corynebacterium glutamicum* (Heikkilä *et al*., 2001; Chang *et al*., 2011; Kikuchi *et al*., 2006), where these homologues are involved in general/specific substrate metabolism or are essential for survival, suggesting a significant role of the extra TatA homologue in the TAT system and this might result in different translocation models to the original TatA(B)C complex, which deserve further consideration.

A previous study suggested that there is only one TatA homologue present in *C. jejuni* (Dilks *et al*., 2003). However, in this chapter, a second *tatA* homologue *cj0786*, which is located in the *nap* operon, shows a typical TatA-structure and is similar to the native TatA (Cj1176c). Here, the role of Cj0786 in the TAT system will be characterized and the relationship of two TatA homologues in *C. jejuni* will be further elucidated.

Table 4.1 Predicted substrates of the twin arginine translocase system in *Campylobacter jejuni* NCTC 11168 (Table adapted from Hitchcock *et al*., 2010)

Gene	Tat sequence*	Predicted Tat substrate		Function	*C. jejuni* cellular location
		TATFIND†	TatP‡		
*Cj0005c***	9 NRRDFLK	Yes	Yes	Sulphite oxidase, SorA	Periplasmic (Myers & Kelly, 2005)
Cj0145 **	2 ERRFFLK	No	Yes	Phosphatase	Periplasmic and confirmed Tat substrate (van Mourik *et al.*, 2008)
*Cj0264c***	3 DRRKFLK	Yes	Yes	TMAO reductase, TorA	Predicted periplasmic
Cj0379c	11 QRRNFLK	Yes	Yes	Unknown, YedY homologue	Predicted periplasmic
Cj0414	7 DRRSFFK	Yes	Yes	Gluconate dehydrogenase	Predicted periplasmic
Cj0437 **	5 SRRDFIK	Yes	Yes	Methyl-menaquionol fumarate reductase, MfrA	Periplasmic (Guccione *et al.*, 2010)
Cj0780 **	2 NRRDFLK	Yes	Yes	Nitrate reductase, NapA	Periplasmic and confirmed Tat substrate (van Mourik *et al.*, 2008)
Cj0781	3 GRREFFV	Yes	Yes	Nitrate reductase, NapG	Predicted membrane-bound
Cj0782§	7 ARRIVQL	No	No	Nitrate reductase, NapH	Predicted membrane-bound
Cj1186c	6 SRRSFMG	Yes	Yes	PetA Rieske subunit	Predicted membrane-bound
Cj1267c	36 SRRDFMK	No	Yes	Hydrogenase, HydA	Periplasmic (Hoffman & Goodman, 1982)
Cj1358c§	4 LRRKILK	No	No	Nitrite reductase, NrfH	Predicted membrane-bound
*Cj1511c***	11 TRRSFLK	Yes	Yes	Formate dehydrogenase, FdhA	Predicted periplasmic
Cj1513c	3 NRREFLK	Yes	Yes	Unknown, periplasmic TAT signal peptide	Predicted periplasmic
Cj1516 **	2 NRRNFLK	Yes	Yes	Multicopper oxidase, CueO	Periplasmic (Hall *et al.*, 2008)

* The numbers correspond to amino acid position in the protein.

** The enzyme activity was measured in this study

†TATFIND v1.4 (http://signalfind.org/tatfind.html; Rose *et al.*, 2002) results for the *C. jejuni* NCTC11168 genome. Predicted substrates are in agreement with those identified by Dilks *et al.* (2003).

‡TatP v1.0 (http://www.cbs.dtu.dk/services/TatP/; Bendtsen *et al.*, 2005) results for the *C. jejuni* NCTC11168 genome. Sequences that gave a positive result with any output parameter were manually analyzed for the presence of a variant of the conserved S/TRRxFLK Tat signal motif (Berks, 1996).

§These membrane-bound proteins were included (despite negative predictions with TATFIND and TatP) due to the presence of a response regulator-containing motif and the possibility that they may be membrane-anchored via an uncleaved TAT sequence.

4.2 Results

4.2.1 Identification of *tatA1* and *tatA2* genes in *C. jejuni* strain NCTC 11168

The TatA protein discovered among different bacteria shares several common structural features: it has an N-out, C-in topology and possesses a hydrophobic N-terminal transmembrane helix (TMH), followed by a hinge-region with a highly conserved FG sequence and then an amphipathic helix (APH) associated with the inner surface of the cytoplasmic membrane (Koch *et al*., 2012; Porcelli *et al*., 2002). Although TatA is widely distributed in various species of bacteria and recognised easily according to the features above, there are still some TatA-like TAT components existing with shorter or truncated structure at their C-terminus and assigned as TatE. The typical TatE protein was demonstrated in the genome of *E. coli* strain MG1655 and it shared all common features with TatA protein despite its shorter C-terminal (Fig. 4.1 a). The *cj1176c* gene in *C. jejuni* NCTC 11168 is located between *gmk* (guanylate kinase) and *argS* (arginyl-tRNA synthetase) genes and encodes a TatA homologue that also has all of these features above (Fig. 4.1 a and b), although no functional studies of this gene have been reported. However, the gene *cj0786* was found in the nitrate reductase (*nap*) operon (Fig. 4.1 a) and thus might be involved in nitrate reduction. But the sequence comparisons and secondary structure predictions of the product of the *cj0786* gene showed that it also encoded a protein with the appropriately placed helices and the FG hinge region (Fig. 4.1 b), although it is shorter than Cj1176 (57 compared to 79 aa) due to truncation at the C-terminus. It is thus more like the *E. coli* TatE protein. Due to this finding, the genes *cj1176c* and *cj0786* were designated here as *tatA1* and *tatA2* in *C. jejuni* strain NCTC 11168.

Furthermore, the bioinformatics analysis of epsilonprobacterial genome sequences indicated that the *tatA1* gene was present in all species examined, whereas *tatA2* was absent in many species. Due to the unusual location at the distal end of the *nap* operon, the *tatA2* gene was only present in the related four species: *C. jejuni*, *C. coli*, *C. lari* and *C. upsaliensis* (Table 4.2 and Fig. 4.2) but the TatA2 proteins in *C. lari* and *C. upsaliensis* lack the conserved glycine of the FG hinge region (Fig. 4.2).

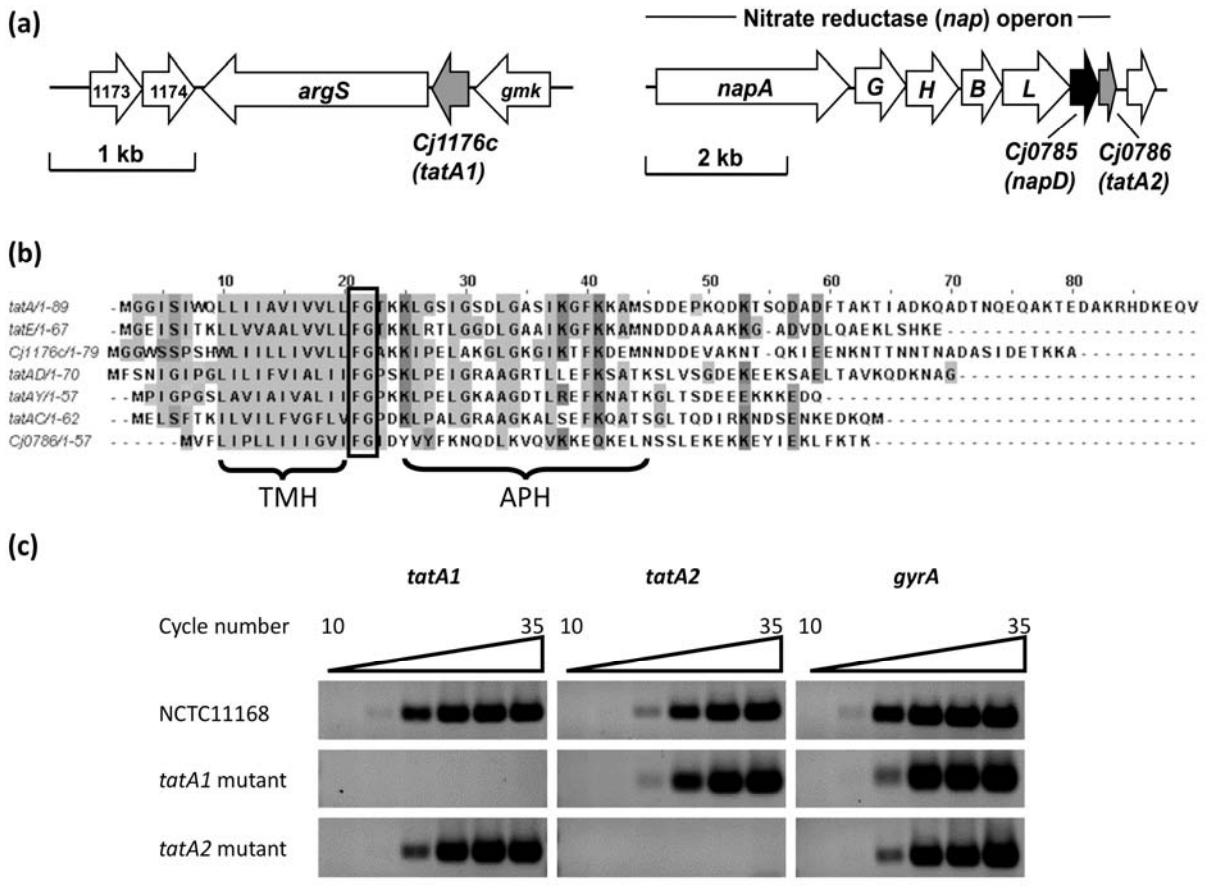

Figure 4.1 The identification of *tatA1* (*cj1176c*) and *tatA2* (*cj0786*) in *C. jejuni* strain NCTC 11168. (a) *tatA1* (*cj1176c*) is located between *gmk* (guanylate kinase) and *argS* (arginyl-tRNA synthetase) genes whereas *tatA2* (*cj0786*) is part of the *nap* (nitrate reductase) operon, immediately downstream of a *napD* homologue (*cj0785*). **(b)** Sequence alignment of TatA/E proteins. TatA and TatE are from *Escherichia coli* strain MG1655. TatAY, TatAD and TatAC are from *Bacillus subtilis* strain 168. The boxed, highly conserved, region is the "FG" hinge between the transmembrane helix (TMH) and amphipathic helix (APH). **(c)** RT-PCR of *tatA1, tatA2* and *gyrA* (control housekeeping gene) expression in *C. jejuni* NCTC 11168, *tatA1* and *tatA2* mutant strains. Primers used for gene specific amplification are listed in section 2.3.6. Agarose gels of amplicons resulting after the number of PCR cycles indicated are shown.

Table 4.2 *nap* operon arrangement and correlation with *tatA2* and *mfr* genes in selected species of Epsilonproteobacteria.

Strain	*nap* operon	*tatA2* gene?	*mfr* genes?
C. jejuni NCTC 11168	*napAGHBLDtatA2*	YES	YES
C. coli Rm2228	*napAGHBLDtatA2*	YES	NO
C. lari RM2100	*napAGHBLDtatA2**	YES	NO
C. upsaliensis RM3195	*napAGHBLDtatA2**	YES	NO
Helicobacter hepaticus ATCC 51449	*napAGHBLD*	NO	NO
C. fetus fetus 82-40	*napAGHBFLD*	NO	NO
C. hominis BAA-381	*napAGHDFLD*	NO	NO
C. concisus 13826	*napAGHBFLD*	NO	YES
C. curvus 525.92	*napAGHBFLD*	NO	YES
Arcobacter butzleri RM4018	*napAGHBFLD1*	NO	NO
Sulfurimonas denitrificans DSM 1251	*napAGHBFL1D23*	NO	NO
Wolinella succinogenes	*napAGHBFLD*	NO	YES

BLAST searches with the *C. jejuni* NCTC 11168 TatA2 were performed on the genomes shown. Where *tatA2* genes are present, they are encoded at the distal end of the *nap* operons. The *tatA2** genes encode TatA2 homologues which lack the conserved glycine residue in the FG hinge region (see Fig. 4.2). The *nap* operons of *A. butzleri* and *S. denitrificans* have additional genes of unknown function denoted by numbers, as described by Kern and Simon (2009a).

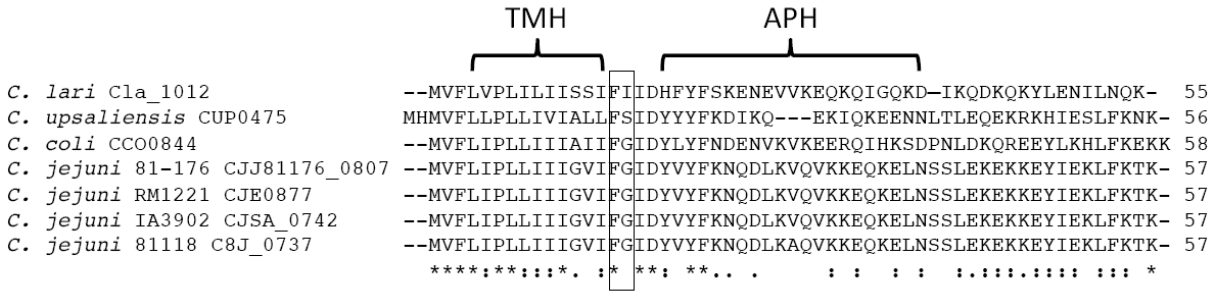

Figure 4.2 Alignment of TatA2 sequences from selected *Campylobacter* strains. In *C. jejuni* and *C. coli*, the sequences are highly similar and possess the conserved FG hinge region (boxed). Note the substitution of the glycine in this motif in the *C. lari* and *C. upsaliensis sequences*. Alignment was performed using Clustal Omega.

4.2.2 Construction of *tatA1*, *tatA2* and *tatA1tatA2* mutants in strain NCTC 11168

The same cloning strategy described in section 3.2.1 was carried out for creating *tatA1* and *tatA2* mutants respectively in strain NCTC 11168. The *cj1176* gene was replaced by a *kan* cassette and the *cj0786* gene was replaced by a chloramphenicol resistant cassette (*Cat*) which was amplified from pAV35 vector (van Vliet *et al*., 1998) by ISACAT-F and ISACAT-R primers. Two ISA reactions were performed with necessary fragments and resulted in pGEM1176kan and pGEM786Cat plasmids. Then both constructs were checked by the pGEM3Zf(-)-specific primer set of 3zf-F and 3zf-R to obtain correct clones with estimated sizes contributed by each fragment. The electroporated wild-type NCTC 11168 with two plasmids above were screened on the blood agar plates supplemented kanamycin or chloramphenicol (30 μg/ml) respectively and the transformants were confirmed by PCR using the forward primer of the antibiotic cassettes and the reverse primer of 3' flanking region. The *tatA1*$^{-}$*tatA2*$^{-}$ double mutant strain was constructed by delivering pGEM1176kan vector into *tatA2*$^{-}$ strain and screened by plates with kanamycin. Then the stable double mutant strain was cultured in MH-S broth supplemented with kanamycin and chloramphenicol. Their phenotypes would be also confirmed by the growth curve and the assays of those TAT-dependent substrates (section 4.2.4 to 4.2.7).

In order to confirm the relationship of gene expression of *tatA1* and *tatA2* in *C. jejuni* strain NCTC 11168, reverse-transcriptase PCR (RT-PCR) was carried out with a housekeeping gene *gyrA* as the internal control. The result of RT-PCR of *tatA1*, *tatA2* and *gyrA* expression in the wild-type and both mutants constructed above is shown in figure 4.1 c. The DNA gel clearly shows that both *tatA* genes were expressed in wild-type cells and the deletion of either *tatA* homologue did not appear to significantly affect expression of the other.

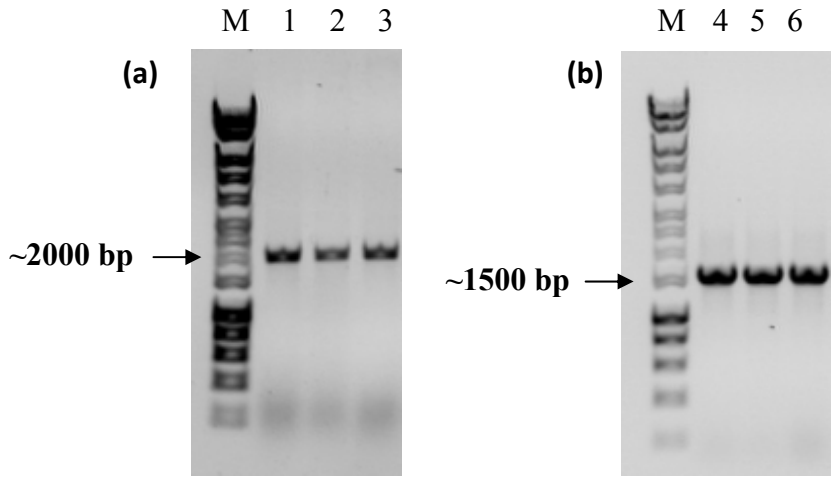

Figure 4.3 Verification of *tatA1 and tatA2* mutant strains of NCTC 11168. (a) Agarose gel electrophoresis confirmation of *tatA1*$^{-}$ mutants. Lane 1 to 3 shows the colony PCR product (*kan* + 3' flanking region of *cj1176*) obtained from *tatA1*$^{-}$ mutants with Kan-F and pGEM1176-3R primers. **(b)** Lane 4 to 6 shows the colony PCR product (*cat* + 3' flanking region of *cj0786c*) obtained from *tatA2*$^{-}$ mutants using ISACAT-F and pGEM0786-3R primers; lane M: HyperLadder^{TM} 1kb molecular weight marker (Bioline).

4.2.3 Construction of *tatA1*$^{+/-}$ and *tatA2*$^{+/-}$ complemented strains

The complementation of *tatA1* and *tatA2* mutants was carried out by using pC*metK* and pK*metK* plasmids (Duncan Gaskin, IFR, UK) where chloramphenicol is the selection marker of pC*metK* and kanamycin is for pK*metK*. Both of them share common features of sequence with pC46 (section 3.2.4). Furthermore, the *metK* promoter is located upstream of *Bsm*BI restriction site which is a moderate and constitutive promoter in gene expression. The *Esp*3I site allows conservation of the reading frame of the inserted fragment initiating at the start codon (ATG in most cases) and this strategy is more specific to *tatA2* since its location is just right after *cj0785* which means they share a promoter located upstream of *napA* (Fig. 4.1 a) and it is inapplicable to adapt the same cloning strategy as *tsdA*$^{+/-}$ in strain 81116 (section 3.2.4). The *tatA1* (*cj1176c*) and *tatA2* (*cj0786*) genes were cloned into pC*metK* and pK*metK* vector respectively via *Esp*3I sites on both vectors and PCR amplified fragments (*tatA1*: 1176c-F and 1176c-R; *tatA2*: 0786c-F and 0786c-R). Correct transformants were confirmed by colony PCR (Fig. 4.4 b and d) and the recovered phenotype was also confirmed by the growth curve and the biochemical analysis, described below.

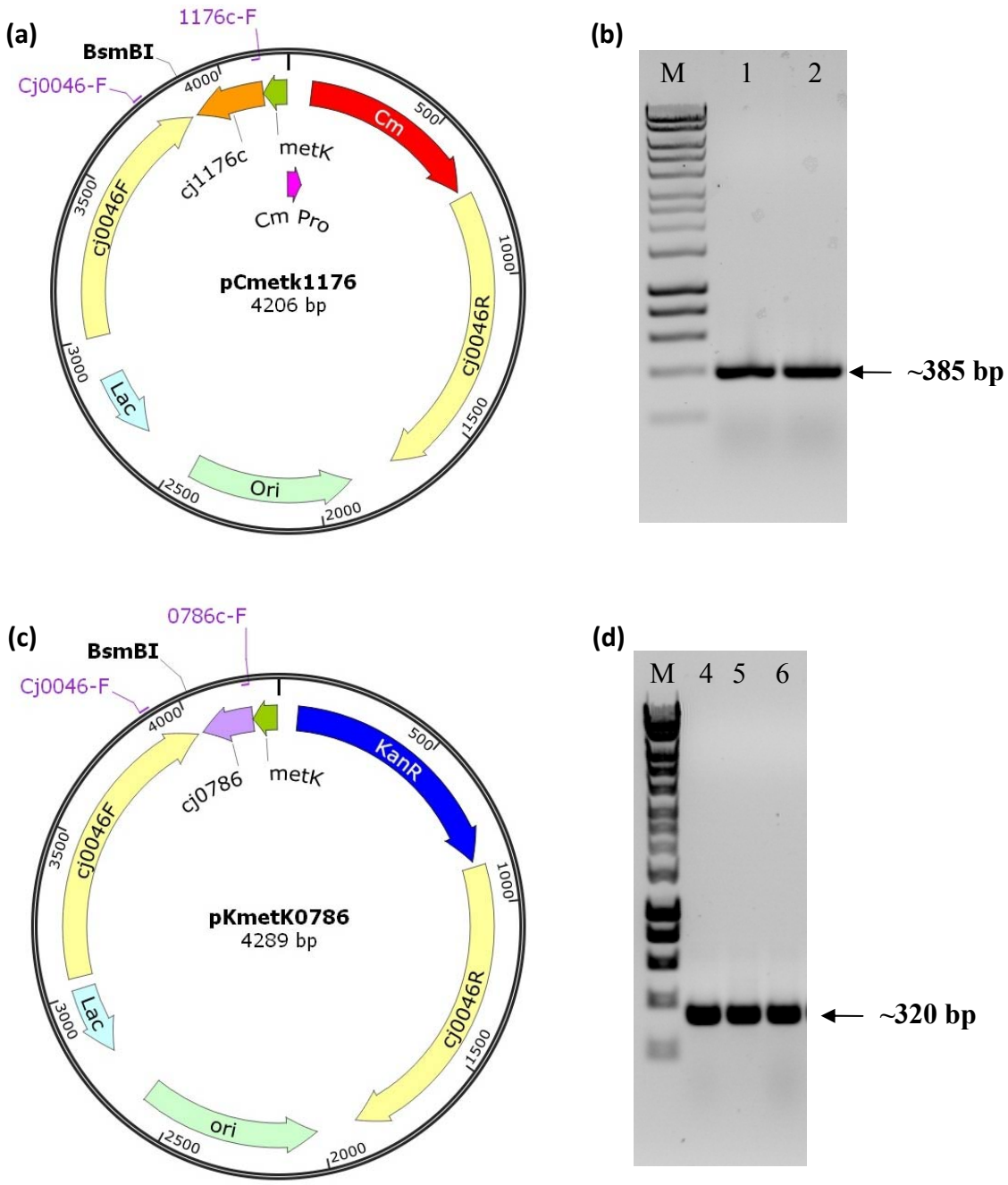

Figure 4.4 Constructions of pC*metK*1176 and pK*metK*0786 plasmids and verification of *tatA1*$^+$ and *tatA2*$^+$ *C. jejuni* strains. (a) The map of pC*metK*1176. The *tatA1* gene (*cj1176c*) was cloned into pC*metK* vector and the gene expression was regulated by *metK* promoter. **(b)** Agarose gel electrophoresis confirmation of the *tatA1*/*tatA1*$^+$ strain. Lane 1 and 2: The colony PCR product obtained from *tatA1*/*tatA1*$^+$ *C. jejuni* transformants amplified by 1176c-F / cj0046-F primers. **(c)** The map of pK*metK*0786. The *tatA2* gene (*cj0786*) was cloned into pK*metK* vector using the same strategy as that of pC*metK*1176. **(d)** Agarose gel electrophoresis confirmation of the *tatA2*/*tatA2*$^+$ strain. Lane 4 to 6: The colony PCR product obtained from *tatA2*/*tatA2*$^+$ *C. jejuni* transformants amplified by 0786c-F / cj0046-F primers. Lane M: HyperLadder^{TM} 1kb molecular weight marker (Bioline).

4.2.4 Growth phenotypes of the *tatA* mutants under microaerobic and oxygen-limited conditions

The growth characteristics of wild type NCTC 11168, mutants and complemented strains under standard microaerobic growth condition is shown in figure 4.5. The *tatA1* mutant showed a severe growth defect under an oxygen-dependent environment but the growth was fully recovered in the complemented strain *tatA1*$^{+/-}$ (Fig. 4.5 a), which indicated the importance of *tatA1* in the aerobic growth of *C. jejuni*. However, the deletion of *tatA2* did not noticeably affect its growth rate or final cell density (Fig. 4.5 b) but interestingly the *tatA1tatA2* double mutant grew less well than the *tatA1* mutant (Fig. 4.5 a and b), suggesting a role for *tatA2*, at least in the absence of TatA1.

Figure 4.6 shows the growth curve of wild type, mutant and their complemented strains under severely oxygen-limited conditions with either nitrate or TMAO as electron acceptors. The periplasmic molybdoenzymes nitrate reductase (NapA) and TMAO reductase (TorA) have previously been shown to be TatC dependent (table 4.1; van Mourik *et al*., 2008; Hitchcock *et al*., 2010) and are the sole reductases for nitrate and TMAO respectively in strain NCTC 11168. The specific role of TatA2 in nitrate reduction under oxygen-limited condition attracted more attention since the *tatA2* gene is located in the *nap* gene cluster. In the presence of nitrate, the oxygen-limited growth of *tatA1* mutant was totally abolished and complementation with the *tatA1* gene restored growth to wild-type levels (Fig. 4.6 a). However, the *tatA2* mutant grew as well as the wild-type with nitrate as electron acceptor under these conditions. In the presence of TMAO, the *tatA1* mutant also showed no growth, but the *tatA2* mutant displayed a slightly lower rate than the wild-type, which was restored by complementation (Fig. 4.6 b). Unsurprisingly, there was not any growth observed in the double *tatA1tatA2* mutant supplemented with either nitrate or TMAO (Fig. 4.6 a and b). None of the strains grew without any exogenous electron acceptors under oxygen limitation (data not shown). Thus, the data suggest that TatA2 is not required for the assembly of the periplasmic nitrate reductase, but that it may have some role in the biogenesis of the TMAO reductase.

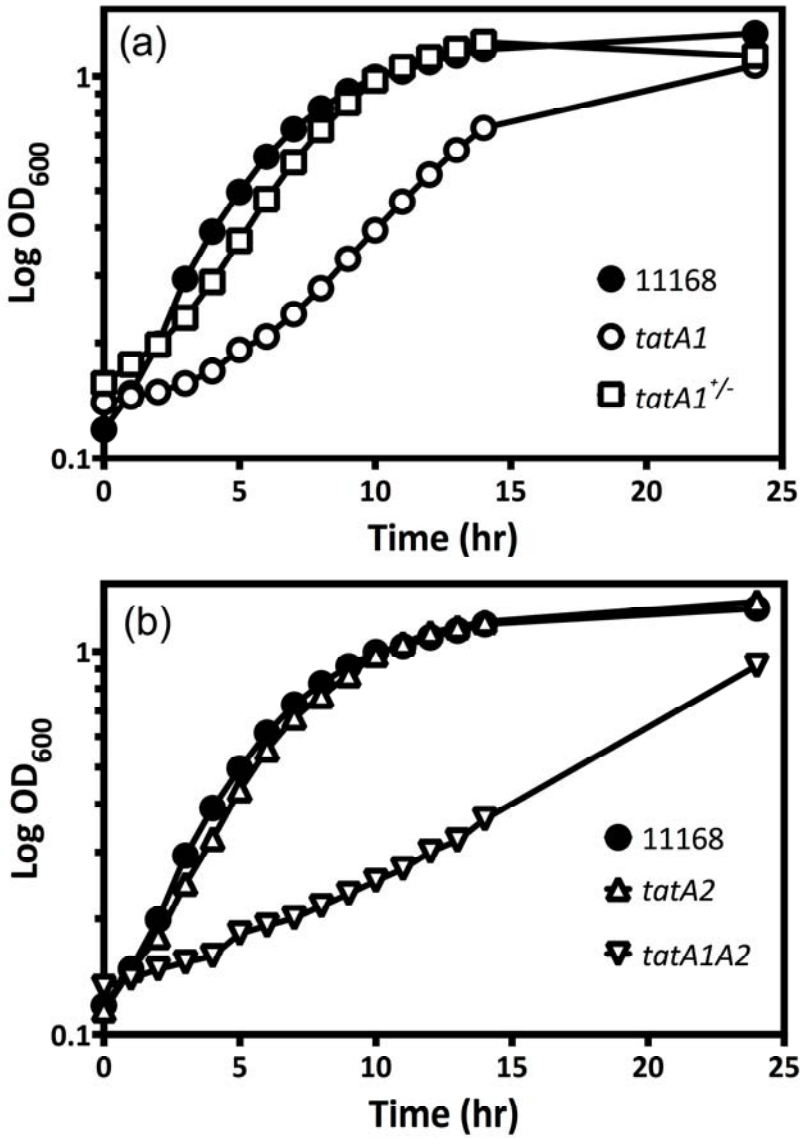

Figure 4.5 Microaerobic growth curves of wild type, mutant and complemented strains in 100 ml volumes of MH-S medium in 250 ml conical flasks shaken at 180 r.p.m. in a microaerobic gas atmosphere of 10% (v/v) oxygen, 5% (v/v) carbon dioxide and 85% (v/v) nitrogen. (a) The *tatA1* mutant shows a growth defect, which could be complemented by integration of the wild-type *tatA1* gene at the *cj0046* pseudogene locus, driven by the *metK* promoter. **(b)** The mutation of *tatA2* did not affect the growth rate under microaerobic conditions. Nevertheless, a double *tatA1tatA2* mutant grew worse than the *tatA1* mutant alone, suggesting a physiological role for TatA2, at least in the absence of TatA1. Data shown is for a single experiment; independent growth experiments were carried out three times with similar results.

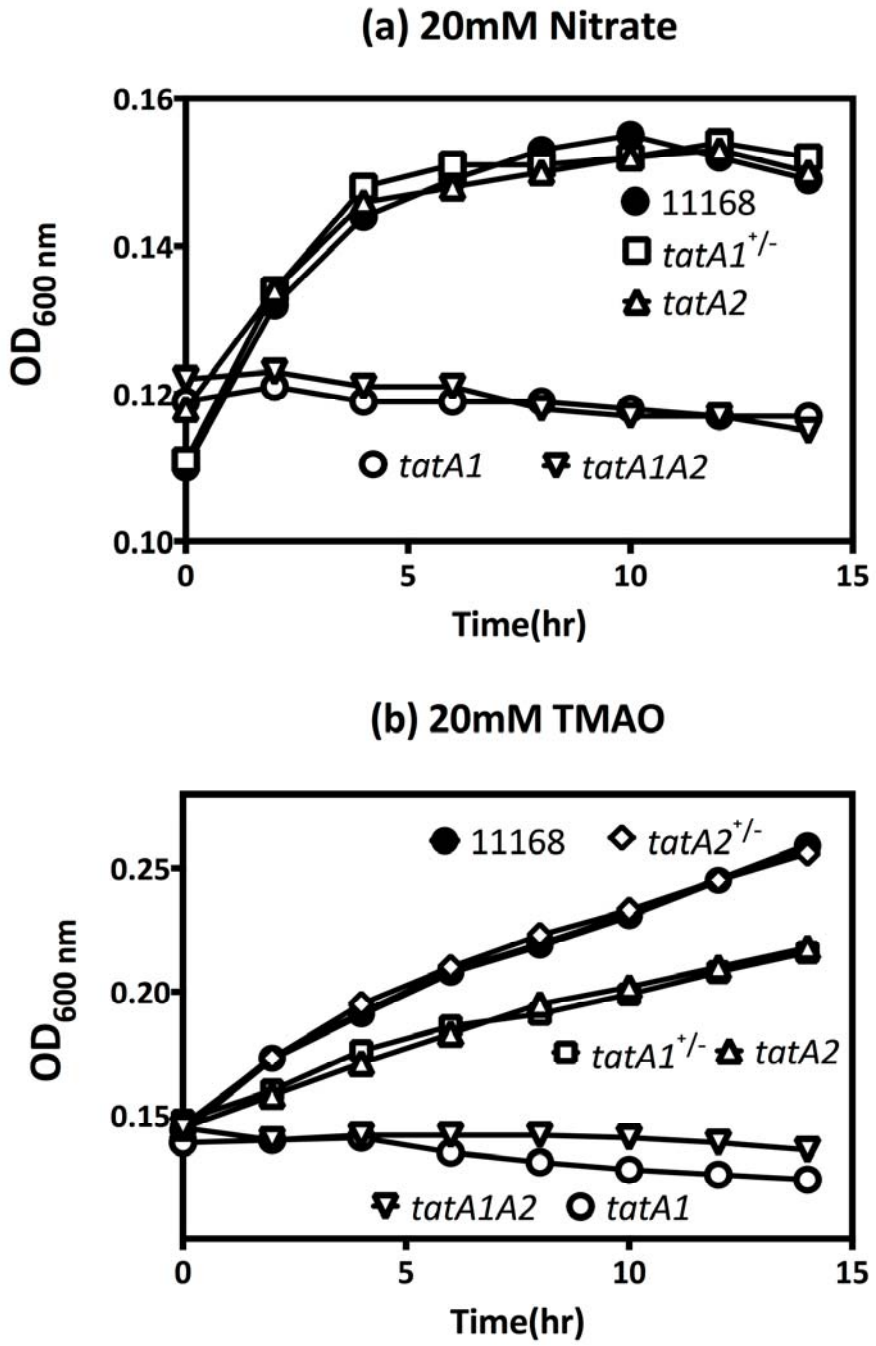

Figure 4.6 Oxygen-limited growth curves of wild type, mutant and complemented strains. Cultures of *C. jejuni* were incubated at 37°C in almost completely filled 500 ml unshaken conical flasks containing BHI medium supplemented with 20 mM nitrate **(a)** or 20mM TMAO **(b)** as electron acceptors. None of the strains grew without any electron acceptors under oxygen limitation (data not shown). The data shown are representative of at least three independent growth experiments.

4.2.5 Dependence of the assembly of cofactor containing electron transport enzymes on TatA1 and TatA2

Seven TAT-dependent periplasmic enzymes were chosen to examine their correct transportations across the cytoplasmic membrane in wild-type, *tatA1* or *tatA2* mutants and complemented strains. Since the transportations of nitrate reductase, sulphite oxidase, formate dehydrogenase, multi-copper oxidase, TMAO reductase and fumarate reductase were affected in a *tatC* mutant (Hitchcock *et al*, 2010), they might be also affected in either *tatA1* or *tatA2* mutants where the TatABC complex was unable to form without the component of TatA and lead to abolished or aberrant protein transportation.

In order to measure the correct export of nitrate reductase subunit NapA to the periplasm, the assay of nitrate-dependent reduced methyl viologen oxidation in intact cells and periplasmic extracts of the strains above was carried out and the oxidation rates were compared. Methyl viologen does not readily cross the inner membrane and in all cases the pattern of activities observed was highly similar in both intact cells (Fig. 4.7 a) and the corresponding periplasmic fractions (Fig. 4.7 b). Mutation of *tatA1* alone resulted in the total abolition of nitrate reductase activity, while mutation of *tatA2* reduced the rate significantly, to about 50% of the wild-type rate. The complemented strains showed a partial restoration of activity, probably due to lower than optimal gene expression from the *metK* promoter. The data above indicates that TatA1 plays the major role in the transportation of NapA, consistent with the growth data above, but also suggests that TatA2 might play a minor role.

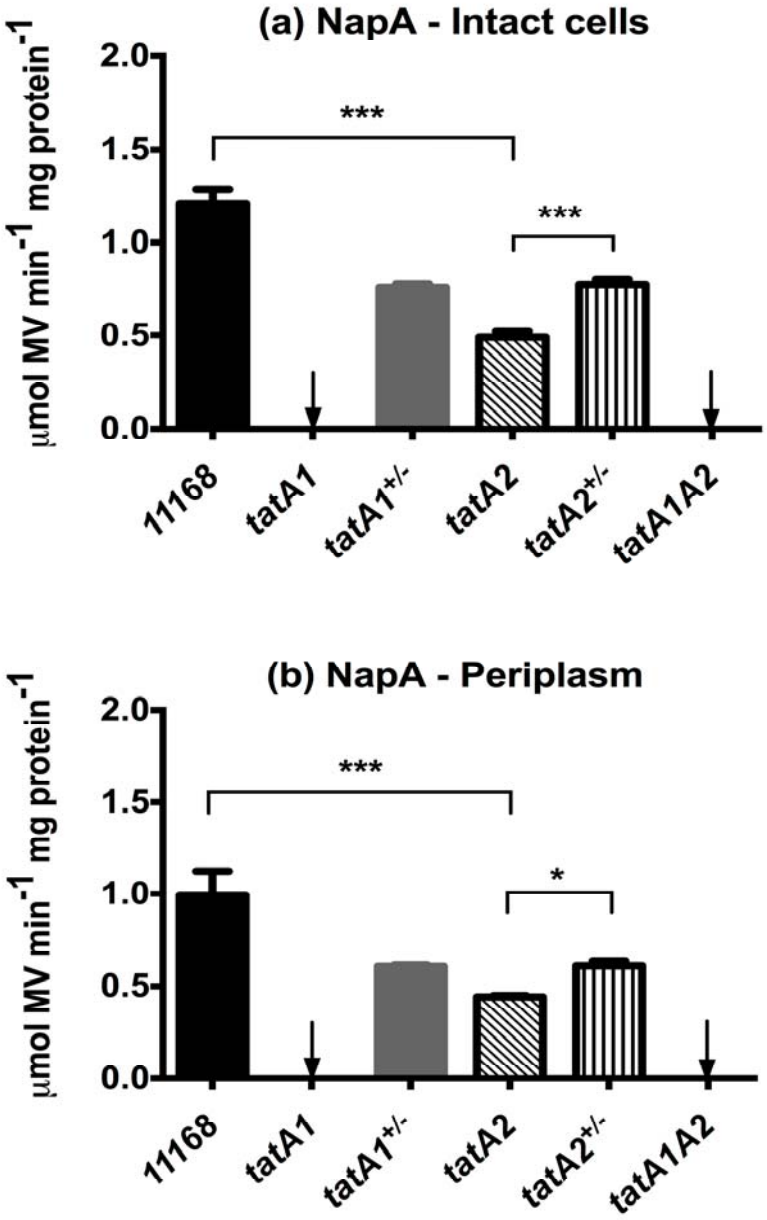

Figure 4.7 Comparison of nitrate reductase activities in (a) intact cells and (b) periplasmic fractions of wild-type, *tatA* mutants and complemented strains. The nitrate dependent oxidation of reduced methyl viologen (MV) was measured as described in Materials and Methods. Relevant significant differences in activity are indicated by *** ($P < 0.001$) and * ($P < 0.05$) according to Students t-test. The data shown are means ± SD of three independent experiments.

Also, an examination of the TatA1 or TatA2 dependency of the activity of several other TAT-dependent cofactor-containing electron transport enzymes in intact cells (TMAO reductase, formate dehydrogenase and sulphite oxidase) or periplasmic fractions (the multi-copper oxidase CueO/Cj1516) is shown in Fig. 4.8. For sulphite oxidase (Fig. 4.8

a), a complete dependency on TatA1 was evidenced by undetectable sulphite respiration in intact cells of the *tatA1* and double mutant, but no significant difference between activities in the wild-type and *tatA2* strain. A very similar pattern was seen for the multi-copper oxidase CueO (Fig. 4.8 b). In contrast, a partial dependency on TatA2 was observed in the case of formate dehydrogenase (Fig. 4.8 c), although, like the case with NapA, mutation of *tatA1* alone resulted in undetectable enzyme activity. With TMAO reductase (Fig. 4.8 d), a significant activity remained in the *tatA1* mutant, indicating continued export of TorA to the periplasm. This could be attributed to TatA2 by the pattern of activities in the *tatA2* and double mutant, the latter exhibiting just a very low residual rate.

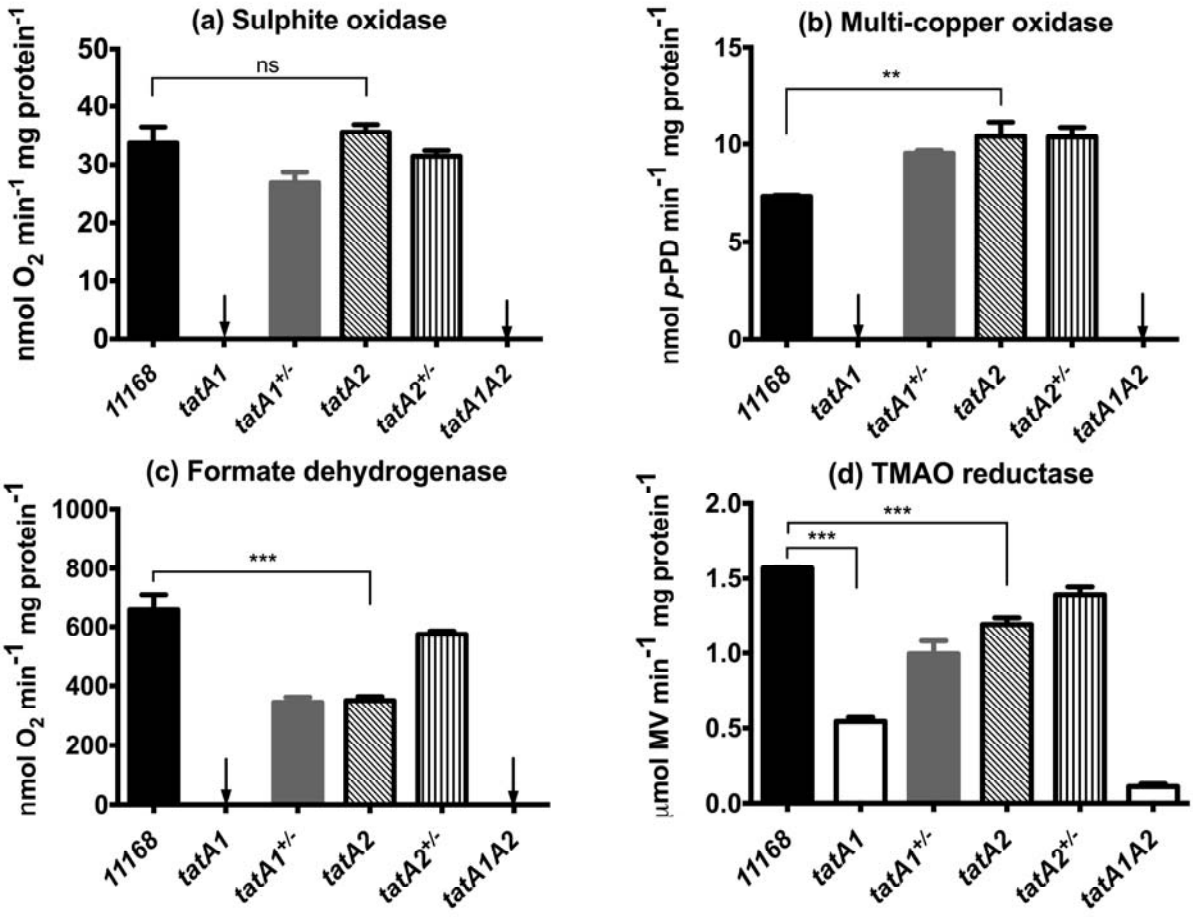

Figure 4.8 The activities of key Tat dependent electron transport enzymes in intact cells of wild-type, mutant and complemented strains. Assay methods were as described in Materials and Methods. Relevant significant differences in activity are indicated by *** ($P < 0.001$) or ** ($P < 0.01$) according to Students t-test (ns; no significant difference). The data shown are means ± SD of at least three independent experiments.

4.2.6 Export of the periplasmic fumarate reductase subunit MfrA occurs via either TatA1 or TatA2

Unusually, *C. jejuni* possesses two fumarate reductases, one acting as a reversible bi-functional succinate dehydrogenase/fumarate reductase (Frd) that is cytoplasmic-facing and non-TAT dependent, while the other (methylmenaquinone fumarate reductase, Mfr) is a periplasmic-facing enzyme that acts as a unidirectional fumarate reductase (Guccione *et al*., 2010). The active site subunit of the latter enzyme, MfrA, has a twin-arginine signal sequence and its export was shown to be unequivocally TAT dependent in studies with a *tatC* mutant (Hitchcock *et al*., 2010). In order to investigate weather MfrA translocation to the periplasm requires either paralogue, an assay measuring fumarate dependent reduced benzyl viologen oxidation in periplasmic extracts was performed, and the MfrA protein was also directly detected by the immunoblotting with anti-MfrA polyclonal antibodies. Figure 4.9 a shows that in marked contrast to the other electron transport enzymes studied above, inactivation of either *tatA1* or *tatA2* individually had no effect on MfrA activity in the periplasm. However, this activity was abolished in the *tatA1tatA2* double mutant. The corresponding immunoblots of the periplasmic fractions (Fig. 4.9 b) show that the MfrA subunit is indeed translocated in both the single *tatA1* and *tatA2* mutants, while it is absent in the double mutant. Interestingly, a higher molecular mass form (~66 kD) corresponding to the size expected of the unprocessed protein is clearly present in the *tatA1* periplasm, accompanied by a smear suggesting some degradation, while in the *tatA2* mutant periplasm only the ~63 kDa band corresponding to the mature form is visible, suggesting normal processing. Complementation with the wild-type *tatA1* gene restored normal processing in the *tatA1* mutant. A similar pattern was seen in total cell-free extracts, but in the double mutant there was no evidence of the accumulation of the unprocessed MfrA, indicating that it is degraded in this mutant background (Fig. 4.9 b). Taken together, these data do suggest redundancy between TatA1 and TatA2 for the translocation of MfrA, but also reveal an unexpected processing defect when the cells are forced to use TatA2 in the *tatA1* mutant background.

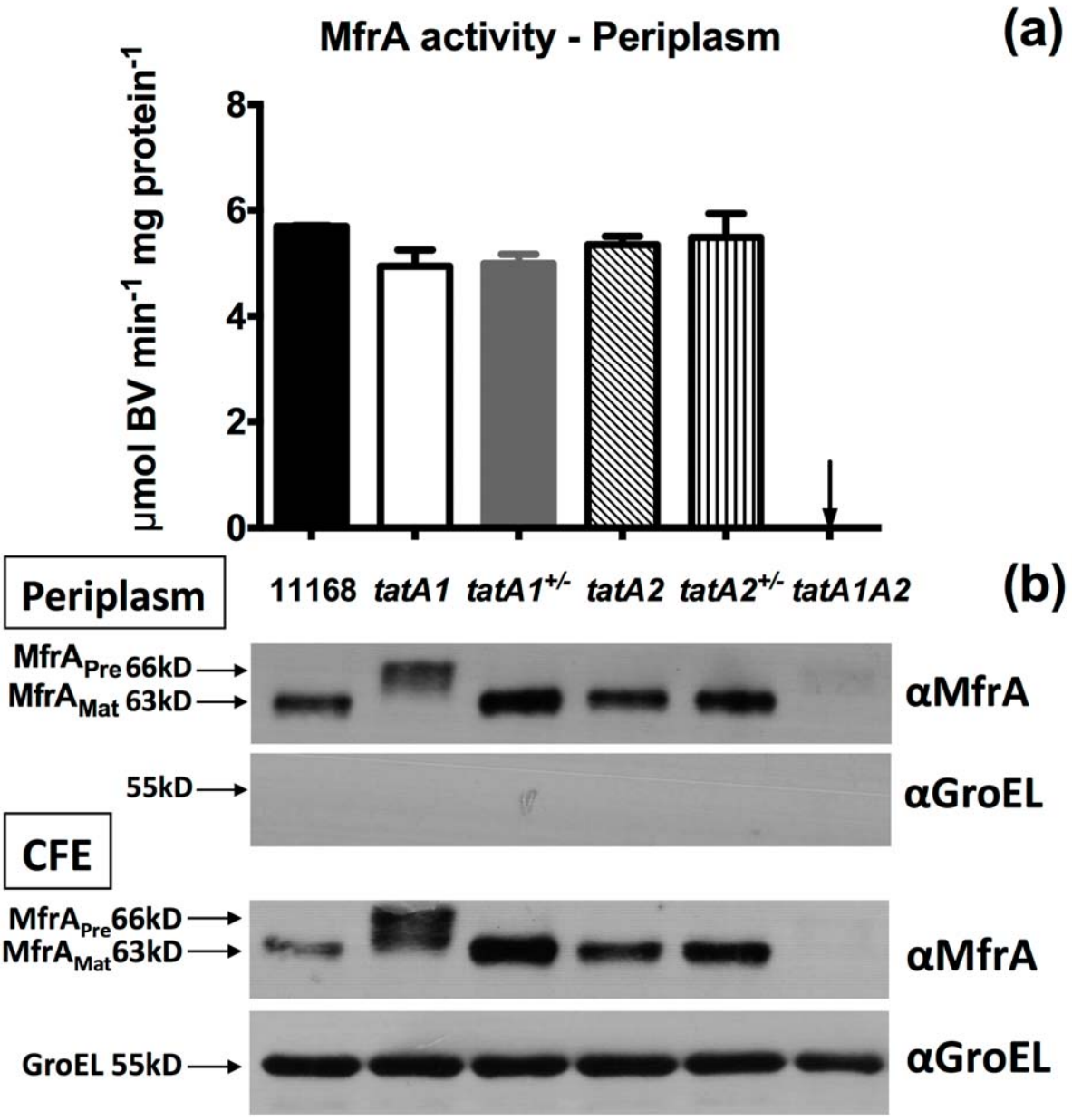

Figure 4.9 Dual dependence of MfrA translocation on TatA1 and TatA2. **(a)** The activity of MfrA in periplasmic extracts of the strains are shown (means and standard deviations of three independent experiments), as measured by the fumarate dependent oxidation of reduced benzyl viologen. In **(b)** corresponding immunoblots are shown of both periplasmic fractions (upper two panels) and cell-free extracts (CFE; lower two panels), probed with either anti-MfrA or anti-GroEL antibodies. The latter was used as a control for cytoplasmic contamination of the periplasm. Approximately 5 µg periplasmic protein and 15 µg CFE protein was loaded in each lane.

4.2.7 The Tat-dependent but cofactorless enzyme alkaline phosphatase (PhoX) is translocated exclusively via TatA1

The alkaline phosphatase (PhoX) is a unique case of TAT-dependent enzyme in the periplasm of *C. jejuni* because all other enzymes studied in the previous section possess complex cofactors, which explain their requirement for transport through the TAT system. Among the TAT substrate proteins in *C. jejuni* (Table 4.1), the alkaline phosphatase encoded by *cj0145* (PhoX; van Mourik *et al*., 2008) is a hydrolytic enzyme that only requires calcium ions and no known cofactor is necessary for its conformational stability and enzyme activity. PhoX may be an example of a TAT substrate that has folding requirements or kinetics that are incompatible with Sec translocation (van Mourik *et al*., 2008). Furthermore, PhoX expression is inducible under conditions of phosphate limitation (Section 2.2.3; Wösten *et al*., 2006). The result of assays for alkaline phosphatase activity in intact cells of wild-type, mutant and complemented strains is shown in Fig. 4.10. Deletion of *tatA1* completely abolished PhoX activity while complementation with the wild type *tatA*1 gene completely restored it. In contrast, deletion of *tatA2* did not affect PhoX activity. The data thus indicate a complete dependence of PhoX translocation on TatA1.

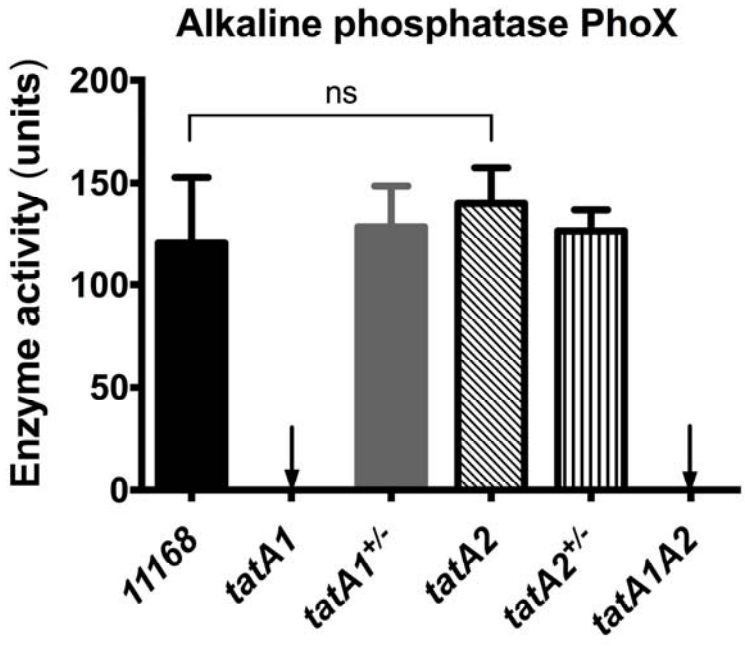

Figure 4.10 The non-cofactor containing enzyme alkaline phosphatase (PhoX) is exclusively translocated via TatA1. Rates of hydrolysis of *p*-nitrophenyl-phosphate were measured in phosphate limited intact cells without lysis using the assay described in Methods. The units of activity are normalised to cell density (see van Mourik *et al*., 2008 and Methods). The data shown are means ± SD of three independent experiments (ns; no significant difference)

4.3 Discussion

Although the genome size of *C. jejuni* is relatively smaller than that of other pathogenic bacteria, it has a highly branched electron transport system including various oxidases and reductases which offer many possibilities to this bacterium for host adaption (Kelly, 2008). Most redox partners in the electron transport chain locate in the periplasm and contain specific co-factors for the enzyme activity. Therefore, in order to maintain the enzyme activity and structural integrity, their transportation across the cytoplasmic membrane becomes a crucial issue. The TAT system not only can avoid ion competition during co-factor acquisition when folding but guarantees holoenzyme transportation (Tottey *et al*., 2008), which means the enzyme is immediately active in the periplasm. The TatA protein is considered as the component for the pore forming or membrane structure weakening activity during the transportation. Two *tatA* homologues were found in *C. jejuni,* suggesting either different roles in the transportation of different substrates or that the same substrate can utilise either of them. In fact, rather few Gram-negative bacteria have been identified which have duplicated *tat* genes. As in *C. jejuni*, the commonest situation is the presence of an additional TatA homologue, which has variably been called TatE or TatA2. In *E. coli*, *tatE* is expressed at low levels and deletion of *tatE* has no effect on TAT transport or cell viability (Jack *et al.,* 2001). TatE is C-terminally truncated compared to TatA, but functional studies show that, like TatA, TatE can translocate substrates of varying size (Baglieri *et al.*, 2012). Interestingly, biofilms cells express the *tatE* gene at a higher level than in planktonic cells (Beloin *et al*., 2004), hinting at a specialised role under stress conditions. In contrast, in the denitrifying bacterium *Pseudomonas stuzeri* a *tatE* gene is located in the *nos* gene cluster, required for nitrous oxide reduction and was shown to be essential for denitrification (Heikkila *et al.,* 2001), presumably because it is specifically required for the translocation of the NosA polypeptide to the periplasm. In the Gram-negative predatory bacterium *Bdellovibrio bacteriovorus*, *tatA1* and *tatA2* genes have also been identified and here TatA2 was shown to be essential for both host-dependent and host-independent growth, while deletion of *tatA1* slowed the rates of growth in each mode (Chang *et al*., 2011). The TAT system in this bacterium clearly has a key role in transporting essential proteins into the prey and the TatA paralogues seem to play distinct roles in this.

Overall, all data in this chapter clearly indicates that TatA1 is the most important TatA paralogue in *C. jejuni*. The deletion of the cognate gene resulted in severe defects in microaerobic or oxygen-limited growth. Also, the enzyme activities of many TAT-dependent substrates were partly/totally abolished in the *tatA1* mutant. Nevertheless, although individual deletion of *tatA2* did not affect microaerobic growth, that growth of the double mutant was more severely inhibited compared to the *tatA1* single mutant does suggest a role for TatA2 under respiratory conditions with oxygen as the electron acceptor. The TAT dependency of the Rieske iron-sulphur subunit of the cytochrome bc_1 complex is the most likely reason for these growth defects (Bachmann *et al*., 2006; Hitchcock *et al.,* 2010) and the data imply TatA1 has a dominant but not exclusive role in its assembly.

Since the *tatA1* gene already existed in the genome of *C. jejuni* strain NCTC 11168, the *tatA2* gene seems redundant in TAT-dependent translocation but the position of *tatA2* immediately downstream of the characterized *nap* gene cluster (Pittman *et al*., 2007; Fig. 4.1 a) initially suggested a specific role in the assembly of the periplasmic nitrate reductase system. Indeed, RNAseq analysis of the NCTC 11168 transcriptome (Dugar *et al*., 2013) has shown that *tatA2* is expressed from the primary *napA* promoter along with all of the *bona fide nap* genes. However, although a reduction in NapA specific activity was found in the periplasm of the *tatA2* mutant, this did not result in a noticeable growth defect under oxygen-limited conditions with nitrate as electron acceptor. These data thus suggest that *tatA2* is not specifically required for NapA translocation.

According to the enzyme activities of all TAT-dependent substrates measured with *tatA1* or *tatA2* mutants in this study, there are three classes of TAT protein substrates that had differing dependency patterns on TatA1 and TatA2. For several enzymes, including sulphite oxidase (SorA), the multicopper oxidase (CueO) and alkaline phosphatase (PhoX), complete dependency on TatA1 was observed as their activities in the *tatA2* mutant were identical to wild-type cells, while they were abolished in the *tatA1* mutant. For nitrate reductase, formate dehydrogenase (FdhA) and TMAO reductase (TorA), a statistically significant reduction of specific activity in the *tatA2* mutant was observed, amounting to ~50% in the case of NapA and FdhA, suggesting that TatA2 could partially substitute for TatA1 (Fig. 4.8 and 4.9). Nevertheless, these activities were still abolished in intact cells of the *tatA1* mutant. This might be explained

if there was some interaction between TatA1 and TatA2 such that a mixed complex was optimal for the translocation process. For TMAO reductase, the results were more complex as significant activity (~30 %) remained in the *tatA1* mutant cells and the reduction in activity in the *tatA2* mutant was less than that observed with NapA and FdhA. However, in the growth experiments with TMAO, no growth was found with the *tatA1* mutant and a significant reduction was apparent with the *tatA2* deletion, supporting the involvement of both paralogues in TMAO reductase assembly.

Although the TatA2 protein plays a minor or totally irrelevant role in the transportation of TAT-dependent substrates mentioned above, an intriguing result was found in the translocation of fumarate reductase (MfrA) in the *tatA2* mutants. MfrA, containing the TAT signal peptide and a flavoprotein active site, is a subunit of unusual periplasmic fumarate reductase consisted of MfrABC. The Mfr enzyme (Juhnke *et al*., 2009) is restricted to a limited number of *Epsilonproteobacteria* and is thought to allow the use of non-transportable fumarate analogues like mesaconate and crotonate as electron acceptors as well as more rapid adaptation to fumarate respiration under low oxygen-conditions (Guccione *et al*., 2010). The specific rate of fumarate reduction catalysed by MfrA was similar in periplasmic fractions of both the *tatA1* and *tatA2* mutants and only deletion of both genes abolished activity (Fig. 4.9 a), indicating redundancy of function of the TatA paralogues for the translocation of MfrA. The result suggests the role of the TatA2 protein could be in MfrA assembly even though the gene is encoded in the *nap* operon. However, the immunoblotting showed that unprocessed MfrA accumulated in the periplasm of the *tatA1* mutant while complementation restored the processing defect to normal. The data imply that the pre-protein form of MfrA can be translocated without the cleavage of signal peptide through TatA2 since it is the sole TatA paralogue in the cells. The processing of the signal peptide is considered as the last step in TAT-dependent translocation and the target protein will be released from the TatABC complex (Yahr *et al*., 2001; Luke *et al*., 2009). However, in the absence of TatA1, although TatA2 must be able to form transport-competent TatA2BC complexes, these complexes do not seem to be functionally equivalent to TatA1BC complexes and/or do not allow signal peptidase 1 to cleave the MfrA pre-protein. Comparing with other TAT-dependent substrates in *C. jejuni*, the signal peptide does not show any obvious differences in the amino acid composition, which might indicate a distinct translocation pathway. Furthermore, the presence of the Mfr complex is not correlated

with the presence of two TatA paralogues; the Mfr-containing *C. curvus, C. concisus* and *Wolinella succinogenes* have only one *tatA* gene (Table 4.2).

Taken together, the result above suggests that the TatA2 is not able to function correctly in the transport of any of the substrates tested without the participation of TatA1. This contrasts with for example the *E. coli* TatE protein which can function independently in the absence of TatA. Significantly, TatA2 is lacking two functionally important residues: Phe39 (at the C-terminus of the APH) and Gln8 (at the N-terminus of the TMH; *E. coli* numbering, Fig. 4.1 b). Phe39 appears to be absolutely conserved across TatA's, but in TatA2 is substituted (non-conservatively) with a glutamate. Position 8 in proteobacteria is conserved as a charged residue, but in TatA2 this is a phenylalanine. Both Gln8 and Phe39 have been shown to be required for TatA translocation function (Greene *et al*., 2007; Hicks *et al.*, 2003) and are key to the latest membrane thinning model of TatA pore formation (Rodriguez *et al.*, 2013). In addition, TatA2 has a truncated N-terminus, which might also have functional implications. Thus, it seems most likely that TatA2 would have to interact with TatA1 to form a fully functional complex. If there is interaction between TatA1 and TatA2, then analysis of single null mutants in each gene might not give a full picture of their roles and other methods will be necessary to determine the precise function of each of these proteins in translocation.

4.4 Conclusions

TatA is a major component of twin-arginine translocation system in bacteria. Two TatA paralogues were found in the genome of *C. jejuni* strain NCTC 11168, TatA1 plays a major role in the transportation of TAT-dependent substrates for maintaining cell viability. Its amino acid sequence also shows high similarity to TatA proteins found in other bacteria which suggests the physiological importance of TatA1 in *C. jejuni* cells. However, although the deletion of TatA2 does not affect the cell growth under the microaerobic condition, it still facilitates the translocation of some TAT-dependent enzymes which reduced alternative electron acceptors in the oxygen-limited growth (TMAO; Fig 4.6 b) and suggests a minor role in the TAT system. Interestingly, without TatA1, the fumarate reductase MfrA was still able to be translocated into the periplasm via the TAT system, where TatA2 was the major component for the pore forming / structure weakening of cytoplasmic membrane. The retention of the signal peptide of MfrA in the periplasm also implies that TatA2 itself is insufficient to deal with

pre-proteins in the TatA2BC complex or maybe the signal peptidase is unable to recognise TatA2 complexes. Furthermore, a few crucial residues in the amino acid sequence of TatA2 are not conserved compared to most TatA proteins, suggesting its supportive role to TatA1.

In short, two issues in the TAT system of *C. jejuni* are still worthy to be investigated. Firstly, the actual evidence of the interaction between TatA1 and TatA2 and the forming of a TatA2BC complex has to be carried out to prove the translocation of MfrA in the *tatA1* mutant is achieved by homo-oligomers formed by TatA2, which lacks crucial residues Gln8 and Phe39. Also, the interactions between the twin-arginine signal peptide of MfrA and the TatA2BC complex is still unclear. Possibly the dynamic model of translocation directed by TatA2 is different from that of TatA1 since the signal peptide of MfrA is not processed. There might be other TAT-dependent substrates like the periplasmic MfrA among different bacteria which are essential for survival and the "tango" between TatA paralogues will allow more flexibility in the electron transport chain and maintain cellular viability.

Chapter 5

Dissection of the function of novel *c*-type cytochromes in *Campylobacter jejuni*

5.1 Introduction

Periplasmic *c*-type cytochromes play a crucial role in the electron transport chain in *C. jejuni* under both microaerobic and more oxygen-limited conditions. Most importantly, they must mediate electron flow from the bc_1 complex to the terminal *cb*-type oxidase or transfer electrons from various substrates via dehydrogenases/oxidoreductases such as the sulphite oxidase SorAB in strain NCTC 11168 (Myers and Kelly, 2005) or the aforementioned thiosulphate dehydrogenase TsdA in strain 81116 (Chapter 3). They also participate in electron transfer to alternative acceptors like nitrate and TMAO/DMSO. The utilisation of a variety of electron donors and acceptors stimulates growth and offers this pathogen the ability to better survive under various environmental conditions; *c*-type cytochromes are key to this process. According to the genome sequence of *C. jejuni* NCTC 11168 (Parkhill *et al*., 2000), several candidate *c*-type cytochromes of unknown function that are not associated with already known electron transport pathways can be identified. These contain one or more typical -CXXCH- haem-binding motifs, and they are encoded by *cj1153*, *cj1020c*, *cj0037c*, *cj0158c*, *cj0854c* and *cj0874c* (see Table 5.1). Most of them harbour only one -CXXCH- motif, are of low molecular weight (10 to 38 kD) and contain typical Sec-dependent signal sequences for periplasmic localisation. The exception is *cj0158c*, which encodes a predicted membrane anchored *c*-type cytochrome, as it contains a lipoprotein signal sequence. Cj1153 seems the most likely candidate amongst these *c*-type cytochrome that might transfer electrons from the bc_1 complex to the terminal *cb* oxidase under normal microaerobic conditions, because it is most similar to cytochrome c_{553} found in the closely related *H. pylori* and a variety of other bacteria which are known to carry out this role. Interestingly, Cj1020 shows significant sequence similarity to Cj1153. The lipoprotein signal peptide predicted at the N-terminus of Cj0158 suggests it is a periplasmic-facing membrane-bound protein but it is not possible to predict if it is anchored to the inner or outer membrane. The location of *cj0854c* is upstream of *hemL*, which is involved in the biogenesis of the haem molecule.

Two of the proteins in strain NCTC 11168 listed in Table 5.1 each have two –CXXCH- motifs indicating they are dihaem cytochromes. Cj0874 was already identified in

Chapter 3 as a pseudogene of *cjTsdA* (*c8j_0815*) in strain 81116 (section 3.2.2). Without fusion to the other two peptides encoded by *cj0873c* and *cj0876c*, the thiosulphate dehydrogenase activity associated with Cj0874 in strain NCTC 11168 is absent (Chapter 3; data not shown) and tetrathionate reductase activity is also undetectable in this strain (see Chapter 3). The other putative dihaem cytochrome, Cj0037, is the homologue of C8j_0040 in strain 81116 (with 99.42% similarity), which has been demonstrated to possess a very low thiosulphate dehydrogenase activity (section 3.2.11). However, as no thiosulphate respiration has been found in strain NCTC 11168, this suggests that Cj0037 is unlikely to play a physiological role as a thiosulphate dehydrogenase.

In this chapter, the corresponding mutants of genes listed in Table 5.1 (with the exception of *cj0874c*) and the complemented strains will be constructed and the growth phenotypes will provide the first evidence indicating if those *c*-type cytochromes are involved in the ETC of *C. jejuni*. Also, biochemical analysis and respiratory assays with different substrates will be carried out to elucidate the role of these candidate cytochromes. Taken together, the study of *c*-type cytochromes in this chapter has provided a more complete and clear picture of the ETC in *C. jejuni*.

Table 5.1 The candidate cytochromes *c* of unknown function in *C. jejuni* NCTC 11168

Genes	Number of CXXCH domains	Putative Mw of product (kDa)	Remark
cj1153	1	10.84	Homology to many *c*-553 cytochromes
cj1020c	1	16.26	Some sequence similarity to Cj1153
cj0158c	1	15.83	Has a signal sequence with a possible lipid attachment site
cj0854c	1	13.26	Located upstream of haem biosynthesis gene (*hemL*)
cj0874c	2	20.70	A pseudogene, which is homologous to part of *c8j_0815* in strain 81116
cj0037c	2	38.84	The homologous gene of *c8j_0040* in strain 81116

5.2 Results

5.2.1 Construction of mutants of *c*-type cytochrome candidates in strain NCTC 11168

The same general cloning strategy (using ISA) described in section 3.2.1 was carried out for creating *cj1153*, *cj1020c*, *cj0158c*, *cj0854c* and *cj0037c* knockout deletion mutants in strain NCTC 11168, where the *cj1020c* gene was replaced by a chloramphenicol resistance cassette (*cat*) and the other genes were replaced by a *kan* cassette (van Vliet *et al*., 1998). Several ISA reactions were performed with primers as detailed in Materials and Methods and resulted in pGEM1153kan, pGEM1020Cat, pGEM158kan, pGEM854kan and pGEM37kan plasmids. All constructs were PCR checked by the pGEM3Zf(-)-specific primer set of 3zf-F and 3zf-R to obtain correct clones with the expected sizes contributed by each fragment. The plasmids were electroporated into wild-type NCTC 11168 and transformants were selected on blood agar plates supplemented kanamycin (50 μg/ml) or chloramphenicol (30 μg/ml) as appropriate. The correct transformants were confirmed by colony PCR using the forward primer of the antibiotic cassettes and the reverse primer of 3' flanking region. However, the transformants with pGEM854kan seem unable to survive on the plates with kanamycin (at least 5 attempts with no colonies growing), suggesting that *cj0854c* might be essential for *C. jejuni* NCTC 11168. Its role is still worthy of future investigation. The phenotypes of the remaining viable mutants will be studied by growth curves and biochemical analysis.

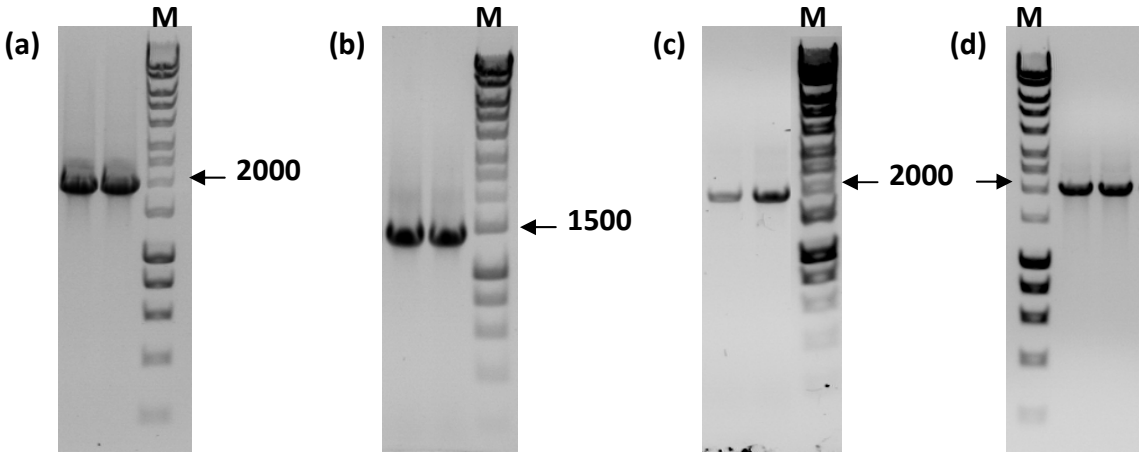

Figure 5.1 Verification of *cj1153*, *cj1020c*, *cj0037c and cj0158c* mutant strains of NCTC 11168. (a) Agarose gel electrophoresis confirmation of *cj1153* mutants, **(b)** *cj1020c* mutants, **(c)** *cj0037c* mutants, **(d)** *cj0158c* mutants. The colony PCR was performed by using Kan-F / corresponding 3R primers in (a), (c) and (d); and ISACAT-F / pGEM1020-3R in (b); lane M: HyperLadder^{TM} 1kb molecular weight marker (Bioline).

5.2.2 Construction of *cj1153*$^{+/-}$, *cj1020c*$^{+/-}$ and *cj0037c*$^{+/-}$ strains

The complementation of the *cj1153* mutant was carried out by using both pC46 and pCfdxA plasmids (Duncan Gaskin, IFR, UK), where chloramphenicol is the selection marker. The *cj1153* gene with its native promoter (an 82 bp upstream fragment) was cloned into pC46 via the *Bsm*BI restriction site whereas the pCfdxA1153 construct only carried the coding region of the *cj1153* gene and uses the *fdxA* vector promoter which is strongly inducible by ferric ions when added to the growth media. The *cj1020c* and *cj0037c* genes were cloned into pKmetK (section 4.2.3) and pCfdxA vectors via the *BsmB*I site with transcription driven by the *metK* or *fdxA* promoters respectively (Duncan 'Gaskin, IFR, UK). The resulting plasmids pC1153, pCfdxA1153, pKmetK1020 and pCfdxA0037 were electroporated into the corresponding mutants. The *C. jejuni* transformants were checked by colony PCR and the orientation-specific primer sets (fdxA-1153-F, metK-1020-F and fdxA-0037-F are forward primers and Cj0046-F is the reverse primer). However, due to the fragment with the native promoter in pC1153, the identification of insert fragments was performed with the primers used in the fragment amplification (pC46-1153-F and 1153com-R). The transformants with correct size of fragments (Fig. 5.2 e) were propagated and preserved in 20% glycerol for further analysis.

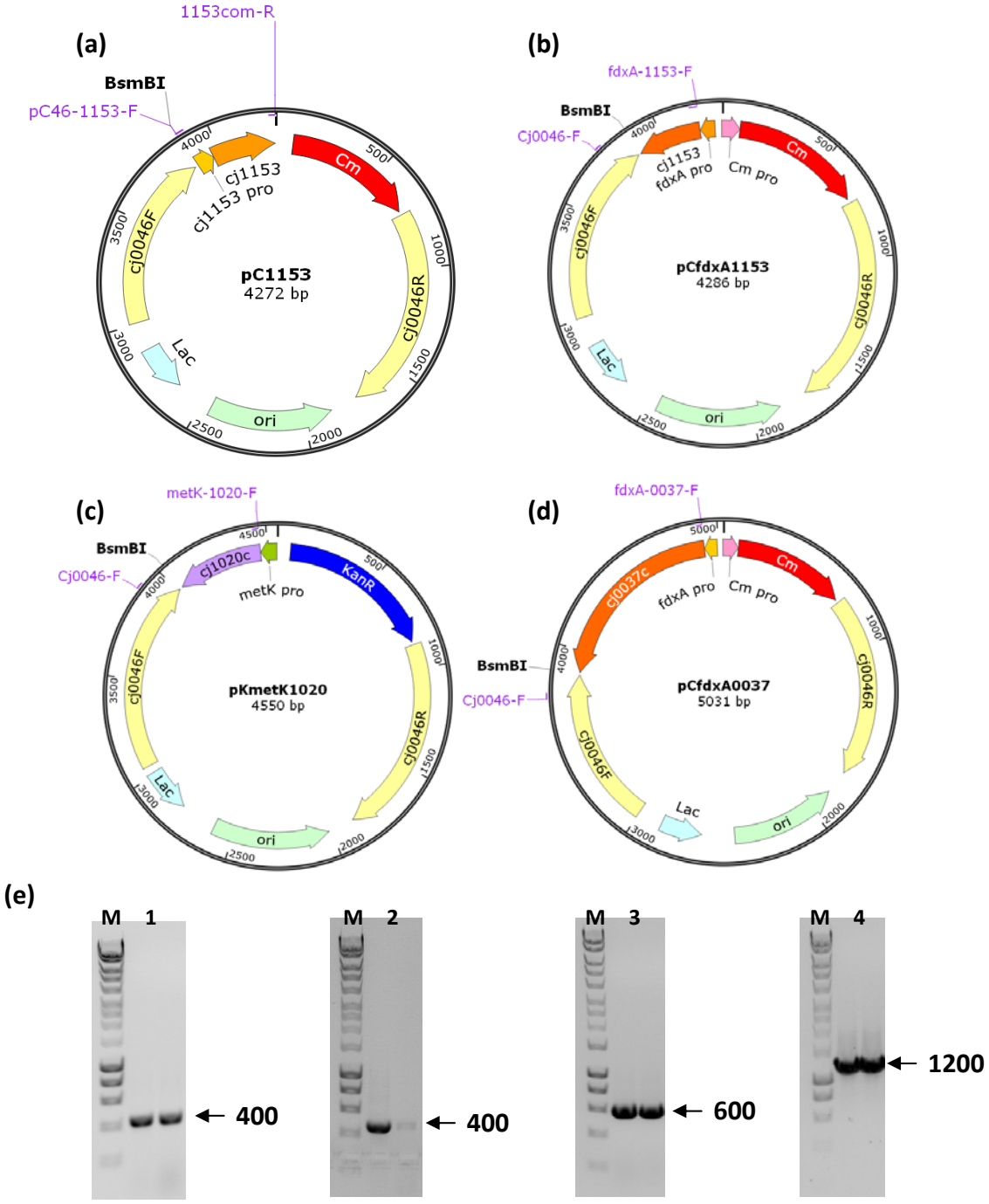

Figure 5.2 Constructions of pC1153, pCfdxA1153, pKmetK1020 and pCfdxA0037 plasmids and verification of corresponding *C. jejuni* complemented mutant strains. **(a)** The map of pC1153. The *cj1153* gene was cloned into pC46 vector with its native promoter. **(b)** The map of pCfdxA1153, where the expression of *cj1153* is regulated by an inducible promoter *fdxA*. **(c)** The map of pKmetK1020, where *cj1020c* is downstream of a constitutive promoter *metK*. **(d)** The map of pCfdxA0037. **(e)** Agarose gel electrophoresis confirmation of the complemented strains. Lane 1: The colony PCR product obtained from *cj1153*$^{+/-}$ with its native promoter. Lane 2: The *fdxA*-driven *cj1153*$^{+/-}$ complemented strains. Lane 3: The metK-driven *cj1020c*$^{+/-}$ strain. Lane 4: The *fdxA*-driven *cj0037c*$^{+/-}$ strain. The size of corresponding PCR products are shown as the number with arrows. Lane M: HyperLadder^{TM} 1kb molecular weight marker (Bioline).

5.2.3 Growth phenotypes of the mutants of *c*-type cytochrome candidates under microaerobic conditions

Microaerobic growth experiments were carried out under the standard atmospheric conditions described in section 2.2.4. The growth characteristics of wild type, mutants and complemented strains are shown in figure 5.3. Both *cj1153* and *cj1020c* mutants showed moderate growth defects which could be fully complemented in *cj1153*$^{+/-}$ (pC1153) and *cj1020*$^{+/-}$ respectively, suggesting a role for *cj1153* and *cj1020c* in growth under aerobic conditions. However, the mutation of *cj0037c* and *cj0158c* did not seem to affect the microaerobic growth of *C. jejuni* NCTC 11168, suggesting these two genes might not be directly involved in aerobic electron transfer or their functions can be compensated by other *c*-type cytochromes.

5.2.4 Haem blots and reduced minus oxidized difference spectra of periplasmic fractions

To obtain a better resolution of low molecular weight periplasmic proteins for haem blots with the wild-type and different mutants, 12% Tricine-SDS-PAGE was used to separate periplasmic *c*-type cytochromes in *cj1153*$^{-}$, *cj1020c*$^{-}$ mutants and their complemented strains and a 10% gel was used for *cj0037*$^{-}$ and *cj0037*$^{+/-}$ strains. The blots of the wild-type periplasm showed a number of reasonably well-resolved bands (Fig. 5.4). From a comparison of the coomassie stained gels and the haem blots, it is clear that Cj1153 is an extremely abundant protein and is clearly absent in the *cj1153* mutant. However, most surprisingly, it was immediately apparent from the blot that no haem signals at all of any other *c*-type cytochromes could be detected in the periplasm of the *cj1153*$^{-}$ mutant (Fig. 5.4 a) and the major absorption peaks at 553 nm (alpha band) 525 nm (beta band) and 420 nm (Soret band) were absent in the dithionite reduced minus air-oxidised difference spectra (Fig. 5.4 d). Taken together, it is clear that all periplasmic soluble *c*-type cytochromes are absent in this mutant. The pelleted cells of the *cj1153* mutant were also a brown colour rather than the pink colour of the wild-type (not shown). The partial recovery of the haem signals of the periplasmic *c*-type cytochromes is apparent in the isogenic *cj1153*$^{+/-}$ pC46 complemented strain, which is based on the expression with the native promoter. However, the recovery is only about 20% according to the magnitude of the two major peaks in the difference spectra (Soret at ~420 nm and alpha band at ~553 nm) of cytochromes in *cj1153*$^{+/-}$ compared to the

wild-type. The haem signals of other *c*-type cytochromes on the blot are also not as obvious as that of Cj1153 (Fig. 5.4 a), suggesting the expression level of Cj1153 is low in this complemented strain. The expression level of *cj1020c* is apparently naturally low in *C. jejuni* NCTC 11168 and the corresponding missing cytochrome *c* signal is not very obvious in the *cj1020c*$^{-}$ mutant but still can be visualised by comparison with the complemented *cj1020*$^{+/-}$ strain (Fig. 5.4 b).

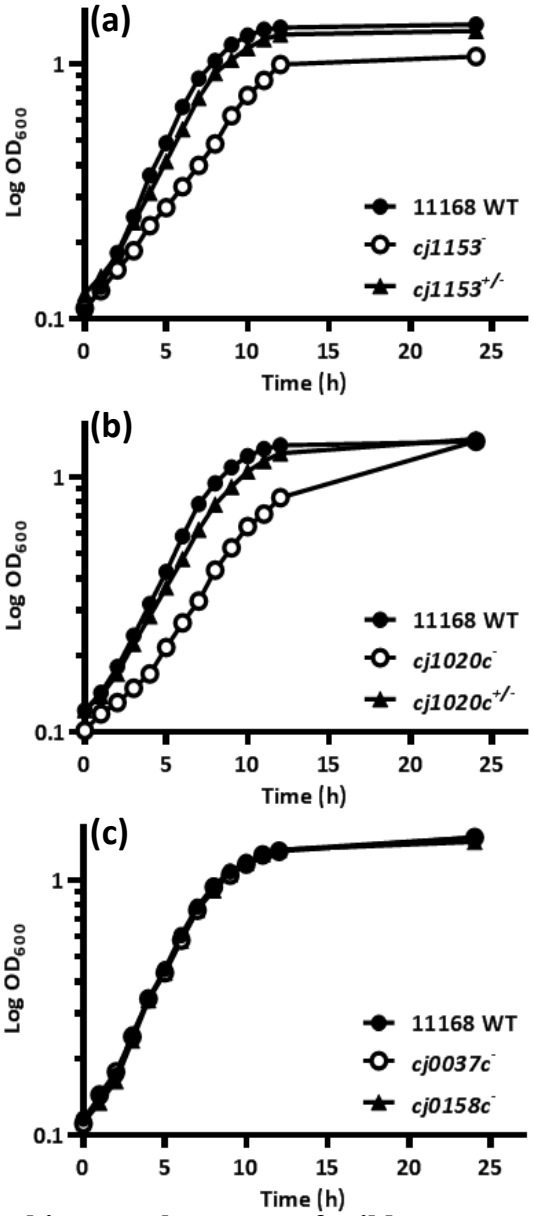

Figure 5.3 Microaerobic growth curves of wild type, mutant and complemented strains. (a) The *cj1153* mutant shows a growth defect, which could be complemented by integration of the wild-type *cj1153* gene with its native promoter at the *cj0046* pseudogene locus in pC46 vector. **(b)** The mutation of *cj1020c* shows a moderate growth defect which can be complemented by the expression of *cj1020c* driven by the *metK* promoter. **(c)** The mutation of *cj0037c* and *cj0158c* did not affect the growth rate under microaerobic conditions. Data shown is for a single experiment; independent growth experiments were carried out three times with similar results.

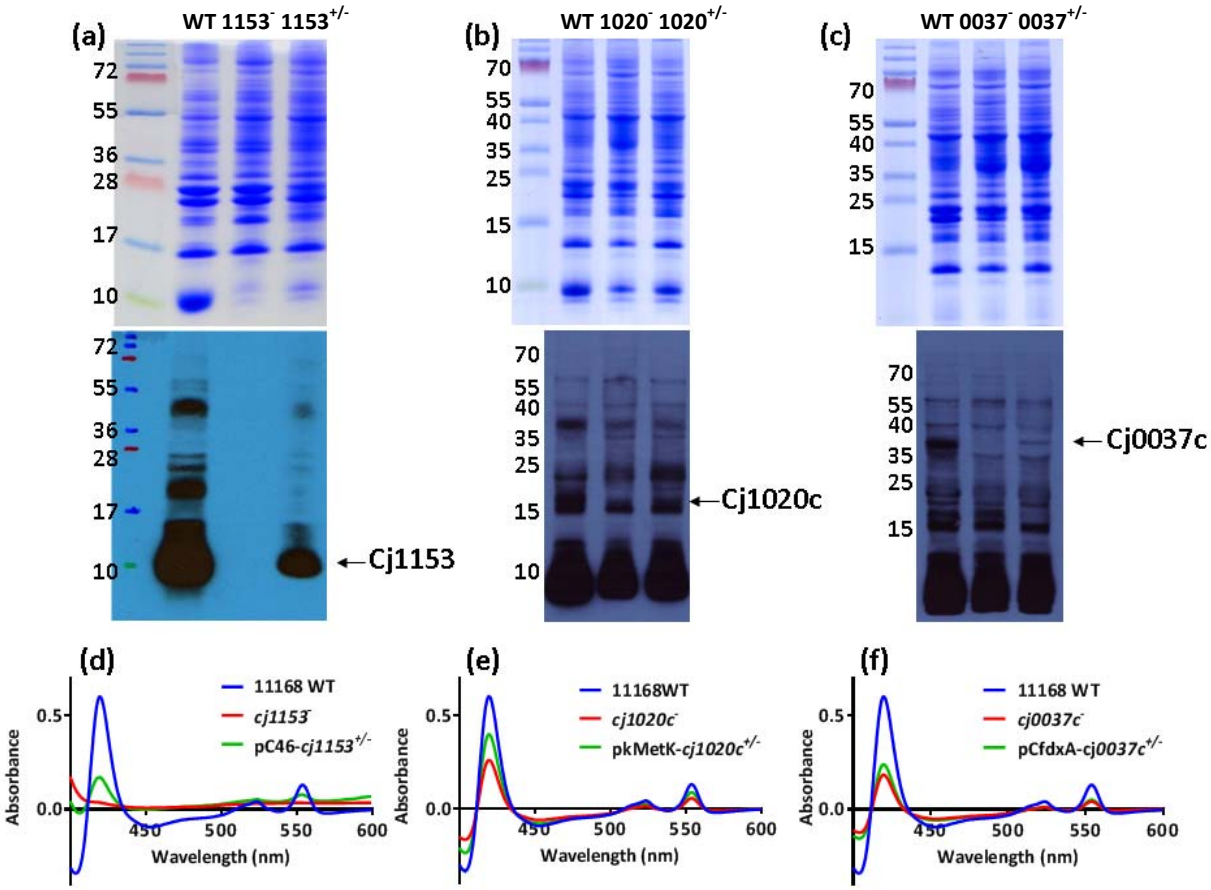

Figure 5.4 Haem blots and reduced minus oxidized difference spectra of periplasmic fractions. (a) The haem blot of periplasm (20 µg per lane) of *cj1153* mutant and the pC1153 complemented strain. **(b)** The haem blot of *cj1020c* and *cj1020*$^{+/-}$, 40 µg per lane. (c) The haem blot of *cj0037c* and *cj0037c*$^{+/-}$, 60 µg per lane. **(d) to (f)** The dithionite reduced minus air oxidised difference spectra of the periplasm (1 mg/ml) of *cj1153*, *cj1020c* and *cj0037c* and their complemented strains.

The signal corresponding to the expected size of Cj0037 is clearly missing in the haem blot of the *cj0037c*$^{-}$ mutant and just detectable again in the complemented strain (Fig. 5.4 c). The reduced minus oxidised difference spectra reveal that the expression level is indeed rather low in the complemented strain even with the highly inducible *fdxA* promoter. The complemented strain was double checked by both colony PCR and sequencing, but more optimal expression might be obtained with its native or a different promoter.

5.2.5 The abundance of *c*-type cytochromes in the complemented *cj1153*$^{+/-}$ strain with expression from different promoters

In order to optimise the expression of Cj1153 protein in the isogenic *cj1153*$^{+/-}$ strain, the *fdxA*-based complemented strain was also constructed and the haem blot and reduced minus oxidised difference spectra were performed to compare the abundance of Cj1153 and other periplasmic *c*-type cytochromes in the two complemented strains. The haem blot in figure 5.5 shows the signal from Cj1153 and all periplasmic cytochromes *c* in *fdxA1153*$^{+/-}$ is much stronger than that when using *pccj1153*$^{+/-}$, suggesting that the expression level of *cj1153* induced by the *fdxA* promoter is higher than that of its native promoter. Significantly, the higher expression level of *cj1153* driven by the *fdxA* promoter also directly correlates with the expression or the protein stability of other *c*-type cytochromes which are more abundant in *fdxA1153*$^{+/-}$ than in the *pccj1153*$^{+/-}$ complemented strain (Fig. 5.5). Also, the difference spectra reveals increased intensities of peaks at 553 nm, 525 nm and 420 nm; the pCfdxA-*1153*$^{+/-}$ strain shows ~60% recovery of total cytochromes *c* to the wild-type while the *pccj1153*$^{+/-}$ strain only retains ~20% of total *c*-type cytochromes. Thus, only the complemented strain driven by the *fdxA* promoter was used in further experiments.

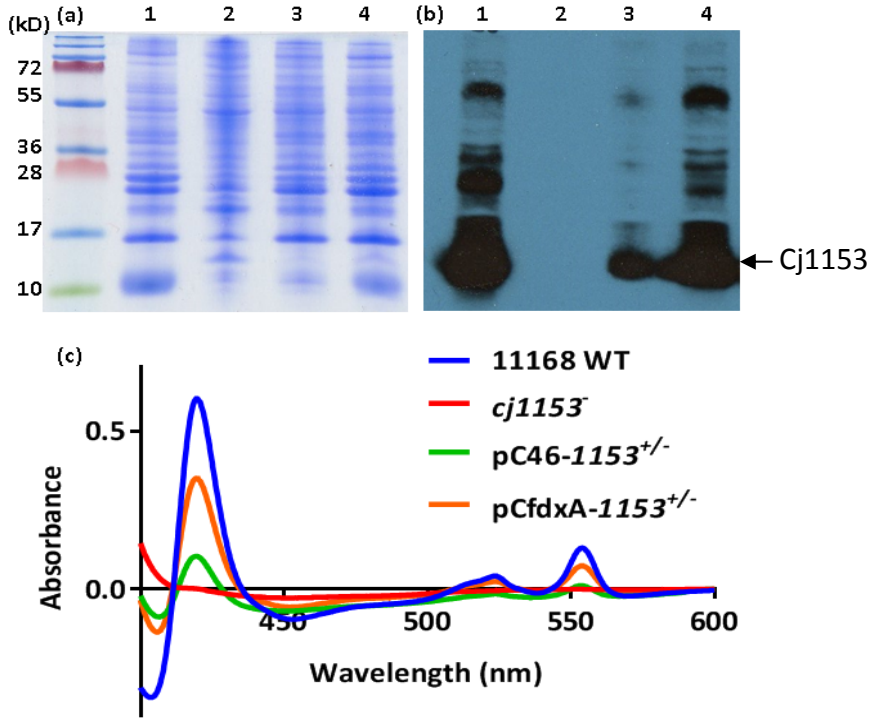

Figure 5.5 Haem blot and dithionite reduced minus air oxidized difference spectra of periplasmic fractions in *cj1153*$^{+/-}$ strains with different promoters. (a) The haem blot of periplasm (20 µg) of wild-type (1), *cj1153* (2) and *cj1153*$^{+/-}$ strains with the native promoter (3) or *fdxA* promoter (4). **(b)** The reduced minus oxidised difference spectra of the periplasm (1 mg/ml protein) of strains used in the haem blot.

5.2.6 Growth phenotypes of the *cj1153* mutant under oxygen-limited conditions

The unexpected phenotype of all cytochrome *c* haem signals being absent in the periplasm of the *cj1153* mutant should be accompanied by the loss of functions of some haem-containing enzymes such as nitrate reductase (Nap) and TMAO reductase (Tor) where NapB and Cj0265 are *c*-type cytochrome subunits which transfer electrons to the active site subunits (NapA and Cj0264 (TorA)) respectively. Oxygen-limited growth experiments were carried out with 500 ml BHI medium in a 500 ml conical flask with 20 mM sodium formate as additional electron donor and alternative electron acceptors (fumarate, nitrate or TMAO) were added to a final concentration of 20 mM. None of strains were able to survive only with electron donor (Fig. 5.6 a) and all of them show similar growth rates when incubated with formate and fumarate (Fig. 5.6 b). Significantly, neither of the two fumarate reductases FrdABC or MfrABE contains any haem *c*-binding subunit, but FrdC is a *b*-type cytochrome, indicating that the pleiotropic effect of the *cj1153* mutation is limited to *c*-type cytochromes. However, the *cj1153*$^{-}$ mutant is clearly unable to utilise nitrate and TMAO as alternative electron acceptors, as no growth was observed during the incubation (Fig. 5.6 c and d) but the complemented strain *cj1153*$^{+/-}$ shows a similar growth rate to the wild-type with nitrate and only a slightly decreased growth rate with TMAO, suggesting the recovery of *c*-type cytochromes in the *cj1153*$^{+/-}$ strain is crucial for the activity of those haem *c*-containing enzymes. This result also suggests that the loss of Cj1153 might cause the degradation of other *c*-type cytochromes in the periplasm of *C. jejuni* NCTC 11168, although this needs confirmation by western blotting with antibodies to the various cytochromes.

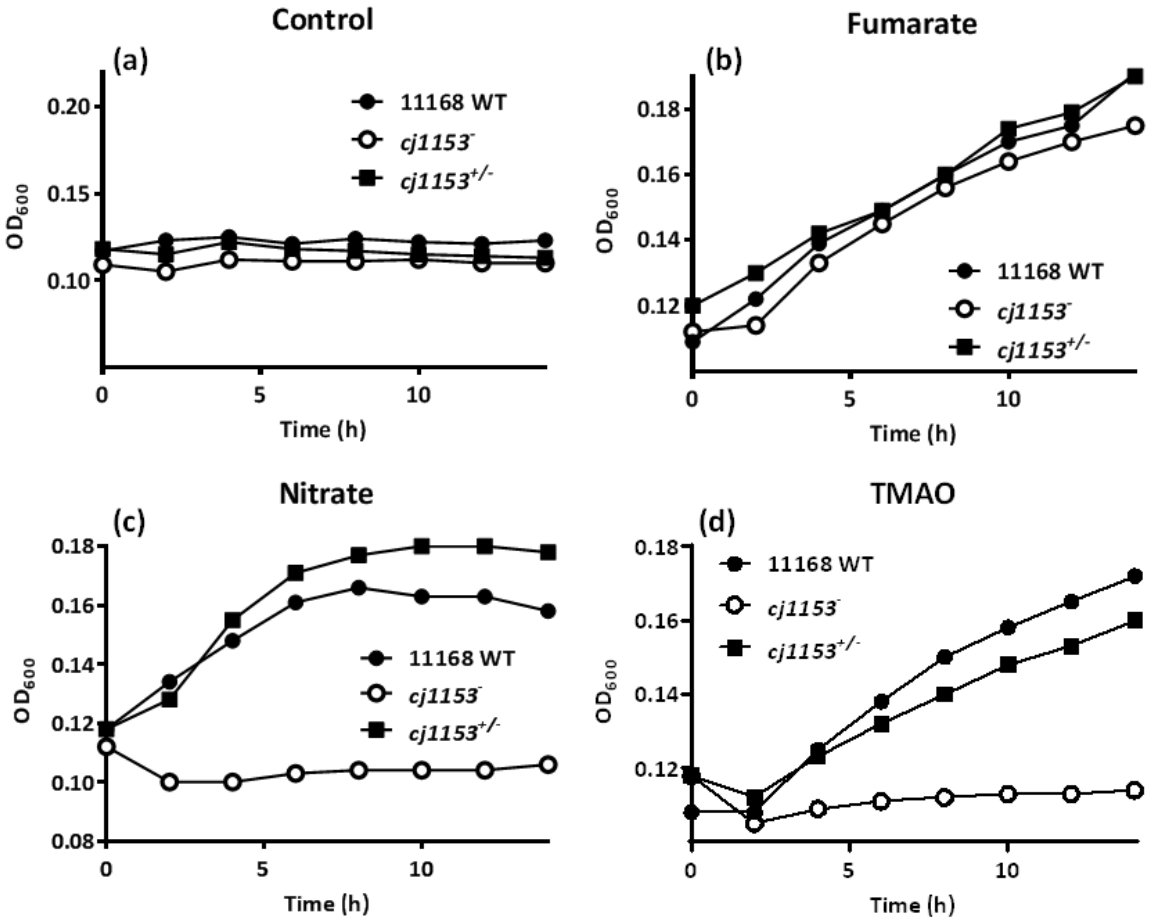

Figure 5.6 Oxygen-limited growth curves of wild type, mutant and complemented *cj1153* strains. Cultures of *C. jejuni* were incubated at 37°C in almost completely filled 500 ml unshaken conical flasks containing BHI medium with 20 mM formate and supplemented with 20 mM fumarate **(b)**, nitrate **(c)** or 20mM TMAO **(d)** as electron acceptors. None of the strains grew without any electron acceptors under oxygen limitation **(a)**. The data shown are representative of at least three independent growth experiments.

5.2.7 Oxygen consumption rates with different electron donors in *C. jejuni* NCTC 11168, *c*-type cytochrome mutants and complemented strains

Several compounds like formate, sulphite and ascorbic acid plus TMPD (*N,N,N′,N′*-tetramethyl-p-phenylenediamine) were chosen as substrates in the respiration measurement of wild-type NCTC 11168, *c*-type cytochrome mutants and their complemented strains. The electrons from formate oxidation by formate dehydrogenase (Fdh) will be transferred to oxygen through two electron transfer routes – to the *cb*-type terminal oxidase via the quinone pool, bc_1 complex and periplasmic *c*-type cytochrome(s) and also directly to the alternative oxidase (CioAB) from the quinone pool. However, as discussed in Chapter 1, the electrons from sulphite oxidation by

sulphite oxidase (SorAB) are thought to bypass the bc_1 complex and SorAB will mediate electron flux to oxygen via *c*-type cytochromes and the *cb*-type oxidase only. As a relatively weak reductant, ascorbic acid is able to reduce high potential periplasmic *c*-type cytochromes, which will transfer electrons to the *cb* oxidase when oxygen is available, whereas TMPD is an artificial electron donor, which is easily able to be reduced by ascorbic acid. The ascorbate/TMPD mixture will be oxidised directly by the *cb* oxidase and can be used to measure its activity in the membrane.

Interestingly, it was found that the *cj1153* mutant showed a significantly higher formate respiration activity than that of the wild-type, while the complemented strain showed a similar activity to the wild-type (Fig. 5.7 a). As expected, due to the absence of *c*-type cytochromes in the periplasm, sulphite respiration activity was totally abolished in *cj1153*$^-$ and recovered in the complemented strain (Fig. 5.7 b). Also, no oxygen respiration was observed after adding ascorbic acid to *cj1153*$^-$ but the rates in the wild-type and complemented strains were similar (Fig. 5.7 c). Again, this is consistent with the total absence of periplasmic *c*-type cytochromes in the *cj1153* mutant. The activity of the *cb*-oxidase, as judged by the rates observed with a mixture of ascorbate and TMPD was still detectable in the *cj1153* mutant, but at a much lower level compared to the wild-type. Importantly, the activity was completely recovered in the complemented strain (Fig. 5.7 c).

Both *cj1020c*$^-$ and *cj0037c*$^-$ mutants showed decreased formate and sulphite respiration activities compared to the wild-type (about 50-70% activity of NCTC 11168; Fig. 5.7 a and b) and these activities recover to the wild-type level in their complemented strains. The mutation of *cj1020c* did not affect the respiration with ascorbic acid alone or in combination with TMPD. However, surprisingly the *cj0037c* mutant showed no respiration rate after adding ascorbic acid and the complemented strain showed only ~ 20% recovery of activity compared to the wild-type but both of them show similar respiration to that of the wild-type with ascorbate plus TMPD, suggesting the overall activity of the *cb* oxidase (*cco* module) is not altered with the loss of the Cj0037 protein. Taken together, these data suggest that Cj0037 itself may play a significant role in electron transport to the *cb*-type terminal oxidase.

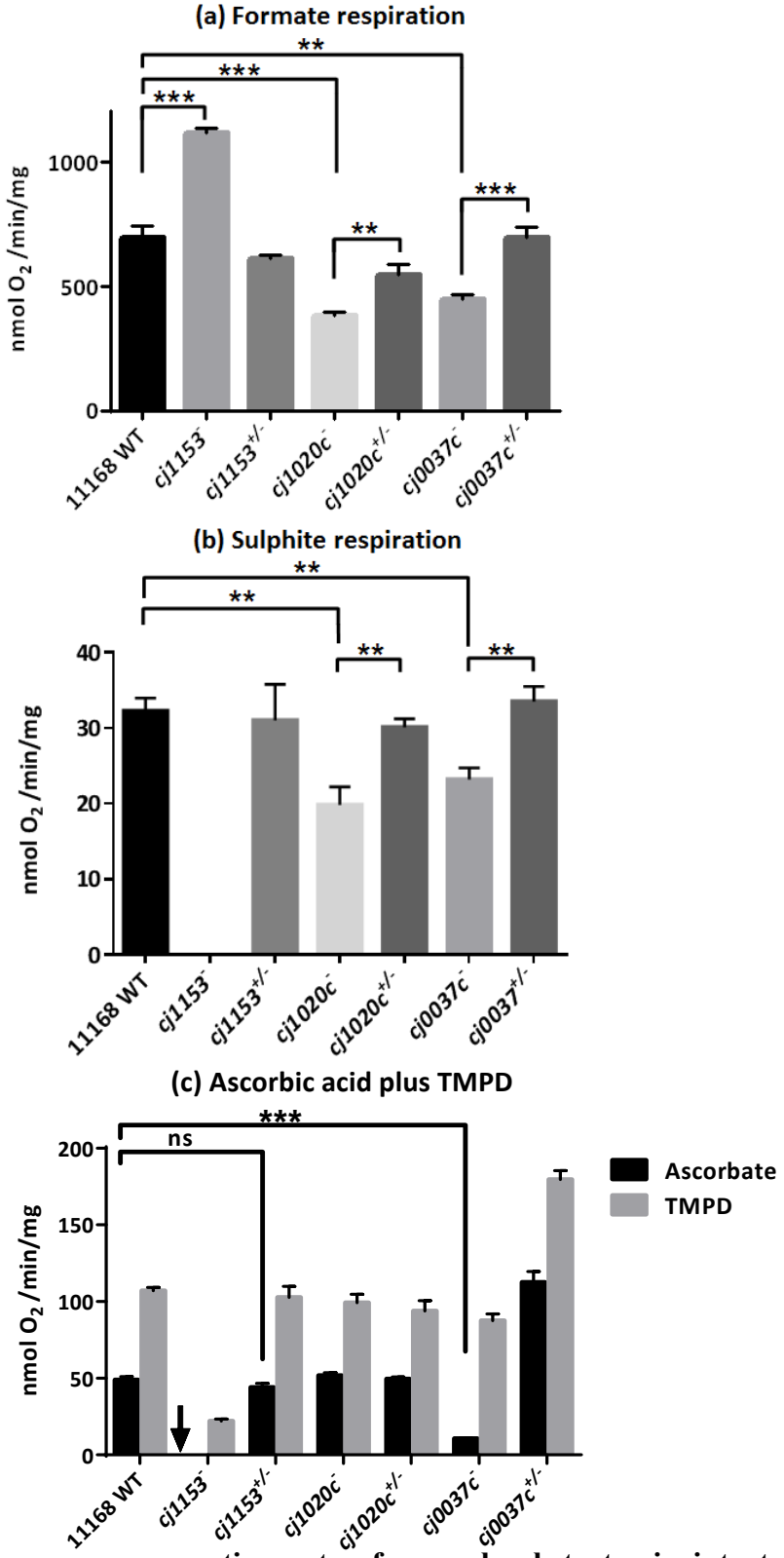

Figure 5.7. The oxygen consumption rate of several substrates in intact cells of wild-type, mutant and complemented strains. (a) 10 mM formate. **(b) 0.**5 mM sulphite. **(c)** 1 mM ascorbic acid alone or with 0.25 mM TMPD. Assay methods were as described in Materials and Methods. Relevant significant differences in activity are indicated by *** ($P < 0.001$) or ** ($P < 0.01$) according to Students t-test (ns; no significant difference). The data shown are means ± SD of at least three independent experiments.

5.2.8 The CXXCH histidine residue is crucial for the stability of Cj1153 and periplasmic *c*-type cytochromes

The unexpected pleiotropic effect of the mutation of *cj1153* might be due to an effect of Cj1153 on the expression or stability of other *c*-type cytochromes, or perhaps the Cj1153 protein is directly involved in the biogenesis of *c*-type cytochromes. The latter possibility seems unlikely as Cj1153 itself contains a *c*-type haem and a typical CXXCH motif for haem binding. However, it does also possess another histidine in the C-terminus and we wanted to test the importance of both histidines in the binding of haem and the stability of the protein by changing these to alanines. The first histidine residue H33 is located in the haem binding motif -CXXCH-, which is considered to be essential for the haem-binding activity. The other histidine residue is H95, located at the C-terminus of Cj1153 (Fig. 5.8). Site-directed point mutations of *cj1153* were carried out by the overlapped PCR method described in section 2.3.13 and the fragments with point mutated H33A and H95A were sequenced (Core Genomic Facility, University of Sheffield Medical School, UK) and ligated to the pCfdxA plasmid and then were transformed into *cj1153*$^{-}$ cells. The transformants were PCR screened and the point-mutated fragments were amplified and sequenced again to confirm that the histidine residues were replaced to alanines correctly. Haem blots and reduced minus oxidised difference spectra were performed with the periplasm of wild-type, H33A, H95A, *cj1153*$^{-}$ and *cj1153*$^{+/-}$ strains. From figure 5.8, it is clear that that H33A and *cj1153*$^{-}$ showed the same phenotype of the absence of Cj1153 itself and all other *c*-type cytochromes in the periplasm, while the H95A strain shows a decreased level (only ~30% of wild-type; Fig. 5.8 b and c) of periplasmic *c*-type cytochromes and Cj1153 itself. This suggests, unsurprisingly, that H33A is essential for the haem ligation in the -CXXCH- motif, but that H95 contributes to the stability of the protein.

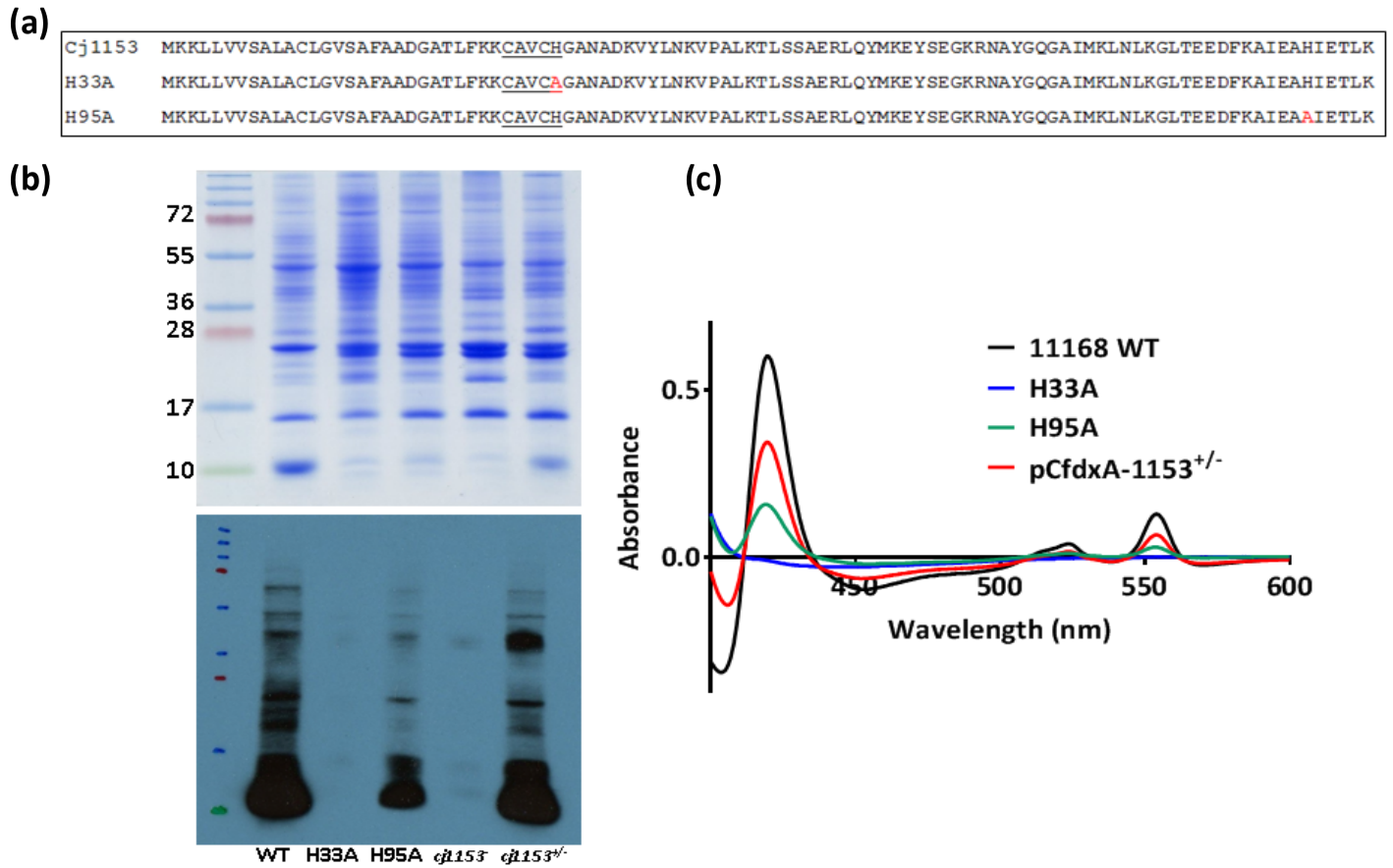

Figure 5.8 Characterisation of *c*-type cytochromes in point-mutated H33A and H95A strains. (a) The multiple sequence alignment of Cj1153, H33A and H95A. The haem binding motif is underlined and the replaced residue is marked in red (b) The CBR stain and haem-blot of the periplasm of wild-type, H33A, H95A, *cj1153*$^{-}$ and *cj1153*$^{+/-}$ strains, 20 µg per lane. (c) The reduced minus oxidised difference spectra of the strains used in the haem blot, the concentration used in measurements is 1 mg/ml.

5.2.9 The growth phenotype of *cb* oxidase mutants and the profile of gene expression in *cj1153*$^-$

The total absence of *c*-type cytochromes in the periplasm of *cj1153*$^-$ should mean that no electrons can be transferred to the terminal *cb*-oxidase from the bc_1 complex, although the *cj1153* mutant is still able to survive under microaerobic conditions, presumably by respiration using the alternative oxidase (CioAB). If this is the case, we would expect a similar aerobic growth phenotype of a *cb*-oxidase mutant compared to the *cj1153* mutant. Two mutants of the *cb*-oxidase were constructed in *C. jejuni* NCTC 11168, these are deletions of *ccoN*$^-$ (*cj1490c*) only and a deletion of the entire *ccoNOQP* (*cj1490c* to *cj1487c*) operon. CcoN is the catalytic subunit of the *cb*-oxidase and mutation of this subunit should result in the loss of oxidase activity (Jackson *et al*., 2007; Weingarten *et al*., 2008). Both *ccoN* and *ccoNOQP* mutants indeed showed similar growth phenotypes to that of *cj1153*$^-$ under microaerobic conditions (Fig. 5.9 a), with a similar reduction in growth rate.

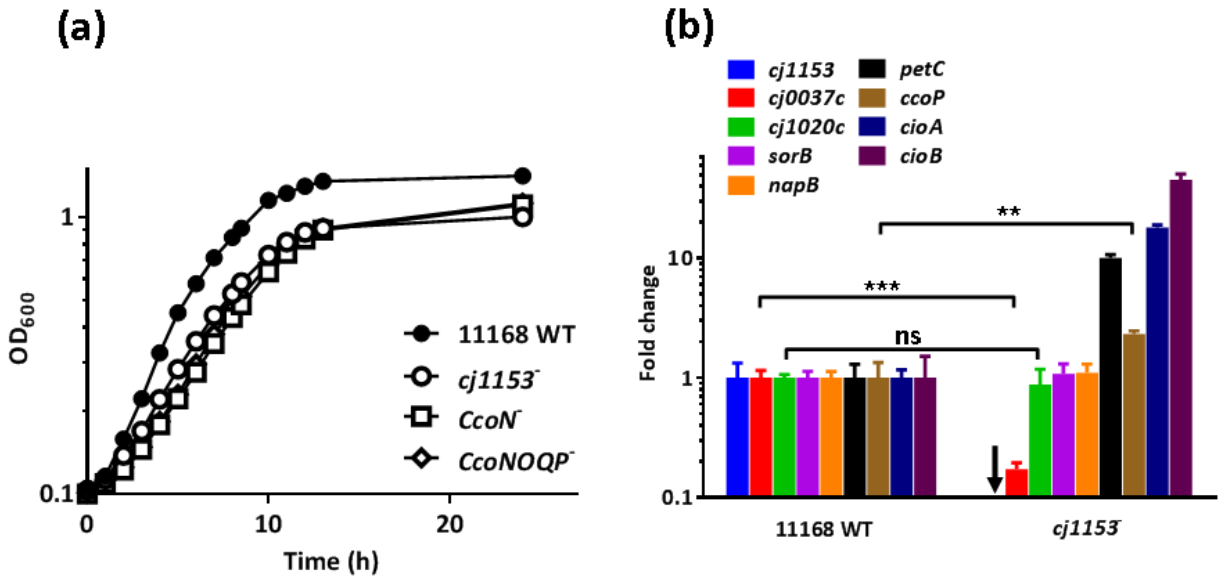

Figure 5.9 Microaerobic growth curves of wild type, *cj1153*$^-$ and the mutant of *cb*-oxidase and the profile of gene expression in *cj1153*$^-$. (a) The *cj1153*, *ccoN* and *ccoNOQP* mutants show similar growth defects to wild type, suggesting both Cj1153 and *cb*-oxidase play similar roles in the microaerobic growth of *C. jejuni* NCTC 11168. **(b)** Real-time PCR reveals the expression profile of different genes in *cj1153*$^-$. Relevant significant differences in fold change are indicated by *** ($P < 0.001$) or ** ($P < 0.01$) according to Students t-test (ns; no significant difference). The data shown are means ± SD of at least three independent experiments.

However, the fact that *cj1153*$^{-}$ only shows mild growth defects compared to wild-type, despite having such a large pleiotropic effect on other cytochromes is surprising. We wanted to test whether there were any gene expression changes in the *cj1153* mutant that could explain its phenotype, particularly the down-regulation of other *c*-type cytochrome genes or perhaps the up-regulation of the alternative oxidase to enable the cells to better adapt to respiration without the *cb*-oxidase, which is important for microaerobic conditions (Pitcher *et al*., 2002). A profile of selected gene expression in *cj1153*$^{-}$ under microaerobic conditions was determined by real-time PCR with gene-specific primers and the DNA gyrase subunit A as an internal control (Fig. 5.9 b). The results showed that although the expression of *cj1153* is totally abolished as expected, the expression of most other periplasmic *c*-type cytochromes measured, such as *cj1020*, *sorB* and *napB* is actually not altered in *cj1153*$^{-}$. This important result strongly argues against a transcriptional effect being the reason for the general absence of *c*-type cytochromes in the mutant. An exception was *cj0037*, where the expression level in *cj1153* is only about 20% of that of wild-type. Very interestingly, the expression of both genes of the cyanide-resistant quinol oxidase encoded by *cioAB* (*cj0081* and *cj0082*) is upregulated by at least 20-40 fold compared to wild-type. Also, the expression of *petC* encoding for the cytochrome c_1 subunit of the bc_1 complex is ten fold upregulated.

5.2.10 The growth phenotype of *c*-type cytochrome mutants in a *cioAB*$^{-}$ background

The large up-regulation of the genes for the quinol oxidase in the *cj1153* mutant might be a compensatory adaptation for growth without the ability to use the *cb*-oxidase route in this strain and the major reason why no severe microaerobic growth defect was observed. It would also consistent with the higher formate respiration activity observed in the *cj1153* mutant. Therefore, in order to better study the role of other *c*-type cytochromes in the ETC of *C. jejuni* NCTC 11168, a deletion mutation of the *cioAB* genes was made, where the genes were replaced by an apramycin resistance cassette (*apr*; Cameron and Gaynor, 2014). This meant that the *cioAB*::*apr* deletion plasmid construct could simply be introduced into the wild-type and each of the previously constructed mutants and complemented strains. The transformants were screened on blood agar plates containing apramycin (60 μg ml^{-1}) and the correct clones were confirmed by colony PCR with primers of apr-F and pGEM0082-3R (data not shown). However, although several attempts were carried out for the construction of

cioAB^{-}*cj1153*$^{-}$ double mutants of *C. jejuni*, no transformants were able to survive on blood agar plates incubated microaerobically. On the contrary, the mutation of *cioAB* could be achieved in the *cj1153*$^{+/-}$ complemented strain (*cj1153* expressed from the *fdxA* promoter), which results in a viable *cioAB*$^{-}$*cj1153*$^{+/-}$ double mutant. Its growth phenotype is similar to the *cioAB* mutant, which grows almost as well as wild-type (Fig. 5.10 a). These results are in line with the evidence above which suggests that no electron flow can occur to the *cb*-oxidase in the *cj1153* mutant and so it is impossible to make a double *cioAB* and *cj1153* mutant strain, except in the complemented background. However, the mutation of *cioAB* was possible in the *cj1020c* and *cj0037c* mutants and their complemented derivatives. The growth phenotype of *cioAB*$^{-}$*cj1020c*$^{-}$ is similar to that of *cj1020c*$^{-}$ and *cioAB*$^{-}$*cj0037c*$^{-}$ shows a mild growth defect compared to *cioAB*$^{-}$ (Fig. 5.10 b and c). Both complemented strains of *cj1020c*$^{-}$and *cj0037c*$^{-}$ in the *cioAB*$^{-}$ background show a recovered growth rate similar to that of *cioAB*$^{-}$ alone.

5.2.11 Expression of *cj1153* in a *cioAB*$^{-}$ strain recovers respiration with different substrates

Although the *cioAB*$^{-}$ *cj1153*$^{-}$ mutant is not viable under microaerobic conditions, the complemented strain *cioAB*$^{-}$ *cj1153*$^{+/-}$ shows a similar growth rate to wild-type, suggesting that the expression of *cj1153* with the inducible promoter *fdxA* is able to recover electron transfer to the *cb*-oxidase, allowing growth to occur. However, the result of real-time PCR experiments showed that the expression level of *cj1153* is only about ~40% of that of wild-type in the complemented *cj1153*$^{+/-}$ strain (Fig. 5.11 a) but this expression level is seemingly enough for a good restoration of respiration with different substrates in the *cioAB*$^{-}$ *cj1153*$^{+/-}$ mutant of *C. jejuni* NCTC 11168 (Fig. 5.11 b to d).

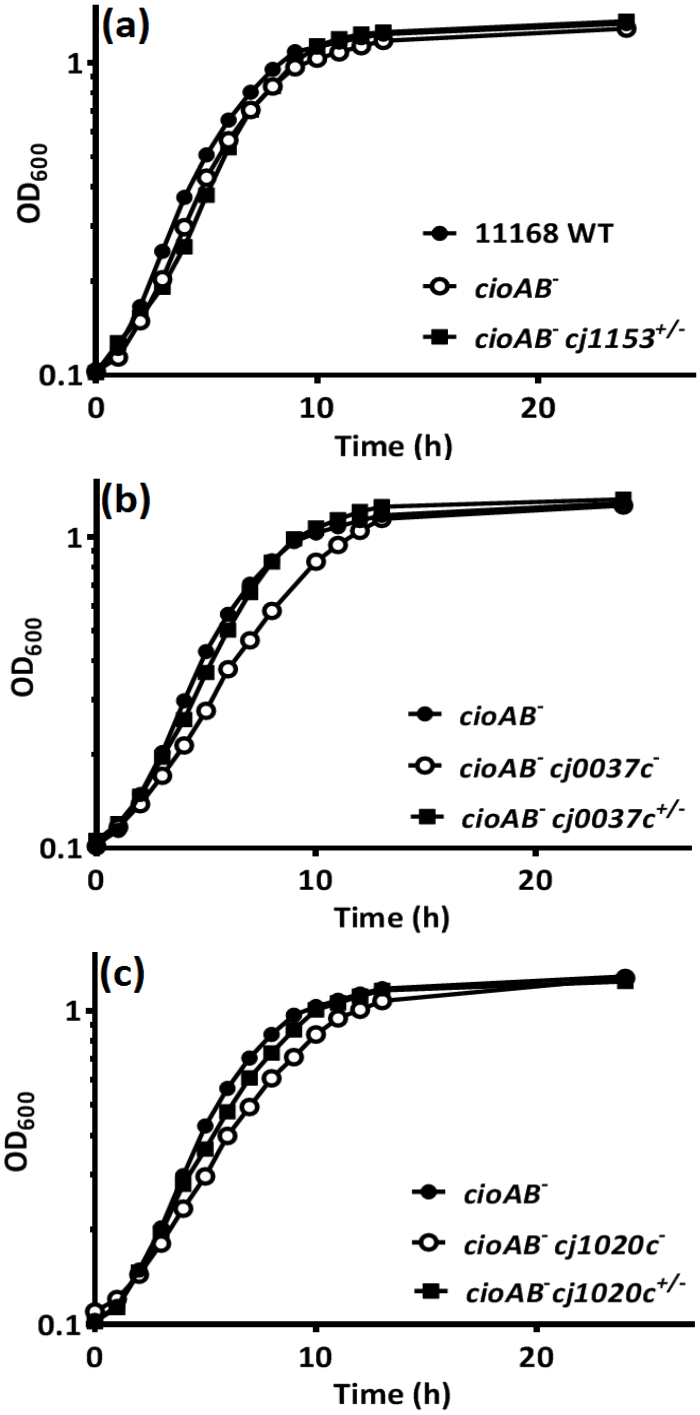

Figure 5.10 Microaerobic growth curves of wild type, mutants and complemented strains without the presence of CioAB oxidase. (a) A growth defect is not obvious in the mutation of *cioAB* and *cioAB*$^{-}$*cj1153*$^{+/-}$ strains, although the double mutant of *cioAB*$^{-}$*cj1153*$^{-}$ in *C. jejuni* NCTC 11168 is not viable**. (b)** The double mutation of *cioAB* and *cj0037c* results in a moderate growth defect compared to *cioAB* only mutant. The function of Cj0037c can be complemented and the strain of *cioAB*$^{-}$*cj0037c*$^{+/-}$ shows a similar growth rate to *cioAB*$^{-}$. **(c)** The mutation of *cj1020c* causes a mild growth defect with the same *cioAB*$^{-}$ background, which can be fully complemented. Data shown is for a single experiment; independent growth experiments were carried out three times with similar results.

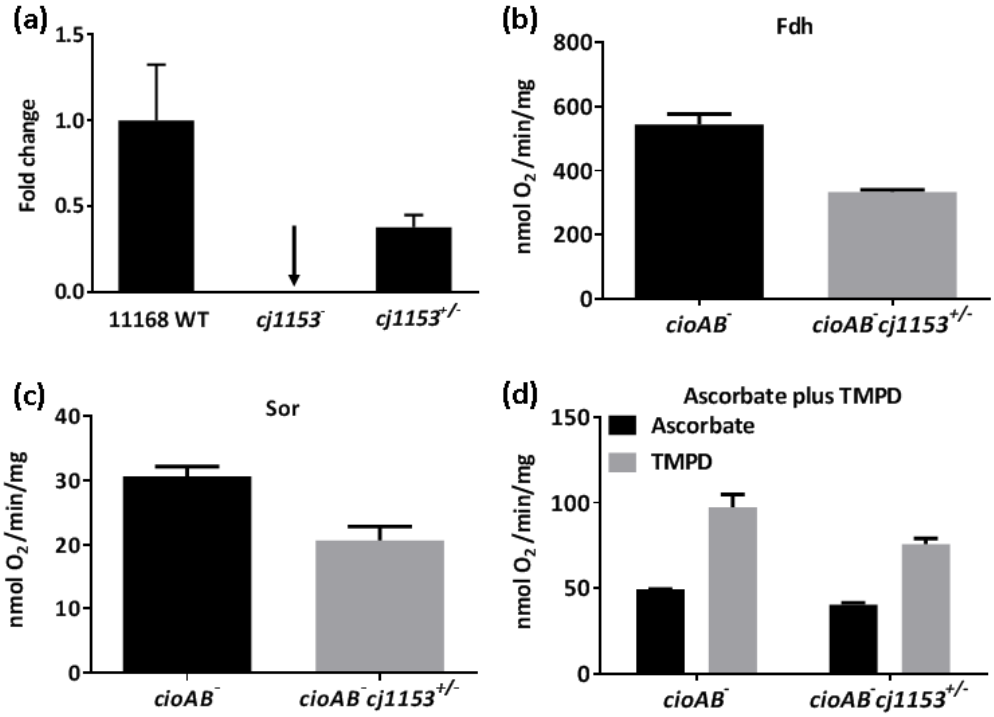

Figure 5.11 The expression level of *cj1153* in the complemented strain and the respiration rate of intact cells of *cioAB*$^-$ and *cioAB*$^-$ *cj1153*$^{+/-}$ with different substrates. (a) The expression of *cj1153* with the *fdxA* promoter in *cj1153*$^{+/-}$ is about ~ 40% of wild-type. **(b)** In *cioAB*$^-$*cj1153*$^{+/-}$ mutant, the formate dehydrogenase activity is about ~60% and **(c)** the sulphite oxidase activity is ~65% to those of *cioAB*$^-$. **(d)** No significant difference in respiration rate of *cioAB*$^-$ and *cioAB*$^-$*cj1153*$^{+/-}$ is observed with ascorbic acid but *cioAB*$^-$*cj1153*$^{+/-}$ shows ~80% oxygen consumption of *cioAB*$^-$ with ascorbate plus TMPD.

5.2.12. Respiration with different substrates in *c*-type cytochrome mutants and complemented strains in the *cioAB*$^-$ background

Since the *cioAB* mutant was introduced into wild-type, all aforementioned mutants (not including *cj1153*$^-$) and complemented strains, the respiration rates with formate, sulphite and ascorbic acid plus TMPD were measured to further study the roles of Cj1020 and Cj0037 in the electron transport chain to the *cb*-oxidase. Without the CioAB quinol oxidase, the respiration rate of the *cioAB*$^-$ strain with formate is about ~75% of that of wild-type whereas both *cioAB*$^-$ *cj1020c*$^-$ and *cioAB*$^-$ *cj0037c*$^-$ strains showed lower oxygen consumption compared to *cioAB*$^-$ itself (Fig. 5.12 a). However, the ratio of respiration rates of both double mutants to *cioAB*$^-$ alone is similar to that of *cj1020c*$^-$ and *cj0037c*$^-$ with functional CioAB in wild-type cells (Fig. 5.7 a), highlighting the role of CioAB in formate respiration. Also, the respiration rate is partially recovered in *cioAB*$^-$ *cj1020c*$^{+/-}$ and fully recovered in *cioAB*$^-$ *cj0037c*$^{+/-}$ compared to the level of

cioAB^{-} (Fig. 5.12 a). However, the *cioAB* mutant showed a similar rate to wild-type in sulphite respiration and the oxygen consumption of double mutants *cioAB*$^{-}$ *cj1020c*$^{-}$ and *cioAB*$^{-}$ *cj0037c*$^{-}$ is only mildly decreased compared to that of wild-type and *cioAB*$^{-}$, which is similar to the ratio of *cj1020c*$^{-}$ and *cj0037c*$^{-}$ to wild-type (Fig. 5.7 b). No respiration with ascorbic acid was observed in the *cioABcj0037c* double mutant (Fig. 5.12 c), which is identical to the situation in *cj0037*$^{-}$ (Fig. 5.7 c), nevertheless the oxygen consumption of *cioAB*$^{-}$ *cj0037c*$^{+/-}$ is still much lower than that of *cioAB*$^{-}$ and wild-type (~20% respiration of both; Fig. 5.12 c), which is similar to the *cj0037*$^{+/-}$ complemented strain (Fig. 5.7 c).

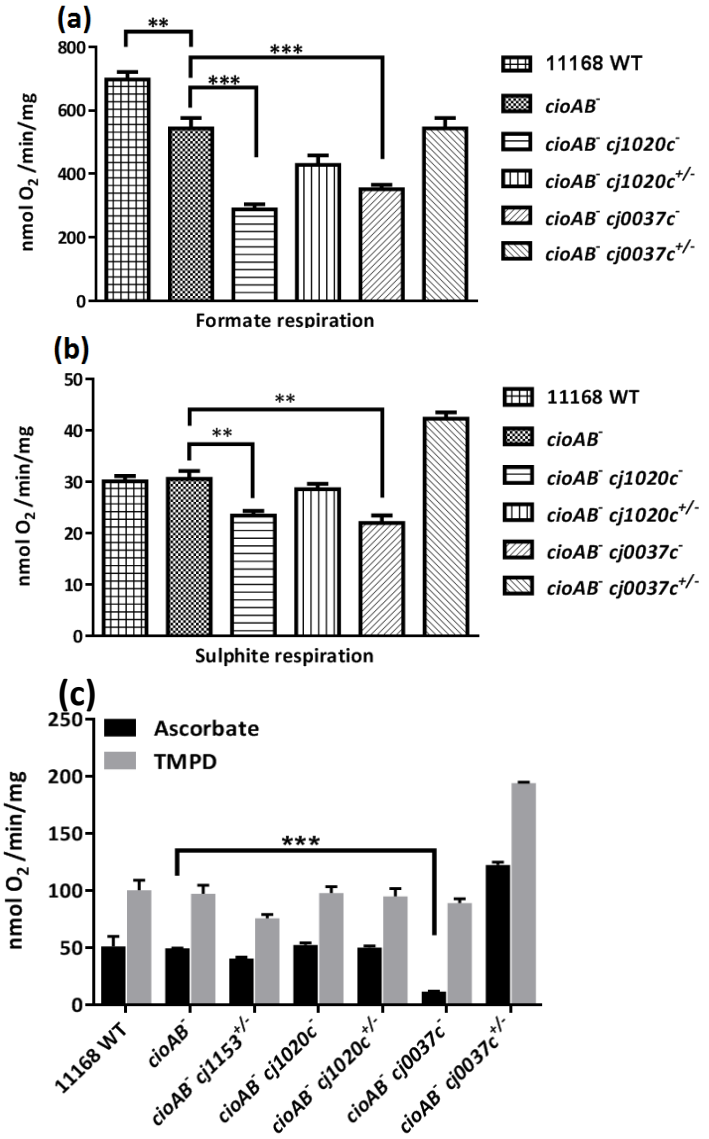

Figure 5.12 The oxygen consumption rate of different substrates in intact cells of wild-type, mutant and complemented strains without intact quinol oxidase CioAB. **(a)** 10 mM formate. **(b)** 5 mM sulphite. **(c)** 1 mM ascorbic acid alone or with 0.25 mM TMPD. Assay methods were as described in Materials and Methods. Relevant significant differences in activity are indicated by *** ($P < 0.001$) or ** ($P < 0.01$) according to Students t-test. The data shown are means ± SD of at least three independent experiments.

5.2.13 Overexpression and purification of recombinant Cj1153 and Cj0037 proteins and their ability to act as electron donors to the *cb*-oxidase

All the data above suggests that Cj0037 (and probably Cj1020) could be electron donors to the *cb*-oxidase, but because of the pleiotropic phenotype of the *cj1153* mutant, it is impossible to dissect out whether this is the case also for Cj1153 from mutant studies alone. We therefore wanted to directly study this with the purified proteins. Unfortunately, only very low yields of Cj1020 were obtained by heterologous expression (data not shown) so it was not further studied. For the overexpression of recombinant Cj1153 and Cj0037 proteins, both genes were amplified from the genomic DNA of *C. jejuni* NCTC 11168 and cloned into the pET21a(+) expression vector. Both constructs were sequenced (Core Genomic Facility, University of Sheffield Medical School, UK) to check for fidelity and to ensure the presence of an in-frame 6X-His tag at the C-terminus of both recombinant proteins. Then the constructs were co-transformed with the pEC86 vector (expressing the *ccm* genes needed for *c*-type cytochrome production in *E. coli*) into *E. coli* BL21(DE3) and the transformants were screened on LB plates containing carbenicillin (50 μg/ml) and chloramphenicol (30 μg/ml). The successful clones were amplified to 1 litre culture and grown overnight (16 to 18 hours) without any induction and the cell free extracts were prepared by sonification. The purification of recombinant proteins was carried out with nickel-affinity then ion-exchange chromatography and the purity was checked by 12% SDS-PAGE (Fig. 5.13 a).

The aim was to use ascorbate reduced purified Cj1153 and Cj0037 in respiration measurements with membrane preparations from the *cj1153* mutant, taking advantage of the fact that these membranes would not be contaminated with any residual *c*-type cytochromes. In order to first confirm that ascorbate can completely reduce the recombinant Cj1153 and Cj0037 proteins, the reduced minus oxidised difference spectra were measured with both recombinant proteins compared to other reductants dithionite (a few grains) and sodium borohydride (final concentration 1 mM) (Fig. 5.13 b and c). The reducing power of all reductants is sufficient to reduce these recombinant *c*-type cytochromes and two major peaks were observed at ~420 and ~550 nm with overlapped spectra. No further reduction occurred after addition of ascorbic acid (final concentration 1mM) in combination with dithionite or sodium borohydride.

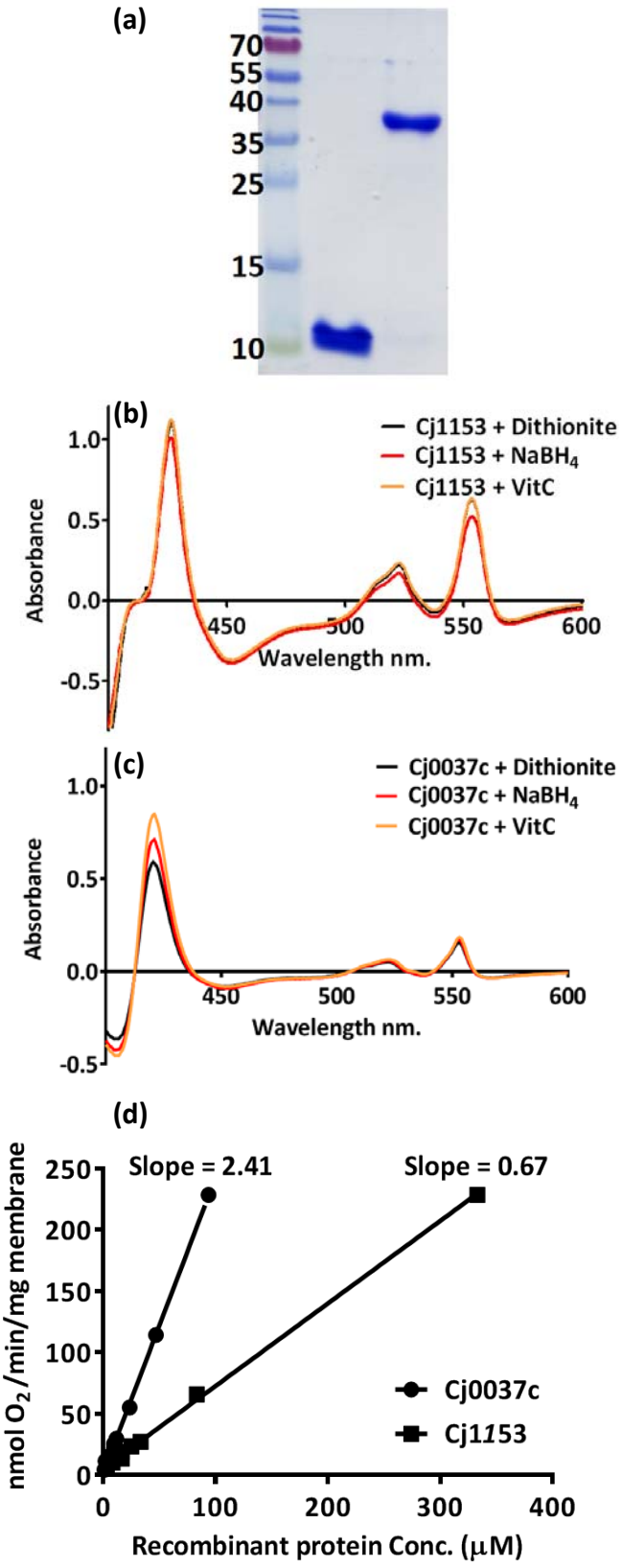

Figure 5.13 The reduced minus oxidised difference spectra of recombinant Cj1153 and Cj0037 and their ability to catalyse oxygen consumption with the *cj1153*$^-$ membrane fraction. (a) Purified Cj1153 and Cj0037c proteins, 10 μg per lane. **(b)** The reduced minus oxidised difference spectra of Cj1153 and (c) Cj0037c with several reductants (1mg/ml protein in each case). (d) *In vitro* respiration assayed by recombinant Cj1153, Cj0037 and the membrane fraction of *cj1153*$^-$. The slope indicates the affinity of recombinant proteins for the *cb*-oxidase.

The assay was carried out with the *cj1153* membrane fraction with different concentrations of recombinant Cj1153 and Cj0037 proteins and the oxygen consumption rate was measured after adding ascorbate. The respiration rate was plotted against the concentration of recombinant proteins (Fig. 5.13 c). The results did not show saturation behaviour but rather a linear relationship with different slopes for the two proteins. The Cj0037 protein showed a steeper slope, suggesting a higher affinity for the *cb*-oxidase in the membrane of *cj1153*$^{-}$ compared to Cj1153 itself. Nevertheless, the data do show clearly that both these cytochromes can act as electron donors to the *cb*-oxidase suggesting they may have partially redundant roles in the electron transport chain of *C. jejuni* NCTC 11168.

5.2.14 Identification of genes involved in the biogenesis of *c*-type cytochromes in *C. jejuni* NCTC 11168

The pleiotropic phenotype of missing periplasmic *c*-type cytochromes in the *cj1153* mutant suggests the mutation of other genes involved in the biogenesis of cytochromes *c* in *C. jejuni* might result in a similar phenotype as *cj1153*$^{-}$. The biogenesis of *c*-type cytochromes in *C. jejuni* is carried out by the Ccs system (System II; Simon and Hederstedt, 2011) which is comprised of several components such as CcsBA (cytochrome *c* synthase), DsbD and ResA (discussed in Chapter 1). The genome sequence revealed several homologues of enzymes in the Ccs system in *C. jejuni* NCTC 11168 (Parkhill *et al*., 2000), including *cj1013c* (*ccsBA*), *cj0603c* (*dsbD*), *cj1207c*, *cj1664* and *cj1665* (possible *resA* like genes). Also regulators like Cj1000 (Dufour *et al*., 2013), which affects respiration and RacRS, which is a two-component regulator involved in heat shock response, motility and the utilisation of fumarate (Apel *et al*., 2012; van der Stel *et al*., 2014) might affect the synthesis of *c*-type cytochromes. The mutation of those genes was carried out with the ISA method and the correct clones in *C. jejuni* NCTC 11168 were checked by colony PCR with the forward primer of antibiotic cassette and the reverse primer of 3' flanking region. No colonies were retrieved from the *cj1013c* mutagenesis, suggesting the homologue of *ccsBA* is essential for survival. The haem blots of periplasm of *cj1664*$^{-}$, *cj1665*$^{-}$, *cj1664*$^{-}$*cj1665*$^{-}$, *cj1000*$^{-}$, *racR*$^{-}$, *racS*$^{-}$ and *racRS*$^{-}$ strains showed a similar haem *c* pattern to the wild-type whereas less intensive bands were found in the periplasm of *cj0603c*$^{-}$ and *cj1207c*$^{-}$ (Fig. 5.14 a) and the intensity of the two major peaks at 553 and 420 nm were much less than that of wild-type in the reduced minus oxidised difference spectra (Fig. 5.14 c), which correlated to their mild growth defect under microaerobic conditions (Fig. 5.14 b). On

the contrary, no growth defect was observed in the *cj1664*, *cj1665* and *cj1664cj1665* and *racRS* (data not shown) mutants (Fig. 5.14 e) and the spectra of *cj1664*, *cj1665*, *cj1664cj1665* and wild-type were almost overlapped, suggesting that these genes are not involved in the biogenesis of *c*-type cytochromes in *C. jejuni*.

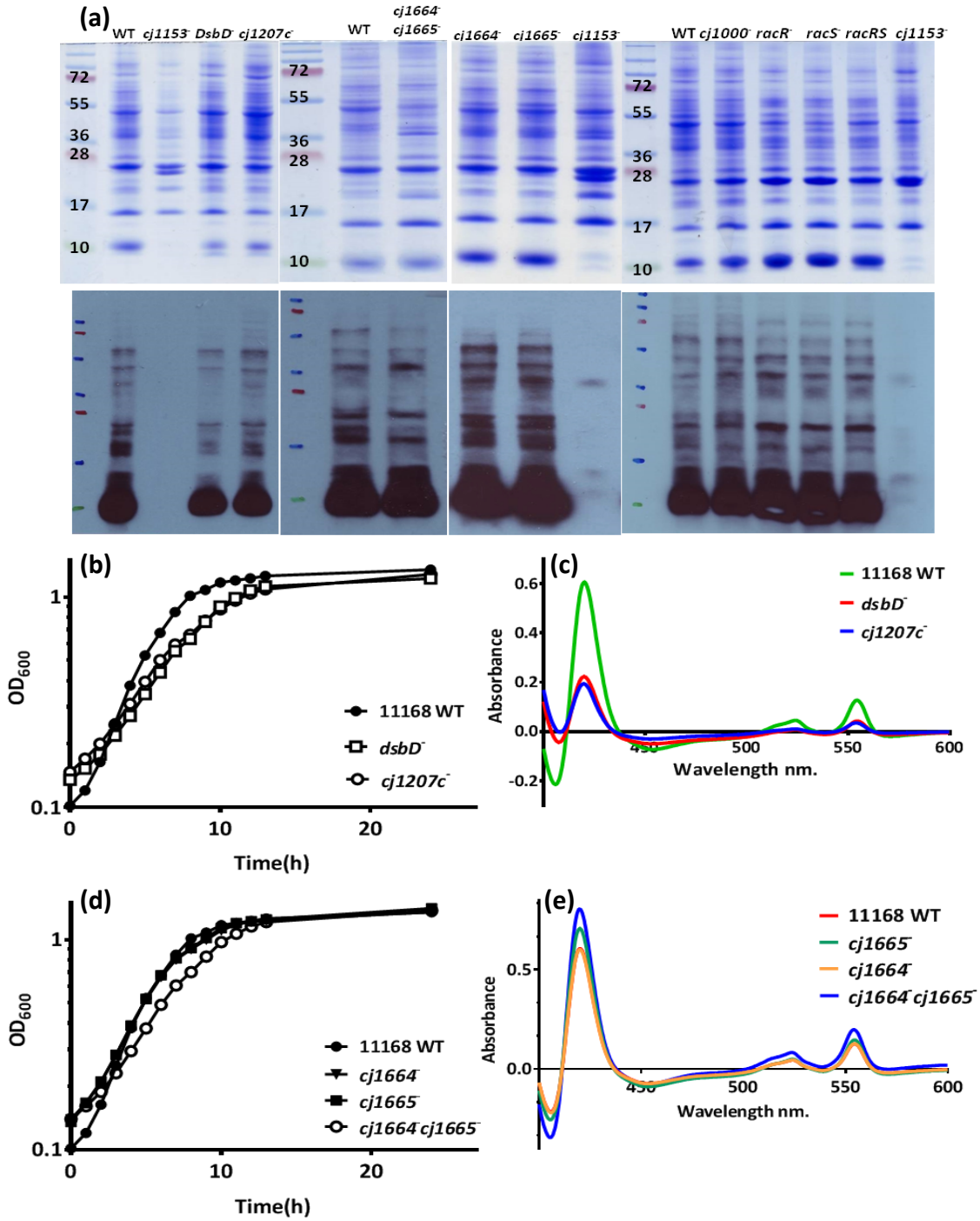

Figure 5.14 The haem blot, microaerobic growth curve and dithionite reduced minus air oxidised difference spectra of mutants involved in the Ccs system of C. jejuni NCTC 11168. (a) The haem blot of the periplasm (20 µg per lane) of wild-type and mutants. (b) and (d) The microaerobic growth curve of wild-type, *dsbD*$^-$ (*cj0603c*$^-$), *cj1207c*$^-$, *cj1664*$^-$, *cj1665*$^-$ and *cj1664*$^-$*cj1665*$^-$. (c) and (e) The difference spectra of the periplasm (1 mg/ml) of wild-type, *dsbD*$^-$, *cj1207c*$^-$, *cj1664*$^-$, *cj1665*$^-$ and *cj1664*$^-$*cj1665*$^-$.

5.2.15 Does Cj1153 form a complex with other cytochromes? Expression of His-tagged Cj1153 in the *cj1153*$^{-}$ mutant, BN-PAGE and periplasmic pull-down assays

The role of Cj1153 in the biogenesis of periplasmic *c*-type cytochromes is still unclear but given the lack of evidence for a large effect on *c*-type cytochrome gene expression, we hypothesised that there might be essential interactions between Cj1153 and other *c*-type cytochromes that is crucial for their stability and that there might be a "supercomplex" of *c*-type cytochromes in the periplasm of *C. jejuni*, which is unable to be formed in the absence of Cj1153. To examine this hypothesis, a pull down assay was carried out with His-tagged Cj1153 protein in *C. jejuni* via expression induced by the *fdxA* promoter. A DNA fragment with 5X His at the 3′ end of *cj1153* was amplified by fdxA-1153-F and 1153com-5XHis-R primers and cloned into the pCfdxA vector via a *Esp3*I restriction site (Gaskin, IFR, UK). The construct of pCfdxA1153His with correct orientation was sequenced (Core Genomic Facility, University of Sheffield Medical School, UK) and transformed into the *cj1153* mutant. The successful complemented strain was designated *cj1153*$^{+/-}$-His. The periplasm was prepared freshly then incubated with different volumes of nickel beads at 4 ^{o}C for 1 hour and then a haem blot was carried out with the set of supernatants and imidazole eluents from the different volumes of nickel beads. A clear haem *c* signal of Cj1153 was observed in the imidazole eluent with different volumes of beads (Fig. 5.15 a, lanes E), which correlated with the massive signal in the periplasm of *cj1153*$^{+/-}$-His (Fig. 5.15 a, lane P). However, no other abundant haem *c* signal was found above the size of Cj1153 in any eluent, suggesting that there was no other *c*-type cytochrome co-precipitating with Cj1153 in the presence of nickel beads. Moreover, all of the other periplasmic *c*-type cytochromes were still retained in the supernatants from after the incubation with the beads, with profiles very similar to the periplasm without beads added (Fig. 5.15 a, lanes SN compared to lane P).

As another approach to detect complex formation, 2-dimensional BN-PAGE fractionation was performed with the periplasm of *C. jejuni* NCTC 11168, in which native BN-PAGE and Tricine-SDS-PAGE were used to separate proteins in the first and second dimension respectively. The aim here was to resolve potential cytochrome containing complexes in the first dimension and then separate the individual proteins in the second and use haem blotting to look for an association with Cj1153. No obvious haem *c* signals caused by the formation of any supercomplex were found in the blot of

the second dimension gel and most of the signals were close to that of Cj1153 which showed a massive band in the bottom right corner of the gel. Taken together, although an interaction might exist between the Cj1153 protein and other periplasmic cytochromes *c*, no direct evidence can be found in several experiments and further work will be required to solve this enigma.

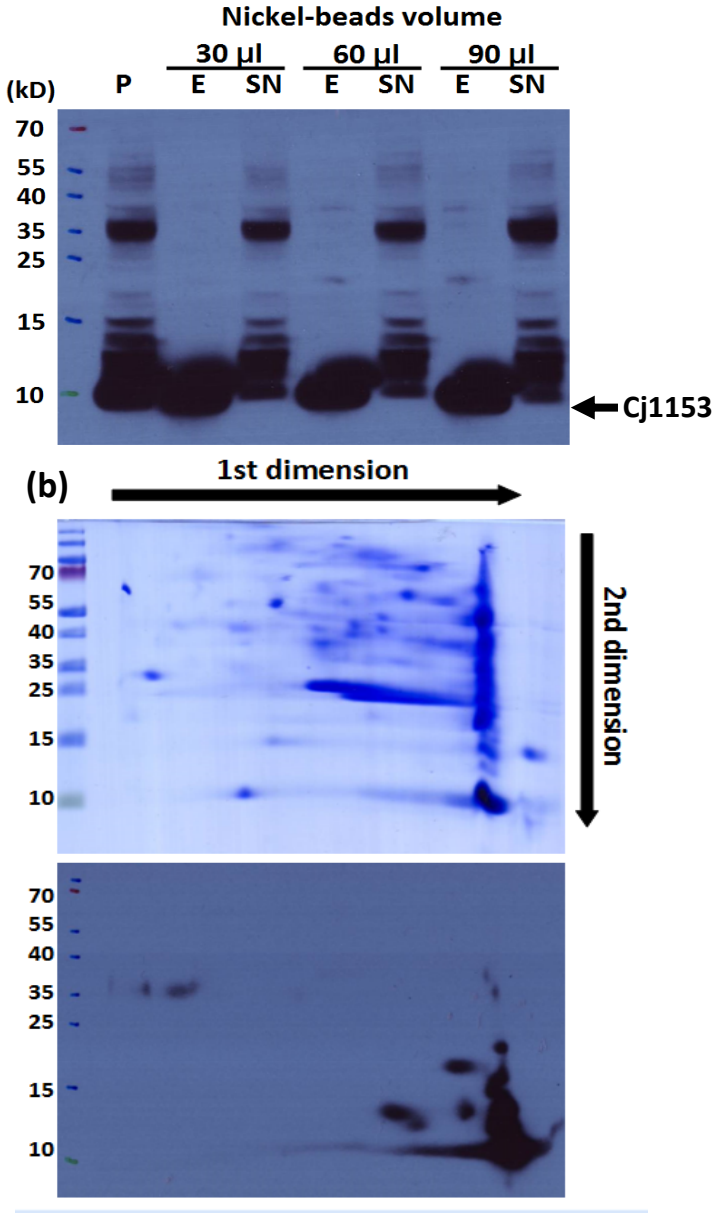

Figure 5.15 The pull down assay of the periplasm of *cj1153*$^{+/-}$-His and BN-PAGE of the periplasm of strain NCTC 11168. (a) The haem blot of the periplasm of *cj1153*$^{+/-}$-His, eluent and supernatants in the pull down assay. P, periplasm of *cj1153*$^{+/-}$-His, 40 µg per lane; E, imidazole eluent; and SN, supernatants after binding. (b) The periplasm of wild-type was separated by two dimensional BN-PAGE and haem blotted. The loading for the first dimension is 80 µg per lane, run on a native (no SDS) BN-PAGE gel strip. This was then cut out and applied to a second dimension Tricine SDS-PAGE gel with staining by coomassie blue. The corresponding haem blot is shown below. The Cj1153 signal is bottom right around 10 kDa.

5.3 Discussion

Several genes encoding *c*-type cytochromes in *C. jejuni* NCTC 11168 were identified and corresponding knockout mutants were constructed successfully via homologous recombination, where the target gene was replaced by an antibiotic resistance cassette. The mutation of *cj1153* and *cj1020c* resulted in mild growth defects that were fully recovered in their complemented strains with the native promoter (*cj1153*) or the *metK* promoter (*cj1020c*). No growth defect was observed in either *cj0037c* or *cj0158c* mutants, giving no clues as to their physiological relevance. One important issue concerns the possible redundancy of these cytochromes and it would be advantageous in future work to construct double or triple mutants in different combinations, although this would not be possible with Cj1153 (see below). However, the *cj0854c* mutant was unviable and thus the gene might be essential for *C. jejuni*. Due to the similarity (33%) of amino acid composition between Cj1153 and cytochrome c_{553} in *H. pylori* (Koyanagi *et al*., 2000), Cj1153 was initially considered likely as the major *c*-type cytochrome which mediates electron flux between the bc_1 complex and terminal *cb*-type oxidase, as has been shown to occur in *H. pylori*. Both *C. jejuni* and *H. pylori* have similar genome size (1.6 Mbp) and only four *c*-type cytochromes are encoded in *H. pylori*, where three of them comprise a typical ETC (not including cytochrome c_{551}; Koyanagi *et al*., 2000), suggesting a significant role of the cytochrome c_{553} homologue Cj1153 in *C. jejuni*, which from this study seems to be by far the most abundant *c*-type cytochrome in the periplasm. Although Cj1020 in full-length shows a low similarity (8%), it still shares some sequence features with Cj1153 and might possibly be involved in electron transfer to the *cb* oxidase. Due to the anticipated difficulty of analysing and expressing recombinant membrane-bound Cj0158 in *E. coli*, this gene was not further pursued in this study.

All periplasmic *c*-type cytochromes in this study harbour Sec-dependent signal peptides at their N-terminus and their actual molecular weights in the periplasm are 9.5 kD (Cj1153), 15.1 kD (Cj1020) and 38.1 kD (Cj0037), as calculated by SignalP 4.1 (http://www.cbs.dtu.dk/services/SignalP/). A dramatic and very unexpected phenotype in the periplasm of the *cj1153* mutant was the total loss of all haem *c* signals on both haem blots and in the difference spectra (Fig. 5.4), indicating that Cj1153 might participate in the biogenesis/maturation of the periplasmic *c*-type cytochromes in *C. jejuni* and/or their stabilities might be affected by the expression level of *cj1153* (Fig.

5.5 b). This is further discussed below. On the contrary, the expression level of *cj1020c* is much lower than *cj1153* with a faint band observed about ~15 kD in the double amount (40 μg) of periplasm of wild-type and *cj1020*$^{+/-}$ strain (Fig. 5.4 b). Furthermore, the growth curve of the *cj1020c* complemented strain driven by the inducible *fdxA* promoter is similar to the *cj1020*$^{-}$ mutant, possibly suggesting a higher expression level of *cj1020c* may lead to an inhibitory effect on growth. Taken together, the expression of *cj1020c* seems tightly controlled in *C. jejuni* although its role in the ETC could be redundant with Cj1153. The expression level of *cj0037c* is also lower than *cj1153* and the strong signal of Cj0037 seen in the haem blot is probably due to the three fold loading of periplasm (60 μg) compared to that needed to detect Cj1153 without overloading (20 μg; Fig. 5.4 a). However, even though the gene is driven by the strong *fdxA* promoter in *cj0037*$^{+/-}$, the protein expression level in this strain was still very low, which is reflected in the haem blot and the difference spectra (Fig. 5.4 c and f) and the expression level could perhaps be optimised using the native promoter, as was the case with *cjtsdA*$^{+/-}$ discussed in chapter 3. Nevertheless, the low expression level in the *cj0037c* complemented strain still supports the recovered growth phenotype and enzyme activities (Fig. 5.7 and 5.10).

The lack of growth of the *cj1153* mutant under oxygen-limited conditions on nitrate and TMAO but not fumarate is clearly a consequence of the pleiotropic loss of the haem signals in the mutant, as the NapB subunit of nitrate reductase (Pittman *et al*., 2007) and the Cj0265 subunit of the TMAO reductase (Sellars *et al*., 2002) are dihaem and monohaem *c*-type cytochromes respectively. The higher expression level of Cj1153 in the *cj1153*$^{+/-}$ strain driven by the *fdxA* promoter gave good restoration of growth and the data suggest that Cj1153 is not only important in the ETC of *C. jejuni* for microaerobic growth but also essential for oxygen-limited growth because of its pleiotropic effect on those cytochromes involved in the utilisation of alternative electron acceptors.

From the difference spectra obtained with the purified protein, Cj1153 seems to be a typical *c*-type cytochrome with an alpha band at 553 nm. Thus, the histidine in the -CXXCH- motif would be expected to be essential for haem binding and the loss of haem will likely lead to protein degradation. However, in the case of Cj1153, the substitution of His33 was found to lead to the loss/instability of <u>*all*</u> periplasmic *c*-type cytochromes, which is the same phenotype observed in the *cj1153*$^{-}$ deletion mutant. Surprisingly, the haem blot of H95A shows lower levels of Cj1153 and also some loss

of other cytochromes, similar to that seen with *cj1153*$^{+/-}$, suggesting His95 also contributes to the stability of Cj1153 itself and all other periplasmic *c*-type cytochromes. Taken together, the results of the null mutagenesis, complementation and point mutation of Cj1153 reveals that its expression level in the periplasm directly affects the level or stability of all other cytochromes *c*. Given this correlation, we did consider the possibility that the histidine residues in Cj1153 are somehow possible haem donors to other *c*-type cytochromes, but this seems highly unlikely given the presence of a typical type II cytochrome *c* biogenesis system (discussed below) and the paradox that Cj1153 would have to obtain its haem from elsewhere. An alternative and more likely explanation is that as the most abundant periplasmic *c*-type cytochrome, Cj1153 is essential for the stability of the less abundant species and perhaps forms a "supercomplex" with other cytochromes to keep structural integrity or for electron transfer kinetic reasons. This idea would be consistent with the lack of change in gene expression of at least some of these cytochromes in the *cj1153* mutant (i.e the phenotype is not mediated at the transcriptional level), but we did not find any positive evidence for complex formation by pull-down or 2D-gel analysis (discussed further below).

The pleiotropic effect caused by the mutation of *cj1153* most likely results in the degradation of all periplasmic *c*-type cytochromes and the electron transfer pathway from the bc_1 complex to *cb*-type oxidase will therefore be interrupted, which means no electrons can be directed to the CcoNOQP module in microaerobic growth. However, unlike the conclusion of previous studies (Jackson *et al*., 2007; Weingarten *et al*., 2008), the successful mutation of *ccoN* alone or the whole *ccoNOQP* module in *C. jejuni* NCTC 11168 in this study resulted in viable mutants. The similar growth defect in *cj1153*$^{-}$ and *ccoNOQP*$^{-}$ mutants suggests that the *c*-type cytochromes are as important as *cb* oxidase in energy conservation in *C. jejuni* under microaerobic conditions. Also, without the presence of *c*-type cytochromes or *cb* oxidase, electron flow to oxygen from the quinone pool will be directly diverted to the cyanide-resistant quinone oxidase CioAB. In order to maintain the growth rate under microaerobic conditions, the upregulated expression of *cioA* and *cioB* in the *cj1153*$^{-}$ mutant observed in this study might be a mechanism to compensate the loss of the more efficient *cb*-oxidase route (which has 3 coupling sites). This may also explain the higher formate respiration seen in *cj1153*$^{-}$ than in the wild-type, if all electrons are routed to CioAB, although the up-regulation of *fdhABCD* cannot be ruled out (this was not measured). The mechanism

of the up-regulation of *cioAB* in the *cj1153* mutant is unknown. No obvious down-regulation of gene expression of other *c*-type cytochromes is observed in the *cj1153* mutant, suggesting Cj1153 shows a post-translational effect on periplasmic cytochromes *c* instead of altering their transcriptional levels. Further RT-PCR evidence to support this (Fig. 5.11), suggests that a moderate level of *cj1153* expression in the complemented strain is sufficient for the recovery of enzyme activities. However, a totally different phenotype was found in the periplasm of *Paracoccus denitrificans,* where the knockout of cytochromes c_{550}, c_{552} and bc_1 solely and in various combinations resulted in the increased expression of other types of cytochromes *c* (Otten *et al*., 2001) and their regulation is more like a parallel relationship which compensates the loss of other *c*-type cytochromes instead of a hierarchy regulatory mode dominated by Cj1153 in *C. jejuni*.

The mutation of *cioAB* results in electron flux only being possible from electron donors to the *cb*-type oxidase during oxygen-dependent microaerobic growth of *C. jejuni* and this explains why the *cioAB*$^-$ *cj1153*$^-$ double mutant is unable to survive under the atmospheric conditions used for growth (containing 5% O_2). We did not test whether it was possible to recover colonies on media containing fumarate, which might allow growth by fumarate respiration. The phenotype of the *cioAB*$^-$ single mutant is similar to that reported in a previous study, in which no major growth defect is distinguishable by optical density measurements (Jackson *et al*., 2007). Mild aerobic growth defects were found in the corresponding mutants of *cj1020c* and *cj0037c* in the *cioAB*$^-$ background, which were reversed in the complemented strains. In particular, unlike the situation with intact CioAB, the *cj0037c*$^-$ *cioAB*$^-$ double mutant showed a more severe growth defect than *cj1020c*$^-$ *cioAB*$^-$ under microaerobic conditions, thus revealing a possible role of Cj0037 in oxygen-dependent electron transfer in *C. jejuni*. As might be expected, formate oxidation rates were slightly lower in the *cioAB* mutant than wild-type but sulphite oxidation rates were the same, consistent with the evidence that electrons derived from sulphite enter the respiratory chain after the bc_1 complex (Myers and Kelly, 2005) and will be transferred directly to cytochromes *c*. Thus, due to the absence of all periplasmic *c*-type cytochromes, no sulphite respiration rate can be measured in *cj1153*$^-$ (Fig. 5.7 b) and a reduced rate was observed in *cj1020c*$^-$ and *cj0037c*$^-$ mutants whether CioAB is present or not (Fig. 5.7 b and Fig. 5.12 b). No respiration with ascorbate alone could be observed in *cj1153*$^-$ or *cj0037c*$^-$ in the *cioAB*$^-$ background, which is explained by the *cj1153* dependent absence of all periplasmic *c*-type cytochromes, which will

include Cj0037. The reason why mutation of *cj0037c* alone leads to an abolished respiration with ascorbate is unknown but no pleiotropic effect on other periplasmic cytochromes *c* is apparent in the *cj0037c*$^{-}$ mutant (Fig. 5.2 c). However, due to the low expression level of *cj0037c* driven by the *fdxA* promoter in *cj0037*$^{+/-}$ (Fig. 5.2 c and f), its oxygen consumption rate with ascorbate is still much lower than wild-type and a better expression level might be obtained with the native promoter, which should be further investigated.

The recombinant his-tagged Cj1153 and Cj0037 were successfully expressed in *E. coli* with the accessory Ccm system in the pEC86 vector, but the expression level of expression of Cj1020 was extremely low. The faint haem *c* signal of purified his-tagged Cj1020 could be seen on an X-ray film in haem blots but no band was found with the corresponding molecular weight in a CBR-stained gel, although the sensitivity of the CBR stain may be too low to visualise the Cj1020 protein. The low expression of Cj1020 in *E. coli* might be due to (i) the overexpression of Cj1020 is unfavourable for cell growth since the expression is tightly controlled in *C. jejuni* and the periplasmic protein level is relatively lower than other *c*-type cytochromes in this study; or (ii) *C. jejuni* adopts the Ccs system for *c*-type cytochrome synthesis and the expression of recombinant cytochromes *c* such as Cj1153 and Cj0037 in *E. coli* is still possible with the *ccm* genes in the pEC86 vector, suggesting both biogenesis systems Ccm and Ccs might tolerate the different mechanisms and be partially interchangeable for the expression of these *c*-type cytochromes, but this is not the case for Cj1020. The interaction of the two purified cytochromes with the *cb*-oxidase was studied in membrane preparations, which showed that both Cj0037 and Cj1153 could act as electron donors for this oxidase. Interestingly, the ascorbate reduced recombinant Cj0037 promoted a higher respiration rate than Cj1153 with the membrane fraction of the *cj1153*$^{-}$ mutant. However, neither cytochrome showed typical Michaelis-Menten saturation behaviour in the steady state kinetics measurements. Significantly, this is similar to the data obtained with purified cbb_3-type oxidase from *Vibrio cholerae* interacting with recombinant cytochrome c_4 or c_5 (Chang *et al*., 2010). These authors proposed that oxidised *c*-type cytochrome affects the oxidase activity and that both V_{max} and K_M increase as the concentration of oxidised cytochrome *c* increases in the reaction. Thus, it was suggested that oxidised *c*-type cytochromes have a strong effect on the activity between *cb*-oxidase and reduced cytochromes *c* and the presence of a relatively small amount of oxidised cytochromes *c* will result in an increasing K_M. If the K_M is too

large, it is impossible to obtain an accurate curve fitting to Michaelis–Menten kinetics. Another factor for Cj0037 is the presence of two haem molecules that may be in a different redox state which, as for the *Vibrio* dihaem cytochrome c_4, will complicate the true values for either V_{max} or K_M (Chang *et al*., 2010). The apparent higher affinity of Cj0037 for the *cb* oxidase might partially explain the respiration data of the *cj0037*⁻ mutant with ascorbate, where the expression of *cj1153* is not affected by the mutation of *cj0037c*. Cj0037 seems to contribute most of the oxygen consumption with ascorbate and Cj1153 might also be involved. In the periplasm of the *cj0037*⁻ mutant, perhaps the concentration of Cj1153 is not high enough to compensate for the rate contributed by Cj0037 with ascorbate. *In vitro*, the actual oxygen consumption might be lower since the assay was carried out with *cj1153*⁻ membranes and purified recombinant proteins. Nevertheless, it is clear that reduced Cj1153 itself does contribute to respiration with the *cb*-oxidase. It seems that Cj1153 is one of the most important *c*-type cytochromes in *C. jejuni* NCTC 11168, and it has a dual role in the ETC: as an electron transfer enzyme and in regulating the stability of all other periplasmic cytochromes *c*.

Still another possibility should be addressed here; the absence of Cj1153 might lead to the degradation of **all** *c*-type cytochromes, which could include the cyt-*c* components CcoP and CcoO of the *cb* oxidase. This would result in the severe reduction or abolition of the function of this oxidase and the measured respiration rate with recombinant Cj0037 and Cj1153 using the membrane fraction of the *cj1153* mutant might therefore be due to the oxidation caused by the *bd*-type quinol oxidase in the membrane (Yang *et al*., 2008). The *bd*-type quinol oxidase is known to be able to oxidise ascorbate reduced TMPD in *E. coli* and a similar situation may occur here. Thus, further respiratory studies should be carried out with recombinant Cj0037 and Cj1153 respectively with the membrane fraction of the *cioAB* mutant to confirm the origin of the respiration observed here.

Finally, the biogenesis of *c*-type cytochromes in *C. jejuni* was investigated, partly inspired by the unexpected *cj1153* phenotype. This depends on the Ccs system and several homologous genes, which might be involved in this system, have been identified. Although the mutation of *ccsBA* (*cj1013c*) is apparently lethal, the mutants of homologues of *dsbD*, *resA* and the two regulator *cj1000* and *racRS* are still viable, suggesting not only the presence of another *dsbD* homologue(s) in *C. jejuni* but the redundancy of all *resA* genes (*cj1207c*, *cj1664* and *cj1665*) investigated in this study.

None of the possible regulators investigated seem to be involved in the biogenesis of *c*-type cytochromes in *C. jejuni*, although Cj1000 has been proposed to be involved in the regulation of several genes involved in both oxidative stress and the ETC, such as *ahpC*, *katA*, *nrfA* and *SorA* (Dufour *et al*., 2013), but the haem blots performed here clearly show a similar haem *c* pattern to wild-type. Also, although the *racRS* two-component regulator is involved in the regulation of several physiological activities relating to nitrate, fumarate and aspartate metabolism in *C. jejuni*, the expression of periplasmic *c*-type cytochrome is not affected in the corresponding mutants. Taken together, the expression of *c*-type cytochromes in *C. jejuni* is likely to be controlled only by the Ccs biogenesis system and the possibility that Cj1153, which has a unique systemic effect on all periplasmic *c*-type cytochromes, might be a novel Ccs component, seems less likely compared to its more probable role in mediating essential interactions between the periplasmic cytochrome network. However, perhaps due to the limitation of the simple analytical techniques used here, no "supercomplex" formation could be proved by the pull-down assay or two-dimensional PAGE, but several other methods such as cross-linking, gel filtration or ultracentrifugation still can be tried to detect such complexes in the periplasm.

5.4 Conclusions

Cytochromes *c* play a crucial role in the electron transport chain of *C. jejuni*, which mediates the main electron flux from the bc_1 complex to the *cb*-type terminal oxidise in microaerobic growth. Also, they transfer electrons directly from electron donors like sulphite and gluconate to the *cb* oxidase by accepting electrons from the corresponding oxidase or dehydrogenase, which bypasses the bc_1 complex. Several *c*-type cytochromes were identified as possible candidates involved in the ETC of *C. jejuni* NCTC 11168 and the periplasmic proteins Cj1153, Cj1020c and Cj0037 might be the major electron transfer enzymes. Although the mutation of *cj0854c* was not possible under microaerobic conditions and no growth defect was observed in the *cj0158c* mutant, both of them might still be significant for some physiological activities. The mutation of *cj1153* and *cj1020c* leads to a growth defect in the corresponding mutants under microaerobic conditions but not with the *cj0037c* mutant. The physiological role of *cj1020c* and *cj0037c* in *C. jejuni* has been elucidated by respiration studies with formate and sulphite where both mutants showed lower oxygen consumption rates to wild-type. However, the *cj0037c* mutant showed an unusual phenotype as no oxygen consumption

was observed when incubated with ascorbate. The expression level of these three genes can be reflected by the haem blot where Cj1153 shows the most intensive haem *c* signal among all periplasmic *c*-type cytochromes while signals of Cj1020 and Cj0037 are far less obvious. The very low expression level of *cj1020c* in *C. jejuni* might explain the difficulty of expressing recombinant Cj1020 in *E. coli*, although the haem *c* signal is still detectable.

The haem blot revealed that Cj1153 is the most abundant *c*-type cytochrome in the periplasm of *C. jejuni* and this might correlate to its physiological activity in microaerobic growth. Cj1153 has been demonstrated as an electron transfer enzyme in the ETC; however, the pleiotropic effect caused by the mutation of *cj1153* suggests that it might be involved in the biogenesis or stability of periplasmic *c*-type cytochromes. This hypothesis is also supported by the anaerobic growth of *cj1153*$^{-}$ and the complemented strain with several alternative electron acceptors. The expression of *cj1153* driven by different promoters indeed affects the intensity of haem *c* signals in the periplasm of complemented strains. However, in the *cj1153* mutant, the transcription level of most *c*-type cytochromes is not altered, suggesting that post-translational interactions might occur between Cj1153 and other *c*-type cytochromes in the periplasm of *C. jejuni*. Interestingly, the expression of cyanide-resistant quinone oxidase encoded by *cioAB* is 20 fold upregulated in *cj1153*$^{-}$ and this explains not only the mild growth defect of *cj1153*$^{-}$ under microaerobic conditions but higher respiration rate to wild-type incubated with formate. No oxygen consumption occurs when *cj1153*$^{-}$ cells are incubated with sulphite or ascorbate and the latter result is similar to that with *cj0037c*$^{-}$ cells but in *cj1153*$^{-}$ the Cj0037 protein might be unstable / degraded without the presence of Cj1153. The significance of Cj1153 in the ETC of *C. jejuni* is equal to that of the terminal *cb*-type oxidase because both *cj1153*$^{-}$ and *ccoNOQP*$^{-}$ showed similar growth rate under microaerobic conditions and all electrons are diverted to CioAB in both cases.

Both recombinant reduced Cj1153 and Cj0037 are able to be oxidised by the membrane fraction of *cj1153*$^{-}$ but the rate with Cj1153 is only about ~20% to that of Cj0037. This phenomenon might be sufficient to explain the zero respiration rate of *cj0037*$^{-}$ incubated with ascorbate. A series of mutants of homologous genes involved in the *c*-type cytochrome biogenesis Ccs system and two regulators was carried out in *C. jejuni* NCTC 11168 but none of mutants showed a similar periplasmic phenotype to *cj1153*$^{-}$,

although the mutation of *cj0603c* (*dsbD*) and a *cj1207c* (one of *resA* homologues) resulted in a mild decrease of all haem *c* signals in the periplasm, which correlates to their growth defect under microaerobic conditions. The absence of cytochromes *c* caused by the mutation of *cj1153* suggests that Cj1153 is likely to from a complex with other *c*-type cytochromes; however, no direct evidence for protein-protein interactions was obtained so far. This topic is still worthy to be investigated since there is still no clear answer for the dramatic phonotype in the *cj1153* mutant. Also, due to the abundance of Cj1153 in the periplasm and its regulatory effect on all periplasmic *c*-type cytochromes, a dilemma should be addressed here: it is impossible to measure an accurate oxygen consumption rate with only one kind of *c*-type cytochrome in the periplasm because the mutation of *cj1153* or any double mutant will lead to the absence of all periplasmic *c*-type cytochromes, including the target and this makes dissection of cytochrome redundancy and specificity very difficult to assess. Finally, all Cj1153, Cj1020 and Cj0037 are involved in the electron transferring from the bc_1 complex or other electron donors to the terminal *cb* type oxidase and they might play parallel roles in the ETC of *C. jejuni*. The possible model is shown in Fig. 1.5.

Chapter 6 General conclusions

The electron transport chain in *C. jejuni* is highly branched, which allows flexibility in energy conservation and supports growth under microaerobic and near-anaerobic conditions, especially in the oxygen-limited environment of the human or avian intestine. At the start of this study, several reductases had already been identified to support oxygen-limited growth of *C. jejuni* via respiration with alternative electron acceptors to oxygen, such as nitrate, nitrite, fumarate and *S*- and *N*-oxides (Pittman *et al*., 2005; Pittman *et al*., 2007; Guccione *et al*., 2010; Sellars *et al*., 2002). Recently,, tetrathionate, a less studied alternative electron acceptor has been identified as being formed in the human intestine, which supports *Salmonella enterica* serotype Typhimurium (*S*. Typhimurium) to outgrow the microbiota during inflammation, in which reactive oxygen species react with endogenous thiosulphate to form tetrathionate (Winter *et al*., 2010). In this study, a novel bi-functional enzyme TsdA has been identified in *C. jejuni* 81116 with both thiosulphate dehydrogenase and tetrathionate reductase activities, which is totally distinct from the Ttr type enzyme in *Salmonella.* We believe that TsdA might be important for growth of *C. jejuni* in the human gut that directly associates to its pathogenicity. An important recent conceptual advance in bacterial pathogenesis has been the demonstration that enteric pathogens can utilise host responses to outgrow the intestinal microbiota (Stecher *et al*., 2007; Lupp *et al*., 2007). Under anaerobic conditions, microbes compete for high-energy resources that are available for fermentation, but fermentation end products cannot be further utilized. By reducing tetrathionate, *C. jejuni* might be able to use fermentation end products which generate a new respiratory electron acceptor as byproduct of the host inflammatory response and this not only changes the composition of the microbiota in the anaerobic environment of the gut, but also provides this pathogen a substantial selective advantage. Some *C. jejuni* strains like 81116 (Pearson *et al*., 2007) or M1 (Friis *et al*., 2010) harbour an active TsdA (C8j_0815) enzyme that catalyses the reduction of tetrathionate to thiosulfate in the presence of additional electron donors like formate while truncated *tsdA* genes are found in the isolates NCTC 11168 (Parkhill *et al*., 2000), RM1221 (Fouts *et al*., 2005) and 81-176 (Hofreuter *et al*., 2006); however, the presence of TsdA might correlate to the pathogenicity of *C. jejuni*. Further animal infection studies are required to clarify if tetrathionate respiration in *C. jejuni* provides a similar benefit for the colonization process as described for *S.* Typhimurium. On the contrary, thiosulphate dehydrogenase activity of TsdA might contribute to microaerobic survival of *C. jejuni*

in the open environment, which is similar to the chemotrophic *Allochromatium vinosum* that harbours a *tsdA* homologue with a dominant activity in thiosulphate oxidation. Furthermore, unlike the three-component molybdoenzyme TtrABC characterized from *S.* Typhimurium (Hinojosa-Leon *et al*., 1986; Hensel *et al*., 1999) and the octahaem Otr enzyme found in *Shewanella* (Mowat *et al*., 2004), the structure of the monomeric di-haem TsdA in *C. jejuni* is much simpler. Thus, the catalytic mechanism of CjTsdA in tetrathionate reduction and thiosulphate oxidation is worthy to be further investigated and is currently being pursued by electrochemical techniques (collaboration of D. Kelly, C. Dahl and J. Butt). The discovery of a totally novel type of tetrathionate reductase will lead to a new insights in bacterial sulphur metabolism since *tsdA* homologues are widely distributed among different bacteria.

Many of the periplasmic enzymes involved in the electron transport chain of *C. jejuni* are transported across the cytoplasmic membrane via the TAT system (Hitchcock *et al*., 2010). Although a compact TAT complex comprised by TatA1, TatB and TatC (encoded by *cj1176c*, *cj0579c* and *cj0578c* respectively) was already known to be present in *C. jejuni* NCTC 11168, a TatA homologue encoded by *cj0786* located in the *nap* operon has here been shown to have typical structural features similar to TatA1 and was named TatA2. The mutation of *tatA2* partially affects the translocation of some TAT-dependent substrates such as nitrate reductase, formate dehydrogenase and TMAO reductase involved in the ETC but other TAT-dependent substrates assayed in this study still function normally whereas the mutation of TatA1 resulted in complete loss of enzyme activities of most TAT-dependent substrates (not including TMAO reductase and Mfr fumarate reductase), suggesting enzyme degradation occurs in the cytoplasm. However, in the *tatA1* mutant an unusual phenomenon was observed where MfrA could be detected in the periplasm, suggesting a role of TatA2 in the transportation of Mfr. Indeed, several TatA2 homologues are found in different bacteria, which are involved in distinct physiological characteristics such as tolerance of salinity, biofilm forming and denitrification (van der Ploeg *et al*., 2011; Beloin *et al*., 2004; Heikkila *et al*., 2001) and TatA2 might be associated with other phenotypes in *C. jejuni* since it shows an atypical translocation of fumarate reductase. Furthermore, unprocessed MfrA was observed in the *tatA1* mutant indicates the translocation was carried out by TatA2 without the cleavage of the TAT signal peptide. Thus, in order to confirm the role of TatA2 in the TAT-dependent translocation, a point mutation of RR to XR, RX or XX (where X can be alanine or lysine) in the twin-arginine motif of MfrA is likely to prove whether

TatA2 is able to transport TAT-dependent substrates without signal peptide recognition, which should occur with TatC (or TatBC complex). In addition, TatA2 is able to transport MfrA possibly due to the uniqueness of the signal peptide at its N-terminus and this hypothesis can be examined by swapping the signal peptide of MfrA to other TAT-dependent substrates like sulphite oxidase SorA, where enzyme activity is measurable in the periplasm. Taken together, the precise relationship between the TAT signal peptide and the translocation occurring with TatA2 assistance still remains to be elucidated in the future. Since TatA2 lacks two crucial residues Gin8 and Phe39 which have been shown to be required for TatA translocation function or in the membrane weakening model (Greene *et al*., 2007; Rodriguez *et al*., 2013), TatA2 seems to have an accessory role which interacts with TatA1. However, TatA2 still possibly forms a TAT complex with TatBC. Thus, to characterise the protein-protein interactions between TatA1 and TatA2, several approaches such as chemical cross-linking, yeast two-hybrid, fluorescence resonant energy transfer (FRET), and co-immunoprecipitation can be carried out. Moreover, the existence of TatA2BC complex can be proved by protein purification in a gentle way (like gel filtration) with Western blotting using anti-TatA2 antibodies. Although structural studies will reveal more direct evidence, expression and purification of recombinant membrane proteins TatB and TatC is difficult. In short, not only the recognition of the signal peptide but formation of translocating units is important for transportation of TAT-dependent substrates and both mechanisms in *C. jejuni* are still unclear.

Several genes encoding periplasmic *c*-type cytochromes have been identified in this study, which mediate electrons flux from the bc_1 complex or electron donors like sulphite to the terminal *cb*-type oxidase in microaerobic growth of *C. jejuni*. However, Cj1153 is not only involved in the electron transfer pathway but regulates the biogenesis/ maturation or maintains the stability of other *c*-type cytochromes, including Cj1020 and Cj0037. Although these three *c*-type cytochromes are able to mediate electron transfer in *C. jejuni*, the mutation of *cj1153* will lead to degradation of all other cytochromes *c* and electrons in the menaquinone pool will be diverted to quinol oxidase CioAB, which is different to the situations in several bacteria, such as *P. denitrificans*, *Neisseria gonorrhoea* and *Neisseria meningitidis* (Otten *et al*., 2001; Li *et al*., 2010; Deeudom *et al*., 2008) where several cytochromes are present in the periplasm and a loss of function in any can be compensated by other cytochromes in the corresponding mutant, suggesting a parallel relationship in electron transfer. Due to the pleiotropic

effect caused by the mutation of *cj1153*, it seems unlikely the similar parallel relationship existing among Cj1020, Cj0037 and Cj0158 and the low expression level of Cj1020 and Cj0037 further restricts analysis. However, haem blots are still a very direct way to show the abundance of *c*-type cytochromes in the periplasm and the low expression level might be solved by concentrating periplasmic fractions before analysing by tricine-PAGE (not including membrane-bound Cj0158). The surprising phenotype of the *cj1153* mutant is unexpected and the amino acid composition and the simple structure of Cj1153 suggests that it is unlikely to function as a chaperone maintaining the correct folding or as a haem lyase for other periplasmic *c*-type cytochromes. Future analytical tools such as global proteomics can be introduced to see how many proteins are affected in the mutant, which may help to resolve the basis of the phenotype. Instead of conventional BN-PAGE, isoelectric focusing (IEF) might result in better separation of several supercomplexes in the periplasm. Furthermore, although the up-regulation of *cioAB* was observed in the *cj1153* mutant, the mechanism is still unclear and *cj1153* might directly or indirectly affect the gene expression of *cioAB*. For this reason, a transcriptomics approach such as microarray analysis will give a more complete profile of gene expression in the absence of *cj1153*. The enigma in the *cj1153* mutant remains until both transcriptomics and proteomics studies are fully accomplished. Unlike the mutation of *cj1153* with diverted electron flux to CioAB, both *cj0854c* and *ccsBA* mutants are unable to survive under microaerobic conditions, although the reason is still unknown. Cj0854 is a soluble *c*-type cytochrome in the periplasm, which shows a ~40% similarity to the subunit III of cytochrome *c* oxidase in *H. pylori* and *ccsBA* (*cj1013c*) is involved in the biogenesis of *c*-type cytochromes in *C. jejuni*. However, due to the lethal phenotype of the *ccsBA* mutant, *cj1013c* might also regulate the expression of other (essential) genes. CcsBA might be a potential target for drug design, which could slow down the spreading of this common pathogen among poultry and indirectly reduce campylobacteriosis in humans.

Chapter 7 References

Ahuja, U. and L. Thony-Meyer (2003). Dynamic features of a heme delivery system for cytochrome *c* maturation. *J Biol Chem* **278**(52): 52061-52070.

Ahuja, U. and L. Thony-Meyer (2005). Ccmd is involved in complex formation between Ccmc and the heme chaperone ccme during cytochrome *c* maturation. *J Biol Chem* **280**(1): 236-243.

Ahuja, U., P. Kjelgaard, B. L. Schulz, L. Thony-Meyer and L. Hederstedt (2009). Haem-delivery proteins in cytochrome *c* maturation system II. *Mol Microbiol* **73**(6): 1058-1071.

Alami, M., I. Luke, S. Deitermann, G. Eisner, H. G. Koch, J. Brunner and M. Muller (2003). Differential interactions between a twin-arginine signal peptide and its translocase in *Escherichia coli*. *Mol Cell* **12**(4): 937-946.

Alderson, D. and C. R. Welbourn (1997). Laparoscopic surgery for gastro-oesophageal reflux disease. *Gut* **40**(5): 565-567.

Aldridge, C., X. Ma, F. Gerard and K. Cline (2014). Substrate-gated docking of pore subunit Tha4 in the Tatc cavity initiates tat translocase assembly. *J Cell Biol* **205**(1): 51-65.

Apel, D., J. Ellermeier, M. Pryjma, V. J. Dirita and E. C. Gaynor (2012). Characterization of *Campylobacter jejuni* racrs reveals roles in the heat shock response, motility, and maintenance of cell length homogeneity. *J Bacteriol* **194**(9): 2342-2354.

Arslan, E., H. Schulz, R. Zufferey, P. Kunzler and L. Thony-Meyer (1998). Overproduction of the *Bradyrhizobium japonicum c*-type cytochrome subunits of the cbb_3 oxidase in *Escherichia coli*. *Biochem Biophys Res Commun* **251**(3): 744-747.

Ashgar, S. S., N. J. Oldfield, K. G. Wooldridge, M. A. Jones, G. J. Irving, D. P. Turner and D. A. Ala'Aldeen (2007). CapA, an autotransporter protein of *Campylobacter jejuni*, mediates association with human epithelial cells and colonization of the chicken gut. *J Bacteriol* **189**(5): 1856-1865.

Atack, J. M. and D. J. Kelly (2007). Structure, mechanism and physiological roles of bacterial cytochrome *c* peroxidases. *Adv Microb Physiol* **52**: 73-106.

Atack, J. M., P. Harvey, M. A. Jones and D. J. Kelly (2008). The *Campylobacter jejuni* thiol peroxidases Tpx and Bcp both contribute to aerotolerance and peroxide-mediated stress resistance but have distinct substrate specificities. *J Bacteriol* **190**(15): 5279-5290.

Atack, J. M. and D. J. Kelly (2009). Oxidative stress in *Campylobacter jejuni*: Responses, resistance and regulation. *Future Microbiol* **4**(6): 677-690.

Atkinson, S. J., C. G. Mowat, G. A. Reid and S. K. Chapman (2007). An octaheme *c*-type cytochrome from *Shewanella oneidensis* can reduce nitrite and hydroxylamine. *FEBS Lett* **581**(20): 3805-3808.

Bachmann, J., B. Bauer, K. Zwicker, B. Ludwig and O. Anderka (2006). The rieske protein from paracoccus denitrificans is inserted into the cytoplasmic membrane by the twin-arginine translocase. *FEBS J* **273**(21): 4817-4830.

Bacon, D. J., R. A. Alm, D. H. Burr, L. Hu, D. J. Kopecko, C. P. Ewing, T. J. Trust and P. Guerry (2000). Involvement of a plasmid in virulence of *Campylobacter jejuni* 81-176. *Infect Immun* **68**(8): 4384-4390.

Bacon, D. J., R. A. Alm, L. Hu, T. E. Hickey, C. P. Ewing, R. A. Batchelor, T. J. Trust and P. Guerry (2002). DNA sequence and mutational analyses of the pVir plasmid of *Campylobacter jejuni* 81-176. *Infect Immun* **70**(11): 6242-6250.

Bacon, D. J., C. M. Szymanski, D. H. Burr, R. P. Silver, R. A. Alm and P. Guerry (2001). A phase-variable capsule is involved in virulence of *Campylobacter jejuni* 81-176. *Mol Microbiol* **40**(3): 769-777.

Bader, J., H. Gunther, E. Schleicher, H. Simon, S. Pohl and W. Mannheim (1980). Utilization of (E)-2-butenoate (Crotonate) by *Clostridium kluyveri* and some other *Clostridium* species. *Arch Microbiol* **125**(1-2): 159-165.

Bageshwar, U. K., N. Whitaker, F. C. Liang and S. M. Musser (2009). Interconvertibility of lipid- and translocon-bound forms of the bacterial Tat precursor pre-Sufi. *Mol Microbiol* **74**(1): 209-226.

Baglieri, J., D. Beck, N. Vasisht, C. J. Smith and C. Robinson (2012). Structure of tatA paralog, tatE, suggests a structurally homogeneous form of tat protein translocase that transports folded proteins of differing diameter. *J Biol Chem* **287**(10): 7335-7344.

Bagos, P. G., E. P. Nikolaou, T. D. Liakopoulos and K. D. Tsirigos (2010). Combined prediction of Tat and Sec signal peptides with hidden Markov models. *Bioinformatics* **26**(22): 2811-2817.

Baillon, M. L., A. H. van Vliet, J. M. Ketley, C. Constantinidou and C. W. Penn (1999). An iron-regulated alkyl hydroperoxide reductase (Ahpc) confers aerotolerance and oxidative stress resistance to the microaerophilic pathogen *Campylobacter jejuni*. *J Bacteriol* **181**(16): 4798-4804.

Bamford, V. A., S. Bruno, T. Rasmussen, C. Appia-Ayme, M. R. Cheesman, B. C. Berks and A. M. Hemmings (2002). Structural basis for the oxidation of thiosulfate by a sulfur cycle enzyme. *EMBO J* **21**(21): 5599-5610.

Barker, P. D. and S. J. Ferguson (1999). Still a puzzle: Why is haem covalently attached in *c*-type cytochromes? *Structure* **7**(12): R281-290.

Barnes, I. H., M. C. Bagnall, D. D. Browning, S. A. Thompson, G. Manning and D. G. Newell (2007). Gamma-glutamyl transpeptidase has a role in the persistent colonization of the avian gut by *Campylobacter jejuni*. *Microb Pathog* **43**(5-6): 198-207.

Beckett, C. S., J. A. Loughman, K. A. Karberg, G. M. Donato, W. E. Goldman and R. G. Kranz (2000). Four genes are required for the system II cytochrome *c* biogenesis pathway in *Bordetella pertussis*, a unique bacterial model. *Mol Microbiol* **38**(3): 465-481.

Beery, J. T., M. B. Hugdahl and M. P. Doyle (1988). Colonization of gastrointestinal tracts of chicks by *Campylobacter jejuni*. *Appl Environ Microbiol* **54**(10): 2365-2370.

Behrendt, J., K. Standar, U. Lindenstrauss and T. Bruser (2004). Topological studies on the twin-arginine translocase component Tatc. *FEMS Microbiol Lett* **234**(2): 303-308.

Beloin, C., J. Valle, P. Latour-Lambert, P. Faure, M. Kzreminski, D. Balestrino, J. A. Haagensen, S. Molin, G. Prensier, B. Arbeille and J. M. Ghigo (2004). Global impact of mature biofilm lifestyle on *Escherichia coli* K-12 gene expression. *Mol Microbiol* **51**(3): 659-674.

Bendtsen, J. D., H. Nielsen, D. Widdick, T. Palmer and S. Brunak (2005). Prediction of twin-arginine signal peptides. *BMC Bioinformatics* **6**: 167.

Berg, B. L., J. Li, J. Heider and V. Stewart (1991). Nitrate-inducible formate dehydrogenase in *Escherichia coli* K-12. I. Nucleotide sequence of the fdnghi operon and evidence that opal (uga) encodes selenocysteine. *J Biol Chem* **266**(33): 22380-22385.

Berks, B. C. (1996). A common export pathway for proteins binding complex redox cofactors? *Mol Microbiol* **22**(3): 393-404.

Berks, B. C., T. Palmer and F. Sargent (2005). Protein targeting by the bacterial twin-arginine translocation (Tat) pathway. *Curr Opin Microbiol* **8**(2): 174-181.

Bertini, I., G. Cavallaro and A. Rosato (2006). Cytochrome *c*: Occurrence and functions. *Chem Rev* **106**(1): 90-115.

Bilous, P. T. and J. H. Weiner (1988). Molecular cloning and expression of the *Escherichia coli* dimethyl sulfoxide reductase operon. *J Bacteriol* **170**(4): 1511-1518.

Bingham-Ramos, L. K. and D. R. Hendrixson (2008). Characterization of two putative cytochrome *c* peroxidases of *Campylobacter jejuni* involved in promoting commensal colonization of poultry. *Infect Immun* **76**(3): 1105-1114.

Biswas, D., U. Fernando, C. Reiman, P. Willson, A. Potter and B. Allan (2006). Effect of cytolethal distending toxin of *Campylobacter jejuni* on adhesion and internalization in cultured cells and in colonization of the chicken gut. *Avian Dis* **50**(4): 586-593.

Blachier, F., A. M. Davila, S. Mimoun, P. H. Benetti, C. Atanasiu, M. Andriamihaja, R. Benamouzig, F. Bouillaud and D. Tome (2010). Luminal sulfide and large intestine mucosa: Friend or foe? *Amino Acids* **39**(2): 335-347.

Black, R. E., M. M. Levine, M. L. Clements, T. P. Hughes and M. J. Blaser (1988). Experimental *Campylobacter jejuni* infection in humans. *J Infect Dis* **157**(3): 472-479.

Blattner, F. R., G. Plunkett, 3rd, C. A. Bloch, N. T. Perna, V. Burland, M. Riley, J. Collado-Vides, J. D. Glasner, C. K. Rode, G. F. Mayhew, J. Gregor, N. W. Davis, H. A. Kirkpatrick, M. A. Goeden, D. J. Rose, B. Mau and Y. Shao (1997). The complete genome sequence of *Escherichia coli* K-12. *Science* **277**(5331): 1453-1462.

Blaudeck, N., P. Kreutzenbeck, R. Freudl and G. A. Sprenger (2003). Genetic analysis of pathway specificity during posttranslational protein translocation across the *Escherichia coli* plasma membrane. *J Bacteriol* **185**(9): 2811-2819.

Blaudeck, N., P. Kreutzenbeck, M. Muller, G. A. Sprenger and R. Freudl (2005). Isolation and characterization of bifunctional *Escherichia coli* tata mutant proteins that allow efficient tat-dependent protein translocation in the absence of tatB. *J Biol Chem* **280**(5): 3426-3432.

Bogsch, E., S. Brink and C. Robinson (1997). Pathway specificity for a delta pH-dependent precursor thylakoid lumen protein is governed by a 'Sec-avoidance' motif in the transfer peptide and a 'Sec-incompatible' mature protein. *EMBO J* **16**(13): 3851-3859.

Bolhuis, A., J. E. Mathers, J. D. Thomas, C. M. Barrett and C. Robinson (2001). TatB and tatC form a functional and structural unit of the twin-arginine translocase from *Escherichia coli*. *J Biol Chem* **276**(23): 20213-20219.

Bradford, M. M. (1976). A rapid and sensitive method for the quantitation of microgram quantities of protein utilizing the principle of protein-dye binding. *Anal Biochem* **72**: 248-254.

Braun, M. and L. Thony-Meyer (2004). Biosynthesis of artificial microperoxidases by exploiting the secretion and cytochrome *c* maturation apparatuses of *Escherichia coli*. *Proc Natl Acad Sci U S A* **101**(35): 12830-12835.

Braun, V. (2001). Iron uptake mechanisms and their regulation in pathogenic bacteria. *Int J Med Microbiol* **291**(2): 67-79.

Brondijk, T. H., D. Fiegen, D. J. Richardson and J. A. Cole (2002). Roles of Napf, Napg and Naph, subunits of the *Escherichia coli* periplasmic nitrate reductase, in ubiquinol oxidation. *Mol Microbiol* **44**(1): 245-255.

Brondijk, T. H., A. Nilavongse, N. Filenko, D. J. Richardson and J. A. Cole (2004). NapGH components of the periplasmic nitrate reductase of *Escherichia coli* K-12: Location, topology and physiological roles in quinol oxidation and redox balancing. *Biochem J* **379**(Pt 1): 47-55.

Bruser, T. (2007). The twin-arginine translocation system and its capability for protein secretion in biotechnological protein production. *Appl Microbiol Biotechnol* **76**(1): 35-45.

Buckel, W. (2001). Unusual enzymes involved in five pathways of glutamate fermentation. *Appl Microbiol Biotechnol* **57**(3): 263-273.

Buelow, D. R., J. E. Christensen, J. M. Neal-McKinney and M. E. Konkel (2011). *Campylobacter jejuni* survival within human epithelial cells is enhanced by the secreted protein CiaI. *Mol Microbiol* **80**(5): 1296-1312.

Burns, B. P., S. L. Hazell and G. L. Mendz (1995). Acetyl-CoA carboxylase activity in *Helicobacter pylori* and the requirement of increased CO_2 for growth. *Microbiology* **141 (Pt 12)**: 3113-3118.

Butzler, J. P. and M. B. Skirrow (1979). Campylobacter enteritis. *Clin Gastroenterol* **8**(3): 737-765.

Byran, F.L. and M.P. Doyle (1995). Health Risks and Consequences of *Salmonella* and *Campylobacter jejuni* in Raw Poultry. *J Food Prot* **58** (3):326-344

Cabiscol, E., J. Tamarit and J. Ros (2000). Oxidative stress in bacteria and protein damage by reactive oxygen species. *Int Microbiol* **3**(1): 3-8.

Cameron, A. and E. C. Gaynor (2014). Hygromycin B and apramycin antibiotic resistance cassettes for use in *Campylobacter jejuni*. *PLoS One* **9**(4): e95084.

Cannon, K. S., E. Or, W. M. Clemons, Jr., Y. Shibata and T. A. Rapoport (2005). Disulfide bridge formation between SecY and a translocating polypeptide localizes the translocation pore to the center of SecY. *J Cell Biol* **169**(2): 219-225.

Carlone, G. M. and F. A. Anet (1983). Detection of menaquinone-*6* and a novel methyl-substituted menaquinone-*6* in *Campylobacter jejuni* and *Campylobacter fetus* subsp. *fetus*. *J Gen Microbiol* **129**(11): 3385-3393.

Carlone, G. M. and J. Lascelles (1982). Aerobic and anaerobic respiratory systems in *Campylobacter fetus* subsp. *jejuni* grown in atmospheres containing hydrogen. *J Bacteriol* **152**(1): 306-314.

Chanal, A., C. Santini and L. Wu (1998). Potential receptor function of three homologous components, TatA, TatB and TatE, of the twin-arginine signal sequence-dependent metalloenzyme translocation pathway in *Escherichia coli*. *Mol Microbiol* **30**(3): 674-676.

Chang, C. Y., L. Hobley, R. Till, M. Capeness, M. Kanna, W. Burtt, P. Jagtap, S. Aizawa and R. E. Sockett (2011). The *Bdellovibrio bacteriovorus* twin-arginine transport system has roles in predatory and prey-independent growth. *Microbiology* **157**(Pt 11): 3079-3093.

Chang, H. Y., Y. Ahn, L. A. Pace, M. T. Lin, Y. H. Lin and R. B. Gennis (2010). The diheme cytochrome c_4 from *Vibrio cholerae* is a natural electron donor to the respiratory cbb_3 oxygen reductase. *Biochemistry* **49**(35): 7494-7503.

Cheesman, M. R., P. J. Little and B. C. Berks (2001). Novel heme ligation in a *c*-type cytochrome involved in thiosulfate oxidation: EPR and MCD of SoxAX from *Rhodovulum sulfidophilum*. *Biochemistry* **40**(35): 10562-10569.

Chen, M., L. P. Andersen, L. Zhai and A. Kharazmi (1999). Characterization of the respiratory chain of *Helicobacter pylori*. *FEMS Immunol Med Microbiol* **24**(2): 169-174.

Christensen, J. E., S. A. Pacheco and M. E. Konkel (2009). Identification of a *Campylobacter jejuni*-secreted protein required for maximal invasion of host cells. *Mol Microbiol* **73**(4): 650-662.

Christensen, O., E. M. Harvat, L. Thony-Meyer, S. J. Ferguson and J. M. Stevens (2007). Loss of ATP hydrolysis activity by CcmAB results in loss of *c*-type cytochrome synthesis and incomplete processing of CcmE. *FEBS J* **274**(9): 2322-2332.

Cline, K. and H. Mori (2001). Thylakoid ΔpH -dependent precursor proteins bind to a cpTatC–Hcf106 complex before Tha4 -dependent transport. *J Cell Biol* **154**(4): 719-729.

Cline, K. and M. McCaffery (2007). Evidence for a dynamic and transient pathway through the TAT protein transport machinery. *EMBO J* **26**(13): 3039-3049.

Colbert, C. L., Q. Wu, P. J. Erbel, K. H. Gardner and J. Deisenhofer (2006). Mechanism of substrate specificity in *Bacillus subtilis* ResA, a thioredoxin-like protein involved in cytochrome *c* maturation. *Proc Natl Acad Sci U S A* **103**(12): 4410-4415.

Collins, M. D., M. Costas and R. J. Owen (1984). Isoprenoid quinone composition of representatives of the genus *Campylobacter*. *Arch Microbiol* **137**(2): 168-170.

Costa, C., A. Macedo, I. Moura, J. J. Moura, J. Le Gall, Y. Berlier, M. Y. Liu and W. J. Payne (1990). Regulation of the hexaheme nitrite/nitric oxide reductase of *Desulfovibrio desulfuricans*, *Wolinella succinogenes* and *Escherichia coli*. A mass spectrometric study. *FEBS Lett* **276**(1-2): 67-70.

Cristobal, S., J. W. de Gier, H. Nielsen and G. von Heijne (1999). Competition between Sec- and Tat-dependent protein translocation in *Escherichia coli*. *EMBO J* **18**(11): 2982-2990.

Crow, A., R. M. Acheson, N. E. Le Brun and A. Oubrie (2004). Structural basis of redox-coupled protein substrate selection by the cytochrome *c* biosynthesis protein ResA. *J Biol Chem* **279**(22): 23654-23660.

Crow, A., A. Lewin, O. Hecht, M. Carlsson Moller, G. R. Moore, L. Hederstedt and N. E. Le Brun (2009). Crystal structure and biophysical properties of *Bacillus subtilis* BdbD. An oxidizing thiol:Disulfide oxidoreductase containing a novel metal site. *J Biol Chem* **284**(35): 23719-23733.

Cunningham, K. and W. Wickner (1989). Specific recognition of the leader region of precursor proteins is required for the activation of translocation ATPase of *Escherichia coli*. *Proc Natl Acad Sci U S A* **86**(22): 8630-8634.

Cunningham, L. and H. D. Williams (1995). Isolation and characterization of mutants defective in the cyanide-insensitive respiratory pathway of *Pseudomonas aeruginosa*. *J Bacteriol* **177**(2): 432-438.

Daltrop, O., J. W. Allen, A. C. Willis and S. J. Ferguson (2002). *In vitro* formation of a *c*-type cytochrome. *Proc Natl Acad Sci U S A* **99**(12): 7872-7876.

Dambe, T., A. Quentmeier, D. Rother, C. Friedrich and A. J. Scheidig (2005). Structure of the cytochrome complex SoxXA of *Paracoccus pantotrophus*, a heme enzyme initiating chemotrophic sulfur oxidation. *J Struct Biol* **152**(3): 229-234.

Day, W. A., Jr., J. L. Sajecki, T. M. Pitts and L. A. Joens (2000). Role of catalase in *Campylobacter jejuni* intracellular survival. *Infect Immun* **68**(11): 6337-6345.

De Buck, E., E. Lammertyn and J. Anne (2008). The importance of the twin-arginine translocation pathway for bacterial virulence. *Trends Microbiol* **16**(9): 442-453.

De Buck, E., L. Vranckx, E. Meyen, L. Maes, L. Vandersmissen, J. Anne and E. Lammertyn (2007). The twin-arginine translocation pathway is necessary for correct membrane insertion of the Rieske Fe/S protein in *Legionella pneumophila*. *FEBS Lett* **581**(2): 259-264.

de Vitry, C. (2011). Cytochrome *c* maturation system on the negative side of bioenergetic membranes: CCB or System IV. *FEBS J* **278**(22): 4189-4197.

Debruyne, L., E. Samyn, E. De Brandt, O. Vandenberg, M. Heyndrickx and P. Vandamme (2008). Comparative performance of different PCR assays for the identification of *Campylobacter jejuni* and *Campylobacter coli*. *Res Microbiol* **159**(2): 88-93.

Deeudom, M., M. Koomey and J. W. Moir (2008). Roles of *c*-type cytochromes in respiration in *Neisseria meningitidis*. *Microbiology* **154**(Pt 9): 2857-2864.

Dekeyser, P., M. Gossuin-Detrain, J. P. Butzler and J. Sternon (1972). Acute enteritis due to related Vibrio: First positive stool cultures. *J Infect Dis* **125**(4): 390-392.

Denkmann, K., F. Grein, R. Zigann, A. Siemen, J. Bergmann, S. van Helmont, A. Nicolai, I. A. Pereira and C. Dahl (2012). Thiosulfate dehydrogenase: A widespread unusual acidophilic *c*-type cytochrome. *Environ Microbiol* **14**(10): 2673-2688.

Deshmukh, M., G. Brasseur and F. Daldal (2000). Novel *Rhodobacter capsulatus* genes required for the biogenesis of various *c*-type cytochromes. *Mol Microbiol* **35**(1): 123-138.

Di Matteo, A., S. Gianni, M. E. Schinina, A. Giorgi, F. Altieri, N. Calosci, M. Brunori and C. Travaglini-Allocatelli (2007). A strategic protein in cytochrome *c* maturation: Three-dimensional structure of CcmH and binding to apocytochrome *c*. *J Biol Chem* **282**(37): 27012-27019.

Dilks, K., R. W. Rose, E. Hartmann and M. Pohlschroder (2003). Prokaryotic utilization of the twin-arginine translocation pathway: A genomic survey. *J Bacteriol* **185**(4): 1478-1483.

D'Mello, R., S. Hill and R. K. Poole (1996). The cytochrome *bd* quinol oxidase in *Escherichia coli* has an extremely high oxygen affinity and two oxygen-binding haems: Implications for regulation of activity *in vivo* by oxygen inhibition. *Microbiology* **142 (Pt 4)**: 755-763.

Dorrell, N., J. A. Mangan, K. G. Laing, J. Hinds, D. Linton, H. Al-Ghusein, B. G. Barrell, J. Parkhill, N. G. Stoker, A. V. Karlyshev, P. D. Butcher and B. W. Wren (2001). Whole genome comparison of *Campylobacter jejuni* human isolates using a low-cost microarray reveals extensive genetic diversity. *Genome Res* **11**(10): 1706-1715.

Driessen, A. J. (2001). SecB, a molecular chaperone with two faces. *Trends Microbiol* **9**(5): 193-196.

Dryden, M. S., R. J. Gabb and S. K. Wright (1996). Empirical treatment of severe acute community-acquired gastroenteritis with ciprofloxacin. *Clin Infect Dis* **22**(6): 1019-1025.

Dufour, V., J. Li, A. Flint, E. Rosenfeld, K. Rivoal, S. Georgeault, B. Alazzam, G. Ermel, A. Stintzi, M. Bonnaure-Mallet and C. Baysse (2013). Inactivation of the LysR regulator Cj1000 of *Campylobacter jejuni* affects host colonization and respiration. *Microbiology* **159**(Pt 6): 1165-1178.

Dugar, G., A. Herbig, K. U. Forstner, N. Heidrich, R. Reinhardt, K. Nieselt and C. M. Sharma (2013). High-resolution transcriptome maps reveal strain-specific regulatory features of multiple *Campylobacter jejuni* isolates. *PLoS Genet* **9**(5): e1003495.

Economou, A. and W. Wickner (1994). SecA promotes preprotein translocation by undergoing ATP-driven cycles of membrane insertion and deinsertion. *Cell* **78**(5): 835-843.

Einsle, O., A. Messerschmidt, P. Stach, G. P. Bourenkov, H. D. Bartunik, R. Huber and P. M. Kroneck (1999). Structure of cytochrome *c* nitrite reductase. *Nature* **400**(6743): 476-480.

Einsle, O., P. Stach, A. Messerschmidt, J. Simon, A. Kroger, R. Huber and P. M. Kroneck (2000). Cytochrome *c* nitrite reductase from *Wolinella succinogenes*. STRUCTURE AT 1.6 Å RESOLUTION, INHIBITOR BINDING, AND HEME-PACKING MOTIFS. *J Biol Chem* **275**(50): 39608-39616.

Elharrif, Z. and F. Mégraud. (1986) Characterization of thermophilic *Campylobacter*. II. enzymatic profiles *Curr. Microbiol*. **13**(6): 317-322

Elvers, K. T., S. M. Turner, L. M. Wainwright, G. Marsden, J. Hinds, J. A. Cole, R. K. Poole, C. W. Penn and S. F. Park (2005). NssR, a member of the Crp-Fnr superfamily from *Campylobacter jejuni*, regulates a nitrosative stress-responsive regulon that includes both a single-domain and a truncated haemoglobin. *Mol Microbiol* **57**(3): 735-750.

Elvers, K. T., G. Wu, N. J. Gilberthorpe, R. K. Poole and S. F. Park (2004). Role of an inducible single-domain hemoglobin in mediating resistance to nitric oxide and nitrosative stress in *Campylobacter jejuni* and *Campylobacter coli*. *J Bacteriol* **186**(16): 5332-5341.

Emerson, D., J. A. Rentz, T. G. Lilburn, R. E. Davis, H. Aldrich, C. Chan and C. L. Moyer (2007). A novel lineage of proteobacteria involved in formation of marine fe-oxidizing microbial mat communities. *PLoS One* **2**(7): e667.

Evans, D. J. and D. G. Evans. (1997) Identification of a formate dehydrogenase associated cytochrome c_{553} in *Helicobacter pylori*. *Gut* **41**(S): A6

Erlendsson, L. S., R. M. Acheson, L. Hederstedt and N. E. Le Brun (2003). *Bacillus subtilis* ResA is a thiol-disulfide oxidoreductase involved in cytochrome *c* synthesis. *J Biol Chem* **278**(20): 17852-17858.

Fabianek, R. A., T. Hofer and L. Thony-Meyer (1999). Characterization of the *Escherichia coli* CcmH protein reveals new insights into the redox pathway required for cytochrome *c* maturation. *Arch Microbiol* **171**(2): 92-100.

Feissner, R. E., C. L. Richard-Fogal, E. R. Frawley and R. G. Kranz (2006). ABC transporter-mediated release of a haem chaperone allows cytochrome *c* biogenesis. *Mol Microbiol* **61**(1): 219-231.

Fekkes, P. and A. J. Driessen (1999). Protein targeting to the bacterial cytoplasmic membrane. *Microbiol Mol Biol Rev* **63**(1): 161-173.

Flanagan, R. C., J. M. Neal-McKinney, A. S. Dhillon, W. G. Miller and M. E. Konkel (2009). Examination of *Campylobacter jejuni* putative adhesins leads to the identification of a new protein, designated FlpA, required for chicken colonization. *Infect Immun* **77**(6): 2399-2407.

Fouts, D. E., E. F. Mongodin, R. E. Mandrell, W. G. Miller, D. A. Rasko, J. Ravel, L. M. Brinkac, R. T. DeBoy, C. T. Parker, S. C. Daugherty, R. J. Dodson, A. S. Durkin, R. Madupu, S. A. Sullivan, J. U. Shetty, M. A. Ayodeji, A. Shvartsbeyn, M. C. Schatz, J. H. Badger, C. M. Fraser and K. E. Nelson (2005). Major structural differences and novel potential virulence mechanisms from the genomes of multiple *Campylobacter* species. *PLoS Biol* **3**(1): e15.

Frawley, E. R. and R. G. Kranz (2009). CcsBA is a cytochrome *c* synthetase that also functions in heme transport. *Proc Natl Acad Sci U S A* **106**(25): 10201-10206.

Friedrich, C. G., D. Rother, F. Bardischewsky, A. Quentmeier and J. Fischer (2001). Oxidation of reduced inorganic sulfur compounds by bacteria: Emergence of a common mechanism? *Appl Environ Microbiol* **67**(7): 2873-2882.

Friedrich, T. (1998). The NADH:Ubiquinone oxidoreductase (complex I) from *Escherichia coli*. *Biochim Biophys Acta* **1364**(2): 134-146.

Friedrich, T., A. Abelmann, B. Brors, V. Guenebaut, L. Kintscher, K. Leonard, T. Rasmussen, D. Scheide, A. Schlitt, U. Schulte and H. Weiss (1998). Redox components and structure of the respiratory NADH:Ubiquinone oxidoreductase (complex I). *Biochim Biophys Acta* **1365**(1-2): 215-219.

Friis, C., T. M. Wassenaar, M. A. Javed, L. Snipen, K. Lagesen, P. F. Hallin, D. G. Newell, M. Toszeghy, A. Ridley, G. Manning and D. W. Ussery (2010). Genomic characterization of *Campylobacter jejuni* strain M1. *PLoS One* **5**(8): e12253.

Fultz, M.L., and R. A. Durst. (1982) Mediator compounds for the electrochemical study of biological redox systems – a compilation. *Anal Chim Acta* **140:** 1–18.

Gerard, F. and K. Cline (2006). Efficient twin arginine translocation (Tat) pathway transport of a precursor protein covalently anchored to its initial cpTatC binding site. *J Biol Chem* **281**(10): 6130-6135.

Gerard, F. and K. Cline (2007). The thylakoid proton gradient promotes an advanced stage of signal peptide binding deep within the Tat pathway receptor complex. *J Biol Chem* **282**(8): 5263-5272.

Gibson, D. G., L. Young, R. Y. Chuang, J. C. Venter, C. A. Hutchison, 3rd and H. O. Smith (2009). Enzymatic assembly of DNA molecules up to several hundred kilobases. *Nat Methods* **6**(5): 343-345.

Goddard, A. D., J. M. Stevens, A. Rondelet, E. Nomerotskaia, J. W. Allen and S. J. Ferguson (2010). Comparing the substrate specificities of cytochrome *c* biogenesis systems I and II: Bioenergetics. *FEBS J* **277**(3): 726-737.

Gohlke, U., L. Pullan, C. A. McDevitt, I. Porcelli, E. de Leeuw, T. Palmer, H. R. Saibil and B. C. Berks (2005). The TatA component of the twin-arginine protein transport system forms channel complexes of variable diameter. *Proc Natl Acad Sci U S A* **102**(30): 10482-10486.

Golden, N. J. and D. W. Acheson (2002). Identification of motility and autoagglutination *Campylobacter jejuni* mutants by random transposon mutagenesis. *Infect Immun* **70**(4): 1761-1771.

Gon, S., J. C. Patte, V. Mejean and C. Iobbi-Nivol (2000). The *torYZ* (*yecK bisZ*) operon encodes a third respiratory trimethylamine *N*-oxide reductase in *Escherichia coli*. *J Bacteriol* **182**(20): 5779-5786.

Gon, S., M. T. Giudici-Orticoni, V. Mejean and C. Iobbi-Nivol (2001). Electron transfer and binding of the *c*-type cytochrome TorC to the trimethylamine *N*-oxide reductase in *Escherichia coli*. *J Biol Chem* **276**(15): 11545-11551.

Goodhew, C. F., A. B. elKurdi and G. W. Pettigrew (1988). The microaerophilic respiration of *Campylobacter mucosalis*. *Biochim Biophys Acta* **933**(1): 114-123.

Goosens, V. J., C. G. Monteferrante and J. M. van Dijl (2014). The Tat system of Gram-positive bacteria. *Biochim Biophys Acta* **1843**(8): 1698-1706.

Gosset, G. (2005). Improvement of *Escherichia coli* production strains by modification of the phosphoenolpyruvate:Sugar phosphotransferase system. *Microb Cell Fact* **4**(1): 14.

Grant, C. C., M. E. Konkel, W. Cieplak, Jr. and L. S. Tompkins (1993). Role of flagella in adherence, internalization, and translocation of *Campylobacter jejuni* in nonpolarized and polarized epithelial cell cultures. *Infect Immun* **61**(5): 1764-1771.

Graubner, W., A. Schierhorn and T. Bruser (2007). Dnak plays a pivotal role in tat targeting of cueo and functions beside slyd as a general tat signal binding chaperone. *J Biol Chem* **282**(10): 7116-7124.

Greene, N. P., I. Porcelli, G. Buchanan, M. G. Hicks, S. M. Schermann, T. Palmer and B. C. Berks (2007). Cysteine scanning mutagenesis and disulfide mapping studies of the tata component of the bacterial twin arginine translocase. *J Biol Chem* **282**(33): 23937-23945.

Grein, F., S. S. Venceslau, L. Schneider, P. Hildebrandt, S. Todorovic, I. A. Pereira and C. Dahl (2010). Dsrj, an essential part of the dsrmkjop transmembrane complex in the purple sulfur bacterium allochromatium vinosum, is an unusual triheme cytochrome c. *Biochemistry* **49**(38): 8290-8299.

Gripp, E., D. Hlahla, X. Didelot, F. Kops, S. Maurischat, K. Tedin, T. Alter, L. Ellerbroek, K. Schreiber, D. Schomburg, T. Janssen, P. Bartholomaus, D. Hofreuter, S. Woltemate, M. Uhr, B. Brenneke, P. Gruning, G. Gerlach, L. Wieler, S. Suerbaum and C. Josenhans (2011). Closely related *Campylobacter jejuni* strains from different sources reveal a generalist rather than a specialist lifestyle. *BMC Genomics* **12**: 584.

Guccione, E., R. Leon-Kempis Mdel, B. M. Pearson, E. Hitchin, F. Mulholland, P. M. van Diemen, M. P. Stevens and D. J. Kelly (2008). Amino acid-dependent growth of *Campylobacter jejuni*: Key roles for aspartase (aspa) under microaerobic and oxygen-limited conditions and identification of aspb (cj0762), essential for growth on glutamate. *Mol Microbiol* **69**(1): 77-93.

Guccione, E., A. Hitchcock, S. J. Hall, F. Mulholland, N. Shearer, A. H. van Vliet and D. J. Kelly (2010). Reduction of fumarate, mesaconate and crotonate by mfr, a novel oxygen-regulated periplasmic reductase in *Campylobacter jejuni*. *Environ Microbiol* **12**(3): 576-591.

Guerry, P., R. A. Alm, M. E. Power, S. M. Logan and T. J. Trust (1991). Role of two flagellin genes in campylobacter motility. *J Bacteriol* **173**(15): 4757-4764.

Guerry, P., C. P. Ewing, M. Schirm, M. Lorenzo, J. Kelly, D. Pattarini, G. Majam, P. Thibault and S. Logan (2006). Changes in flagellin glycosylation affect campylobacter autoagglutination and virulence. *Mol Microbiol* **60**(2): 299-311.

Gundogdu, O., S. D. Bentley, M. T. Holden, J. Parkhill, N. Dorrell and B. W. Wren (2007). Re-annotation and re-analysis of the *Campylobacter jejuni* nctc11168 genome sequence. *BMC Genomics* **8**: 162.

Gupta, R. S. (2006). Molecular signatures (unique proteins and conserved indels) that are specific for the epsilon proteobacteria (campylobacterales). *BMC Genomics* **7**: 167.

Haddock, B. A. and C. W. Jones (1977). Bacterial respiration. *Bacteriol Rev* **41**(1): 47-99.

Haider, S., B. A. Hall and M. S. Sansom (2006). Simulations of a protein translocation pore: SecY. *Biochemistry* **45**(43): 13018-13024.

Hall, S. J., A. Hitchcock, C. S. Butler and D. J. Kelly (2008). A multicopper oxidase (Cj1516) and a CopA homologue (Cj1161) are major components of the copper homeostasis system of *Campylobacter jejuni*. *J Bacteriol* **190**(24): 8075-8085.

Hanahan, D. (1983). Studies on transformation of *Escherichia coli* with plasmids. *J Mol Biol* **166**(4): 557-580.

Hartl, F. U., S. Lecker, E. Schiebel, J. P. Hendrick and W. Wickner (1990). The binding cascade of SecB to SecA to SecY/E mediates preprotein targeting to the *E. coli* plasma membrane. *Cell* **63**(2): 269-279.

Hartshorne, R. S., M. Kern, B. Meyer, T. A. Clarke, M. Karas, D. J. Richardson and J. Simon (2007). A dedicated haem lyase is required for the maturation of a novel bacterial cytochrome *c* with unconventional covalent haem binding. *Mol Microbiol* **64**(4): 1049-1060.

Hatzixanthis, K., D. J. Richardson and F. Sargent (2005). Chaperones involved in assembly and export of *N*-oxide reductases. *Biochem Soc Trans* **33**(Pt 1): 124-126.

He, G., R. A. Shankar, M. Chzhan, A. Samouilov, P. Kuppusamy and J. L. Zweier (1999). Noninvasive measurement of anatomic structure and intraluminal oxygenation in the gastrointestinal tract of living mice with spatial and spectral EPR imaging. *Proc Natl Acad Sci U S A* **96**(8): 4586-4591.

Heikkila, M. P., U. Honisch, P. Wunsch and W. G. Zumft (2001). Role of the Tat ransport system in nitrous oxide reductase translocation and cytochrome cd_1 biosynthesis in *Pseudomonas stutzeri*. *J Bacteriol* **183**(5): 1663-1671.

Hendrixson, D. R., B. J. Akerley and V. J. DiRita (2001). Transposon mutagenesis of *Campylobacter jejuni* identifies a bipartite energy taxis system required for motility. *Mol Microbiol* **40**(1): 214-224.

Hendrixson, D. R. and V. J. DiRita (2004). Identification of *Campylobacter jejuni* genes involved in commensal colonization of the chick gastrointestinal tract. *Mol Microbiol* **52**(2): 471-484.

Hensel, M., A. P. Hinsley, T. Nikolaus, G. Sawers and B. C. Berks (1999). The genetic basis of tetrathionate respiration in *Salmonella typhimurium*. *Mol Microbiol* **32**(2): 275-287.

Hensen, D., D. Sperling, H. G. Truper, D. C. Brune and C. Dahl (2006). Thiosulphate oxidation in the phototrophic sulphur bacterium *Allochromatium vinosum*. *Mol Microbiol* **62**(3): 794-810.

Hicks, M. G., E. de Leeuw, I. Porcelli, G. Buchanan, B. C. Berks and T. Palmer (2003). The *Escherichia coli* twin-arginine translocase: Conserved residues of TatA and TatB family components involved in protein transport. *FEBS Lett* **539**(1-3): 61-67.

Hinojosa-Leon, M., M. Dubourdieu, J. A. Sanchez-Crispin and M. Chippaux (1986). Tetrathionate reductase of *Salmonella thyphimurium*: A molybdenum containing enzyme. *Biochem Biophys Res Commun* **136**(2): 577-581.

Hinsley, A. P., N. R. Stanley, T. Palmer and B. C. Berks (2001). A naturally occurring bacterial Tat signal peptide lacking one of the 'invariant' arginine residues of the consensus targeting motif. *FEBS Lett* **497**(1): 45-49.

Hinton, A., Jr. (2006). Growth of *Campylobacter* in media supplemented with organic acids. *J Food Prot* **69**(1): 34-38.

Hitchcock, A., S. J. Hall, J. D. Myers, F. Mulholland, M. A. Jones and D. J. Kelly (2010). Roles of the twin-arginine translocase and associated chaperones in the biogenesis of the electron transport chains of the human pathogen *Campylobacter jejuni*. *Microbiology* **156**(Pt 10): 2994-3010.

Hodson, C. T., A. Lewin, L. Hederstedt and N. E. Le Brun (2008). The active-site cysteinyls and hydrophobic cavity residues of ResA are important for cytochrome *c* maturation in *Bacillus subtilis*. *J Bacteriol* **190**(13): 4697-4705.

Hoffman, P. S. and T. G. Goodman (1982). Respiratory physiology and energy conservation efficiency of *Campylobacter jejuni*. *J Bacteriol* **150**(1): 319-326.

Hofreuter, D., J. Tsai, R. O. Watson, V. Novik, B. Altman, M. Benitez, C. Clark, C. Perbost, T. Jarvie, L. Du and J. E. Galan (2006). Unique features of a highly pathogenic *Campylobacter jejuni* strain. *Infect Immun* **74**(8): 4694-4707.

Hofreuter, D., V. Novik and J. E. Galan (2008). Metabolic diversity in *Campylobacter jejuni* enhances specific tissue colonization. *Cell Host Microbe* **4**(5): 425-433.

Holzapfel, E., M. Moser, E. Schiltz, T. Ueda, J. M. Betton and M. Muller (2009). Twin-arginine-dependent translocation of SufI in the absence of cytosolic helper proteins. *Biochemistry* **48**(23): 5096-5105.

Howe, G. and S. Merchant (1992). The biosynthesis of membrane and soluble plastidic *c*-type cytochromes of *Chlamydomonas reinhardtii* is dependent on multiple common gene products. *EMBO J* **11**(8): 2789-2801.

Howlett, R. M., B. M. Hughes, A. Hitchcock and D. J. Kelly (2012). Hydrogenase activity in the foodborne pathogen *Campylobacter jejuni* depends upon a novel ABC-type nickel transporter (Nikzyxwv) and is slyD-independent. *Microbiology* **158**(Pt 6): 1645-1655.

Hugdahl, M. B., J. T. Beery and M. P. Doyle (1988). Chemotactic behavior of *Campylobacter jejuni*. *Infect Immun* **56**(6): 1560-1566.

Hughes, N. J., P. A. Chalk, C. L. Clayton and D. J. Kelly (1995). Identification of carboxylation enzymes and characterization of a novel four-subunit pyruvate:flavodoxin oxidoreductase from *Helicobacter pylori*. *J Bacteriol* **177**(14): 3953-3959.

Hughes, N. J., C. L. Clayton, P. A. Chalk and D. J. Kelly (1998). *Helicobacter pylori* porCDAB and oorDABC genes encode distinct pyruvate:flavodoxin and 2-oxoglutarate:acceptor oxidoreductases which mediate electron transport to NADP. *J Bacteriol* **180**(5): 1119-1128.

Ingledew, W. J. and R. K. Poole (1984). The respiratory chains of *Escherichia coli*. *Microbiol Rev* **48**(3): 222-271.

Iwata, S., C. Ostermeier, B. Ludwig and H. Michel (1995). Structure at 2.8 Å resolution of cytochrome *c* oxidase from *Paracoccus denitrificans*. *Nature* **376**(6542): 660-669.

Ize, B., I. Porcelli, S. Lucchini, J. C. Hinton, B. C. Berks and T. Palmer (2004). Novel phenotypes of *Escherichia coli* Tat mutants revealed by global gene expression and phenotypic analysis. *J Biol Chem* **279**(46): 47543-47554.

Jack, R. L., F. Sargent, B. C. Berks, G. Sawers and T. Palmer (2001). Constitutive expression of *Escherichia coli* Tat genes indicates an important role for the twin-arginine translocase during aerobic and anaerobic growth. *J Bacteriol* **183**(5): 1801-1804.

Jack, R. L., G. Buchanan, A. Dubini, K. Hatzixanthis, T. Palmer and F. Sargent (2004). Coordinating assembly and export of complex bacterial proteins. *EMBO J* **23**(20): 3962-3972.

Jackson, R. J., K. T. Elvers, L. J. Lee, M. D. Gidley, L. M. Wainwright, J. Lightfoot, S. F. Park and R. K. Poole (2007). Oxygen reactivity of both respiratory oxidases in *Campylobacter jejuni*: The *cydAB* genes encode a cyanide-resistant, low-affinity oxidase that is not of the cytochrome *bd* type. *J Bacteriol* **189**(5): 1604-1615.

Jacobs, B. C., A. van Belkum, & H. P. Endtz. (2008). Guillain-Barre Syndrome and *Campylobacter* Infection. In: *Campylobacter*. Third edition. Nachamkin, I., Szymanski, C.M.and Blaser, M.J. Eds. ASM Press, Washington D.C.

Jacobs-Reitsma, W., U. Lyths, and J. Wagenaar. (2008) *Campylobacter* in the food supply. In: *Campylobacter*. Third edition. Nachamkin, I., Szymanski, C.M.and Blaser, M.J. Eds. ASM Press, Washington D.C.

Jiang, X. and M. P. Doyle (2000). Growth supplements for *Helicobacter pylori*. *J Clin Microbiol* **38**(5): 1984-1987.

Jin, S., A. Joe, J. Lynett, E. K. Hani, P. Sherman and V. L. Chan (2001). JlpA, a novel surface-exposed lipoprotein specific to *Campylobacter jejuni*, mediates adherence to host epithelial cells. *Mol Microbiol* **39**(5): 1225-1236.

Joly, J. C. and W. Wickner (1993). The SecA and SecY subunits of translocase are the nearest neighbors of a translocating preprotein, shielding it from phospholipids. *EMBO J* **12**(1): 255-263.

Jong, W. S., C. M. ten Hagen-Jongman, P. Genevaux, J. Brunner, B. Oudega and J. Luirink (2004). Trigger factor interacts with the signal peptide of nascent Tat substrates but does not play a critical role in Tat-mediated export. *Eur J Biochem* **271**(23-24): 4779-4787.

Jongbloed, J. D., U. Martin, H. Antelmann, M. Hecker, H. Tjalsma, G. Venema, S. Bron, J. M. van Dijl and J. Muller (2000). TatC is a specificity determinant for protein secretion via the twin-arginine translocation pathway. *J Biol Chem* **275**(52): 41350-41357.

Jongbloed, J. D., U. Grieger, H. Antelmann, M. Hecker, R. Nijland, S. Bron and J. M. van Dijl (2004). Two minimal Tat translocases in *Bacillus*. *Mol Microbiol* **54**(5): 1319-1325.

Joshi, M. V., S. G. Mann, H. Antelmann, D. A. Widdick, J. K. Fyans, G. Chandra, M. I. Hutchings, I. Toth, M. Hecker, R. Loria and T. Palmer (2010). The twin arginine protein transport pathway exports multiple virulence proteins in the plant pathogen *Streptomyces scabies*. *Mol Microbiol* **77**(1): 252-271.

Jourlin, C., A. Bengrine, M. Chippaux and V. Mejean (1996). An unorthodox sensor protein (Tors) mediates the induction of the tor structural genes in response to trimethylamine *N*-oxide in *Escherichia coli*. *Mol Microbiol* **20**(6): 1297-1306.

Juhnke, H. D., H. Hiltscher, H. R. Nasiri, H. Schwalbe and C. R. Lancaster (2009). Production, characterization and determination of the real catalytic properties of the putative 'succinate dehydrogenase' from *Wolinella succinogenes*. *Mol Microbiol* **71**(5): 1088-1101.

Kakuda, T. and V. J. DiRita (2006). Cj1496c encodes a *Campylobacter jejuni* glycoprotein that influences invasion of human epithelial cells and colonization of the chick gastrointestinal tract. *Infect Immun* **74**(8): 4715-4723.

Kanungpean, D., T. Kakuda and S. Takai (2011). Participation of CheR and CheB in the chemosensory response of *Campylobacter jejuni*. *Microbiology* **157**(Pt 5): 1279-1289.

Karlyshev, A. V., O. L. Champion, C. Churcher, J. R. Brisson, H. C. Jarrell, M. Gilbert, D. Brochu, F. St Michael, J. Li, W. W. Wakarchuk, I. Goodhead, M. Sanders, K. Stevens, B. White, J. Parkhill, B. W. Wren and C. M. Szymanski (2005). Analysis of *Campylobacter jejuni* capsular loci reveals multiple mechanisms for the generation of structural diversity and the ability to form complex heptoses. *Mol Microbiol* **55**(1): 90-103.

Kather, B., K. Stingl, M. E. van der Rest, K. Altendorf and D. Molenaar (2000). Another unusual type of citric acid cycle enzyme in *Helicobacter pylori*: The malate:Quinone oxidoreductase. *J Bacteriol* **182**(11): 3204-3209.

Kelle, K., J. M. Pages and J. M. Bolla (1998). A putative adhesin gene cloned from *Campylobacter jejuni*. *Res Microbiol* **149**(10): 723-733.

Kelly, D. J. (2001). The physiology and metabolism of *Campylobacter jejuni* and *Helicobacter pylori*. *Symp Ser Soc Appl Microbiol*(30): 16S-24S.

Kelly, D. J. (2008). Complexity and versatility in the physiology and metabolism of *Campylobacter jejuni.* In: *Campylobacter*. Third edition. Nachamkin, I., Szymanski, C.M.and Blaser, M.J. Eds. ASM Press, Washington D.C.

Kelly, D.P., L. A. Chambers and P. A. Trudinger. (1969) Cyanolysis and spectrophotometric estimation of trithionate in mixture with thiosulfate and tetrathionate. *Anal Chem* **41:** 898–901.

Kelly, M. J., R. K. Poole, M. G. Yates and C. Kennedy (1990). Cloning and mutagenesis of genes encoding the cytochrome *bd* terminal oxidase complex in *Azotobacter vinelandii*: Mutants deficient in the cytochrome *d* complex are unable to fix nitrogen in air. *J Bacteriol* **172**(10): 6010-6019.

Kendall, J. J., A. M. Barrero-Tobon, D. R. Hendrixson and D. J. Kelly (2014). Hemerythrins in the microaerophilic bacterium *Campylobacter jejuni* help protect key iron-sulphur cluster enzymes from oxidative damage. *Environ Microbiol* **16**(4): 1105-1121.

Kern, M., A. M. Mager and J. Simon (2007). Role of individual nap gene cluster products in napc-independent nitrate respiration of *Wolinella succinogenes*. *Microbiology* **153**(Pt 11): 3739-3747.
Kern, M. and J. Simon (2008). Characterization of the NapGH quinol dehydrogenase complex involved in *Wolinella succinogenes* nitrate respiration. *Mol Microbiol* **69**(5): 1137-1152.

Kern, M. and J. Simon (2009a). Electron transport chains and bioenergetics of respiratory nitrogen metabolism in *Wolinella succinogenes* and other epsilonproteobacteria. *Biochim Biophys Acta* **1787**(6): 646-656.

Kern, M. and J. Simon (2009b). Periplasmic nitrate reduction in *Wolinella succinogenes*: Cytoplasmic NapF facilitates NapA maturation and requires the menaquinol dehydrogenase NapH for membrane attachment. *Microbiology* **155**(Pt 8): 2784-2794.

Kern, M., F. Eisel, J. Scheithauer, R. G. Kranz and J. Simon (2010). Substrate specificity of three cytochrome *c* haem lyase isoenzymes from *Wolinella succinogenes*: Unconventional haem *c* binding motifs are not sufficient for haem *c*attachment by nrfi and ccsa1. *Mol Microbiol* **75**(1): 122-137.
Kern, M. and J. Simon (2011). Production of recombinant multiheme cytochromes *c* in *Wolinella succinogenes*. *Methods Enzymol* **486**: 429-446.

Kern, M., C. Winkler and J. Simon (2011a). Respiratory nitrogen metabolism and nitrosative stress defence in ε-proteobacteria: The role of NssR-type transcription regulators. *Biochem Soc Trans* **39**(1): 299-302.

Kern, M., J. Volz and J. Simon (2011b). The oxidative and nitrosative stress defence network of *Wolinella succinogenes*: Cytochrome *c* nitrite reductase mediates the stress response to nitrite, nitric oxide, hydroxylamine and hydrogen peroxide. *Environ Microbiol* **13**(9): 2478-2494.

Ketley, J. M. (1997). Pathogenesis of enteric infection by *Campylobacter*. *Microbiology* **143 (Pt 1)**: 5-21.

Kikuchi, Y., M. Date, H. Itaya, K. Matsui and L. F. Wu (2006). Functional analysis of the twin-arginine translocation pathway in *Corynebacterium glutamicum* ATCC 13869. *Appl Environ Microbiol* **72**(11): 7183-7192.

Koch, S., M. J. Fritsch, G. Buchanan and T. Palmer (2012). *Escherichia coli* TatA and TatB proteins have N-out, C-in topology in intact cells. *J Biol Chem* **287**(18): 14420-14431.

Konkel, M. E., S. G. Garvis, S. L. Tipton, D. E. Anderson, Jr. and W. Cieplak, Jr. (1997). Identification and molecular cloning of a gene encoding a fibronectin-binding protein (CadF) from *Campylobacter jejuni*. *Mol Microbiol* **24**(5): 953-963.

Konkel, M. E., B. J. Kim, V. Rivera-Amill and S. G. Garvis (1999). Bacterial secreted proteins are required for the internaliztion of *Campylobacter jejuni* into cultured mammalian cells. *Mol Microbiol* **32**(4): 691-701.

Konkel, M. E., M. R. Monteville, V. Rivera-Amill and L. A. Joens (2001). The pathogenesis of *Campylobacter jejuni*-mediated enteritis. *Curr Issues Intest Microbiol* **2**(2): 55-71.

Konkel, M. E., J. D. Klena, V. Rivera-Amill, M. R. Monteville, D. Biswas, B. Raphael and J. Mickelson (2004). Secretion of virulence proteins from *Campylobacter jejuni* is dependent on a functional flagellar export apparatus. *J Bacteriol* **186**(11): 3296-3303.

Koonin, E. V. and A. E. Gorbalenya (1992). Autogenous translation regulation by *Escherichia coli* ATPase SecA may be mediated by an intrinsic rna helicase activity of this protein. *FEBS Lett* **298**(1): 6-8.

Korolik, V. & J. Ketley. (2008). Chemosensory Signal Transduction Pathway of *Campylobacter jejuni*. In: *Campylobacter*. Third edition. Nachamkin, I., Szymanski, C.M.and Blaser, M.J. Eds. ASM Press, Washington D.C.

Kouwen, T. R. and J. M. van Dijl (2009). Interchangeable modules in bacterial thiol-disulfide exchange pathways. *Trends Microbiol* **17**(1): 6-12.

Koyanagi, S., K. Nagata, T. Tamura, S. Tsukita and N. Sone (2000). Purification and characterization of cytochrome *c*-553 from *Helicobacter pylori*. *J Biochem* **128**(3): 371-375.

Kranz, R. G., C. Richard-Fogal, J. S. Taylor and E. R. Frawley (2009). Cytochrome *c* biogenesis: Mechanisms for covalent modifications and trafficking of heme and for heme-iron redox control. *Microbiol Mol Biol Rev* **73**(3): 510-528, Table of Contents.

Krieg, N. R. and P. S. Hoffman (1986). Microaerophily and oxygen toxicity. *Annu Rev Microbiol* **40**: 107-130.

Kudva, R., K. Denks, P. Kuhn, A. Vogt, M. Muller and H. G. Koch (2013). Protein translocation across the inner membrane of Gram-negative bacteria: The Sec and Tat dependent protein transport pathways. *Res Microbiol* **164**(6): 505-534.

Kumamoto, C. A. (1989). *Escherichia coli* SecB protein associates with exported protein precursors *in vivo*. *Proc Natl Acad Sci U S A* **86**(14): 5320-5324.

Lancaster, C. R. (2002). Succinate:quinone oxidoreductases: An overview. *Biochim Biophys Acta* **1553**(1-2): 1-6.

Lancaster, C. R., U. S. Sauer, R. Gross, A. H. Haas, J. Graf, H. Schwalbe, W. Mantele, J. Simon and M. G. Madej (2005). Experimental support for the "E pathway hypothesis" Of coupled transmembrane e^- and h^+ transfer in dihemic quinol:Fumarate reductase. *Proc Natl Acad Sci U S A* **102**(52): 18860-18865.

Lara-Tejero, M. and J. E. Galan (2001). CdtA, CdtB, and CdtC form a tripartite complex that is required for cytolethal distending toxin activity. *Infect Immun* **69**(7): 4358-4365.

Leach, S., P. Harvey and R. Wali (1997). Changes with growth rate in the membrane lipid composition of and amino acid utilization by continuous cultures of *Campylobacter jejuni*. *J Appl Microbiol* **82**(5): 631-640.

Lee, A., J. L. O'Rourke, P. J. Barrington and T. J. Trust (1986). Mucus colonization as a determinant of pathogenicity in intestinal infection by *Campylobacter jejuni*: A mouse cecal model. *Infect Immun* **51**(2): 536-546.

Lee, D., K. Pervushin, D. Bischof, M. Braun and L. Thony-Meyer (2005). Unusual heme-histidine bond in the active site of a chaperone. *J Am Chem Soc* **127**(11): 3716-3717.

Lee, H. C. and H. D. Bernstein (2001). The targeting pathway of *Escherichia coli* presecretory and integral membrane proteins is specified by the hydrophobicity of the targeting signal. *Proc Natl Acad Sci U S A* **98**(6): 3471-3476.

Lee, J. H., E. M. Harvat, J. M. Stevens, S. J. Ferguson and M. H. Saier, Jr. (2007). Evolutionary origins of members of a superfamily of integral membrane cytochrome *c* biogenesis proteins. *Biochim Biophys Acta* **1768**(9): 2164-2181.

Lemos, R. S., A. S. Fernandes, M. M. Pereira, C. M. Gomes and M. Teixeira (2002). Quinol:fumarate oxidoreductases and succinate:quinone oxidoreductases: Phylogenetic relationships, metal centres and membrane attachment. *Biochim Biophys Acta* **1553**(1-2): 158-170.

Leon-Kempis Mdel, R., E. Guccione, F. Mulholland, M. P. Williamson and D. J. Kelly (2006). The *Campylobacter jejuni* PEB1a adhesin is an aspartate/glutamate-binding protein of an ABC transporter essential for microaerobic growth on dicarboxylic amino acids. *Mol Microbiol* **60**(5): 1262-1275.

Letoffe, S., G. Heuck, P. Delepelaire, N. Lange and C. Wandersman (2009). Bacteria capture iron from heme by keeping tetrapyrrol skeleton intact. *Proc Natl Acad Sci U S A* **106**(28): 11719-11724.

Lewin, A., A. Crow, C. T. Hodson, L. Hederstedt and N. E. Le Brun (2008). Effects of substitutions in the CXXC active-site motif of the extracytoplasmic thioredoxin ResA. *Biochem J* **414**(1): 81-91.

Li, Y., A. Hopper, T. Overton, D. J. Squire, J. Cole and N. Tovell (2010). Organization of the electron transfer chain to oxygen in the obligate human pathogen *Neisseria gonorrhoeae*: Roles for cytochromes c_4 and c_5, but not cytochrome c_2, in oxygen reduction. *J Bacteriol* **192**(9): 2395-2406.

Lindenstrauss, U., C. F. Matos, W. Graubner, C. Robinson and T. Bruser (2010). Malfolded recombinant Tat substrates are Tat-independently degraded in *Escherichia coli*. *FEBS Lett* **584**(16): 3644-3648.

Lindmark, B., P. K. Rompikuntal, K. Vaitkevicius, T. Song, Y. Mizunoe, B. E. Uhlin, P. Guerry and S. N. Wai (2009). Outer membrane vesicle-mediated release of cytolethal distending toxin (CDT) from *Campylobacter jejuni*. *BMC Microbiol* **9**: 220.

Line, J. E., K. L. Hiett, J. Guard-Bouldin and B. S. Seal (2010). Differential carbon source utilization by *Campylobacter jejuni* 11168 in response to growth temperature variation. *J Microbiol Methods* **80**(2): 198-202.

Linton, D., N. Dorrell, P. G. Hitchen, S. Amber, A. V. Karlyshev, H. R. Morris, A. Dell, M. A. Valvano, M. Aebi and B. W. Wren (2005). Functional analysis of the *Campylobacter jejuni N*-linked protein glycosylation pathway. *Mol Microbiol* **55**(6): 1695-1703.

Liu, T. W., C. W. Ho, H. H. Huang, S. M. Chang, S. D. Popat, Y. T. Wang, M. S. Wu, Y. J. Chen and C. H. Lin (2009). Role for alpha-l-fucosidase in the control of *Helicobacter pylori*-infected gastric cancer cells. *Proc Natl Acad Sci U S A* **106**(34): 14581-14586.

Liu, Y. W., K. Denkmann, K. Kosciow, C. Dahl and D. J. Kelly (2013). Tetrathionate stimulated growth of *Campylobacter jejuni* identifies a new type of bi-functional tetrathionate reductase (TsdA) that is widely distributed in bacteria. *Mol Microbiol* **88**(1): 173-188.

Louwen, R., A. Heikema, A. van Belkum, A. Ott, M. Gilbert, W. Ang, H. P. Endtz, M. P. Bergman and E. E. Nieuwenhuis (2008). The sialylated lipooligosaccharide outer core in *Campylobacter jejuni* is an important determinant for epithelial cell invasion. *Infect Immun* **76**(10): 4431-4438.

Luirink, J., G. von Heijne, E. Houben and J. W. de Gier (2005). Biogenesis of inner membrane proteins in *Escherichia coli*. *Annu Rev Microbiol* **59**: 329-355.

Lüke, I., J. I. Handford, T. Palmer and F. Sargent (2009). Proteolytic processing of *Escherichia coli* twin-arginine signal peptides by LepB. *Arch Microbiol* **191**(12): 919-925.

Lupp, C., M. L. Robertson, M. E. Wickham, I. Sekirov, O. L. Champion, E. C. Gaynor and B. B. Finlay (2007). Host-mediated inflammation disrupts the intestinal microbiota and promotes the overgrowth of enterobacteriaceae. *Cell Host Microbe* **2**(2): 119-129.

Maillard, J., C. A. Spronk, G. Buchanan, V. Lyall, D. J. Richardson, T. Palmer, G. W. Vuister and F. Sargent (2007). Structural diversity in twin-arginine signal peptide-binding proteins. *Proc Natl Acad Sci U S A* **104**(40): 15641-15646.

Marcelli, S. W., H. T. Chang, T. Chapman, P. A. Chalk, R. J. Miles and R. K. Poole (1996). The respiratory chain of *Helicobacter pylori*: Identification of cytochromes and the effects of oxygen on cytochrome and menaquinone levels. *FEMS Microbiol Lett* **138**(1): 59-64.

Marchant, J., B. Wren and J. Ketley (2002). Exploiting genome sequence: Predictions for mechanisms of *Campylobacter* chemotaxis. *Trends Microbiol* **10**(4): 155-159.

Markwell, M. A., S. M. Haas, L. L. Bieber and N. E. Tolbert (1978). A modification of the lowry procedure to simplify protein determination in membrane and lipoprotein samples. *Anal Biochem* **87**(1): 206-210.

McClelland, M., K. E. Sanderson, J. Spieth, S. W. Clifton, P. Latreille, L. Courtney, S. Porwollik, J. Ali, M. Dante, F. Du, S. Hou, D. Layman, S. Leonard, C. Nguyen, K. Scott, A. Holmes, N. Grewal, E. Mulvaney, E. Ryan, H. Sun, L. Florea, W. Miller, T. Stoneking, M. Nhan, R. Waterston and R. K. Wilson (2001). Complete genome sequence of *Salmonella enterica* serovar Typhimurium LT2. *Nature* **413**(6858): 852-856.

McCrindle, S. L., U. Kappler and A. G. McEwan (2005). Microbial dimethylsulfoxide and trimethylamine-*N*-oxide respiration. *Adv Microb Physiol* **50**: 147-198.

McDevitt, C. A., G. Buchanan, F. Sargent, T. Palmer and B. C. Berks (2006). Subunit composition and *in vivo* substrate-binding characteristics of *Escherichia coli* Tat protein complexes expressed at native levels. *FEBS J* **273**(24): 5656-5668.

McNally, D. J., J. P. Hui, A. J. Aubry, K. K. Mui, P. Guerry, J. R. Brisson, S. M. Logan and E. C. Soo (2006). Functional characterization of the flagellar glycosylation locus in *Campylobacter jejuni* 81-176 using a focused metabolomics approach. *J Biol Chem* **281**(27): 18489-18498.

McNally, D. J., M. P. Lamoureux, A. V. Karlyshev, L. M. Fiori, J. Li, G. Thacker, R. A. Coleman, N. H. Khieu, B. W. Wren, J. R. Brisson, H. C. Jarrell and C. M. Szymanski (2007). Commonality and biosynthesis of the *O*-methyl phosphoramidate capsule modification in *Campylobacter jejuni*. *J Biol Chem* **282**(39): 28566-28576.

McNicholas, P. M., R. C. Chiang and R. P. Gunsalus (1998). Anaerobic regulation of the *Escherichia coli dmsABC* operon requires the molybdate-responsive regulator ModE. *Mol Microbiol* **27**(1): 197-208.

McSweegan, E. and R. I. Walker (1986). Identification and characterization of two *Campylobacter jejuni* adhesins for cellular and mucous substrates. *Infect Immun* **53**(1): 141-148.

Méjean, V., C. Iobbi-Nivol, M. Lepelletier, G. Giordano, M. Chippaux and M. C. Pascal (1994). TMAO anaerobic respiration in *Escherichia coli*: Involvement of the *tor* operon. *Mol Microbiol* **11**(6): 1169-1179.

Meyer, E. H., P. Giege, E. Gelhaye, N. Rayapuram, U. Ahuja, L. Thony-Meyer, J. M. Grienenberger and G. Bonnard (2005). AtCCMH, an essential component of the *c*-type cytochrome maturation pathway in *Arabidopsis* mitochondria, interacts with apocytochrome *c*. *Proc Natl Acad Sci U S A* **102**(44): 16113-16118.

Mickael, C. S., P. K. Lam, E. M. Berberov, B. Allan, A. A. Potter and W. Koster (2010). *Salmonella enterica* serovar Enteritidis *tatB* and *tatC* mutants are impaired in Caco-2 cell invasion *in vitro* and show reduced systemic spread in chickens. *Infect Immun* **78**(8): 3493-3505.

Miles, C. S., F. D. Manson, G. A. Reid and S. K. Chapman (1993). Substitution of a haem-iron axial ligand in flavocytochrome b_2. *Biochim Biophys Acta* **1202**(1): 82-86.

Miller, C. E., P. H. Williams and J. M. Ketley (2009). Pumping iron: Mechanisms for iron uptake by *Campylobacter*. *Microbiology* **155**(Pt 10): 3157-3165.

Miller, W. G., A. H. Bates, S. T. Horn, M. T. Brandl, M. R. Wachtel and R. E. Mandrell (2000). Detection on surfaces and in Caco-2 cells of *Campylobacter jejuni* cells transformed with new *gfp*, *yfp*, and *cfp* marker plasmids. *Appl Environ Microbiol* **66**(12): 5426-5436.

Mitra, K., J. Frank and A. Driessen (2006). Co- and post-translational translocation through the protein-conducting channel: Analogous mechanisms at work? *Nat Struct Mol Biol* **13**(11): 957-964.

Mohammed, K. A., R. J. Miles and M. A. Halablab (2004). The pattern and kinetics of substrate metabolism of *Campylobacter jejuni* and *Campylobacter coli*. *Lett Appl Microbiol* **39**(3): 261-266.

Möller, M. C. and L. Hederstedt (2008). Extracytoplasmic processes impaired by inactivation of *trxA* (thioredoxin gene) in *Bacillus subtilis*. *J Bacteriol* **190**(13): 4660-4665.

Monds, R. D., P. D. Newell, J. A. Schwartzman and G. A. O'Toole (2006). Conservation of the Pho regulon in *Pseudomonas fluorescens* Pf0-1. *Appl Environ Microbiol* **72**(3): 1910-1924.

Monteville, M. R., J. E. Yoon and M. E. Konkel (2003). Maximal adherence and invasion of INT 407 cells by *Campylobacter jejuni* requires the CadF outer-membrane protein and microfilament reorganization. *Microbiology* **149**(Pt 1): 153-165.

Mori, H. and K. Cline (2002). A twin arginine signal peptide and the pH gradient trigger reversible assembly of the thylakoid ΔpH/Tat translocase. *J Cell Biol* **157**(2): 205-210.

Mowat, C. G., E. Rothery, C. S. Miles, L. McIver, M. K. Doherty, K. Drewette, P. Taylor, M. D. Walkinshaw, S. K. Chapman and G. A. Reid (2004). Octaheme tetrathionate reductase is a respiratory enzyme with novel heme ligation. *Nat Struct Mol Biol* **11**(10): 1023-1024.

Muller, A., G. H. Thomas, R. Horler, J. A. Brannigan, E. Blagova, V. M. Levdikov, M. J. Fogg, K. S. Wilson and A. J. Wilkinson (2005). An ATP-binding cassette-type cysteine transporter in *Campylobacter jejuni* inferred from the structure of an extracytoplasmic solute receptor protein. *Mol Microbiol* **57**(1): 143-155.

Müller, M. and R. B. Klosgen (2005). The Tat pathway in bacteria and chloroplasts (review). *Mol Membr Biol* **22**(1-2): 113-121.

Muraoka, W. T. and Q. Zhang (2011). Phenotypic and genotypic evidence for L-fucose utilization by *Campylobacter jejuni*. *J Bacteriol* **193**(5): 1065-1075.

Myer, Y. P., A. F. Saturno, B. C. Verma and A. Pande (1979). Horse heart cytochrome *c*. The oxidation-reduction potential and protein structures. *J Biol Chem* **254**(22): 11202-11207.

Myers, J. D. and D. J. Kelly (2005). A sulphite respiration system in the chemoheterotrophic human pathogen *Campylobacter jejuni*. *Microbiology* **151**(Pt 1): 233-242.

Nagata, K., S. Tsukita, T. Tamura and N. Sone (1996). A *cb*-type cytochrome-*c* oxidase terminates the respiratory chain in *Helicobacter pylori*. *Microbiology* **142 (Pt 7)**: 1757-1763.

Naikare, H., J. Butcher, A. Flint, J. Xu, K. N. Raymond and A. Stintzi (2013). *Campylobacter jejuni* ferric-enterobactin receptor CfrA is TonB3 dependent and mediates iron acquisition from structurally different catechol siderophores. *Metallomics* **5**(8): 988-996.

Naikare, H., K. Palyada, R. Panciera, D. Marlow and A. Stintzi (2006). Major role for FeoB in *Campylobacter jejuni* ferrous iron acquisition, gut colonization, and intracellular survival. *Infect Immun* **74**(10): 5433-5444.

Natale, P., T. Bruser and A. J. Driessen (2008). Sec- and Tat-mediated protein secretion across the bacterial cytoplasmic membrane-distinct translocases and mechanisms. *Biochim Biophys Acta* **1778**(9): 1735-1756.

Nauta, M., A. Hill, H. Rosenquist, S. Brynestad, A. Fetsch, P. van der Logt, A. Fazil, B. Christensen, E. Katsma, B. Borck and A. Havelaar (2009). A comparison of risk assessments on *Campylobacter* in broiler meat. *Int J Food Microbiol* **129**(2): 107-123.

Nicholls, D.G. & J. S. Ferguson. (2002). In Bioenergetics 3, Academic Press, London/San Diego.

Novik, V., D. Hofreuter and J. E. Galan (2010). Identification of *Campylobacter jejuni* genes involved in its interaction with epithelial cells. *Infect Immun* **78**(8): 3540-3553.

Ochsner, U. A., A. Snyder, A. I. Vasil and M. L. Vasil (2002). Effects of the twin-arginine translocase on secretion of virulence factors, stress response, and pathogenesis. *Proc Natl Acad Sci U S A* **99**(12): 8312-8317.

Odum, L. and L. P. Andersen (1995). Investigation of *Helicobacter pylori* ascorbic acid oxidating activity. *FEMS Immunol Med Microbiol* **10**(3-4): 289-294.

Oelschlaeger, T. A., P. Guerry and D. J. Kopecko (1993). Unusual microtubule-dependent endocytosis mechanisms triggered by *Campylobacter jejuni* and *Citrobacter freundii*. *Proc Natl Acad Sci U S A* **90**(14): 6884-6888.

Olson, C.K., S. Ethelberg, W. van Pelt & R. V. Tauxe. (2008). Epidermiology of *Campylobacter jejuni* Infections in Industrialized Nations. In: *Campylobacter*. Third edition. Nachamkin, I., Szymanski, C.M. and Blaser, M.J. Eds. ASM Press, Washington D.C.

Olson, J. W. and R. J. Maier (2002). Molecular hydrogen as an energy source for *Helicobacter pylori*. *Science* **298**(5599): 1788-1790.

Oltmann, L. F., V. P. Claassen, P. Kastelein, W. N. Reijnders and A. H. Stouthamer (1979). Influence of tungstate on the formation and activities of four reductases in *Proteus mirabilis*: Identification of two new molybdo-enzymes: chlorate reductase and tetrathionate reductase. *FEBS Lett* **106**(1): 43-46.

Otten, M. F., J. van der Oost, W. N. Reijnders, H. V. Westerhoff, B. Ludwig and R. J. Van Spanning (2001). Cytochromes c_{550}, c_{552}, and c_1 in the electron transport network of paracoccus denitrificans: Redundant or subtly different in function? *J Bacteriol* **183**(24): 7017-7026.

Page, M. L., P. P. Hamel, S. T. Gabilly, H. Zegzouti, J. V. Perea, J. M. Alonso, J. R. Ecker, S. M. Theg, S. K. Christensen and S. Merchant (2004). A homolog of prokaryotic thiol disulfide transporter CcdA is required for the assembly of the cytochrome b_6f complex in *Arabidopsis* chloroplasts. *J Biol Chem* **279**(31): 32474-32482.

Pajaniappan, M., J. E. Hall, S. A. Cawthraw, D. G. Newell, E. C. Gaynor, J. A. Fields, K. M. Rathbun, W. A. Agee, C. M. Burns, S. J. Hall, D. J. Kelly and S. A. Thompson (2008). A temperature-regulated *Campylobacter jejuni* gluconate dehydrogenase is involved in respiration-dependent energy conservation and chicken colonization. *Mol Microbiol* **68**(2): 474-491.

Palmer, T. and B. C. Berks (2012). The twin-arginine translocation (Tat) protein export pathway. *Nat Rev Microbiol* **10**(7): 483-496.

Palmer, T., B. C. Berks and F. Sargent (2010). Analysis of tat targeting function and twin-arginine signal peptide activity in *Escherichia coli*. *Methods Mol Biol* **619**: 191-216.

Palyada, K., Y. Q. Sun, A. Flint, J. Butcher, H. Naikare and A. Stintzi (2009). Characterization of the oxidative stress stimulon and PerR regulon of *Campylobacter jejuni*. *BMC Genomics* **10**: 481.

Palyada, K., D. Threadgill and A. Stintzi (2004). Iron acquisition and regulation in *Campylobacter jejuni*. *J Bacteriol* **186**(14): 4714-4729.

Pande, A. and Y. P. Myer (1978). The redox potential of horse heart cytochrome. *Biochem Biophys Res Commun* **85**(1): 7-13.

Parkhill, J., B. W. Wren, K. Mungall, J. M. Ketley, C. Churcher, D. Basham, T. Chillingworth, R. M. Davies, T. Feltwell, S. Holroyd, K. Jagels, A. V. Karlyshev, S. Moule, M. J. Pallen, C. W. Penn, M. A. Quail, M. A. Rajandream, K. M. Rutherford, A. H. van Vliet, S. Whitehead and B. G. Barrell (2000). The genome sequence of the food-borne pathogen *Campylobacter jejuni* reveals hypervariable sequences. *Nature* **403**(6770): 665-668.

Parsons, C. M. and D. H. Baker (1982). Effect of dietary protein level and monensin on performance of chicks. *Poult Sci* **61**(10): 2083-2088.

Pearson, B. M., D. J. Gaskin, R. P. Segers, J. M. Wells, P. J. Nuijten and A. H. van Vliet (2007). The complete genome sequence of *Campylobacter jejuni* strain 81116 (nctc11828). *J Bacteriol* **189**(22): 8402-8403.

Pei, Z., C. Burucoa, B. Grignon, S. Baqar, X. Z. Huang, D. J. Kopecko, A. L. Bourgeois, J. L. Fauchere and M. J. Blaser (1998). Mutation in the *peb1A* locus of *Campylobacter jejuni* reduces interactions with epithelial cells and intestinal colonization of mice. *Infect Immun* **66**(3): 938-943.

Pesci, E. C., D. L. Cottle and C. L. Pickett (1994). Genetic, enzymatic, and pathogenic studies of the iron superoxide dismutase of *Campylobacter jejuni*. *Infect Immun* **62**(7): 2687-2694.

Peterson, J. H., C. A. Woolhead and H. D. Bernstein (2003). Basic amino acids in a distinct subset of signal peptides promote interaction with the signal recognition particle. *J Biol Chem* **278**(46): 46155-46162.

Pisa, R., T. Stein, R. Eichler, R. Gross and J. Simon (2002). The *nrfI* gene is essential for the attachment of the active site haem group of *Wolinella succinogenes* cytochrome *c* nitrite reductase. *Mol Microbiol* **43**(3): 763-770.

Pitcher, R. S., T. Brittain and N. J. Watmough (2002). Cytochrome cbb_3 oxidase and bacterial microaerobic metabolism. *Biochem Soc Trans* **30**(4): 653-658.

Pittman, M. S. and D. J. Kelly (2005). Electron transport through nitrate and nitrite reductases in *Campylobacter jejuni*. *Biochem Soc Trans* **33**(Pt 1): 190-192.

Pittman, M. S., K. T. Elvers, L. Lee, M. A. Jones, R. K. Poole, S. F. Park and D. J. Kelly (2007). Growth of *Campylobacter jejuni* on nitrate and nitrite: Electron transport to NapA and NrfA via NrfH and distinct roles for NrfA and the globin Cgb in protection against nitrosative stress. *Mol Microbiol* **63**(2): 575-590.

Pohlschröder, M., K. Dilks, N. J. Hand and R. Wesley Rose (2004). Translocation of proteins across archaeal cytoplasmic membranes. *FEMS Microbiol Rev* **28**(1): 3-24.

Pommier, J., V. Mejean, G. Giordano and C. Iobbi-Nivol (1998). TorD, a cytoplasmic chaperone that interacts with the unfolded trimethylamine *N*-oxide reductase enzyme (TorA) in *Escherichia coli*. *J Biol Chem* **273**(26): 16615-16620.

Poock, S. R., E. R. Leach, J. W. Moir, J. A. Cole and D. J. Richardson (2002). Respiratory detoxification of nitric oxide by the cytochrome *c* nitrite reductase of *Escherichia coli*. *J Biol Chem* **277**(26): 23664-23669.

Poole, R. K. and G. M. Cook (2000). Redundancy of aerobic respiratory chains in bacteria? Routes, reasons and regulation. *Adv Microb Physiol* **43**: 165-224.

Pop, O., U. Martin, C. Abel and J. P. Muller (2002). The twin-arginine signal peptide of PhoD and the TatAd/Cd proteins of *Bacillus subtilis* form an autonomous Tat translocation system. *J Biol Chem* **277**(5): 3268-3273.

Porat, A., S. H. Cho and J. Beckwith (2004). The unusual transmembrane electron transporter DsbD and its homologues: A bacterial family of disulfide reductases. *Res Microbiol* **155**(8): 617-622.

Porcelli, I., E. de Leeuw, R. Wallis, E. van den Brink-van der Laan, B. de Kruijff, B. A. Wallace, T. Palmer and B. C. Berks (2002). Characterization and membrane assembly of the TatA component of the *Escherichia coli* twin-arginine protein transport system. *Biochemistry* **41**(46): 13690-13697.

Potter, L. C. and J. A. Cole (1999). Essential roles for the products of the *napABCD* genes, but not *napFGH*, in periplasmic nitrate reduction by *Escherichia coli* K-12. *Biochem J* **344 Pt 1**: 69-76.

Potter, L. C., P. Millington, L. Griffiths, G. H. Thomas and J. A. Cole (1999). Competition between *Escherichia coli* strains expressing either a periplasmic or a membrane-bound nitrate reductase: Does Nap confer a selective advantage during nitrate-limited growth? *Biochem J* **344 Pt 1**: 77-84.

Potter, L., H. Angove, D. Richardson and J. Cole (2001). Nitrate reduction in the periplasm of Gram-negative bacteria. *Adv Microb Physiol* **45**: 51-112.

Price, A., A. Economou, F. Duong and W. Wickner (1996). Separable ATPase and membrane insertion domains of the SecA subunit of preprotein translocase. *J Biol Chem* **271**(49): 31580-31584.

Pryjma, M., D. Apel, S. Huynh, C. T. Parker and E. C. Gaynor (2012). FdhTU-modulated formate dehydrogenase expression and electron donor availability enhance recovery of *Campylobacter jejuni* following host cell infection. *J Bacteriol* **194**(15): 3803-3813.

Purdy, D., C. M. Buswell, A. E. Hodgson, K. McAlpine, I. Henderson and S. A. Leach (2000). Characterisation of cytolethal distending toxin (CDT) mutants of *Campylobacter jejuni*. *J Med Microbiol* **49**(5): 473-479.

Rahman, H., R. M. King, L. K. Shewell, E. A. Semchenko, L. E. Hartley-Tassell, J. C. Wilson, C. J. Day and V. Korolik (2014). Characterisation of a multi-ligand binding chemoreceptor CcmL (Tlp3) of *Campylobacter jejuni*. *PLoS Pathog* **10**(1): e1003822.

Rajashekara, G., M. Drozd, D. Gangaiah, B. Jeon, Z. Liu and Q. Zhang (2009). Functional characterization of the twin-arginine translocation system in *Campylobacter jejuni*. *Foodborne Pathog Dis* **6**(8): 935-945.

Rappaport, F., I. Hirschberg and N. Konforti (1956). Modified tetrathionate enrichment medium for certain Salmonellae. *Acta Med Orient* **15**(3): 84-87.

Reid, E., J. Cole and D. J. Eaves (2001). The *Escherichia coli* CcmG protein fulfils a specific role in cytochrome *c* assembly. *Biochem J* **355**(Pt 1): 51-58.

Reijerse, E. J., M. Sommerhalter, P. Hellwig, A. Quentmeier, D. Rother, C. Laurich, E. Bothe, W. Lubitz and C. G. Friedrich (2007). The unusal redox centers of SoxXA, a novel *c*-type heme-enzyme essential for chemotrophic sulfur-oxidation of *Paracoccus pantotrophus*. *Biochemistry* **46**(26): 7804-7810.

Ren, Q., U. Ahuja and L. Thony-Meyer (2002). A bacterial cytochrome *c* heme lyase. CcmF forms a complex with the heme chaperone CcmE and CcmH but not with apocytochrome *c*. *J Biol Chem* **277**(10): 7657-7663.

Rhodes, K. M. and A. E. Tattersfield (1982). Guillain-Barre syndrome associated with *Campylobacter* infection. *Br Med J (Clin Res Ed)* **285**(6336): 173-174.

Ribardo, D. A. and D. R. Hendrixson (2011). Analysis of the LIV system of *Campylobacter jejuni* reveals alternative roles for LivJ and LivK in commensalism beyond branched-chain amino acid transport. *J Bacteriol* **193**(22): 6233-6243.

Richard-Fogal, C. and R. G. Kranz (2010). The CcmC:heme:CcmE complex in heme trafficking and cytochrome *c* biosynthesis. *J Mol Biol* **401**(3): 350-362.

Richard-Fogal, C. L., E. R. Frawley, E. R. Bonner, H. Zhu, B. San Francisco and R. G. Kranz (2009). A conserved haem redox and trafficking pathway for cofactor attachment. *EMBO J* **28**(16): 2349-2359.

Richard-Fogal, C. L., E. R. Frawley and R. G. Kranz (2008). Topology and function of CcmD in cytochrome *c* maturation. *J Bacteriol* **190**(10): 3489-3493.

Ridley, K. A., J. D. Rock, Y. Li and J. M. Ketley (2006). Heme utilization in *Campylobacter jejuni*. *J Bacteriol* **188**(22): 7862-7875.

Rivera-Amill, V., B. J. Kim, J. Seshu and M. E. Konkel (2001). Secretion of the virulence-associated *Campylobacter* invasion antigens from *Campylobacter jejuni* requires a stimulatory signal. *J Infect Dis* **183**(11): 1607-1616.

Robertson, I. B., J. M. Stevens and S. J. Ferguson (2008). Dispensable residues in the active site of the cytochrome *c* biogenesis protein CcmH. *FEBS Lett* **582**(20): 3067-3072.

Robinson, C. and A. Bolhuis (2004). Tat-dependent protein targeting in prokaryotes and chloroplasts. *Biochim Biophys Acta* **1694**(1-3): 135-147.

Robinson, D. A. (1981). *Campylobacter* infection. *R Soc Health J* **101**(4): 138-140.

Rodriguez, F., S. L. Rouse, C. E. Tait, J. Harmer, A. De Riso, C. R. Timmel, M. S. Sansom, B. C. Berks and J. R. Schnell (2013). Structural model for the protein-translocating element of the twin-arginine transport system. *Proc Natl Acad Sci U S A* **110**(12): E1092-1101.

Rollauer, S. E., M. J. Tarry, J. E. Graham, M. Jaaskelainen, F. Jager, S. Johnson, M. Krehenbrink, S. M. Liu, M. J. Lukey, J. Marcoux, M. A. McDowell, F. Rodriguez, P. Roversi, P. J. Stansfeld, C. V. Robinson, M. S. Sansom, T. Palmer, M. Hogbom, B. C. Berks and S. M. Lea (2012). Structure of the TatC core of the twin-arginine protein transport system. *Nature* **492**(7428): 210-214.

Rose, R. W., T. Bruser, J. C. Kissinger and M. Pohlschroder (2002). Adaptation of protein secretion to extremely high-salt conditions by extensive use of the twin-arginine translocation pathway. *Mol Microbiol* **45**(4): 943-950.

Sałamaszyńska-Guz, A. and D. Klimuszko (2008). Functional analysis of the *Campylobacter jejuni cj0183* and *cj0588* genes. *Curr Microbiol* **56**(6): 592-596.

Sambrook, J. and D. W. Russell (2001) *Molecular Cloning: A laboratory manual*. Third Edition. Cold Spring Harbor Laboratory Press. New York.

Sanders, C., S. Turkarslan, D. W. Lee and F. Daldal (2010). Cytochrome *c* biogenesis: The Ccm system. *Trends Microbiol* **18**(6): 266-274.

Sargent, F., E. G. Bogsch, N. R. Stanley, M. Wexler, C. Robinson, B. C. Berks and T. Palmer (1998). Overlapping functions of components of a bacterial Sec-independent protein export pathway. *EMBO J* **17**(13): 3640-3650.

Sargent, F., N. R. Stanley, B. C. Berks and T. Palmer (1999). Sec-independent protein translocation in *Escherichia coli*. A distinct and pivotal role for the TatB protein. *J Biol Chem* **274**(51): 36073-36082.

Sauve, V., S. Bruno, B. C. Berks and A. M. Hemmings (2007). The SoxYZ complex carries sulfur cycle intermediates on a peptide swinging arm. *J Biol Chem* **282**(32): 23194-23204.

Schagger, H. (2006). Tricine-SDS-PAGE. *Nat Protoc* **1**(1): 16-22.

Schiött, T., C. von Wachenfeldt and L. Hederstedt (1997). Identification and characterization of the *ccdA* gene, required for cytochrome *c* synthesis in *Bacillus subtilis*. *J Bacteriol* **179**(6): 1962-1973.

Schroder, W. and I. Moser (1997). Primary structure analysis and adhesion studies on the major outer membrane protein of *Campylobacter jejuni*. *FEMS Microbiol Lett* **150**(1): 141-147.

Schulz, H., H. Hennecke and L. Thony-Meyer (1998). Prototype of a heme chaperone essential for cytochrome *c* maturation. *Science* **281**(5380): 1197-1200.

Seaver, L. C. and J. A. Imlay (2004). Are respiratory enzymes the primary sources of intracellular hydrogen peroxide? *J Biol Chem* **279**(47): 48742-48750.

Segel, I.H. (1993) *Enzyme Kinetics: Behavior and Analysis of Rapid Equilibrium and Steady-State Enzyme Systems*. New York: Wiley-Interscience.

Sellars, M. J., S. J. Hall and D. J. Kelly (2002). Growth of *Campylobacter jejuni* supported by respiration of fumarate, nitrate, nitrite, trimethylamine-*N*-oxide, or dimethyl sulfoxide requires oxygen. *J Bacteriol* **184**(15): 4187-4196.

Shanmugham, A., H. W. Wong Fong Sang, Y. J. Bollen and H. Lill (2006). Membrane binding of twin arginine preproteins as an early step in translocation. *Biochemistry* **45**(7): 2243-2249.

Shaw, F. L., F. Mulholland, G. Le Gall, I. Porcelli, D. J. Hart, B. M. Pearson and A. H. van Vliet (2012). Selenium-dependent biogenesis of formate dehydrogenase in *Campylobacter jejuni* is controlled by the *fdhTU* accessory genes. *J Bacteriol* **194**(15): 3814-3823.

Shouldice, S. R., B. Heras, P. M. Walden, M. Totsika, M. A. Schembri and J. L. Martin (2011). Structure and function of DsbA, a key bacterial oxidative folding catalyst. *Antioxid Redox Signal* **14**(9): 1729-1760.

Simon, J., R. Gross, O. Einsle, P. M. Kroneck, A. Kroger and O. Klimmek (2000). A NapC/NirT-type cytochrome *c* (NrfH) is the mediator between the quinone pool and the cytochrome *c* nitrite reductase of *Wolinella succinogenes*. *Mol Microbiol* **35**(3): 686-696.

Simon, J., M. Sanger, S. C. Schuster and R. Gross (2003). Electron transport to periplasmic nitrate reductase (NapA) of *Wolinella succinogenes* is independent of a NapC protein. *Mol Microbiol* **49**(1): 69-79.

Simon, J. and L. Hederstedt (2011). Composition and function of cytochrome *c* biogenesis system II. *FEBS J* **278**(22): 4179-4188.

Skirrow, M. B. and M. J. Blaser. (2000). Clinical aspects of *Campylobacter* infection. In: *Campylobacter*. Third Edition. Nachamkin,I., Szymanski, C. M. and Blaser, M. J Eds. ASM Press, Washington D.C.

Smart, J. P., M. J. Cliff and D. J. Kelly (2009). A role for tungsten in the biology of *Campylobacter jejuni*: Tungstate stimulates formate dehydrogenase activity and is transported via an ultra-high affinity ABC system distinct from the molybdate transporter. *Mol Microbiol* **74**(3): 742-757.

Smith, M. A., M. Finel, V. Korolik and G. L. Mendz (2000). Characteristics of the aerobic respiratory chains of the microaerophiles *Campylobacter jejuni* and *Helicobacter pylori*. *Arch Microbiol* **174**(1-2): 1-10.

Song, Y. C., S. Jin, H. Louie, D. Ng, R. Lau, Y. Zhang, R. Weerasekera, S. Al Rashid, L. A. Ward, S. D. Der and V. L. Chan (2004). FlaC, a protein of *Campylobacter jejuni* TGH9011 (ATCC43431) secreted through the flagellar apparatus, binds epithelial cells and influences cell invasion. *Mol Microbiol* **53**(2): 541-553.

Sparacino-Watkins, C., J. F. Stolz and P. Basu (2014). Nitrate and periplasmic nitrate reductases. *Chem Soc Rev* **43**(2): 676-706.

St Maurice, M., N. Cremades, M. A. Croxen, G. Sisson, J. Sancho and P. S. Hoffman (2007). Flavodoxin:quinone reductase (FqrB): A redox partner of pyruvate:ferredoxin oxidoreductase that reversibly couples pyruvate oxidation to NADPH production in *Helicobacter pylori* and *Campylobacter jejuni*. *J Bacteriol* **189**(13): 4764-4773.

Stahl, M., J. Butcher and A. Stintzi (2012). Nutrient acquisition and metabolism by *Campylobacter jejuni*. *Front Cell Infect Microbiol* **2**: 5.

Stahl, M., L. M. Friis, H. Nothaft, X. Liu, J. Li, C. M. Szymanski and A. Stintzi (2011). L-fucose utilization provides *Campylobacter jejuni* with a competitive advantage. *Proc Natl Acad Sci U S A* **108**(17): 7194-7199.

Stanley, N. R., K. Findlay, B. C. Berks and T. Palmer (2001). *Escherichia coli* strains blocked in Tat-dependent protein export exhibit pleiotropic defects in the cell envelope. *J Bacteriol* **183**(1): 139-144.

Stanley, N. R., T. Palmer and B. C. Berks (2000). The twin arginine consensus motif of Tat signal peptides is involved in Sec-independent protein targeting in *Escherichia coli*. *J Biol Chem* **275**(16): 11591-11596.

Stecher, B., R. Robbiani, A. W. Walker, A. M. Westendorf, M. Barthel, M. Kremer, S. Chaffron, A. J. Macpherson, J. Buer, J. Parkhill, G. Dougan, C. von Mering and W. D. Hardt (2007). *Salmonella enterica* serovar Typhimurium exploits inflammation to compete with the intestinal microbiota. *PLoS Biol* **5**(10): 2177-2189.

Stevens, J. M., O. Daltrop, J. W. Allen and S. J. Ferguson (2004). *C*-type cytochrome formation: Chemical and biological enigmas. *Acc Chem Res* **37**(12): 999-1007.

Stevens, J. M., D. A. Mavridou, R. Hamer, P. Kritsiligkou, A. D. Goddard and S. J. Ferguson (2011). Cytochrome *c* biogenesis system I. *FEBS J* **278**(22): 4170-4178.

Stevenson, L. G., K. Strisovsky, K. M. Clemmer, S. Bhatt, M. Freeman and P. N. Rather (2007). Rhomboid protease AarA mediates quorum-sensing in *Providencia stuartii* by activating TatA of the twin-arginine translocase. *Proc Natl Acad Sci U S A* **104**(3): 1003-1008.

Sun, G., E. Sharkova, R. Chesnut, S. Birkey, M. F. Duggan, A. Sorokin, P. Pujic, S. D. Ehrlich and F. M. Hulett (1996). Regulators of aerobic and anaerobic respiration in *Bacillus subtilis*. *J Bacteriol* **178**(5): 1374-1385.

Szymanski, C. M., D. H. Burr and P. Guerry (2002). *Campylobacter* protein glycosylation affects host cell interactions. *Infect Immun* **70**(4): 2242-2244.

Szymanski, C. M., R. Yao, C. P. Ewing, T. J. Trust and P. Guerry (1999). Evidence for a system of general protein glycosylation in *Campylobacter jejuni*. *Mol Microbiol* **32**(5): 1022-1030.

Takamiya, M., A. Ozen, M. Rasmussen, T. Alter, T. Gilbert, D. W. Ussery and S. Knochel (2011). Genome sequence of *Campylobacter jejuni* strain 327, a strain isolated from a turkey slaughterhouse. *Stand Genomic Sci* **4**(2): 113-122.

Takata, T., S. Fujimoto and K. Amako (1992). Isolation of nonchemotactic mutants of *Campylobacter jejuni* and their colonization of the mouse intestinal tract. *Infect Immun* **60**(9): 3596-3600.

Tareen, A. M., J. I. Dasti, A. E. Zautner, U. Gross and R. Lugert (2010). *Campylobacter jejuni* proteins Cj0952c and Cj0951c affect chemotactic behaviour towards formic acid and are important for invasion of host cells. *Microbiology* **156**(Pt 10): 3123-3135.

Tareen, A. M., J. I. Dasti, A. E. Zautner, U. Gross and R. Lugert (2011). Sulphite : cytochrome *c* oxidoreductase deficiency in *Campylobacter jejuni* reduces motility, host cell adherence and invasion. *Microbiology* **157**(Pt 6): 1776-1785.

Tarry, M. J., E. Schafer, S. Chen, G. Buchanan, N. P. Greene, S. M. Lea, T. Palmer, H. R. Saibil and B. C. Berks (2009). Structural analysis of substrate binding by the TatBC component of the twin-arginine protein transport system. *Proc Natl Acad Sci U S A* **106**(32): 13284-13289.

Taveirne, M. E., M. L. Sikes and J. W. Olson (2009). Molybdenum and tungsten in *Campylobacter jejuni*: Their physiological role and identification of separate transporters regulated by a single ModE-like protein. *Mol Microbiol* **74**(3): 758-771.

Thauer, R. K., K. Jungermann and K. Decker (1977). Energy conservation in chemotrophic anaerobic bacteria. *Bacteriol Rev* **41**(1): 100-180.

Thiennimitr, P., S. E. Winter, M. G. Winter, M. N. Xavier, V. Tolstikov, D. L. Huseby, T. Sterzenbach, R. M. Tsolis, J. R. Roth and A. J. Baumler (2011). Intestinal inflammation allows *Salmonella* to use ethanolamine to compete with the microbiota. *Proc Natl Acad Sci U S A* **108**(42): 17480-17485.

Thomas, M. T., M. Shepherd, R. K. Poole, A. H. van Vliet, D. J. Kelly and B. M. Pearson (2011). Two respiratory enzyme systems in *Campylobacter jejuni* NCTC 11168 contribute to growth on L-lactate. *Environ Microbiol* **13**(1): 48-61.

Thompson, B. J., D. A. Widdick, M. G. Hicks, G. Chandra, I. C. Sutcliffe, T. Palmer and M. I. Hutchings (2010). Investigating lipoprotein biogenesis and function in the model Gram-positive bacterium *Streptomyces coelicolor*. *Mol Microbiol*. **77**(4): 943–957

Thöny-Meyer, L., D. Ritz and H. Hennecke (1994). Cytochrome *c* biogenesis in bacteria: A possible pathway begins to emerge. *Mol Microbiol* **12**(1): 1-9.

Thöny-Meyer, L. (1997). Biogenesis of respiratory cytochromes in bacteria. *Microbiol Mol Biol Rev* **61**(3): 337-376.

Thöny-Meyer, L. and P. Kunzler (1997). Translocation to the periplasm and signal sequence cleavage of preapocytochrome *c* depend on *Sec* and *Lep*, but not on the *ccm* gene products. *Eur J Biochem* **246**(3): 794-799.

Tian, P. and I. Andricioaei (2006). Size, motion, and function of the SecY translocon revealed by molecular dynamics simulations with virtual probes. *Biophys J* **90**(8): 2718-2730.

Tottey, S., K. J. Waldron, S. J. Firbank, B. Reale, C. Bessant, K. Sato, T. R. Cheek, J. Gray, M. J. Banfield, C. Dennison and N. J. Robinson (2008). Protein-folding location can regulate manganese-binding versus copper- or zinc-binding. *Nature* **455**(7216): 1138-1142.

Trumpower, B. L. (1990). Cytochrome bc_1 complexes of microorganisms. *Microbiol Rev* **54**(2): 101-129.

Ullers, R. S., J. Luirink, N. Harms, F. Schwager, C. Georgopoulos and P. Genevaux (2004). SecB is a bona fide generalized chaperone in *Escherichia coli*. *Proc Natl Acad Sci U S A* **101**(20): 7583-7588.

Urban, P.J. (1961) Colorimetry of sulfur anions. I. An improved colorimetric method for the determination of thiosulfate. *Z Analyt Chem* **179**: 415–422.

Vandamme, P. (2008). Taxonomy of the family *Campylobacteraceae*. In: *Campylobacter*. Third edition Edition. Nachamkin,I., Szymanski, C. M. and Blaser, M. J. ASM Press, Washington D.C.

van der Ploeg, R., J. P. Barnett, N. Vasisht, V. J. Goosens, D. C. Pother, C. Robinson and J. M. van Dijl (2011). Salt sensitivity of minimal twin arginine translocases. *J Biol Chem* **286**(51): 43759-43770.

van der Sluis, E. O. and A. J. Driessen (2006). Stepwise evolution of the Sec machinery in proteobacteria. *Trends Microbiol* **14**(3): 105-108.

van der Stel, A. X., A. van Mourik, L. Heijmen-van Dijk, C. T. Parker, D. J. Kelly, C. H. van de Lest, J. P. van Putten and M. M. Wosten (2014). The *Campylobacter jejuni* RacRS system regulates fumarate utilization in a low oxygen environment. *Environ Microbiol*. doi: 10.1111/1462-2920.12476.

van der Wolk, J. P., J. G. de Wit and A. J. Driessen (1997). The catalytic cycle of the *Escherichia coli* SecA ATPase comprises two distinct preprotein translocation events. *EMBO J* **16**(24): 7297-7304.

van Mourik, A., N. M. Bleumink-Pluym, L. van Dijk, J. P. van Putten and M. M. Wosten (2008). Functional analysis of a *Campylobacter jejuni* alkaline phosphatase secreted via the Tat export machinery. *Microbiology* **154**(Pt 2): 584-592.

van Vliet, A. H., K. G. Wooldridge and J. M. Ketley (1998). Iron-responsive gene regulation in a *Campylobacter jejuni fur* mutant. *J Bacteriol* **180**(20): 5291-5298.

van Vliet, A. H. and J. M. Ketley (2001). Pathogenesis of enteric *Campylobacter* infection. *Symp Ser Soc Appl Microbiol*(30): 45S-56S.

Vargas, C., A. G. McEwan and J. A. Downie (1993). Detection of *c*-type cytochromes using enhanced chemiluminescence. *Anal Biochem* **209**(2): 323-326.

Vegge, C. S., L. Brondsted, Y. P. Li, D. D. Bang and H. Ingmer (2009). Energy taxis drives *Campylobacter jejuni* toward the most favorable conditions for growth. *Appl Environ Microbiol* **75**(16): 5308-5314.

Velayudhan, J. and D. J. Kelly (2002). Analysis of gluconeogenic and anaplerotic enzymes in *Campylobacter jejuni*: An essential role for phosphoenolpyruvate carboxykinase. *Microbiology* **148**(Pt 3): 685-694.

Velayudhan, J., M. A. Jones, P. A. Barrow and D. J. Kelly (2004). L-serine catabolism via an oxygen-labile L-serine dehydratase is essential for colonization of the avian gut by *Campylobacter jejuni*. *Infect Immun* **72**(1): 260-268.

Véron, M., A. Lenvoisé-Furet, and P. Beaune. (1981). Anaerobic respiration of fumarate as a differential test between *Campylobacter fetus* and *Campylobacter jejuni*. *Curr. Microbiol*. **6:**349-354.

Vignais, P. M., B. Billoud and J. Meyer (2001). Classification and phylogeny of hydrogenases. *FEMS Microbiol Rev* **25**(4): 455-501.

Wacker, M., D. Linton, P. G. Hitchen, M. Nita-Lazar, S. M. Haslam, S. J. North, M. Panico, H. R. Morris, A. Dell, B. W. Wren and M. Aebi (2002). *N*-linked glycosylation in *Campylobacter jejuni* and its functional transfer into *E. coli*. *Science* **298**(5599): 1790-1793.

Wai, S. N., T. Takata, A. Takade, N. Hamasaki and K. Amako (1995). Purification and characterization of ferritin from *Campylobacter jejuni*. *Arch Microbiol* **164**(1): 1-6.

Walker, G. C., C. J. Kenyon, A. Bagg, P. J. Langer and W. G. Shanabruch (1982). Mutagenesis and cellular responses to DNA damage. *Natl Cancer Inst Monogr* **60**: 257-267.

Walther, T. H., C. Gottselig, S. L. Grage, M. Wolf, A. V. Vargiu, M. J. Klein, S. Vollmer, S. Prock, M. Hartmann, S. Afonin, E. Stockwald, H. Heinzmann, O. V. Nolandt, W. Wenzel, P. Ruggerone and A. S. Ulrich (2013). Folding and self-assembly of the TatA translocation pore based on a charge zipper mechanism. *Cell* **152**(1-2): 316-326.

Wang, Z., E. Klipfell, B. J. Bennett, R. Koeth, B. S. Levison, B. Dugar, A. E. Feldstein, E. B. Britt, X. Fu, Y. M. Chung, Y. Wu, P. Schauer, J. D. Smith, H. Allayee, W. H. Tang, J. A. DiDonato, A. J. Lusis and S. L. Hazen (2011). Gut flora metabolism of phosphatidylcholine promotes cardiovascular disease. *Nature* **472**(7341): 57-63.

Wassenaar, T. M., N. M. Bleumink-Pluym and B. A. van der Zeijst (1991). Inactivation of *Campylobacter jejuni* flagellin genes by homologous recombination demonstrates that *flaA* but not *flaB* is required for invasion. *EMBO J* **10**(8): 2055-2061.

Wassenaar, T. M., B. A. van der Zeijst, R. Ayling and D. G. Newell (1993). Colonization of chicks by motility mutants of *Campylobacter jejuni* demonstrates the importance of flagellin A expression. *J Gen Microbiol* **139 Pt 6**: 1171-1175.

Watson, R. O. and J. E. Galan (2008). *Campylobacter jejuni* survives within epithelial cells by avoiding delivery to lysosomes. *PLoS Pathog* **4**(1): e14.

Weatherspoon-Griffin, N., G. Zhao, W. Kong, Y. Kong, Morigen, H. Andrews-Polymenis, M. McClelland and Y. Shi (2011). The CpxR/CpxA two-component system up-regulates two Tat-dependent peptidoglycan amidases to confer bacterial resistance to antimicrobial peptide. *J Biol Chem* **286**(7): 5529-5539.

Weerakoon, D. R. and J. W. Olson (2008). The *Campylobacter jejuni* NADH:ubiquinone oxidoreductase (complex I) utilizes flavodoxin rather than NADH. *J Bacteriol* **190**(3): 915-925.

Weerakoon, D. R., N. J. Borden, C. M. Goodson, J. Grimes and J. W. Olson (2009). The role of respiratory donor enzymes in *Campylobacter jejuni* host colonization and physiology. *Microb Pathog* **47**(1): 8-15.

Weiner, J. H., G. Shaw, R. J. Turner and C. A. Trieber (1993). The topology of the anchor subunit of dimethyl sulfoxide reductase of *Escherichia coli*. *J Biol Chem* **268**(5): 3238-3244.

Weingarten, R. A., J. L. Grimes and J. W. Olson (2008). Role of *Campylobacter jejuni* respiratory oxidases and reductases in host colonization. *Appl Environ Microbiol* **74**(5): 1367-1375.

Weingarten, R. A., M. E. Taveirne and J. W. Olson (2009). The dual-functioning fumarate reductase is the sole succinate:quinone reductase in *Campylobacter jejuni* and is required for full host colonization. *J Bacteriol* **191**(16): 5293-5300.

Westfall, H. N., D. M. Rollins and E. Weiss (1986). Substrate utilization by *Campylobacter jejuni* and *Campylobacter coli*. *Appl Environ Microbiol* **52**(4): 700-705.

Wexler, M., F. Sargent, R. L. Jack, N. R. Stanley, E. G. Bogsch, C. Robinson, B. C. Berks and T. Palmer (2000). TatD is a cytoplasmic protein with DNase activity. No requirement for TatD family proteins in Sec-independent protein export. *J Biol Chem* **275**(22): 16717-16722.

Wickner, W. T. (1994). How ATP drives proteins across membranes. *Science* **266**(5188): 1197-1198.

Winter, S. E., P. Thiennimitr, M. G. Winter, B. P. Butler, D. L. Huseby, R. W. Crawford, J. M. Russell, C. L. Bevins, L. G. Adams, R. M. Tsolis, J. R. Roth and A. J. Baumler (2010). Gut inflammation provides a respiratory electron acceptor for *Salmonella*. *Nature* **467**(7314): 426-429.

Winter, S. E., M. G. Winter, M. N. Xavier, P. Thiennimitr, V. Poon, A. M. Keestra, R. C. Laughlin, G. Gomez, J. Wu, S. D. Lawhon, I. E. Popova, S. J. Parikh, L. G. Adams, R. M. Tsolis, V. J. Stewart and A. J. Baumler (2013). Host-derived nitrate boosts growth of *E. coli* in the inflamed gut. *Science* **339**(6120): 708-711.

Wittig, I., H. P. Braun and H. Schagger (2006). Blue native PAGE. *Nat Protoc* **1**(1): 418-428.

Woodall, C. A., M. A. Jones, P. A. Barrow, J. Hinds, G. L. Marsden, D. J. Kelly, N. Dorrell, B. W. Wren and D. J. Maskell (2005). *Campylobacter jejuni* gene expression in the chick cecum: Evidence for adaptation to a low-oxygen environment. *Infect Immun* **73**(8): 5278-5285.

Wösten, M. M., J. A. Wagenaar and J. P. van Putten (2004). The FlgS/FlgR two-component signal transduction system regulates the *fla* regulon in *Campylobacter jejuni*. *J Biol Chem* **279**(16): 16214-16222.

Wösten, M. M., C. T. Parker, A. van Mourik, M. R. Guilhabert, L. van Dijk and J. P. van Putten (2006). The *Campylobacter jejuni* PhosS/PhosR operon represents a non-classical phosphate-sensitive two-component system. *Mol Microbiol* **62**(1): 278-291.

Wright, J. A., A. J. Grant, D. Hurd, M. Harrison, E. J. Guccione, D. J. Kelly and D. J. Maskell (2009). Metabolite and transcriptome analysis of *Campylobacter jejuni in vitro* growth reveals a stationary-phase physiological switch. *Microbiology* **155**(Pt 1): 80-94.

Yahr, T. L. and W. T. Wickner (2001). Functional reconstitution of bacterial Tat translocation *in vitro*. *EMBO J* **20**(10): 2472-2479.

Yamasaki, M., S. Igimi, Y. Katayama, S. Yamamoto and F. Amano (2004). Identification of an oxidative stress-sensitive protein from *Campylobacter jejuni*, homologous to rubredoxin oxidoreductase/rubrerythrin. *FEMS Microbiol Lett* **235**(1): 57-63.

Yang, K., V. B. Borisov, A. A. Konstantinov and R. B. Gennis (2008). The fully oxidized form of the cytochrome *bd* quinol oxidase from *E. coli* does not participate in the catalytic cycle: Direct evidence from rapid kinetics studies. *FEBS Lett* **582**(25-26): 3705-3709.

Yao, R., D. H. Burr, P. Doig, T. J. Trust, H. Niu and P. Guerry (1994). Isolation of motile and non-motile insertional mutants of *Campylobacter jejuni*: The role of motility in adherence and invasion of eukaryotic cells. *Mol Microbiol* **14**(5): 883-893.

Young, K. T., L. M. Davis and V. J. Dirita (2007). *Campylobacter jejuni*: Molecular biology and pathogenesis. *Nat Rev Microbiol* **5**(9): 665-679.

Young, N. M., J. R. Brisson, J. Kelly, D. C. Watson, L. Tessier, P. H. Lanthier, H. C. Jarrell, N. Cadotte, F. St Michael, E. Aberg and C. M. Szymanski (2002). Structure of the *N*-linked glycan present on multiple glycoproteins in the Gram-negative bacterium, *Campylobacter jejuni*. *J Biol Chem* **277**(45): 42530-42539.

Zehnder, A. J. and K. Wuhrmann (1976). Titanium (III) citrate as a nontoxic oxidation-reduction buffering system for the culture of obligate anaerobes. *Science* **194**(4270): 1165-1166.

Zhou, J. and Z. Xu (2005). The structural view of bacterial translocation-specific chaperone SecB: Implications for function. *Mol Microbiol* **58**(2): 349-357.

Zientz, E., I. G. Janausch, S. Six and G. Unden (1999). Functioning of DcuC as the C4-dicarboxylate carrier during glucose fermentation by *Escherichia coli*. *J Bacteriol* **181**(12): 3716-3720.

Ziprin, R. L., C. R. Young, J. A. Byrd, L. H. Stanker, M. E. Hume, S. A. Gray, B. J. Kim and M. E. Konkel (2001). Role of *Campylobacter jejuni* potential virulence genes in cecal colonization. *Avian Dis* **45**(3): 549-557.

Appendix I Media and Buffer

Media used in this study

LB (Luria-Bertani) broth	
LB powder (Melford)	20 g
Dissolved in 1 litre of dH_2O and autoclaved	

LB agar	
LB powder (Melford)	8 g
Micro agar (Melford)	4 g
Dissolved in 400 ml of dH_2O and autoclaved	

Columbia blood agar base	
Columbia blood agar powder (Oxoid)	15.6 g
Dissolved in 400 ml of dH_2O and autoclaved	

Muller-Hinton (MH) broth	
MH powder (Oxoid)	2.1 g
L-Serine (Sigma)	0.21 g
Dissolved in 100 ml of dH_2O and autoclaved	

Brain-Heart Infusion (BHI) broth	
BHI powder (Oxoid)	18.5 g
Dissolved in 500 ml of dH_2O and autoclaved	

MH agar	
MH agar powder (Oxoid)	15.2 g
Dissolved in 400 ml of dH_2O and autoclaved	

dYT	
Tryptone (Oxoid)	1.6 g
Yeast extract (Oxoid)	1 g
NaCl	0.5 g
Dissolved in 100 ml of ddH_2O and autoclaved	

NZCYM broth	
NZCYM powder (Amresco)	23 g
Dissolved in 1 litre of dH_2O and autoclaved	

DMEM basal medium	
Phosphate-free DMEM medium (Gibco)	
L-serine	20 mM
HEPES	25 mM
KH_2PO_4	1.6 mM for growth or 0.08 mM for AP induction
L-serine and KH2PO4 are suitable for autoclaving and HEPES is filter sterilised	

Buffers used in this study

10X TAE buffer	
Tris base	48.4 g
EDTA, disodium salt	3.7 g
Glacial acetic acid	11.4 ml
Dissolved in 800 ml dH_2O, filled to 1 litre with dH_2O and diluted to 1X	

6X DNA loading buffer	
Bromophenol blue	25 mg
Xylene cyanol FF	25 mg
Glycerol	3.3 ml
Dissolved in 3.3 ml glycerol, filled to 10 ml with ddH_2O	

5 × ISA buffer	
1M Tris-HCl, pH 7.5 (VWR)	3 ml
2M $MgCl_2$ (BDH)	150 µl
100 mM dGTP (Promega)	60 µl
100 mM dCTP (Promega)	60 µl
100 mM dTTP (Promega)	60 µl
100 mM dATP (Promega)	60 µl
1M DTT (Melford)	300 µl
PEG-8000 (BDH)	1.5 g
100 mM NAD (Sigma)	300 µl
Filled to 6 ml with ddH_2O and aliquoted into 40 µl	

RF1 buffer

KCl	0.745 g
$MnCl_2 \cdot 4H_2O$	0.98 g
Potassium acetate	0.29 g
$CaCl_2 \cdot 2H_2O$	0.246 g
Glycerol	15 g

Adjust pH to 5.8 with diluted acetic acid and filled to 100ml with ddH_2O, filter sterilised

RF2 buffer

MOPS	50 mg
KCl	15 mg
$CaCl_2 \cdot 2H_2O$	220 mg
Glycerol	3 g

Adjust pH to 6.8 with diluted NaOH and filled to 20ml with ddH_2O, filter sterilized

Washing buffer for competent *C. jejuni* cells

Sucrose	4.5 g
Glycerol	7.5 g

Dissolved in 35 ml dH_2O and filled to 50 ml with dH_2O, autoclaved

1M Tris-HCl, pH 8.0

Tris base	12.11 g

Adjust pH to 8.0 with HCl and filled to 50ml with ddH_2O, autoclaved

100 mM EDTA

EDTA, disodium salt	3.72 g

Adjust pH to 8.0 with HCl and filled to 100ml with ddH_2O, autoclaved

STE buffer

40% sucrose solution	10 ml
1M Tris-HCl, pH 8.0	0.6 ml
100 mM EDTA	0.2 ml

Filled to 20 ml with ddH_2O, filter sterilized

10 mM Tris-HCl, pH 8.0

Tris base	0.61 g

Adjust pH to 8.0 with HCl and filled to 500ml with ddH_2O, autoclaved

20 mM Tris-HCl, pH 8.0	
Tris base	1.22 g
Adjust pH to 8.0 with HCl and filled to 500ml with ddH_2O, autoclaved	

20 (25) mM phosphate buffer, pH 7.4	
0.5 M Na_2HPO_4	77.4 ml
1 M NaH_2PO_4	11.3 ml
Filled to 500 ml with ddH_2O than diluted 5X (4X) with ddH_2O to make final concentration of 20 (25) mM	

Lowry assay, solution A	
Sodium carbonate	20 g
Sodium hydroxide	4 g
Sodium tartrate	1.6 g
SDS	10 g
Dissolved in 1 litre of ddH_2O, warmed slightly to dissolved SDS	

Lowry assay, solution B	
$CuSO4 \cdot 5H_2O$	0.4 g
Dissolved in 10 ml of ddH_2O	

Lowry assay, solution C	
Solution A	100 ml
Solution B	1 ml

4X reduced sample buffer of SDS-PAGE	
Glycerol	4 ml
β-mercaptoethanol	0.5 ml
1M Tris-HCl, pH 6.8	2.4 ml
SDS	0.8 g
Bromophenol blue	4 mg
Filled to 10 ml with ddH_2O	

4X non-reduced sample buffer of Tricine-PAGE	
Glycerol	2 ml
1M Tris-HCl, pH 8.0	1.24 ml
SDS	0.46 g
Bromophenol blue	4 mg
Filled to 10 ml with ddH_2O	

50% acrylamide/bis solution	
Acrylamide	48 g
Bisacrylamide	1.5 g

Dissolved in 100 ml of ddH_2O, filter sterilized

Stock solution of SDS-PAGE

Stock solution	Chemicals	Conc.(M)	Weight per 100 ml (g)
Buffer A	Acrylamide/Bis-acrylamide, 30% solution (29: 1)		
Buffer B	Tris base	1.5	18.2
	TEMED		0.4 ml
	pH	8.8	
Buffer C	Tris base	0.5	6.06
	TEMED		0.5 ml
	pH	6.8	

Stock solution of BN-PAGE (first dimension)

Stock solution	Chemicals	Conc	%	Weight per 500 ml (g)
Anode buffer (1X)	Imidazole	25 mM		0.85
	pH	7.0 by HCl		
Cathode buffer (1X)	Tricine	50 mM		4.48
	Imidazole	7.5		0.26
	CBG		0.02	0.1
	pH	~7.0		
Gel buffer (3×)	Imidazole	75 mM		0.51 per 100 ml
	6-Aminohexanoic acid	1.5 M		19.68 g per 100 ml
	pH	7.0 by HCl		

SDS running buffer 10X	
Tris base	30.3 g
Glycine	144 g
SDS	10 g

Filled to 1 litre with ddH_2O

Stock solution of Tricine-PAGE

Stock solution	Chemicals	Conc.(M)	%	Weight per 100 ml (g)
Anode buffer (10 ×)	Tris base	1		12.11
	HCl	0.225		3.75
	pH		8.90	
Cathode buffer (10 ×)	Tris base	1		12.11
	Tricine	1		17.92
	SDS		1	1.00
	pH		~8.25	
Gel buffer (3×)	Tris base	3		36.34
	HCl	1		16.67
	SDS		0.3	0.30
	pH		8.45	

CBR stain	
CBR (Brilliant R)	1 g
Methanol	250 ml
Acetic acid	50 ml
Dissolve CBR powder in 250 ml ddH_2O then add 250 ml methanol and 50 ml acetic acid	

Destain	
Methanol	300 ml
Acetic acid	100 ml
Pour methanol and acetic acid in ddH_2O and filled to 1 litre	

Transfer buffer	
Tris base	30.3 g
Glycine	144 g
Adjust pH to 8.3 with HCl and filled to 900ml with ddH_2O then add 100 ml of methanol to make final concentration of 10%	

10 × PBS	
NaCl	80 g
Na_2HPO_4	11.5 g
KH_2PO_4	2 g
KCl	2 g
Adjusted pH to 7.4 with HCl and filled to 1 litre with ddH_2O	

Binding buffer (1 litre)	
20 mM phosphate buffer, pH 7.4	
0.5 M NaCl	29.22 g
Filled to 1 litre with 20 mM phosphate buffer	

Washing buffer (1 litre)	
20 mM phosphate buffer, pH 7.4	
0.5 M NaCl	29.22 g
20 mM Imidazole	1.36 g
Adjust pH to 7.4 with diluted HCl and filled to 1 litre with 20 mM phosphate buffer	

Elution buffer (1 litre)	
20 mM phosphate buffer, pH 7.4	
0.5 M NaCl	29.22 g
500 mM Imidazole	34.1 g
Adjust pH to 7.4 with HCl and filled to 1 litre with 20 mM phosphate buffer	

Buffer W (100 ml)	
100 mM Tris	1.21 g
150 mM NaCl	0.88 g
1 mM EDTA-2Na	0.037 g
Adjust pH to 8.0 with HCl and filled to 100 ml with ddH_2O	

Buffer E (100 ml)	
100 mM Tris	1.21 g
150 mM NaCl	0.88 g
1 mM EDTA-2Na	0.037 g
2.5 mM desthiobiotin	0.054 g
Adjust pH to 8.0 with HCl and filled to 100 ml with ddH_2O	

Buffer R (100 ml)	
100 mM Tris	1.21 g
150 mM NaCl	0.88 g
1 mM EDTA-2Na	0.037 g
2-(4-Hydroxyphenylazo)benzoic acid (HABA)	0.024 g
Adjust pH to 8.0 with HCl and filled to 100 ml with ddH_2O	

50 mM Tris-HCl, pH 8.0 (1 litre)	
Tris base (Fisher)	6.06 g
Adjust pH to 8.0 with HCl and filled to 1 litre with ddH_2O, autoclaved	

1 × PBS	
NaCl (Fisher)	8 g
Na_2HPO_4 (Fisher)	1.15 g
KH_2PO_4 (Fisher)	0.2 g
KCl (BDH)	0.2 g
Adjust pH to 7.4 with HCl and filled to 1 litre with ddH_2O, autoclaved	

Gelatin-NET	
Gelatin	1.25 g
NaCl	4.38 g
EDTA-2Na	0.9 g
Tris	3.03 g
Tween-20	0.25 ml
Adjust pH to 8.0 with HCl and filled to 500 ml with ddH_2O, autoclaved	

PBST	
Tween-20	0.25 ml
Adjust the volume to 500 ml by PBS	

Urea-PBST	
Urea	180.2 g
Adjust the volume to 500 ml by PBST	

ECI buffer	
Bovine serum albumin (BSA)	1 g
Polyvinylpyrrolidone (PVP) Mw 40000	10 g
Dissolve both in PBST and adjust the volume to 500 ml, autoclaved	

100 mM ammonium acetate, pH 5	
ammonium acetate	3.85 g
Dissolved in 500 ml ddH_2O and pH adjusted to 5 by acetic acid	

2% titanium (III) citrate oxygen scavenger solution	
Potassium citrate	4.86g
12% titanium chloride solution	9.38 ml
Dissolve potassium citrate in 48.75 ml ddH_2O then sparge the solution by oxygen-free argon for 10 mins then add 9.38 ml titanium chloride solution and adjust pH to 7 by saturated potassium carbonate solution, sparge the solution by argon for another 30 mins	

100 mM Tris-HCl, pH 7.5	
Tris base	1.21 g
Dissolved in 100 ml ddH_2O and adjust pH to 7.5 by HCl	

25 mM ammonium acetate, pH 5.5 (or 5.7 for Phenoloxidase assay)	
ammonium acetate	0.97 g
Dissolved in 500 ml ddH_2O and pH adjusted to 5.5 (or 5.7) by acetic acid	

$Fe(NO_3)_3$ solution for thiosulphate and tetrathionate assays	
$Fe(NO_3)_3 \cdot 9H_2O$	30 g
65% HNO_3	34 ml
Dissolve $Fe(NO_3)_3 \cdot 9H_2O$ in HNO_3 then filled ddH_2O to 100 ml	